Summer 2015

Role of the dewetting mechanism on moisture damage in asphalt pavements

Nibert Elijah Saltibus
Louisiana Tech University

ROLE OF THE DEWETTING MECHANISM ON MOISTURE DAMAGE IN ASPHALT PAVEMENTS

by

Nibert Elijah Saltibus, B.S., M.S.

A Dissertation Presented in Partial Fulfillment
of the Requirements of the Degree
Doctor of Philosophy

COLLEGE OF ENGINEERING AND SCIENCE
LOUISIANA TECH UNIVERSITY

August 2015

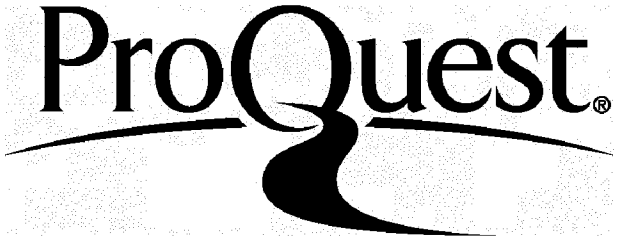

LOUISIANA TECH UNIVERSITY

THE GRADUATE SCHOOL

JULY 6, 2015
Date

We hereby recommend that the thesis prepared under our supervision by **Nibert Elijah Saltibus**, B.S., M.S.

entitled **Role of the Dewetting Mechanism on Moisture Damage in Asphalt Pavements**

be accepted in partial fulfillment of the requirements for the Degree of

Doctor of Philosophy in Engineering

Supervisor of Thesis Research

JDP
Head of Department
Civil Engineering
Department

Recommendation concurred in:

Advisory Committee

Approved:

Director of Graduate Studies

JDP
Dean of the College

Approved:

Dean of the Graduate School

GS Form 13
(8/10)

ABSTRACT

Moisture damage is a major form of pavement distress that causes state and federal highways to undergo high maintenance cost (Bhasin, 2006). According to Hicks et al., (2003), in a survey conducted by the Colorado Department of Transportation, mainly including US agencies (1 Canadian Province), 82% of these agencies required the use of anti-strip treatment (additives) to avert moisture damage. Additionally, 87% of these agencies test for moisture susceptibility. Despite extensive research performed on the moisture damage mechanisms in flexible pavements, it has been a challenge to obtain one single test that can comprehensively quantify the damage and to also predict the material performance in the field (Caro et al., 2008; Solaimanian et al., 2003). In this study, the role of the dewetting mechanism in moisture damage of asphalt pavements was investigated. Three main asphalts, mainly two anti-strip additives, and a warm mix additive were utilized. Tests, such as Pull-off, Surface free energy, Modified boil and microscopic analysis of dewetting were performed. A unique dewetting-based moisture damage test procedure was developed consisting of a moisture conditioning procedure and quantitative analysis of the dewetting with the use of a microscope and NI Vision (2012) software. The dewetting analysis procedure includes measurements of the total dewetted area and number of dewetted holes. It was observed that the dewetting phenomenon occurs primarily under a trapped air bubble in the asphalt film submerged in water. Most of the dewetting pattern followed that of an exponential growth. Polymer

(Styrene Butadiene Styrene) in PG 76-22M asphalt did aid in reducing dewetting. At high pH, 10, the Adhere LOF 6500 additive increased dewetting for all three asphalts. The critical film thickness can be defined as the minimum thickness above which very few dewetted holes was observed, which indicate a proposed threshold parameter for asphalt film thickness in the pavement mixes. The critical film thickness for all three asphalts was estimated experimentally and found to be 300 μm.

The findings of this study on understanding the role of dewetting on moisture damage in asphalt pavements will assist in the implementation of a unique dewetting-based moisture damage test procedure and analysis.

APPROVAL FOR SCHOLARLY DISSEMINATION

The author grants to the Prescott Memorial Library of Louisiana Tech University the right to reproduce, by appropriate methods, upon request, any or all portions of this Dissertation. It is understood that "proper request" consists of the agreement, on the part of the requesting party, that said reproduction is for his personal use and that subsequent reproduction will not occur without written approval of the author of this Dissertation. Further, any portions of the Dissertation used in books, papers, and other works must be appropriately referenced to this Dissertation.

Finally, the author of this Dissertation reserves the right to publish freely, in the literature, at any time, any or all portions of this Dissertation.

Author 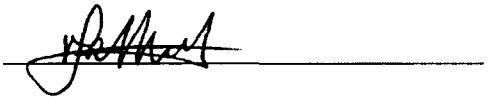

Date 7/31/2015

DEDICATION

To God and His Only Begotten Son Jesus Christ.

TABLE OF CONTENTS

LIST OF TABLES

LIST OF FIGURES

ACKNOWLEDGMENTS

I would like to express my gratitude to my advisor, Dr. Nazimuddin Wasiuddin, for his help, support, and guidance throughout my academic term at Louisiana Tech University. Additionally, I would like to acknowledge the help and guidance of Dr. Jay Wang, Dr. Erez Allouche, Dr. Henry Cardenas, and Dr. Aziz Saber for all the ways they helped in my research and from the knowledge gained from the invaluable instruction that they provided. Special thanks also to Dr. Norman Pumphrey, Jr., and Dr. Sanjay Tewari for helping to serve on my committee, at a time when their help was needed.

Also, I extend gratitude to past research colleagues, Amanda Marshall, Kisler Wilson, and Rajan Saha. Special thanks to Md Readul Islam for his insightful comments on my research.

I would like to take the time to thank my wife, Eola Saltibus, for her great patience with me during the course of my academic pursuit. Additionally, I want to thank my parents, my brothers and sister for their patience with my being away for so long.

Moreover, I would like to thank Louisiana Transportation and Research Center (LTRC) for providing funding during much of my tenure at Louisiana Tech University.

Finally, I would like to thank Louisiana Tech University for allowing me the opportunity to study in the field of Civil Engineering within its walls, and specifically, the College of Engineering and Science for its much needed support.

CHAPTER 1

INTRODUCTION

1.1 Introduction

Moisture damage is a major form of pavement distress that causes state and federal highways to undergo high maintenance cost (Bhasin, 2006). Some of these major distresses include, but are not limited to, stripping, raveling and fatigue damage. In total, moisture damage leads to an annual extra vehicle operating cost estimated in excess of $ 54 billion (Caro et al., 2008; Copeland, 2005).

According to Hicks et al. (2003), in a survey conducted by the Colorado Department of Transportation, mainly including US agencies (1 Canadian Province), 82% of these required the use of anti-strip treatment (additives) to avert moisture damage. Additionally, 87% of these agencies test for moisture susceptibility.

Caro et al. (2008) define moisture damage as it pertains to asphalt mixtures as the deterioration of the mechanical properties of the material as a result of the infiltration of moisture in a liquid or vapor phase. The mechanisms at work in moisture damage are complex (Caro, 2008; Bonner, 2001), and asphalt to aggregate adhesion is dependent on a set of variables in which the principal factors involved are the nature of the aggregates and the bitumen, to a lesser extent (Bonner, 2001). The aggregate properties that affect adhesion are the mineralogy, surface texture, porosity, surface coatings and dust, mechanical durability, surface area, absorption, moisture content, abrasion, pH,

weathering grade, exposure history, shape and the type of additive that is used. Concerning the bitumen (asphalt), the factors that affect aggregate adhesion is the viscosity, surface tension, and polarity (Bonner, 2001). Moreover, due to the multiplicity of the mechanisms involved, the identification of the fracture mechanisms of asphalt-aggregate systems in the presence of water is very challenging and a synergistic interaction of the mechanisms involved is most of the time left to be best explained by the moisture damage process (Kim et al., 2008).

In spite of the extensive research performed on the moisture damage mechanisms in flexible pavements, it has been a challenge to obtain one single test that can comprehensively quantify the damage and to also predict the material behavior in the field (Caro et al., 2008; Solaimanian et al., 2003). Despite the many variables in the field that restrict good correlation of test methods in the lab (Solaimanian et al., 2003), the development of these correlations is still of paramount importance. Also, in the presence of moisture, specifically at the asphalt/air/water interface, it is observed that asphalt dewets under an air bubble, and in the literature, particularly in the oil recovery research field, it has been further observed that oil spreads at the air/water interface. Surface tension has been shown to be a key parameter in the spreading of the oil on the two interfaces. Fromm (1974) observed that asphalt spreads on the air/water interface which he termed "pull back", and he also observed the holes that were formed in the asphalt when it was left to moisture condition for some time. The literature on spreading and wetting/dewetting dynamics is immense as the wetting phenomenon is important when it comes to industries such as the printing, lithography and packaging. The fundamentals will be highlighted in the literature review.

Therefore, there is a pressing need to develop a mechanism-based moisture damage test procedure and analysis.

1.2 Objectives

1. To identify and characterize the role of the dewetting mechanism on moisture damage in asphalt pavements:
    - Perform exploratory adhesion/cohesion testing such as pull-off testing.
    - Determine surface energy components of asphalt binder and aggregates.
    - Perform AASHTO T 283 Test on moisture damage samples.
2. Examine influence of various parameters on dewetting:
    - Develop experimental set up for dewetting after identifying the mechanism.
    - Adapt program (NI Vision Builder 2012) to aid in establishing behavioral change in radius as a function of time.
    - Explore influence of dewetting for different variables (temperature/asphalt type/additives).
3. Develop a test method for moisture susceptibility utilizing the mechanism involved:
    - Quantify and analyze dewetted area.
    - Quantify and analyze dewetted hole density.
    - Analyze and quantify the effect of pH on dewetting of asphalt films.
    - Analyze the effects of additives on dewetting of asphalt films.
    - Conduct modified boiling test (Modified ASTM 3625) to assess moisture damage.

- Validate the developed dewetting-based moisture damage test with modified boiling test.

1.3 Outline

The outline of the dissertation is as follows: Chapter 1 presents a brief overview as to the background, objectives and outline of the dissertation. Chapter 2 gives a comprehensive literature review on moisture damage in asphalt pavements and that of wetting phenomena which includes dewetting and interfacial tension. Chapter 3 discusses the use of surface free energy to measure some of the main asphalt binders and aggregate types used in asphalt pavements particular that of the state of Louisiana and also a measure of the cohesive and adhesive strengths of asphalt and substrates with and without moisture damage.

Chapter 4 analyzes the dewetting of asphalt binders in the presence of moisture under an air bubble with glass and, Chapter 5, aggregate substrates at various film thicknesses, temperature increases, anti-strip additives and pH. Chapter 6 employs the development of a moisture damage test method to assess moisture damage in three asphalt binders (PG 58-28, PG 64-22, and PG 76-22M) with and without additives (Adhere HP Plus and Adhere LOF 6500), together with the effects of film thicknesses. The effects of pH will also be analyzed on the total dewetted area of the glass plate samples on all asphalt types.

Chapter 7 provides the analysis of a modified boil test (Modified ASTM D3625) results and the correlation with the dewetted area observed in the developed dewetting moisture damage test. Chapter 8 provides information on the distribution of the dewetted holes in the asphalt films based on selected asphalt types. The information will also help

understand the dewetting patterns in the films. Chapter 9 presents the necessary conclusions and recommendations.

CHAPTER 2

LITERATURE REVIEW

2.1 Moisture Damage in Hot Mix Asphalt

2.1.1 Introduction

The literature review seeks to give a comprehensive examination of the literature from the earliest time to the present. Additionally, the literature review will explore spreading and wetting phenomena as they pertain to thin and thick films and will include interfacial phenomena as all three topics are the basis of the present research. Primarily, moisture damage in asphalt pavements result in the loss of adhesion between the asphalt film or mastic and the aggregate or failure could result in loss of cohesion in the asphalt film. There are many mechanisms that have been put forward in the literature in an attempt to explain moisture damage in asphalt pavements or the premature failure of the asphalt mix.

2.1.2 Mechanisms for Loss of Adhesion

The reduction of asphalt adhesion from the aggregate has been identified and is as a result of a broad spectrum of mechanisms. These mechanisms include displacement, detachment, film rupture, blistering and pitting, spontaneous emulsification, hydraulic scouring, pore pressure, and chemical disbonding (Lavin, 2002; Ensley,1975; Bagampadde, 2004). Some of these mechanisms are summarized in Table 2-1.

Table 2-1: Mechanisms of stripping (loss of adhesion) at the bitumen aggregate interface (Adapted from Bagampadde, 2004).

Process	Theory	Mechanism
Displacement	Thermodynamic and chemical reaction	Water with lower surface energy and higher dipole moment than bitumen displaces it from aggregate surface.
Detachment	Thermodynamic and chemical reaction	Water with lower surface energy and higher dipole moment than bitumen displaces it from aggregate surface.
Spontaneous emulsification	Electrostatics	Emulsion formation, due to presence of agents like clay coatings, weakens the bonding at the interface.
Pore Pressure	Mechanical break	High pore pressure in undrained conditions causes a break in bitumen film allowing water to enter the interface.
Chemical disbonding	Chemical reaction and electrostatic	Chemical and electrostatic interaction between water and some aggregates favor removal of bitumen from them.
Microbial activity	Bacterial metabolism	Microbial metabolic processes at the interface give by-products that break adhesion at the interface.
Osmosis	Diffusion	Concentration gradient across the bitumen film causes water to be transported to the interface.

2.1.2.1 Displacement

This mechanism is due to the entry of water to the interface of the asphalt film and the aggregate surface with a break in the asphalt film (Lavin, 2002; Little and Jones, 2003; Kiggundu and Roberts, 1988). Little and Jones (2003) explained that the source of the break in the asphalt film can be attributed to insufficient coating of the aggregate surface, the rupture of the film at the aggregate coatings that are sharp or the edges and due to the type of aggregate coatings pinholes that originate in the asphalt film. Thelen (1958) relate that dust on the aggregate surface can increase the production of blisters and pits. Little and Jones (2003) also highlighted that the process of the displacement mechanism can occur as a result of changes in the pH of the water at the aggregate surface that migrate through the point of discontinuity. The thermodynamic and chemical reaction theory may help explain this mechanism (Bagampadde, 2004).

2.1.2.2 Detachment

Unlike the displacement mechanism by which the asphalt film is separated from the aggregate with a break or discontinuity in the film, detachment is defined as the disjoining of the asphalt film from the aggregate surface without an apparent break in the film by a relatively thin layer of water (Bagampadde, 2004; Little and Jones 2003; Lavin 2002). The thermodynamic and chemical reaction theory is also used to explain the detachment mechanism (Bagampadde, 2004).

2.1.2.3 Spontaneous emulsification

Spontaneous emulsification, according to Fromm (1974), is the process whereby water droplets travel through the asphalt film to the substrate which results in total loss of adhesion. Fromm concluded that by spontaneous emulsification, water may go through

and infiltrate asphalt films, but that with the use of various additives, the rate and degree of the emulsification process may be made worse or decrease. However, Little and Jones (2003) noted that commercial amine-based asphalt additives, being organic amine compounds, varied chemically from cationic asphalt emulsifiers and that it is not possible for them to function as emulsifiers in their amine form to produce normal oil in water-asphalt emulsions. Fromm (1974) also concluded that the composition of the asphalt plays an important function in determining how they vary in their rate of emulsification. This process as noted by researchers can be aggravated when subjected to traffic on mixtures that are burdened with water (Kiggundu and Roberts, 1988). Calcareous minerals and some fines are materials that have been observed to improve the probability of inverted asphalt emulsions (Kiggundu and Roberts, 1988).

2.1.2.4 Film rupture

Film rupture as has been noted under the displacement mechanism, for moisture damage may happen as a result of construction loads, the operation of traffic during service conditions, and can occur by environmental effects such as freeze-thaw cycling (Kiggundu and Roberts, 1988).

2.1.2.5 Pore pressure

According to Kiggundu and Roberts (1988), this mechanism precipitate from the occurrence of water in the pore configuration of the HMA locations where there is a prevalence of segregation at the layer boundaries when heavy traffic loading takes place and during freeze-thaw cycling. Lottman et al. (1969) in proposing the pore pressure mechanism, concluded that due to the internal surging of water pressure in the voids of the mixture, stripping is enacted and is caused primarily as a result of differential thermal

expansion of asphaltic binder, the asphalt mixture and the water present in the void. In keeping water out of the mixtures, high asphalt content and mixture densities will assist, but test observations and analysis signify that the voids must be a minimum of two percent (Lottman et al., 1969). It was also noted that the possibility exists for pavement flushing to occur at the two percent air voids or less. The mechanical theory was attributed to these mechanisms (Bagampadde, 2004).

2.1.2.6 Hydraulic scour

This mechanism is caused as a result of capillary tension or compression taking place within the vicinity of a moving heavy traffic wheel on a HMA (Hot Mix Asphalt) saturated structure (Kiggundu and Roberts, 1988). Additionally, Martin et al. (2003) asserted that in front of the tire, water is compressed into the pavement which gives rise to a compressive stress within the void structure. At the passage of the tire, a vacuum is formed, which draws the water back out of the interconnected voids. This hydraulic scour, Martin et al. (2003) maintains can also give rise to two other mechanisms such as displacement or spontaneous emulsification.

2.1.3 Additional Mechanisms

2.1.3.1 Environmental effects

According to Hicks (1991), climate and traffic loads are some of the environmental considerations that affect stripping after construction and can include variation in temperature, freeze thaw cycles, and wet dry cycles. Hicks (1991) noted that pore pressure build up and hydraulic scoring were connected with the damage due to cyclic loads of asphalt concrete by traffic. It, therefore may be affirmed, Hicks continued,

that as all other facts are equal, the increase in traffic loading would accelerate moisture damage.

2.1.3.2 pH instability

It is possible to attain a strong chemical bond between aggregate and asphalt cement that resists pH shifts and a high pH environment (Tarrer, 1996; Little and Jones, 2003). Concerning pH shifts and chemical bond between aggregates and asphalt cement, Little and Jones (2003) highlighted that the magnitude of the pH variations should be kept in the right perspective. It is not expected that a pH as high as 9 or 10 will remove amines (organic compounds) from acidic surfaces of aggregates, neither affecting hydrated lime (Little and Jones, 2003). It was further stated by Little and Jones (2003) that pH values more than 10 were generally not developed in asphalt mixes, unless lime was added. Moreover, pH values below 4, which can dislodge amines from the surface of an aggregate is able to dissolve lime based on the selection of the acid; however in hot mix asphalt, the low specified pH values are not found.

Tarrer (1996) concluded in his assessment of chemical additive on moisture damage that chemical bonds formed with liquid anti-strip additives (ASA's) were weak and susceptible to shifts in pH. Moreover, it was also noted that hydrated lime or lime added as calcium hydroxide had a good performance at all pH levels (pH 3-pH 11). According to Kiggundu and Roberts (1988), the wetting characteristics of the interface region was affected due to pH of contacting water enabling the change of the pH value of the contacting water. Yoon and Tarrer (1988) assessed moisture damage by the boiling test subjected to various pH values. Significant effects on stripping were observed due to variations in the pH of the water. It was noted therein that stripping became more severe

for crushed chert gravel at a pH range of 3.0 to 13.0, depicted in Figure 2-1. Anti-stripping additives were also subjected to the boiling test at various pH values with granite as the aggregate. The pH values were found also to affect the coating retention of the aggregate. This result can also be seen in Figure 2-2.

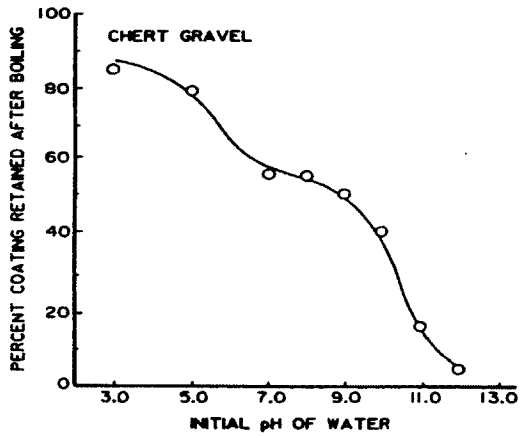

Figure 2-1: Effect of pH of water used in the boiling water test on chert gravel (Yoon and Tarrer, 1988).

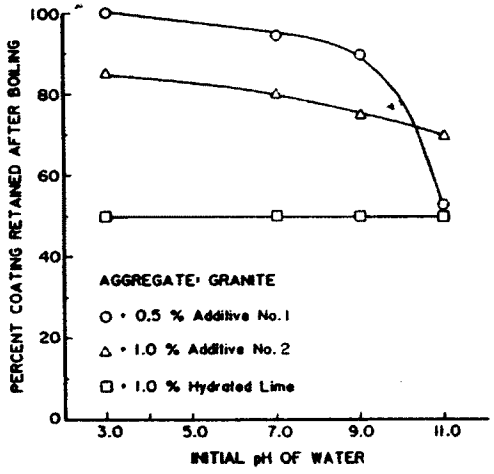

Figure 2-2: Effect of pH of water used in the boiling water test when using additive (Yoon and Tarrer, 1988).

However, hydrated lime performed relatively well as opposed to the other anti-strip additives. Yoon and Tarrer (1988) assessed the changes of the pH values of water with the addition of various aggregate powders. They observed that two aggregates, dolomite and limestone (basic aggregates), enabled the pH of the contacting water to rise to a relatively high pH value. Moreover, the effect of pH on moisture damage had not been an established mechanism. Additionally, Kiggundu and Roberts (1988) asserted that this suggested mechanism was under continuous investigation in an effort to improve its definition, its implication to aggregate surface properties, and the performance of hot mix asphalt.

2.1.3.3 Interfacial pulling

It has been observed in the literature that asphalt or bitumen spreads at the air/water interface (Fromm, 1974; Thelen, 1958; Lelinki et al., 2004). Although Fromm (1974) proposed that apart from spontaneous emulsification, another possible moisture damage mechanism was rupture of the film by interfacial tension (pull-back) at the three phase air/water/asphalt interface, little attention has been given to this process as a moisture damage mechanism. In regards to pulling and breaking of the asphalt film at the air/water/asphalt interface, Fromm (1974) concluded that no technique was found to avert the occurrence. The phenomena of air bubble bitumen attachment have been and continue to be a source of great interest in North America in particular the floatation industry, in which bitumen liberation has been studied extensively (Czarnecki et al., 2005; Drelich,1993). In the process of spreading the oil or bitumen tends to dewet the substrate while it wets the air/water surface in water submerged condition. In water, in the presence of an air bubble, it was observed that at the asphalt vapor interface dewetting took place

under the bubble cap. It is a strong possibility that at the air/water/asphalt interface in asphalt pavements dewetting takes place due to the numerous air voids of which the asphalt mix is composed. In investigating the influence of the gas-water interface in relation to the transport of colloidal particles through porous media, Wan and Wilson (1992) observed that the motion of the gas/water interface stripped particles successfully from the solid surfaces moving them along. Concerning air generation in subsurface environments, Wan and Wilson (1992) highlighted that in the saturated zone, the formation of gas bubbles may be formed by various processes such as entrapment of air as the water table fluctuates, organic and biogenic activities or gas emanating from the solution as the aqueous phase pressure drops. Moreover, due to the compacted air voids present in asphaltic pavements, it would seem that based on Wan and Wilson (1992), even pavements in saturated conditions have a very high probability of generating air bubbles, aiding in moisture damage of the asphaltic binder and the overall integrity of the pavement.

2.1.3.4 Diffusion

Diffusion is the process by which matter is transported from one part of a system to another as a result of random molecular motions (Crank, 1975). There are many factors that affect transport in polymer systems which can also be extended to other systems and materials as well. These factors include the nature of the polymer, the nature of the cross links, effect of plasticizers, the nature of the penetrant, fillers and that of temperature. George et al. (2000) emphasized that the nature of the polymer is of vital importance, noting that the transport behavior for a given penetrant varies from one polymer to another, with the transport properties being a function of free volume within the polymer

and also the segmental mobility of the polymer chains while the glass transition temperature has a significant influence on transport properties (George et al., 2000; Feng, 2001). Substituents being bulky or polar, on the polymer chains, also influence the transport process.

In relation to moisture damage in hot mix asphalt, diffusion has further been proposed as a contributing mechanism by many researchers in the field. Many studies to assess the vapor diffusion coefficient of asphalt materials have been undertaken. Arambula et al. (2010) utilized Fick's first law of diffusion to estimate the diffusivity coefficient of fine aggregate mixtures (FAM) and hot mix asphalt (HMA). The aggregates used in the FAM were that of limestone and sandstone with the binder type PG 70-22 (PG-Performance Graded). The aggregate fraction utilized for the fine aggregate mixtures pass through No. 4 sieve. These specimens were 70 mm in diameter and that of 4-5 mm thick. Moreover, for the HMA, 70 mm diameter was employed with the thickness varying from 6-7 mm. The specimen were sealed inside a container via a rubber washer and caulk seal, with the cylindrical container having a capacity of 118 mL and 60 mm in diameter opening. In conducting the experiment, initial weights of ensembles were taken, initial mass M_0 and all samples were placed in a controlled chamber for 40 days at 35°C and relative humidity, (RH) of 15%. The mass was assessed daily. The graph for periodic ratio to initial aging vs. time taken was plotted and reflected a downward linear relation. Generally, from the results (Arambula et al., 2010), the average effective coefficient of diffusion D_{eff} (mm^2/h) was found to be higher for HMA mixtures tested than that of FAM with values of 23.70×10^{-1} and 9.16×10^{-1}, respectively. Numerical simulation in the FAM was additionally conducted by the

researchers. Table 2-2 shows the approximate effective diffusion coefficients including those for aggregates as well.

Table 2-2: Mass evaporation rate, molar flux, and effective diffusion coefficients (Arumbula et al., 2010).

Material Type	Sample id	Mass evaporation rate W_{H2O}/dt ($x10^{-5}$ g/h)	Molar flux $\langle J \rangle$($x\ 10^{-9}$ g/mm^2-h)	Effective diffusion coefficient D_{eff} (mm^2/h)
Limestone aggregate	L2-2	1.22	4.33	9.02×10^{-1}
	L2-6	1 17	4.15	8.63×10^{-1}
	Average	.20	4.24	8.82×10^{-1}
Sandstone aggregate	S1-18	2.00	7.08	6.31×10^{-1}
	S1-19	1.82	6.44	5.74×10^{-1}
	Average	1.91	6.76	6.03×10^{-1}
FAM	FM-2	1.76	6.22	9.25×10^{-1}
	FM-3	1.92	6.78	9.07×10^{-1}
	Average	1.84	6.50	9.16×10^{-1}
HMA mixture	AM-1	4.02	14.22	25.40×10^{-1}
	AM-3	3.22	11.40	22.00×10^{-1}
	Average	3.62	12.81	23.70×10^{-1}
Sealed plastic containers	W-1	0.14	0.49	1.45×10^{-2a}
	W-2	0.12	0.44	1.31×10^{-2a}
	Average	0.13	0.46	1.38×10^{-2}

[a]Assuming a container of L = 1 mm.

Kasem et al. (2009) determined diffusion coefficient for asphalt mixtures being compacted to 7% air voids (air voids in the asphalt mix). In evaluating the moisture coefficient with the percent air void and air void sizes, Kasem et al. (2009) found a better correlation with connected air voids than that of total percent air voids. To investigate the internal structure of the asphalt mixture samples, Kasem et al. utilized X-ray CT. Vasconcelos (2010) also conducted diffusion studies on asphalt binder in which the film thickness varied from 0.66 to 1.5 μm. As a substrate, the MultiBounce ATR ZnSE (Zinc

Silenide) was used. The Fourier Transform Infrared-Attenuated Total Reflectance (FTIR-ATR) method was employed for this study. Moreover, the tests were conducted on four asphalts, namely, PG 58-22 AAB, PG 58-22 AAD, PG 64-10 AAF, and PG 58-10 ABD. From the results it was observed that the average diffusivity values for PG 58-22 set of samples was higher (9.39 nm^2/s) than that of PG64-10 binder (0.96 nm^2/s). Using a similar technique of the FTIR-ATR/MIR-(Multiple Internal Reflection), Nguyen et al. (1996) assessed moisture transport in asphalt films to that of a model siliceous aggregate. The substrate utilized was that on a hydrated, SiO_2 – covered Si IRE (Internal Reflection Element) representative of the model for siliceous aggregate. The results showed that the thickness of the water layer at the asphalt aggregate siliceous substrate varied for the five asphaltic materials that were used, with thicknesses including 91.2 nm. The asphalt films prepared were approximately 60 μm ± 10 and 63 μm ± 10 at other instances. It was also noted that apart from the asphalt (AAD) that did not absorb water after 50 h, the balance of the asphalt specimens continued to absorb water for more than 100 h. Nguyen et al. (1996) asserted that based on the results of the investigation, that diffusion is not uniform, but the transport process is governed by pores in the asphalt, opened as water dissolves these areas occupied by the hydrophilic area within the asphalt. Additionally, the researchers found evidence of varying water film thicknesses collected at the interface to the asphalt film thickness, noting water present at the interface of the films, but lesser amount than that of thicker films.

However, Thelen (1958) underscored that the diffusion of water through asphalt is a very slow process, and therefore, it is not expected to be a significant cause of water damage such as stripping and blistering. According to Thelen (1958), Beckman et al.

(1941), reported that instead of diffusion, it was the discontinuities in the asphalt film that are the most likely means of ingress of water.

2.1.3.5 Osmosis

Osmosis was also cited as another possible moisture damage process. Materials such as salts at the substrate surface, which are water soluble, have a tendency to attract water molecules forming more dilute solutions (Thelen, 1958).

2.1.4 Theories Relating to Moisture Damage

Due to the many factors that affect the failure of binder adhesion to the aggregate surface, many theories have been put forward to describe the process. These theories will be investigated briefly and include Mechanical Theory, Chemical Reaction Theory, Molecular Orientation Theory, and the Surface Energy Theory (Hicks, 1991; Little and Jones, 2003; Kiggundu and Roberts, 1988; Rice, 1959).

A single theory does not describe adhesion, and there is a strong possibility that a combination of mechanisms occur synergistically to produce adhesion (Little and Jones, 2003). Hicks (1991) agrees that under each theory, adhesion is partially explained.

2.1.4.1 Mechanical theory

This theory is based on the assumption that the binder is forced into the irregularities of the aggregate surface, whereby a mechanical interlock is produced. (Hicks, 1991; Caro et al., 2008). Kiggundu and Roberts (1988) added that the strength of the bond is assumed to be derived from the cohesion in the binder and the interlocking properties of the aggregate particles including the individual crystal faces, the porosity of the aggregate, absorption, surface coating and angularity. In the event that a robust interlocking network of the aforementioned properties is absent, their absence is assumed

to render the system, hot mix asphalt, to the deleterious effects of water (Kiggundu and Roberts, 1988).

2.1.4.2 Chemical reaction theory

According to Caro et al. (2008), this theory relates that the bond of adhesion between the asphalt binder and the aggregate results from a chemical reaction between these two materials. The claim of this theory is due to acidic and basic components being present in each asphalt-aggregate system and that the respective components yield an end result of water-soluble compounds based on their reaction (Kiggundu and Robberts, 1988). Moreover, the bonding between these two materials due to their surface free energy (to be discussed later) or that of their electrostatic interactions also relies on the chemical nature of the materials (Bhasin et al., 2007). Additionally, Yoon and Tarrer (1988) observed that the chemical and electrochemical properties of the aggregate surface under the influence of water had a significant effect on stripping. Curtis et al. (1993) concluded that the composition and surface chemistry of the aggregate strongly influences asphalt aggregate interactions and that for active sites (those sites containing metals or charges species) on the aggregate surface, the polar functional groups from asphalt compounds are highly competitive for these sites. Curtis et al. (1993) also noted that some of these polar compounds that adhere competitively to the surface of the aggregate are highly vulnerable to water and can be easily removed from the aggregate surface. Changes in pH, Curtis et al. (1993) continued, mainly very basic pH, can be detrimental to the asphalt-aggregate bond.

2.1.4.3 Molecular orientation theory

According to this theory, when asphalt cement and aggregate make contact with each other, the molecules present in the asphalt orient themselves in order to satisfy the energy demands of the aggregates (Hicks, 1991), whereupon the molecules specifically seat themselves according to the polarization of the aggregate ions. In the direction of polarization of the aggregate ions is where the asphalt cement may orient themselves (Hicks, 1991). Hicks (1991) further noted that water molecules are dipolar as opposed to asphalt molecules being generally nonpolar though containing some polar components. Therefore, due to the water molecules being more polar, they can more effortlessly satisfy the energy demands of the surface of the aggregate. Kiggundu and Roberts (1988) and Rice (1958) classified the molecular orientation theory together with the surface energy theory. Little and Jones (2003) expounded that the two are coupled as both are part of a theory that reflects structuring of the asphalt molecules at the asphalt-aggregate interface made upon the assumption that asphalt aggregate adhesion is facilitated by a surface energy reduction at the surface of the aggregate when asphalt is adsorbed to the surface.

2.1.4.4 Surface energy theory

Extensive research has been performed on the investigation of this theory. Surface free energy (SFE) measured in ergs/cm^2, is defined as the amount of external work done on a material in order to facilitate the creation of a new unit of surface area in a vacuum. Surface free energies of a material comprises of polar and apolar components. Accordingly, the equations by Fowkes (1983), van Oss et. al (1987), and van Oss (1994)

states these polar and apolar components of the free energies of the interfacial interaction are additive (Equations 2-1 and 2-2).

$$\Delta G = \Delta G^{LW} + \Delta G^{AB}$$

$$\Delta G_{ii} \equiv -2\gamma_i \qquad \textbf{Eq. 2-1}$$

$$\gamma_i = \gamma_i^{LW} + \gamma_i^{AB} \qquad \textbf{Eq. 2-2}$$

$$\gamma_i^{AB} \equiv 2\sqrt{\gamma_i^+ \gamma_i^-}$$

Where, γ_i = SFE of the solid or liquid,

γ_i^{LW} = Lifshitz-van der Waals component of the surface free energy

γ_i^{AB} = Lewis acid-base interactions

γ_i^+ = Electron-acceptor parameter

γ_i^- = Electron-donor parameter of substance, i.

In some literature, γ_i^+ is called the Lewis acid component of surface interaction and γ_i^- is called the Lewis base component of surface interactions (Wasiuddin et al., 2008; Cheng, 2002). Surface free energy of solids cannot be calculated directly and as a result in calculating the surface free energy components of asphalt binders, the Young-Dupré (van Oss, 1994) equation (Equation 2-3) is used which is given below:

$$(1 + cos\theta)\gamma_L = 2\left(\sqrt{\gamma_S^{LW}\gamma_L^{LW}} + \sqrt{\gamma_S^+\gamma_L^-}\sqrt{\gamma_S^-\gamma_L^+}\right)$$

$$\gamma_L = \gamma^{LW} + 2\sqrt{\gamma_L^+\gamma_L^-} \qquad \textbf{Eq. 2-3}$$

where,

γ_L= total surface free energy

$\gamma_S^{LW}, \gamma_S^+, \gamma_S^-$ = surface free energy components of the solid (asphalt)

$\gamma_L^{LW}, \gamma_L^+, \gamma_L^-$ = surface free energy components of the liquid

θ = contact angle

γ_L= total surface free energy.

A minimum of three liquids called probe liquids are used to determine the three unknowns, $\gamma_S^{LW}, \gamma_S^+, \gamma_S^-$ where the contact angles of these liquids are measured and their surface free energies are known. In conducting research on surface free energy components of asphalt, Cheng (2002) utilized glycerol, formamide, and distilled water as the solvents due to their relatively large surface energies, immiscibility with asphalt, and differing surface energy components.

The interaction of two materials 1 and 2 and the presence of a third liquid can be assessed. In that case, that would be the surface free energy of asphalt and aggregate in the presence of water. Equation 2-4 is given (van Oss, 1994):

$$\Delta G_{132} = 2\left[\sqrt{\gamma_1^{LW}\gamma_3^{LW}} + \sqrt{\gamma_2^{LW}\gamma_3^{LW}} - \sqrt{\gamma_1^{LW}\gamma_2^{LW}} - \gamma_3^{LW} + \sqrt{\gamma_3^+}\left(\sqrt{\gamma_1^-} + \sqrt{\gamma_2^-} - \sqrt{\gamma_3^-}\right) + \gamma_3^-\left(\gamma_1^+ + \gamma_2^+ - \gamma_3^+\right) - \sqrt{\gamma_1^+\gamma_2^-} - \sqrt{\gamma_1^-\gamma_2^+}\right] \quad \textbf{Eq. 2-4}$$

where,

$\gamma_1^{LW}, \gamma_1^-, \gamma_1^+$ = surface free energy components of asphalt

$\gamma_2^{LW}, \gamma_2^-, \gamma_2^+$ = surface free energy components of aggregates

$\gamma_3^{LW}, \gamma_3^+, \gamma_3^-$ = surface free energy components of water.

This equation was utilized by Wasiuddin (2007) and Cheng (2002) in assessing the surface free energy of asphalt and aggregate in the presence of water. Cheng (2002) assessed asphalt and aggregates as they pertain to moisture damage by the use of the

surface free energy method. The Wilhelmy plate was utilized to measure the surface free energy of asphalt while for aggregates, the sorption method was used. It was concluded that the surface free energy of high cure rubber asphalt was reduced as a result of aging for both wetting and dewetting modes. Cheng (2002) also related that due to the assessment of adhesion, the surface free energy method can help with the selection of compatible asphalt-aggregate combination to ensure performance. Further noted was that the fundamental parameter in fatigue and healing models developed, based on Schapery's fundamental law of fracture mechanics for materials that are viscoelastic, is from surface free energy.

Moreover, Wasiuddin (2007) assessed the effect of additives on surface free energy characteristics of aggregates and binders in hot mix asphalt. It was concluded that liquid amine anti-strip additives can significantly alter the SFE characteristics of asphalts. It was also observed by Wasiuddin (2007) that the SFE characteristics of asphalt binders with liquid anti-strip additives were altered by aging of asphalts. Bhasin and Little (2007), found that the dispersive and base components of the surface energy of aggregates play a very important role in adhesion with bitumen. Wei et al. (2010) concluded that after adding wax to asphalt (Sasobit®), the wax increased the hydrophobicity of asphalt binders and reduced their surface free energy and the wettability of asphalts on aggregate surface may also be increased. Moreover, Hefer et al. (2006) in assessing bitumen surface energy characterization by the approach of the use of the contact angle, concluded that the components of surface energy of various bitumen evaluated with this method are consistent with the chemical characteristic, weak acid and weak base of the bitumen. Additionally, Hefer et al. (2006) noted that the calculation of

polar components from the advancing plate angle were more representative of the true polar component values. The advancing plate angle values, they believed, was due to the reasonableness of the results for the high acid and base component values and that the receding angle measurement may be affected by the probe-liquid interfacial interactions.

More recently, a study was conducted by Nejad et al. (2013) with the use of the surface free energy method in evaluating the effect of hydrated lime on moisture damage in hot mix asphalt. The aggregates used in this study were limestone and granite. It was concluded that hydrated lime increased the base SFE while it reduced the SFE acid component of both aggregates and that these changes significantly improved the adhesion between the acidic aggregate and asphalt binder that is more prone to moisture damage. In an almost similar conclusion but different treatment on the aggregates, Arabani and Habani (2011) concluded that PE (polyethylene) treatment reduced the acid SFE while it increased the base SFE of all the aggregates used in the study (limestone, granite, and quartzite), thereby supporting adhesion. Some of the methods that are utilized in assessing the surface and interfacial tensions are: the Drop-weight method, the Ring method, the Wilhelmy plate method, and the Pendant drop method (Davies et al., 1961) which are expounded upon by the authors.

Moreover, surface energy is related to the wetting ability of the asphalt cement when making contact with the aggregate surface. Figure 2-3 illustrates the concept of interfacial tension and is given by the Equation 2-5 (DiBenedetto, 1970):

$$\gamma_{SV} = \gamma_{SL} + \gamma_{LV}\text{Cos}\,\theta \text{ (at equilibrium)} \qquad \textbf{Eq. 2-5}$$

where, γ is the interfacial tension measured in ergs/cm^2

SV= solid vapor interface

LV= liquid vapor interface

SL= solid liquid interface

$\text{Cos } \theta = (\gamma_{SV} - \gamma_{SL}) / \gamma_{LV}$.

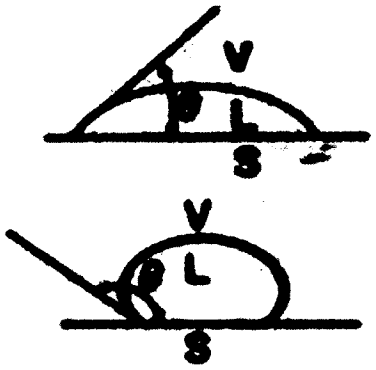

Figure 2-3: Fluid drop resting on a solid surface (Dibenedetto, 1970).

The units of interfacial tension are measured in the unit ergs/cm^2. This phenomenon is explained according to DiBenedetto (1970). Good wetting is denoted by a small contact angle while poor wetting is reflected in a large contact angle. Equation 2-5 places the limits when absolutely no wetting takes place and for spontaneous wetting. When $\gamma_{SV} \geq \gamma_{LV} + \gamma_{SL}$, θ will equal zero giving rise to spontaneous wetting. If, however, $\gamma_{SL} \geq \gamma_{SV} + \gamma_{SL}$, θ will equal 180 degrees, meaning that it is not possible for the liquid (L) to wet the solid layer (S). It is important to note that wetting is favored when there is no contamination of the substrate (γ_{SV} is maximum), when the affinity for the substrate is favored (γ_{SL} is low), producing low interfacial tension, or when the adhesive has a low surface tension (γ_{LV} is low). Moreover, surface roughness modifies wetting characteristics due to the fact that the fluid must move up and over asperities. When

spreading occurs on the rising side of an asperity, wetting may be hindered, but is likely to be aided on the falling side.

2.1.5 Moisture Susceptibility Test

Many tests have been developed and are available to evaluate the stripping potential or moisture damage of asphalt mixes. It is worth noting that the development of these tests have had their origins as far back as the 1930's (Hicks, 1991).The tests that have been developed can be subjected to two main categories, namely, qualitative and quantitative (Solaimanian et al., 2003).The tests that have gained wide acceptance in industry and academia will now be surveyed (Hicks, 1991).

2.1.5.1 AASHTO T 283-07 Resistance of compacted hot mix asphalt (HMA) to moisture induced damage

Currently, the Superpave system recommends this test method as the standard test. This test is normally called the "modified Lottman test". In determining HMA moisture susceptibility, this test is one of the most commonly used (Solaimanian et al., 2003). At least six samples are produced, half to be conditioned and the other half to be tested dry. Typically, the specimens measure 4 in. in diameter by 2.5 in. in height and are compacted to 7.0 ± 0.5% air voids. The dry specimens are stored at room temperature, and before testing they are wrapped with leak proof plastic bag and placed in a water bath at 25 ± 0.5°C (77 ± 1°F) for approximately 2 h. The conditioned samples are subjected to a vacuum of 10 to 26 in. Hg partial pressure for approximately 5 to 10 min. The degree of saturation is then determined where the degree of saturation should be between 70 and 80%. The specimens are then wrapped in a plastic bag with 10 ± 0.5 mL of water and placed in a freezer at a temperature of -18 ± 3°C (0 ± 5°F) for a minimum of 16 h. The specimens are then placed in a submerged water bath at 60 ± 1°C for approximately 24 h.

The specimens are further conditioned in a water bath at 25 ± 1°C (77 ± 1°F) for approximately 2 h. The tensile strength of both dry and wet condition specimens are determined by Equation 2-6:

$$S_t = \frac{2000\,P}{\pi\,t\,D} \qquad \textbf{Eq. 2-6}$$

where:

S_t = tensile strength, kPa

P = maximum load, N

t = specimen thickness, mm

D = specimen diameter, mm.

The numerical index of resistance of HMA (Hot Mix Asphalt) is expressed in terms of the Tensile Strength Ratio or TSR:

$$TSR = \frac{S_2}{S_1} \qquad \textbf{Eq. 2-7}$$

where:

S_1 = average tensile strength of the dry subset, kPa (psi); and

S_2 = average tensile strength of the conditioned subset, kPa (psi).

Based on an earlier AASHTO T 283 version, Hicks (1991) relates that a retained TSR ratio of 70 percent is recommended. According to Hicks (1991), some of the advantages of this test include: (1) it can be conducted on lab mixes, field mixes and core samples, (2) it is a severe test, (3) it can differentiate between additive levels, (4) it gives high correlation and (5), it does not give bias results toward additives (liquid) or lime. The disadvantages of this test are that is time consuming and that the amount and the type

of equipment required is not always readily available. Solaimanian et al. (2003) asserts that as pertains to this method, state highway agencies reported mix success. Furthermore, Kim et al. (2008) highlight that this test, along with the Hamburg and APA (Asphalt Pavement Analyzer), is limited in the ability to corroborate the mechanisms of moisture damage in hot mix asphalt due to these tests exposed to completely diverse boundary conditions, time frames and moisture infiltration modes detected in the field. Lastly, Kim et al. (2008) recommend tests that are quicker and more fundamentally sound to be developed to better estimate and predict damage associated with moisture.

The AASHTO T 283-03 test was conducted in a lab in this study with four samples: two tested dry and two conditioned with a TSR ratio of 1.06. The additive used was Perma-Tac® 99, with a PG 64-22 asphalt.

2.1.5.2 Tunnicliff and root test (ASTM D 4867) Standard test for effect of moisture on asphalt concrete paving mixtures

This test is similar to that of AASHTO T283-03. A minimum of six samples for each test both for dry and for wet condition with compacted air voids of 7 ± 1% air voids are prepared The specimens measure 4 in. in diameter and 2.5 in. in height. According to Hicks (1991), the conditioned samples are to be saturated between 55-80%. The partial vacuum is at 20 in. of Hg for about 5 min. If the degree of saturation is over 80%, the samples must be discarded. The treated samples are placed in distilled water for 24 h at 60 ± 1°C. A freeze-thaw option follows if desired by the researcher. The 24 h soak time is followed by 1 h of soak time at 25 ± 1.0°C. According to Hicks (1991), there is no conditioning before testing for the dry samples. The tensile strengths of each specimen are calculated and the tensile strength ratio of wet specimens and dry specimens are, thus, determined as a percentage. Moreover, instead of a minimum ratio a statistical student's

t-test is conducted to ascertain the desired confidence level used to determine the effectiveness of a specific additive.

According to Hicks (1991), some of the advantages of this test includes: (1) it can utilize cores from the field and that of lab, plant, or field mixes, (2) testing mixtures can be done with or without additives, (3) moderate time is required. Also, good correlations in the field have been observed. Some disadvantages include: (1) it may require trial specimens to acquire degree of saturation of air void levels and (2) it may not be a severe enough test.

2.1.5.3 Boiling water test (ASTM D3625-96) Standard practice for effect of water on bituminous-coated aggregate using boiling water

This test is conducted on loose asphalt mixes. Approximately 250 g (1/2 lb) of bituminous coated aggregate is placed in boiling distilled water of a 1000-2000 mL container approximately half full. The water is to be brought back to boiling and boiling should be maintained for 10 min ± 15 s. Excessive manipulation of the bituminous-coated aggregate mixture is to be avoided. After the test, the container is removed from the heat source, and to prevent recoating, free bitumen from the surface of the water is to be skimmed. The water is cooled to room temperature, decanted and emptied onto a white paper towel for observation of retained coating. According to Hicks (1991) if there is less than 95% of mixture remaining, then there is an indication that moisture susceptible problem is evident. The advantages of this test include: (1) it can be utilized for initial screening; (2) a minimum amount of equipment is required, (3) it tests the effectiveness of additives and (4) it may be used for quality control. The disadvantages are: (1) un-compacted mix; (2) subjective analysis; (3) the coating retention is affected by water

polarity; (4) does not coincide with field experience and (5) highly dependent on asphalt viscosity (Hicks, 1991).

2.1.5.4 Freeze thaw pedestal

As a modification of the water susceptibility test procedure proposed by Plancher et al. (1980) at the Western Research Institute, the Texas-freeze thaw pedestal test was proposed (Solaimanian et al., 2003; Kennedy et al., 1982). The particulars of the test based on Solaimanian et al. (2003), Kennedy et al. (1982) is given. The test makes use of uniform-sized aggregate. It is prepared of the hot mix based on aggregate passing No. 20 (0.85 mm) and retained on No. 35 (0.50 mm) sieve and asphalt at 150°C temperature. To preserve uniformity of temperature the mixed is kept in the oven at 150°C at 2 h being stirred every hour. The mix is then removed from the oven after 2 h elapse, left to cool at room temperature, reheated to 150°C and afterwards compacted to an approximate load of 28 kN for 15 min in order to form a briquette 41 mm in diameter measuring 19 mm in height. Further, after the briquette is cured for 3 days at room temperature, it is placed on a pedestal submerged in a covered jar of distilled water. Next, it is subjected to 15 h at -12°C of thermal cycling, which is followed by 9 h at 49°C. At the completion of each cycle, the briquette surface is checked assessed for cracking. A measure of the water susceptibility is determined by the number of cycles required to induce cracking which is approximately 10 freeze-thaw cycles. In terms of advantages, this test carries none as it is used primarily for research (Hicks 1991). Some disadvantages extracted from Hicks (1991) include: (1) uses only a small amount of the mix, where the void content is not known, (2) the correlation between the field and lab results are only fair, and (3) requires special equipment.

2.1.5.5 Lottman indirect tension test

This test is based on Lottman (1978) where the report was prepared for National Cooperative Highway Research Program (NCHRP). The tests are conducted on laboratory specimens measuring 4 in. in diameter by 2.5 in. thick or high. The test specimens are divided into three sets (3 samples each). The first set is not conditioned. Before testing the first set is placed in metallic jars and submerged in water bath for 5 hours at 55 ± 1.8°F or 73 ± 1.8°F with the top lid being above the water surface. Sets 2 and 3 are vacuum saturated at 26 in. of mercury for approximately 30 min then at atmospheric pressure for 30 min. The second set is vacuum saturated. Set 2 is immersed in water bath at 55 ± 1.8°F or 73 ± 1.8°F for 3 h before testing. Set 3 is frozen for 15 h at -0.4 ± 3.6°F, followed by a water bath of 24 h at 140 ± 3.6°F. Moreover, the specimens are submerged in water at a temperature of 55 ± 1.8°F or 73 ± 1.8°F for 3 h then tested. This is considered accelerated conditioning procedure. In an effort to assess moisture damage, tensile strength ratios are calculated (deformation rate of 0.065 in per min. at 55 ± 1.8°F) and that of the resilient modulus.

Some of the advantages of this test include (Hicks 1991): (1) It can be conducted on lab mixes, field mixes and core samples, (2) it is a severe test,(3) it can differentiate between additive levels, (4) gives high correlation and (5), does not give bias results toward additives (liquid) or lime. One of the disadvantages of this test is that is time consuming.

2.1.5.6 Immersion compression test (AASTO T165-86) Effect of water on cohesion of compacted bituminous mixtures

At least 6 cylindrical specimens are used for this test each measuring 4 x 4 inches. The specimens are divided into two groups, 3 specimens each. Group 1 is tested at

25 ± 1°C to determine their compressive strengths. Group 2 specimens are submerged in water for 4 days at 49 ± 1°C then are transferred to another water bath which is maintained at 25 ± 1°C after which they are tested for their compressive strengths. There is an alternate procedure for group 2 where the test specimens are submerged in water at 60 ± 1°C for 24 hours then transferred to a water bath at 25 ± 1°C for 2 h. The compressive strength of the specimens are then determined. A ratio as the index of retained strength is then calculated as a percentage with compressive strength of conditioned to that of unconditioned specimens. A 70% ratio as the passing limit is utilized by most agencies (Solaimanian et al., 2003). Some disadvantages of this test given by Hicks (1991) are: (1) it is time consuming, (2) poor reproducibility, (3) a significant role is played by the air void level, (4) water type (ions and salt) can affect the moisture sensitivity, (5) equipment may not be available readily. It utilizes the actual mix which is an advantage.

2.1.5.7 Static immersion test (AASTO T182)

According to Solaimanian et al. (2003), before being cured to room temperature, the asphalt-aggregate mixture is cured for 2 h at a temperature of 60°C. Next, it is placed in a glass jar and is covered with distilled water measuring 600 mL. The samples in the jar, the jar being capped, are immersed in a water bath at 25°C and for 16 to 18 h. An established criteria of 95% is used to assess the total visible area of the aggregate being either less than or greater than that number. Solaimanian et al. (2003) further asserts that this a major test limitation as the test results are decided solely on the basis of a subjective estimate of greater than or less than the 95% mark. It was noted also that when

samples are placed at 60°C bath instead of the 25°C for 18 h, the amount of coating is reduced.

2.1.5.8 Rolling bottle test

Isacsson and Jorgensen of Sweden (1987) develop this test (Solaimanian et al., 2003). Coated binder with aggregate chips is covered with water in glass jars. In order that the contents of the glass be agitated, the jars are rotated. Visually, the coating of the stones is estimated periodically.

2.1.5.9 Hamburg wheel tracking device (Tex-242-F)

This test method is used to determine the premature failure susceptibility of bituminous mixtures based on the weakness in the aggregate structure, inadequate binder stiffness or moisture damage and other factors which include inadequate adhesion between the asphalt binder and aggregate. It measures rut depth and a number of passes to failure (Tex-242-F). The test apparatus consists of reciprocating steel wheels with a diameter of 8 in. (203 mm) and a width of 1.85 in. (47 mm). The load applied to the wheel is 158 ± 5 lbs (705 ± 22 N) and must be capable of completing 50 ± 2 passes across the test specimen per min. The test specimens are tested in a water bath at a temperature range of 77-158°F (25-70°C), where the cylindrical test specimens measure 6 in. (150 mm) in diameter and a height of 2.4 ± 10.1 in. (62 ± 2 mm). Typical length of slabs are 12.6 in. (320 mm) and 10.24 in. (260 mm) wide and they can range at 1.5, 3, or 4.7 in. (38,76, or 119 mm, respectively) in thickness (Yildirim et al., 2007). The measurement system houses a linear variable differential transformer (LVDT) which is capable of measuring the rut depth within 0.0004 in. (0.01 mm) over a minimum range of 0.8 in. (20 mm). According to (Yildirim et al., 2007) for 20 000 wheel passes

approximately 6.5 h are needed, noting that the devise will automatically stop if the deformation in the slab was to exceed a measure of 30 mm. It was observed that the total time needed to perform such a test from beginning to the end, including the fabrication of the specimen was three days.

The results obtained from the hamburg wheel tracking device (HWTD) consists of rut depth, post-compaction, creep slope, stripping inflection point (SIP), and stripping slope are expanded upon below (Yildirim et al., 2007):

Post compaction consolidation

The post compaction consolidation is the deformation recorded in mm at 1000 wheel passes which occurs rapidly within the first few minutes of the test. As it is assumed that the wheel is densifying the mixture within the first 1000 wheel passes, the test is thereby referred to as post-compaction consolidation.

Creep slope

The creep slope is a measure of the susceptibility of rutting, and is the inverse of the deformation rate that is within the linear region of the deformation curve after post compaction and prior to stripping, if stripping takes place. The creep slope also measures the accumulation of permanent deformation primarily as a result of a mechanism other than moisture damage.

Stripping Slope

The stripping slope is the inverse of the deformation rate within the linear deformation of the curve of deformation, after the start of stripping. Moreover, the number of wheel passes, which corresponds to the intersection of the creep slope and the stripping slope, is called the "stripping inflection point". Furthermore, the accumulation

of permanent deformation that results from moisture damage is measured by the stripping slope. Its use is to estimate the relative resistance of the HMA sample to induced-moisture damage.

It was also reported that less damage was indicated by higher creep slopes, stripping points, and stripping slopes as both creep and stripping slopes utilized inverse slopes, whereby these slopes could be reported together with the number of wheel passess at the stripping inflection point.

In a typical Hamburg wheel-tracking test results, Yildirim et al. (2007) noted that a final region, called the "tertiary region" is an indication of specimen failing rapidly and is primarily related to moisture damage as opposed to other mechanisms, such as viscous flow that are attributed to permanent deformation. Moreover, it was also highlighted that susceptibility of mixtures to moisture damage is indicated when they start to lose fine aggregates around the stripping inflection point.

2.1.5.10 Environmental conditioning system (ECS)

As part of Strategic Highway Research Program (SHRP), the Environmental Conditioning System (ECS) test protocol was developed at the Oregon State University (Aschenbrener al.,1994, Solaimanian et al., 2003). Based on Solaimanian et al. (2003), the test procedure follows. In this procedure, a specimen membrane-encapsulated is subjected to cycles of temperature, moisture conditioning and repeated loading. The specimen measures 102 ± 4 mm in diameter and 102 ± 4 mm in height and must have an air void content in the range of 7.5 ± 0.5%. The loose asphalt concrete mixtures are prepared according to AASHTO TP4-93, Edition 1B, and based on AASHTO PP2-94, they are short-term aged. Moreover, the short-term aged mixtures are compacted with the

utilization of an SGC per AASHTO TP4-93, and are left at room temperature overnight to cool to room temperature. A latex membrane is then placed around the specimen and sealed with a silicone sealant. The specimens are then laid aside to dry for a minimum of 15 h. After the specimen is placed inside the ECS load frame, the air permeability and the dry resilient modulus (M_R) are determined, where the air permeability is assessed by allowing air to flow through the specimen at 68 kPa vacuum level. Concerning the resilient modulus of the specimen, it is determined by the application of a load in the form of a haversine wave with a loading period of 0.1 s and a 0.9 s rest period. The specimen is then saturated by pulling de-aired distilled water through it at a vacuum level of 68 kPa. Within the next step, the water permeability of the specimen is determined. The temperature of the saturated specimen is increased to 60°C for 6 h while it is subjected to the haversine loading, termed a "hot cycle". The specimen is then cooled to room temperature of 25°C for a minimum of 2 h and at the end of the 8 h water permeability and the conditioned M_R are determined. Additionally, this procedure is repeated for two more cycles, 6 h of loading and heating at 60°C which is then followed by 2 h of cooling.

Moisture susceptibility is based on a ratio. If the ratio of the conditioned M_R to the unconditioned M_R is less than 0.70, the mixture is classified as being moisture susceptible. However, if the said ratio is greater than 0.70, the mixture is classified as being acceptable. One advantage that was noted of this test procedure was its inclusion of the influence of traffic loading and the resulting effect of the pore water pressure. Aschenbrener et al. (1994) evaluated the laboratory data with the use of the ECS and HWTD and correlated them with 20 field test sections together with other tests. Using a

minimum of 0.70 criteria, the data of the ECS-M_R was compared on a pass-fail basis with site performance in three various ways namely, High Maintenance, Complete Rehabilitation, and Disintegrator.

Aschenbrener et al. (1994) further noted that good correlation was generally detected for pavements which had good field performance categories for all the three types of correlation that was mentioned earlier. The researchers concluded that the procedure for the ECS test moisture conditions the test very mildly and that with the use of the M_R ratio that three out of a total of thirteen sites with poor performance actually failed in the lab. It was further concluded that additional research would be needed to assess the ECS test procedure's ability to predict moisture damage.

A modified test procedure was undertaken by Alam (1998) based on recommendations of Aschenbrener et al. (1994) for further research and can be found in Alam (1998).

2.1.5.11 Pneumatic adhesion tensile testing instrument (P.A.T.T.I.) testing

This test method measures pull off strength of coatings using portable adhesion testers and is found in ASTM D4541. Kanitpong (2005) modified this test procedure in assessing the moisture susceptibility of asphalt binders (cohesion and adhesion), and noted some advantages of this test to be: that aggregate surface can be utilized as the substrate, conditioning of specimen in water after the application of asphalt between pull-stub and aggregate surface, and observation of the failure surface to determine adhesive or cohesive failure. In the study, glass plate and aggregate surfaces were used. To control film thickness, Kanitpong (2005) did not use 200 μm glass beads as did Youtcheff and Aurilio (1997), but rather, metal blocks placed under the modified pull stub. Kanitpong

(2005) concluded based on the P.A.T.T.I. results, that asphalt binder composition and the composition of the aggregates significantly affected asphalt-aggregate adhesion and the measured pull-off tensile strength was able to explain the effect of moisture conditioning of the adhesive bond. Copeland (2007) also modified the test by using aggregate substrate rather than glass plate to determine the pull-strength between aggregate and asphalt in wet and dry condition. Copeland (2007) similarly concluded that both aggregate and binder type affect the pull-off tensile strength in dry condition, and that the bond strength of asphalt on aggregate decreased as a result of moisture conditioning.

2.1.5.12 Asphalt pavement analyzer (APA)

According to Skok et al. (2002), after a volumetric design, the APA permit an accelerated evaluation of rutting potential, where the typical testing time for complete rutting evaluation is approximately 135 min for 8000 cycles. By placing samples in the form of a beam or cylindrical mould subjected to repetitive wheel loads and measuring the permanent deformation, rutting susceptibility is assessed. The APA's data acquisition system displays rutting measurements in a format that is either graphic or numeric, where five measurements can be recorded in a single wheel pass. Each specimen can be subjected to a different load level that can go up to 113 kg (250 lb), which resulted in contact pressures of 1378 kPa (200 psi). In terms of testing, the three beam or six cylindrical samples in three sample molds is able to be evaluated at a controlled temperature and in dry or submerged conditions. The cylindrical samples are compacted to 4%, 7%, or other air void content, whereas, beams are compacted to 7% air voids, and allowed field samples to be evaluated. Furthermore, the test samples could be evaluated for moisture susceptibility, and asphalt concrete beams could be tested for fatigue. After

asphalt samples are placed in the testing chamber, the chamber temperature is adjusted as required by the operator from 5 to 70°C (41 to 160°F). Furthermore, the rut testing of the APA is designed to simulate actual conditions in the field by rolling a concave metal wheel over a pressurized rubber hose which measures 689 to 827 kPa (100 to 120 psi) in order to create the effect of various tire pressures. Automated or manual measuring modes can be used in the evaluation of the test. The manufacture of the APA is Pavement Technology Inc. (PTI) Covington, GA.

In evaluating granite and limestone mixes with known histories of stripping performance, West et al. (2004) concluded that the use of steel wheels for the loading of specimens was more severe than the use of air field hoses. Additionally, West et al. noted that these harsh conditions appeared to accelerate the failure of the mixture which was prone to stripping and thereby possibly help to distinguish between good and unacceptable mix performance. Moreover, West et al. (2004) maintain that based on large variations of some test results among replicates, the reproducibility and repeatability of the APA moisture test may be of concern.

2.1.6 Distresses in Pavements (Moisture Related Damage)

2.1.6.1 Stripping and raveling

As mentioned earlier, stripping and raveling are major pavement distresses that are caused by moisture damage. In asphalt concrete pavements (AC), two cases may be the media through which moisture damage takes place (Hicks, 1991). In the first instance, water can interact with the asphalt cement and, hence, cause a reduction in the cohesion with an associated reduction in the stiffness and strength of the mixture. In the second instance, water takes the place of the binder as it gets between the interfaces, breaks the

adhesive bond between the aggregate and the asphalt and detaches (strips) the asphalt from the aggregate surface. Hicks (1991) further asserted that the stripping failure takes on a two step process whereas the first stage is the stripping failure itself and second stage is induced under the influence of traffic. Three stages of stripping in pavements are shown in Figure 2-4. They are: (1) The deposition of water transported aggregate fines or dust from the partially stripped aggregates, (2) The movement of the asphalt binder to the road surface (also known as flushing), and (3) Pothole development in the flushed area.

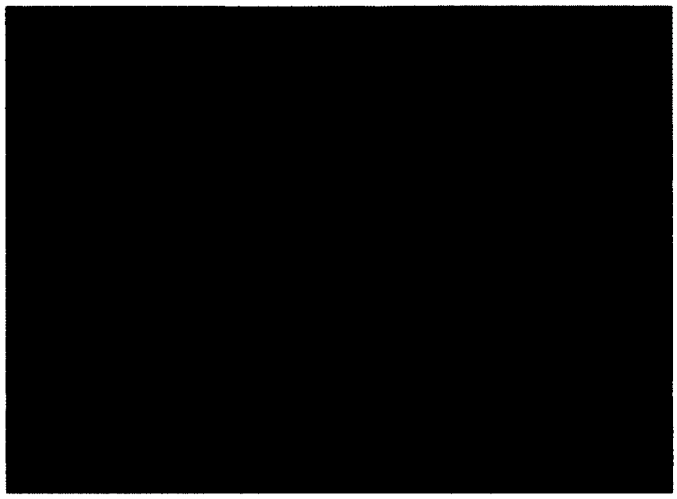

Figure 2-4: Three stages of stripping: white stains, flushing and pothole (I-40) (Kendal and Richards, 2001).

Raveling, another form of pavement distress, is associated with moisture damage. It is defined as the distress manifestation that is characterized by the dislodgement of the aggregate particles in the mixture from the pavement surface (Caro et al., 2008).

Also, the damage may be as a direct result of poor compaction, inferior aggregates, and low asphalt content, high fines content and may be further aggravated

by the action of traffic (Hicks et al., 2003). Figure 2-5 shows the different stages connected to this type of pavement distress.

Figure 2-5: Pavement distress: raveling, (a) early stages, (b) advanced stages (Hicks et al. 2003).

2.1.6.2 Bleeding or flushing

Excess bitumen, bleeding, or flushing, leaves a thin film of asphalt on the pavement surface. These two pavement failures can be as a result of improper seal coat, excess asphalt in the mix, too heavy of a prime or tack coat, or excessive sealant in the cracks or the joints under an overlay (Asphalt Handbook, 2007). The aforementioned failures can also be caused by water present in the mix (Hicks et al., 2003).

2.1.6.3 Cracking

The Asphalt Handbook (2007) relates that various types of cracking can occur in an HMA pavement and depending on the type of cracking present, the appropriate type of repair would be needed. Cracking falls into these main subgroups: alligator (fatigue), block, edge, longitudinal, reflective, and slippage. Some cracking, for instance alligator cracking, would indicate load deterioration that necessitates a different maintenance strategy than block cracking, which is normally caused by block cracking.

2.1.6.4 Rutting

A rut is a surface depression located in the wheel paths which may have transverse displacement along the rut sides. Rutting occurs as a result of consolidation or lateral movement of any of the pavement layers or that of the subgrade subjected to traffic. Furthermore, it may occur as a result of insufficient design thickness, lack of compaction, weakness in the pavement layers as a result of moisture infiltration, or weak asphalt mixtures (Asphalt Handbook 2007).

2.1.7 Additives Used in Asphalt Concrete

In an effort to minimize stripping or moisture damage of asphalt binder in the field, anti-stripping additives are employed in the asphalt mix. Moreover, there are two broad types of additives currently being used for this purpose. They are chemical additives and lime, the former being the most used.

2.1.7.1 Chemical additives

Most of the liquid anti-stripping additives are surface active agents that reduce the surface tension of the asphalt-cement interface and, therefore favor more uniform wetting on the aggregate surface (Hicks, 1991). It has also been noted that the improvement of adhesion between asphalt cement and aggregate is due to the anti-stripping agents changes and produce in the asphalt cement an electrical charge. This electric charge is most of the times opposite to that of the aggregate surface. Liquid anti-stripping agents that have the form of cationic surface-active agents, specifically amines, have been in use for many years (Curtis, 1990). In separate studies, Wasiuddin et al. (2007a; 2007b) evaluated the effects that liquid anti-strip additives have on the surface free energy to analyze moisture susceptibility in that of asphalt pavements. Thermal degradation of

liquid anti-stripping additives was also evaluated with the use of the surface free energy method. In another study, Wasiuddin et al. (2008) used the SFE (surface free energy) method to analyze the effect of liquid anti-stripping agent (Sasobit® and Asphamene) on aggregate-asphalt adhesion and reported that Sasobit improved the wettability of asphalt binders on the aggregate surface. Kanitpong and Bahia (2005), using a pneumatic adhesion tensile testing instrument reported that the adhesive property of asphalt can be altered with the influence of anti-stripping additives, but that influence does significantly alter the cohesive property of the asphalt binder.

Recently, Xiao et al. (2010) reported that the dry indirect tensile strength (ITS) of the mixtures of Warm Mix Asphalt (WMA) liquid additives were higher while that containing liquid additives were lower. Wei et al. (2010) further found that the addition of wax-based additives increased the hydrophobicity of the asphalt binders and lowered their surface free energy with the probability that doing so may increase the wettability of binders on the aggregate surfaces as observed by Wasiuddin et al. (2008). Moreover, Thelen (1958) contends that a completely effective anti-stripping agent, based on prior calculations, must be capable of chemisorption to that of the aggregate surface or to the innermost layers of the water film that are adsorbed. Moreover, a wetting agent that is not being chemisorbed but simply behaves in a manner so as to reduce the interfacial tensions between binder and water and between asphalt and stone surface, theoretically, cannot give complete resistance to stripping, although it may have a profound effect on the reduction in the stripping potential (Thelen, 1958).

Shute et al. (1989) analyzed three field sections that contained amine anti-strip additives at various percentages of 0.3%, 0.3%, and 0.5%. The third test section, although

not classified as none stripping, had the highest percentage additive of 0.5%. From a core sample of the road section with the highest additive, it was observed that the aggregate was 100% coated with a relatively thick film thickness. The thickness was based on observation and the value not given and could very well be that of a mastic film. It must be noted that in one of the sections under analysis, 0.3% additive, the core data indicated that stripping was prevalent in that project and the aggregate was observed to have an asphalt coating of about 40%, having a dry thickness of that particular asphalt film. Shute et al. (1989) also noted that field observations did not correlate well with the IRS ratio even though the ratio, in some cases, was as high as 100%. Based on their data, they noted that the IRS (AASHTO T165) does not provide a reliable indication of mixes prone to moisture susceptibility despite that of the ratio selected as that of a decision criterion.

2.1.7.2 Lime additives

In asphalt pavements, hydrated lime can reduce stripping, rutting, cracking and aging (National Lime Association, 2006). The Association relates that hydrated lime substantially improves each of the aforementioned properties when used solely and works with polymer additives in the process assisting pavement systems that will perform for many years at very high expectations. Furthermore, a study conducted by Kim et al. (2008) shows that asphalt mixes treated with hydrated lime performed better than original mixes due to the combination of effects of the hydrated lime. The two findings are: (1) the increase in the strength, stiffness and toughness of mastic that encourages better resistance of mastic against deterioration of the mastic in the presence of moisture, and (2) the enhancement of the interfacial bonding of asphalt-aggregate that gives better stripping performance. Maupin (1995) in investigating the effectiveness of anti-stripping

additives reported that hydrated lime reflected less stripping than the projects containing chemical additives. Moreover, Little and Epps (2001) noted that the most widely used anti-strip additive in the United States is hydrated lime, but noted that road contractors normally prefer liquid anti-strip additives as they are relatively easy to use.

2.1.7.3 Sasobit®

According to Hurley and Prowell (2005), there have become available new processes and products which do have the ability to reduce hot mix asphalt mixing and compaction temperature without a direct compromise of the pavement performance. Sasobit®, one of these products, is a product of Sasol Wax. Sasobit® was employed by Wasiuddin et al. (2007c) and Wasiuddin and Saltibus (2010) to assess its effect on the surface free energy of asphalt binders.

2.2 Dewetting

2.2.1 Spreading Coefficient and Wetting

Wetting is controlled by a coefficient called the "spreading coefficient". For total wetting, the spreading coefficient would have to be positive and for that of partial wetting mode, the spreading coefficient is negative. The spreading coefficient is given below:

$$S = \gamma_{SO} - (\gamma_{SL} + \gamma) \qquad \textbf{Eq. 2-8}$$

where, γ_{SO}= surface tension of the solid/air, γ_{SL}= surface tension of the solid/liquid, and γ = surface tension of the liquid/air interfaces. Moreover, it is noted that when S < 0, a film will dewet below a critical thickness, e_c(deGennes et al., 2010). This critical thickness is given by deGennes et al. (2010):

$$e_c = 2\kappa^{-1} \cdot \sin\left(\frac{\theta_E}{2}\right) \qquad \textbf{Eq. 2-9}$$

where, θ_E= equilibrium contact angle, κ^{-1} is the capillary length defined by:

$$\kappa^{-1} = \sqrt{\frac{\gamma}{\rho g}} \qquad \textbf{Eq. 2-10}$$

where, ρ = density of the liquid and g = 9.8 m/s^2, the acceleration due to gravity. The order of the capillary length is that of a millimeter. For thick micrometer films, where the long range forces can be taken as negligible, the gravity term is added. Moreover, the sum of the energies, both interfacial and that of gravitational as a function of the thickness is given by the following equation (deGennes et al., 2010):

$$F(e) = \gamma_{SL} + \gamma + \frac{1}{2}\rho g e^2 \qquad \textbf{Eq. 2-11}$$

where, ρ = density of the liquid and g = 9.8 m/s^2 as mentioned earlier.

According to Czarnecki et al. (2005), the critical film thickness also depends on the substrate's wettability, and on the initial hole size. The critical thickness is given by (Czarnecki et al. (2005) as acknowledged, it was derived by Sharma (1993):

$$\mathrm{h} = r_m ln\left(\frac{2\sin\theta}{r_m(1+\cos\theta}\sqrt{\frac{\gamma}{\rho g}}\right) \qquad \textbf{Eq. 2-12}$$

where, r_m is the minimum radius of the hole, γ is the interfacial tension of the asphalt/water interface, ρ is the density difference between water and asphalt, g is the acceleration due to gravity, and θ is the contact angle of the asphalt film on the substrate.

2.2.2 Dewetting of Films

There are many factors involved in the detachment of the binder film from the substrate or mineral surface in the presence of moisture. In order for good adhesion to take place between the binder and the substrate interface, significant wetting of the binder to the substrate must be in order, together with the surface energy properties of that substrate, mineral in our case. As in most adhesion systems, wetting affects the bond that

exists between the bitumen binder and that of the aggregate in the mix. The reverse of spreading or dewetting of a film from a substrate deserves attention as there is a loss of adhesion due to that process.

Dewetting is the opposite of the spreading of a liquid film over a substrate. Reiter (2005) defines dewetting as the drying of a substrate that has been covered with a film of liquid. Composto and Chung (2005) expounds that dewetting is the breaking up of a film in order to attain a minimum of free energy of the system as it reduce the surface or interfacial energy. Meredith et al. (2000) adds that the variables critical in determining film stability and dewetting are thickness, molecular mass, surface chemistry and temperature. The dewetting of a thin film is also that of a complex phenomenon that have been gaining a lot of research interest, particularly in the industrial engineering field (Reiter, 2013; Bertrand et al. 2010).

2.2.3 Types of Dewetting

There are many types of dewetting in the literature. Generally, the main types are called "Spinodal dewetting" and "Nucleated dewetting" (de Gennes, 2010). These types are explored and briefly discussed.

2.2.3.1 Nucleation and growth or nucleated dewetting

Nucleated dewetting as defined by Lorenz-Haas (2002), is an instability of an original continuous film which normally occurs as a result of impurities inside the film. These defects may also include dust particles on the surface of the film. In thicker films that are in the microscopic range, gravity is taken into consideration. After the formation of the holes, they grow in size and a receding rim forms at the edge of the hole (Lee et al., 2004). Redon et al. (1991) was one of the first to study this concept of dewetting in depth.

Figure 2-6 shows a cross section of a hole as it dewets, where, l(t) is the length of the ridge or rim, R(t) is the growth of the hole radius with respect to time, θ_d is the dynamic contact angle, e, is the film thickness.

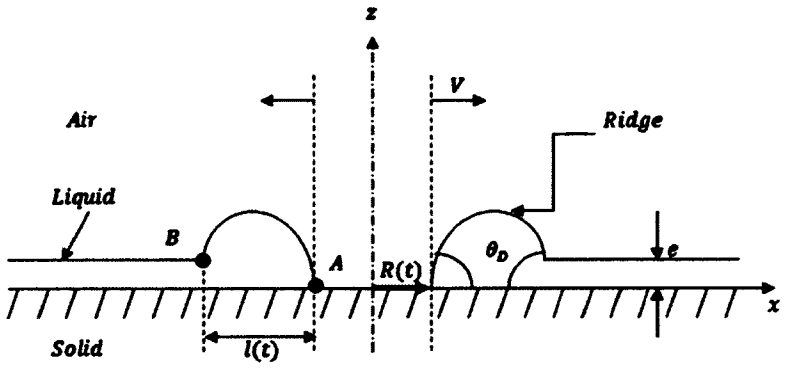

Figure 2-6: Schematic diagram of a film's profile during dewetting. A circular ridge is bounded by the contact line A, which recedes on the dry solid, and by point B, which advances on the wet solid. ©Springer, Capillarity and Wetting Phenomena, 2010, 163, Dewetting, de Gennes et al.7.6.,with kind permission from Springer Science and Business Media.

In the dewetting literature, films are classified as unstable, metastable, and stable. Moreover, according to de Gennes et al. (2010), in the case of thick films, where gravity dominates, the curvature of F(e) is positive, (F''(e) >0) and the film is metastable. Drying will require the nucleation of a dry zone, and will, therefore, expand on the basis that its radius exceeds a critical value $R_c \approx e$.

2.2.3.2 Spinodal dewetting or decomposition

Spinodal dewetting is the process which a film dewets according to spinodal decomposition, where holes breakup at the same time, their average distance being given by the wavelength of the node which dominates (Lorenz-Haas et al., 2002). In the analysis of thin films typically ($e << 1\mu m$), gravity is not considered (de Gennes et

al., 2010), e, representing the thickness of the film. Therefore, it is considered that long range forces between the liquid and substrate does the dominating. This concept is shown in Equation 2.5 de Gennes et al. (2010), thus:

$$F(e) = \gamma_{SL} + \gamma + P(e) \qquad \textbf{Eq. 2-13}$$

where, $P(e)$ is defined as a decreasing function of the film thickness, and e is the film thickness. In such a case when the long range force is that of van der Waals forces,

$$P(e) = \frac{A}{12\pi e^2} \qquad \textbf{Eq. 2-14}$$

where, γ_{SL} = interfacial tension between the solid and the liquid, γ = surface tension of the liquid and the air phase, and A = Hamaker constant which is defined later. Jacobs et al. (1998) notes that thermal fluctuations in the thickness of the film, experiences a driving force that would grow exponentially as a function of time ultimately which leads to dewetting whenever the amplitude arrives at the size of the film thickness.

Furthermore, in terms of microscopic films, as de Gennes (2010) asserts, the curvature of F (e) becomes negative (F" (e) < 0) allowing the film to be unstable. The capillary waves become amplified and the film spontaneously breaks up into a multitude of droplets which is assembled in a pattern similar to a polygon. The graph in Figure 2-7 depicts the two dewetting system.

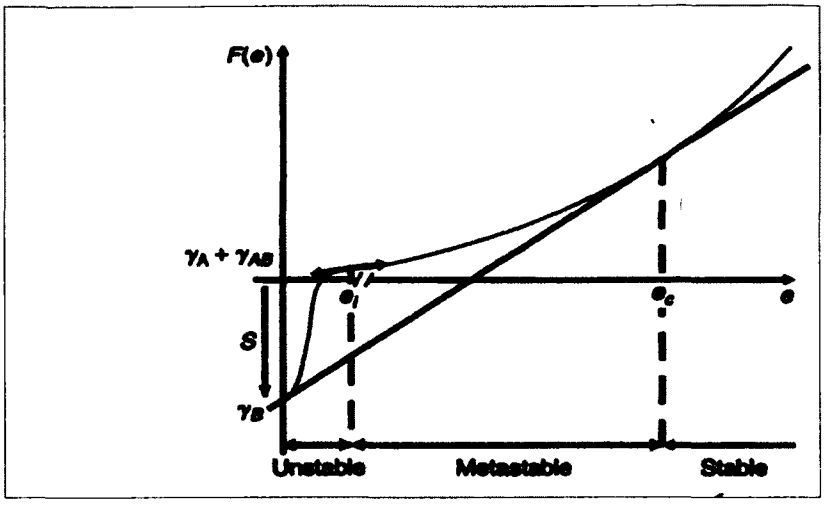

Figure 2-7: Two dewetting regimes: "spinodal" and "nucleation and growth." Depicted here is the energy F(e) of a film whose thickness ranges from a nm to a mm, in a partial wetting regime, with the long range forces included. Depending on the curvature of F(e), one predicts two possible mechanisms for dewetting when $e < e_c$. If $F''(e) < 0$, the film is metastable and dewets by nucleation and growth of a dry zone; If $F''(e) < 0$, the film is unstable and breaks up spontaneously (spinodal decomposition). The thickness e_i at the inflection point is of the order of 10 nm. (De Gennes, 2010). ©Springer, Capillarity and Wetting Phenomena, 2010, 158, Dewetting, de Gennes et al.7.3., with kind permission from Springer Science and Business Media.

Moreover, Lee et al. (2004) investigated dewetting by the use of solvent. It was observed that the rim displays type-1 instability, in an apolar solvent, where the rim undulation does not allow for finger formation. In contrast with a polar solvent, the rim goes through type 2 instability whereby the end result is the formation of droplets.

2.2.3.3 Rupture/dewetting caused by air bubble (pressure)

Jacobs et al. (1998) investigated whether trapped gas has an effect on the rupture process or dewetting of a polymer film. Four varying atmospheres were used to carry out the experiments. These atmospheres include air, nitrogen, argon, and

helium. Generally, it was concluded that at the performance of the experiments in vacuum, less than pressure of 1mbar, rupture was suppressed completely, noting that the substrate must be properly cleaned. Moreover, whichever of the gases were utilized, a pressure of a minimum of 10 mbar induced the formation of holes while a pressure of a maximum of 1 mbar suppressed the rupture. Additionally, for thin wetting films on heterogeneous substrates, rupture is also thought to occur as a result of nanobubbles at the interface of a wetting film and that of the substrate. Slavchove et al. (2005) presented a model with a thin liquid film resting on nanobubbles together with the forces acting therein. In their model, the nanobubbles in the analysis were considered to be spherical and only the surface deformation of the wetting film was taken into account.

2.2.4 Surface Forces/Hamaker Constant

Surface tensions, according to Reynolds (2005), are related to intermolecular forces and underscore that the Hamaker constants equally relate to the intermolecular forces, especially when the dispersion forces dominate. Specifically, Donaldson and Alam (2008) add that the Hammaker constant (A) is a coefficient relating the interactive van der Waals energy to the separation distance of two molecules where the interactive force is a pair-wise additive and is also independent of the intervening media. Hyrodcarbon films and their instability were investigated by Francisca et al. (2003). The films were evaluated in the presence of three different fluids. It was noted that the films do not allow for the formation of double layers on the mineral surface.

In the absence of osmotic pressure, as was observed, and if the van der

Waals forces dominate, the free energy G, per unit area is given as (Francisca et al., 2003):

$$G = \frac{-A12(3)}{12\pi h^2} \qquad \textbf{Eq. 2-15}$$

where, $A_{12(3)}$ is the Hamaker constant between media 1 and 2 across the medium 3 (which is the film), h, being the film thickness. The constant $A_{12(3)}$ can be obtained from the equation (Francisca et al., 2003):

$$A12(3) = \left(\sqrt{A1} - \sqrt{A33}\right)\left(\sqrt{A22} - \sqrt{A33}\right). \qquad \textbf{Eq. 2-16}$$

In the event that media 1 and 2 are equal, the Hamaker constant A_{ii} remains positive giving rise to an attraction between two layers of the same nature. However, the Hamaker constant for three different phases of $A_{12(3)}$ is negative based on these two conditions: $A_{11}>A_{33}>A_{22}$; $A_{11}<A_{33}<A_{22}$. Concerning a mineral substrate, Francisca et al. (2003) concluded that the rate of film thinning leading to rupture is a function of the Hamaker constant $A_{12(3)}$, and also on the viscosity of the fluid (this one being organic) by which the thin film is composed, noting that more difficulty exists in displacing higher-viscosity fluids from mineral surfaces.

2.2.5 Equipment Used in Dewetting Analysis

Currently, analysis of dewetting of thin film is performed with optical microscopy and Atomic Force Microscopy (AFM). The possibility to image liquid structures on the scale of the nanometer by an AFM extends the range by three orders of magnitude to that of the optical contact angle goniometry (Mugele et al., 2005). In Mugele et al.'s investigation on comparing AFM technique to determine the line tension of a three phase contact line, as compared to the optical microscopy

measurements, the researchers realized that the specific, long range interfacial forces allow for a microscopic analysis of that of the force induced distortions concerning the liquid vapor interface within the immediate vicinity of the contact line. Furthermore, Herminghaus (2005) concluded that values are of the same order of magnitude when comparing theoretical calculations and using SFM (Scanning Force Microscopy) in determining the contact line tension.

In concluding, the complexity of the dewetting process has attracted and continues to attract much attention. The types of dewetting, namely nucleated and spinodal have been cited in thin polymer films on various substrate types and testing conditions. In this process, holes which alter the bulk of the material are formed and later droplets, as have been observed. It must be noted that there is not a single parameter that affects wettability of a thin film on a substrate but rather a myriad of factors all working together. Some of the major factors that have been found to affect wettability are surface tension, surface forces between the molecules, capillary pressure, the contact angle of a fluid drop, and spreading coefficient. Other factors that contribute to wettability are the substrate material content and that of pH level of its surface. Although much of research has been done in this area, there is still a need to understand dewetting behavior in relation to the debonding of binder on mineral surface.

CHAPTER 3

SURFACE FREE ENERGY AND PULL OFF TEST

3.1 Background and Objectives

This Chapter and its sub sections, draws primarily from publications from Wasiuddin and Saltibus (2010) and Wasiuddin, Saltibus, and Mohammad (2011a; 2011b). According to Wasiuddin and Saltibus (2010), a modified pull-off test method was proposed. It was therein reported that a novel moisture conditioning procedure that was able to produce adhesive failure and which can be quantified by the modified pull-off test was developed. Additionally, a new moisture damage mechanism along with related theories was proposed. After extensive study of the dewetting literature, from then, based on these results, it was noted that similar hole observations were made (not termed dewetting) caused by air bubbles and termed "pull back" by Fromm (1974) as mentioned previously, and also observed by Field and Fang (1967) and Brown and Kuntze (1972). It was found, as far as can be known, that most of the samples tested in the asphalt literature (Fromm, 1974; and Field and Fang, 1967) were in submerged condition at room temperature; whereas, in Wasiuddin and Saltibus (2010), and Wasiuddin et al. (2011b), the submerged samples were placed directly in an oven at 64°C, allowed to arrive at the said temperature, and tested within 24 h. Additionally, as noted in the literature review, research has been undertaken to assess the motion of bitumen at an air/water interface to better understand oil extraction in Canada (Lilinki et al., 2004). Based on Wasiuddin and

Saltibus (2010), and Wasiuddin et al. (2011b), the moisture damage mechanism and theory were attributed to dewetting of the film from a substrate. In the following chapters (4-8), the investigation was based on the understanding that the dewetting in the asphalt film occurred primarily under an air bubble as observed when examined by a microscope to determine their cause.

3.2 Development of Modified Pull-Off Test and Moisture Conditioning Procedure

As noted earlier, the development of the original pull-off test method was to measure adhesive characteristics (i.e. bond strength) of coatings which is specified in ASTM D 4541 (Pull-off Strength of Coatings using Portable Adhesion Testers, ASTM D 4541). In the asphalt industry, a modified version has been utilized to measure adhesive properties of asphalt binders and in evaluation of their ability to resist moisture damage (Copeland et al., 2006a, 2006b; Kanitpong and Bahia, 2003 and 2005). The modified procedure utilized by Wasiuddin and Saltibus (2010), and Wasiuddin et al. (2011b) is described.

The plain glass plates that are coated with asphalt binder hereafter are termed "asphalt samples". The plain glass plates that are coated with the asphalt binder and that of a pull stub attached to it is termed pull-stub samples. The dimensions of the glass plates are 2 in. x 2 in. and ¼ in. in thickness. The asphalt binders that contain or do not contain additives, the glass plates and the sand blasted aluminum pull stubs were heated at approximately 167°C for 2 h in an oven. Moreover, the glass plate top surface was coated and asphalt samples prepared. For pull-stub samples, the top surface of the glass plate and the bottom surface of the pull stub were coated and adhered. The samples (Figure 3-1) were then kept for overnight before pull-off test with the use of the

Pneumatic Adhesion Tensile Testing Instrument (P.A.T.T.I.) to obtain the dry strength or dry cohesive strength of the asphalt binders.

Figure 3-1: Sample preparation for dry cohesive strength: (a) asphalt samples, (b) asphalt samples in desiccators, and (c) pull-stub samples. Reprinted with permission. Wasiuddin, N.M, Saltibus, N.E, 2010. Theoretical and Experimental Determination of Adhesion between Asphalt Binders and Aggregates in Wet and Dry conditions. *Report*, LTRC, LA. With permission from ASCE. This material may be downloaded for personal use only. Any other use requires prior permission of the American Society of Civil Engineers. Wasiuddin, N, Saltibus, N., and Mohammad, L., 2011a. Effects of a Wax-Based Warm Mix Additive on Cohesive Strengths of Asphalt Binders, *Proceeings*, 528-537, T&DI Congress, 2011.Reproduced with permission. Nazimuddin M. Wasiuddin, Nibert E. Saltibus, and Louay N. Mohammad, 2011. Novel-Moisture Conditioning Method for Adhesive Failure of Hot- and Warm-Mix Asphalt Binders. *Transportation Research Record: Journal of the Transportation Research Board,* No. 2208, [Adapted] Figure 1, p. 109, Washington, D.C., 2011.

Earlier, Copeland et al. (2006a; 2006b) utilized the P.A.T.T.I. to evaluate cohesive and adhesive strength of asphalts. For dry samples, the pull-off tensile strength was termed a measure of cohesive strength; whereas, the adhesive strength was established after moisture conditioning in their study. Cohesive failure of asphalt binder when tested dry, was observed. After moisture conditioning, the failure mode was changed from cohesive to mix mode or adhesive failure (Kanitpong and Bahia, 2005). The pull-off test was used by Kanitpong and Bahia (2005) to measure asphalt aggregate adhesive strengths, and in combination with measurements of cohesive strengths, predicted mixture performance in the laboratory. Making use of a two-part epoxy glue,

Copeland et al. (2006a; 2006b) applied a porous ceramic stub to the pull-stub. The porous stub enabled water to consistently migrate through to the asphalt film. Moreover, a small amount of asphalt binder (<10g) was mixed with 1% (by weight) of 200 μm glass beads to ensure a uniform film thickness. With the use of a hot plate, the sample was then heated to approximately 100°C. The sample was then applied to the ceramic stub, and by the test operator, the pull-stub was pressed onto the glass substrate. The samples were left to cure in room temperature for 24 h. Dry specimens, (specimens not soaked), were tested after curing. Moisture conditioned specimens were submerged at 25°C in distilled water and then withdrawn from the water bath at four, eight, and twenty-four h soak time before being tested (Wasiuddin and Saltibus, 2010; Wasiuddin et al., 2011b).

In this study, (Wasiuddin and Saltibus, 2010; Wasiuddin et al. 2011a, 2011b) the glass beads of 200 μm were not added to the asphalt binder. Neither was the porous ceramic stub adhered to the pull-stub. Wasiuddin and Saltibus (2010), Wasiuddin et al. (2011b), instead, prepared asphalt samples as described earlier and kept the samples overnight for curing at room temperature. For conditioning of the asphalt samples, these samples were submerged in water in a pyrex container, and the foil covered container was placed and left in a force draft oven overnight at a temperature of 64°C (Figure 3-2). The asphalt samples were removed after moisture conditioning and were taken out to visually assess them for any damage. Wasiuddin and Saltibus (2010), Wasiuddin et al. (2011b) further relate that the asphalt samples, after inspection, were submerged in water in room temperature in a different container, and were kept for 30 min. The asphalt samples were then removed from the water and checked whether the asphalt film was able to be peeled off from the glass plate corner or from the sides. Additionally, the

asphalt samples were checked at the middle in order to observe whether the asphalt film can be peeled off easily with a soft scratch. It was hypothesized that the state of adhesion failure by moisture conditioning was accomplished if the asphalt film was able to be peeled off from the glass plate without breaking of the film. The conditioned samples were then carefully wiped with Kim® wipes and for 30 min air dried. A thin film of superglue® was utilized to add a pull-stub to the conditioned asphalt sample. The samples that were prepared using this procedure are termed "conditioned-pull stub samples" hereafter. At a room temperature for 10 min, the conditioned pull-stub samples were then cured. The procedure for preparing the conditioned pull-stub samples are shown in Figure 3-2.

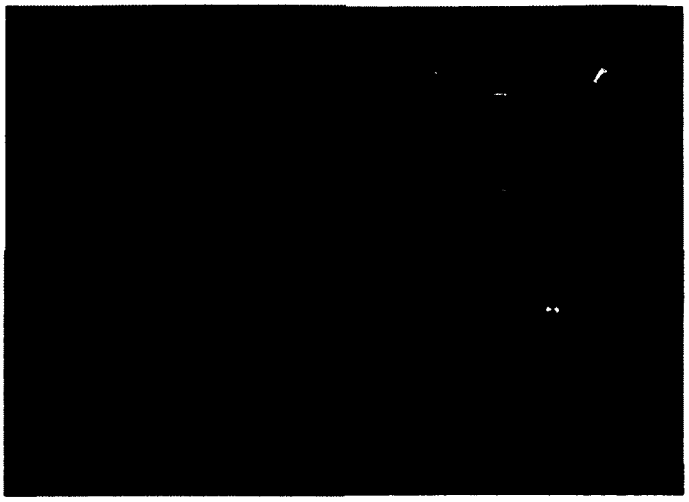

Figure 3-2: Sample preparation for wet adhesive strength: (a) asphalt samples, (b) moisture conditioning: overnight inside the oven at 64°C in submerged condition, (c) asphalt samples after conditioning with holes and (d) conditioned pull-stub samples. Reprinted with permission. Wasiuddin, N.M, Saltibus, N.E 2010. Theoretical and Experimental Determination of Adhesion between Asphalt Binders and Aggregates in Wet and Dry conditions. *Report*, LTRC, LA. With permission from ASCE. This material may be downloaded for personal use only. Any other use requires prior permission of the American Society of Civil Engineers. Wasiuddin, N, Saltibus, N., and Mohammad, L., 2011a. Effects of a Wax-Based Warm Mix Additive on Cohesive Strengths of Asphalt Binders, *Proceeings*, [Adapted] Figure 1, 528-537, T&DI Congress, 2011. Reproduced with permission. Nazimuddin M. Wasiuddin, Nibert E. Saltibus, and Louay N. Mohammad, 2011. Novel-Moisture Conditioning Method for Adhesive Failure of Hot- and Warm-Mix Asphalt Binders. *Transportation Research Record: Journal of the Transportation Research Board, No. 2208, [Adapted] Figure 1, p. 109, Washington, D.C., 2011.*

Wasiuddin and Saltibus (2010), and Wasiuddin et al. (2011b) at the beginning of this study, prepared pull stub samples and then conditioned them by allowing the samples to be submerged in water at 64°C inside the oven overnight. No significant decrease in strength for the conditioned samples compared to dry cohesive strength was observed. Possibly, this result is due to the asphalt film being covered by the pull-stub on top and the glass plate at the bottom. Therefore, asphalt samples prepared by the researchers, were conditioned and the pull-stub was then added to them to make conditioned pull-stub samples. Commercially available superglue® was utilized as the asphalt film in the

conditioned sample does not take much strength for pull-off as was compared by peeling off the asphalt film by nails. The pull-off testing procedure using a P.A.T.T.I. is described in Figure 3-3.

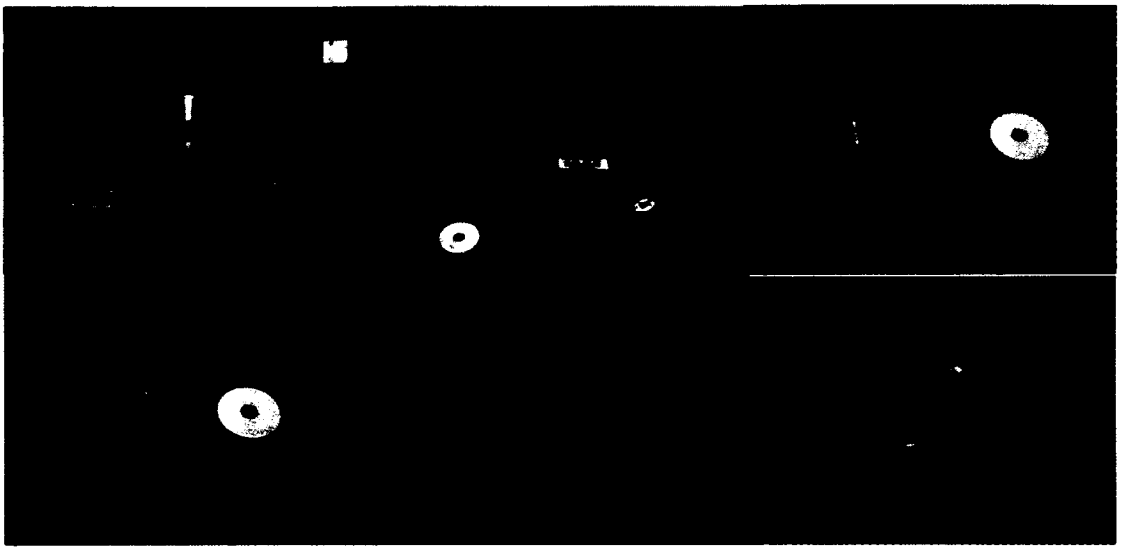

Figure 3-3: (a) P.A.T.T.I., (b) pull-stub sample, gasket (blue) and reaction plate (white), (c) pull-stub Inside the gasket and beside the reaction plate (white), (d) pull-stub sample inside gasket and reaction plate, (e) cohesive failure and (f) adhesive failure. Reprinted with permission. Wasiuddin, N.M, Saltibus, N.E 2010. Theoretical and Experimental Determination of Adhesion between Asphalt Binders and Aggregates in Wet and Dry conditions. *Report*, LTRC, LA. With permission from ASCE. This material may be downloaded for personal used only. Any other use requires prior permission of the American Society of Civil Engineers. Wasiuddin, N, Saltibus, N., and Mohammad, L., 2011a. Effects of a Wax-Based Warm Mix Additive on Cohesive Strengths of Asphalt Binders, *Proceeings*, [Adapted] Figure 1, 528-537, T&DI Congress, 2011. Reproduced with permission. Nazimuddin M. Wasiuddin, Nibert E. Saltibus, and Louay N. Mohammad, 2011. Novel-Moisture Conditioning Method for Adhesive Failure of Hot- and Warm-Mix Asphalt Binders. *Transportation Research Record: Journal of the Transportation Research Board,* No. 2208, [Adapted] Figure 2, p. 109, Washington, D.C., 2011.

According to Wasiuddin and Saltibus (2010), Wasiuddin et al. (2011b) in the study by Copeland et al. (2006a; 2006b), the asphalt binder was mixed with glass beads, and a porous-ceramic-stub headed pull-stub was added to the glass plate by soaking at different durations the samples were conditioned. When the samples were conditioned,

the failure mode was changed from cohesive to mixed or adhesive mode. After moisture conditioning, the failure strength attained was termed bond strength by Copeland et al. (2006a; 2006b) which indicated adhesive strength. Based on the moisture conditioning method developed, pure adhesive failure was observed with the absence of the porous stub. Mixed mode of failure was observed in a few of the cases and, in most cases, the asphalt film peeled off from the glass plate in a pure adhesive mode. Therefore, adhesive strength or wet adhesive strength is the term used for the pull-off strength of the conditioned pull-stub samples. Figure 3-4 depicts some samples failed in adhesion.

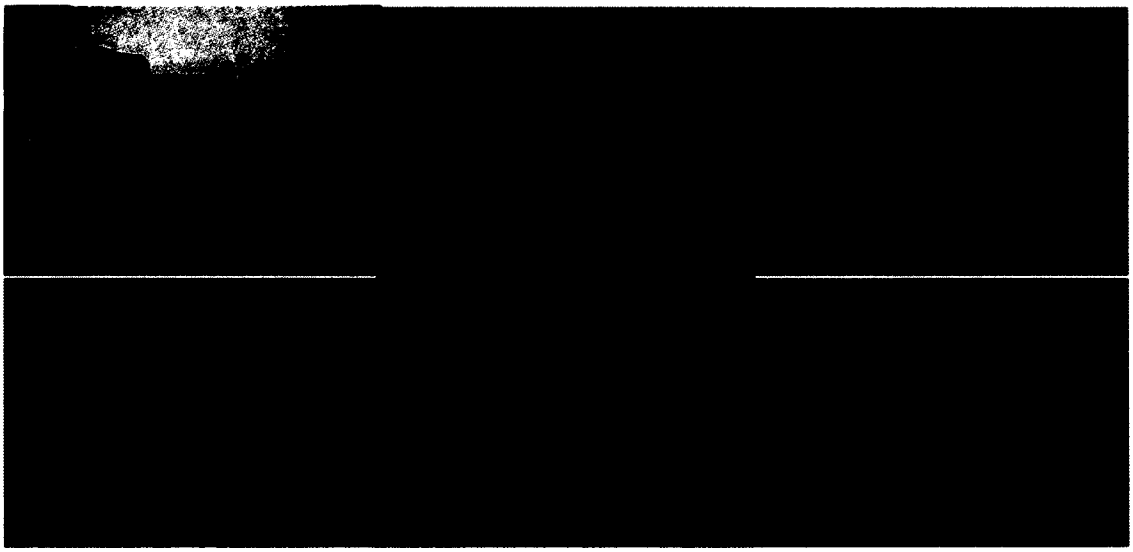

Figure 3-4: Glass Plates with Randomly Distributed Holes, Novaculite with Holes, Adhesive Failures in PG 64-22 (AC30) Samples with and without Additives. Reprinted with permission. Wasiuddin, N.M, Saltibus, N.E 2010. Theoretical and Experimental Determination of Adhesion between Asphalt Binders and Aggregates in Wet and Dry conditions. *Report*, LTRC, LA. Reproduced with permission. Nazimuddin M. Wasiuddin, Nibert E. Saltibus, and Louay N. Mohammad, 2011. Novel-Moisture Conditioning Method for Adhesive Failure of Hot- and Warm-Mix Asphalt Binders. *Transportation Research Record: Journal of the Transportation Research Board*, No. 2208, [Adapted] Figure 2, p. 109, Washington, D.C., 2011.

3.3 Proposed Moisture Damage Mechanism

Initially, it was reported that a novel observation based on the moisture damage mechanism was made. Upon further investigating the cause of the holes via microscope and probing more literature on moisture damage, holes were cited by other researchers in the asphalt film after being exposed to moisture (Fromm, 1974; Field and Phang 1967; Brown and Kuntze, 1972). The researchers, Wasiuddin and Saltibus (2010), Wasiuddin et al. (2011b), proposed that based on the observation that moisture penetrates into the interface of asphalt-aggregate (asphalt-glass plate in this case) by the production of holes on the asphalt film, some of the characteristics of the aforementioned holes reported by Wasiuddin and Saltibus (2010), Wasiuddin et al. (2011b) are mentioned:

(1) The holes are generated from the top surface of the asphalt samples during their conditioning at 64°C inside the oven in submerged water

(2) The holes are cylindrical

(3) The holes are randomly distributed

(4) The diameter and number of holes increases with time for up to about 8 hours

(5) The holes are visible within about 2 hours of conditioning

(6) The hole diameter varies from microscopic to more than 1 mm

(7) The holes arrive at the bottom of the glass surface and a clear glass surface can be observed. Similar observations were also made for polished aggregate surface

(8) The asphalt film from the asphalt samples that generated holes can be peeled off easily after taking the asphalt sample out from the conditioning and

cooling it at room temperature. A pull-off test using PATTI also gives adhesion failure for these sample

(9) After reaching the interface through the holes, moisture start replacing asphalt film from the substrate surface (in this case glass plates) and adhesive failure or stripping is observed [proposed theory].

(10) Therefore, a new moisture damage mechanism can be proposed as follows. Under submerged condition at pavement service temperatures, water develops randomly distributed micro and macro scale cylindrical holes on asphalt film within reasonable time period that penetrates up to the asphalt-substrate interface and start replacing asphalt film from the substrate surface and adhesive failure or stripping is observed. The first process called dewetting of asphalt film from substrate and second process will be called spreading of moisture on substrate.

(Wasiuddin and Saltibus, 2010; Wasiuddin et al., 2011b)

Based on the mechanism that was identified (Wasiuddin and Saltibus, 2010; Wasiuddin et al., 2011b), a theory of the proposed moisture damage mechanism was put forward and in depth studies were conducted to assess the role of dewetting in moisture damage of asphalt pavements. The formation of holes, as proposed by Xu et al. (2007) could be due to water molecules penetrating the polymer film (in our case asphalt film), and the capillary force then drives the formation of the holes and also that of hole growth. Moreover, the capillary force needs be strong enough to drive the process of hole formation. The following equation is the approximate value given for the capillary force:

$$P = \frac{2\gamma cos\theta}{R} \qquad \textbf{Eq. 3-1}$$

where, P is the additional pressure, γ, the surface tension/energy at the polymer-water interface (asphalt-water interface in this study), θ the contact angle of water on polymer film, (asphalt film in this case), and R, the radius of the hole, obtained from the early stages of hole formation. The additional pressure, based on the formula, can arrive at several MPa in the early stage of hole formation, being strong enough to drive both hole formation and growth. The Xu et al. (2007) hypotheses that was developed in that regard was proposed in this study for the asphalt-aggregate system. The dewetting of asphalt film, therefore, is a function of the value P. The asphalt film is more susceptible to dewetting, based on a high value of P.

Moreover, as it pertains to spreading coefficient, Wasiuddin et al. (2008) determined the spreading coefficient of asphalt binders over aggregates in order to assess moisture susceptibility of various aphalt-aggregate systems with and without anti-strip additives. Spreading coefficient as has already noted can be calculated thus:

$$S_{L/S} = \Gamma_S + \Gamma_{SL} - \Gamma_{LV} \qquad \textbf{Eq. 3-2}$$

where, $S_{L/S}$ = Spreading coefficient of liquid L on solid S, Γ_S= SFE of solid S, ergs/cm^2, Γ_{SL}= Solid-liquid interfacial energy, ergs/cm^2, and Γ_{LV} = SFE of liquid L, ergs/cm^2. In terms of the asphalt-aggregate systems, the equation is rewritten thus:

$$S_{water/aggregate} = \Gamma_{asphalt/aggregate} + \Gamma_{water/aggrgate} - \Gamma_{asphalt/water.} \qquad \textbf{Eq. 3-3}$$

For spontaneous spreading, based on the aforementioned equation, the free energy change of the spreading coefficient is positive. Spreading of water over aggregate by

replacing the asphalt film, therefore, is a function of S. As S increases, the higher the susceptibility of the asphalt film is to the spreading of water.

According to Wasiuddin and Saltibus (2010), and Wasiuddin et al. (2011b), a hypothesis on moisture damage mechanisms in asphalt pavements was therefore proposed which follows.

There is a two-step process involved the adhesive failure or stripping in an asphalt-aggregate system: That asphalt film dewets from the aggregate which forms randomly distributed holes in the asphalt film in water at pavement service temperatures followed by the spreading of water on aggregate and in the process replacing asphalt films. The dewetting of the asphalt film from that of the aggregate will be a function of the dewetting coefficient, P, which can be described as the additional pressure that is derived from capillary force. Moreover, the spreading of water on the aggregate surface is to be dependent on the spreading coefficient, S. This parameter, S, can be defined in terms of the reduction in surface free energy on losing the asphalt-aggregate surface which will then form new water-aggregate and asphalt-water interface. Therefore, the higher the values of P and S (coefficients), the higher would be the moisture susceptibility.

After understanding that the holes formed in this study were predominantly formed under a bubble cap, the investigation in later chapters (4-8) focused in that regard and not on the additional pressure, although it may be caused by P.

3.4 Cohesive and Adhesive Strengths using Pneumatic Adhesion Tensile Testing Instrument (P.A.T.T.I.)

3.4.1 Materials

Based on the study by Wasiuddin and Saltibus (2010), Wasiuddin et al. (2011b) two asphalt binders were used in this study, PG 64-22 (also known as AC 30) and PG 76-22 M (also known as PAC 40) being obtained from Ergon Asphalt and Emulsions, Inc., Jackson, Mississsippi. PG 64-22 is not a modified asphalt binder, as opposed to PG 76-22M being a polymer modified binder. According to the Louisiana Department of Transportation and Development (DOTD), the product source codes are referred to as 41-BT and 41-AT, respectively. A product of Sasol Wax, Sasobit®, from South Africa was utilized in this study. Sasobit® is a modifier or an "asphalt flow improver" and is produced in a process called "FT synthesis", in which carbon monoxide is converted into higher hydrocarbons in catalytic hydrogenation, then followed by a distillation process. According to Edwards and Redelius (2003), the end product is comprised of mainly fine crystalline long chain aliphatic polymethylene hydrocarbon chains having 40 to 100 carbon atoms. Macroscrystalline bituminous paraffin waxes, on the other hand, contain carbon chain lengths ranging from 25 to 50. In Sasobit®, the longer carbon chains lead to a higher melting point, and the distribution of the wider wax molecule results in broader melting temperature range and an enlarged plasticity span. Butz et al. (2001) relate that in the range of 60°C to 90°C, natural asphalt wax is normally completely melted out while the melting temperatures of asphalt having Sasobit® are higher (approximately between 100°C and 130°C).

The anti-strip additive utilized in this study, is an amine-based liquid anti-strip additive, called Adhere LOF 6500 or AD-Here® LOF 6500 (referred to LOF 6500 hereafter) from ArrMaz Custom Chemicals, Florida. The rates of 2% and 1% were used for Sasobit® and LOF 6500 respectively.

3.4.2 Pull-Off Test of Dry Pull Stub Samples for Dry Cohesive Strengths

The cohesive strengths of asphalt binders that contain and do not contain additives are shown in Table 3-1. In the P.A.T.T.I. testing, the maximum gasket pressure needed to pull-off is obtained in psi. The pull-off strength in psi was obtained with the use of the equation recommended by the manual. Additionally, to record the elapsed time needed for pull-off, a stop watch was used, and the pressure rate was computed by dividing the pull-off strength by the time required.

Table 3-1: P.A.T.T.I. test results.

Asphalt	Dry Cohesive Strengths (psi) (MPa)	Effect of Film Thickness (psi)	Adhesive Strength of Conditioned Pull-Stub Samples/psi (MPa)	Conditioned and Oven Dry Samples to Check for Healing/psi (MPa)
PG64-22	284.9 ± 21.3 (1.96)	244.6 ± 38.4	Adhesive 150.7 (1.0)	Cohesive 283.5(2.0)
PG64-22 + 2% Sasobit®	212.9 ± 11.3 (1.5)	207.0 ± 3.5	Adhesive 157.2 (1.1)	Cohesive 209.1(1.4)
PG64-22+ 1% LOF 6500	211.9 ± 24.1 (1.5)		Mixed 148.7(1.0)	Cohesive 246.1(1.7)
PG64-22 + 2% Sasobit® + 1% LOF 6500	172.7 ± 22.1 (1.2)		Adhesive 130.2(0.9)	Cohesive 207.6(1.4)
PG76-22M	299.9 ± 15.3 (2.1)	246.9 ± 23.2	Adhesive 238.1(1.6)	Cohesive 246.6(1.7)
PG76-22M + 2% Sasobit®	218.0 ± 17.7 (1.5)	210.1 ± 21.1	Mixed 234.6(1.6)	Cohesive 277.5(1.9)

Table 3-1: P.A.T.T.I. test results (Continued).

Asphalt	Dry Cohesive Strengths (psi) (MPa)	Effect of Film Thickness (psi)	Adhesive Strength of Conditioned Pull-Stub Samples/psi (MPA)	Conditioned and Oven Dry Samples to Check for Healing/psi (MPA)
PG 76-22M + 1% LOF 6500	268.0 ± 33.4 (1.8)		144.7(0.1)	Cohesive 143.7(0.9)
PG 76-22M + 2% Sasobit® + 1% LOF 6500	149.7 ± 10.4 (1.0)		142.7(1.0)	Cohesive 132.7(0.9)

*Values in (MPa) are rounded to one decimal place.

3.4.3 Effects of Polymer on Dry Cohesive Strengths of Asphalt Binders

A polymer is generally used to improve performance grading of asphalt binders. However, it was observed that polymer does not increase the dry cohesive strength significantly (obtained from the pull-off test) compared to the stiffness that is obtained from the dynamic shear rheometer. The pull-off strengths are shown in Table 3-1 depicting the pull-off strength of PG64-22 to be 284.9 psi with a standard deviation of 21.3 psi, as compared to the pull-off strength of PG 76-22M of 299.9 with a standard deviation of 15.3 psi.

3.4.4 Effects of Wax-Based Warm Mix Asphalt (WMA) Additive Sasobit® on Dry Cohesive Strength of Asphalt Binders

In asphalt binders and Hot Mix Asphalt (HMA), (Wasiuddin and Saltibus 2010) the effects of Sasobit®, had previously been studied by many researchers (Hurley and Prowell, 2005; Edwards and Redelius, 2003; Edwards et al., 2006). Moreover, Sasobit® was known to improve the flow of the asphalt mixes (viscosity depressant) and to reduce the mixing and compaction temperatures by approximately 18-54°C (Wasiuddin et al.,

2007c; Kristjánsdóttir et al., 2007). Additionally, Hurley and Prowell, (2005) report that Sasobit® improved the resistance to deformation at higher temperatures for asphalt binder and HMA (rutting); therefore, a significant increase in the high temperature grading of an asphalt binder was realized. However, an increase in the creep stiffness and the reduction in the creep rate (m) based on low temperature grading may be a concern, specifically in the case of overdosing (Wasiuddin et al., 2007c). It has been noted that a lower mixing and compaction temperature can result in incomplete drying of the aggregate. Moisture damage may be as a result of the residual water that is trapped in the coated aggregate (Hurley and Prowell, 2005). Moreover, some researchers reported a reduced-aging property of Sasobit®. Notwithstanding the significant research that has been undertaken in the past two decades on the effect of commercial wax including Sasobit® on asphalt binder and HMA and also the increase in recent interests on Warm mix asphalt (WMA), an understanding of the effects of the wax on the performance on the adhesion between the binder and aggregate and on cohesion are still seriously lacking (Edwards and Redelius, 2003). In this regard, in this study direct pull-off strength was determined to assess the dry cohesive strength of asphalt binders with 2% Sasobit®. It is observed that Sasobit® reduces the dry cohesive strength of PG 64-22 and PG 76-22M which is a polymer modified binder as shown in Table 3-1. It was observed that there was a reduction in dry cohesive strengths by Sasobit® of PG 64-22 from 284.9 psi to 212.9 psi; whereas in the case of PG 76-22, the reduction was from 299.9 psi down to 218.0 psi. For these values, the standard deviations were 21.3, 11.3, 15.3 and 17.7 psi, respectively. When the standard deviations are compared, they showed that the reductions are significant. There was a reduction of 72.0 psi which was 25.3% in the case of PG 64-22

while the reduction was 81.9 psi for PG 76-22M being 27.3%. (Wasiuddin and Saltibus, 2010; Wasiuddin et al., 2011a, 2011b)

3.4.5 Effects of Liquid Amine Anti-Strip Additive (Adhere LOF 6500) on Dry Cohesive Strengths of Asphalt Binders

According to Wasiuddin and Saltibus (2010), Wasiuddin et al., (2011b) for the reduction in stripping and an improvement in adhesion, liquid amine anti-strip additives have been used extensively in hot mix asphalt. In Table 3-1, it was observed that the dry cohesive strengths of asphalt binders are reduced by the use of LOF 6500. For PG 64-22, the dry cohesive strength with the use of 1% LOF 6500 was reduced from 284.9 psi to 211.9 psi. The reduction obtained was 73.0 psi which is 25.6%. Moreover, there was a reduction in cohesive strength from 268.9 psi to 211.9 psi for PG 76-22 M. The reduction in strength of 31.8 psi was 11% of the original cohesive strength, which demonstrated that the reduction was less in the case of PG 76-22M.

3.4.6 Effects of Sasobit and Adhere LOF 6500 on Dry Cohesive Strengths of Asphalt Binders

The combination of 2% Sasobit® and 1% LOF 6500 significantly reduced the dry cohesive strength of asphalt binders (Table 3-1). In the case of PG 64-22 asphalt, the reduction in dry cohesive strength was from 284.9 psi of the original binder to 172.7 psi with a standard deviation of 22.1 psi. Moreover, for PG 76-22M, the strength was reduces from 299.9 psi of the original binder to 149.7 psi having a standard deviation of 10.4 psi. For PG 64-22, the reduction was 25.3%; whereas for PG 76-22M, it was 50.1%.

3.4.7 Effects of Film Thickness of Dry Cohesive Strengths of Asphalt Binders

An average film thickness of approximately 0.1 mm was used in this study. The gravimetric technique was utilized in obtaining the film thickness. The film thickness was

determined by obtaining the asphalt film volume from asphalt film weight then the volume was divided by the glass plate area. It must be noted that in this exploratory study, two samples were used to estimate the thicknesses. It is observed from Table 3-1, that asphalt thickness has a significant influence on dry cohesive strengths of asphalt binders. If the thickness was smaller than 0.1 mm, the dry cohesive strength will be reduced. For example, with the reduction of thickness, the dry cohesive strength of PG 76-22M reduces to from 299.9 psi to 246.9 psi. For PG 64-22 asphalt binder, a similar reduction in dry cohesive strength was observed. However, as it pertains to the reduction in thickness for both of the asphalt binders, there was no significant reduction in strength when Sasobit® was added.

3.4.8 Effects of Polymer on Adhesive Strengths of Asphalt Binders

After the PG 64-22 asphalt binder was conditioned, pure adhesive failure between the asphalt binder and the glass plate was observed when the failure was examined by the peeling off of the sides or corner and also by scratching of at the middle. Moreover, the adhesive strength was measured quantitatively by the pull-off test performed using the P.A.T.T.I. As depicted in Table 3-1, the adhesive strength of PG 64-22 asphalt binder was much lower than that of the dry cohesive strength, where it was shown to reduce from 284.9 psi to 150.7 psi. Pure adhesive failure between asphalt binder and that of the glass plate for PG 76-22M was also observed by the peeling off of the sides or corner and also by scratching of at the middle. The adhesive strength as shown in Table 5-5 for PG 76-22M was 238.1 psi, being much lower than its dry cohesive strength of 299.9 psi. For PG 64-22 asphalt binder, the reduction was 20.6%; whereas for PG 76-22M, the reduction was 47.1%. (Wasiuddin and Saltibus, 2010, Wasiuddin et al., 2011a, 2011b)

3.4.9 Effects of Sasobit® on Adhesive Strengths of Asphalt Binders

For PG 64-22 and PG 76-22M, in the case of Sasobit® added asphalt binders, the strength reduced from 212.9 psi to 148.7 psi and from 218.0to 144.7 psi, respectively, where the reductions were 30.1% and 33.6%, respectively, as well. In the case of PG 64-22, a mixed mode of failure was observed, and the failure was fully cohesive for PG 76-22M. Even though the strengths reduced significantly (30.1% and 33.6 %), the failure mode remained mostly or fully cohesive. Based on the results, it may wrongly be assessed that Sasobit® performs comparatively better than normal asphalt in the resistance of moisture damage which was not the case as the reductions presented here were based on the dry cohesive strengths of Sasobit® added asphalt. It should be noted that for regular asphalt binders, the adhesive strengths are still greater than those when Sasobit® is included. The hand peel-off test was performed where it was observed that the asphalt film was not able to be peeled off from the glass plates when Sasobit® was added to the asphalt binders. Sasobit®, this result indicates, does have a positive effect in the resistance of moisture damage obtained from the moisture condition method used in this study.

3.4.10 Effects of Adhere LOF 6500 on Adhesive Strengths of Asphalt Binders

According to Wasiuddin and Saltibus (2010), and Wasiuddin et al., (2011b) adhesive failure was exhibited in PG 64-22 with 1% LOF 6500, while a mixed mode of failure was exhibited by PG 76-22M with 1% LOF 6500 after the moisture conditioning procedure was followed. After moisture conditioning, it was possible to peel off the asphalt film of PG 64-22 with 1% LOF 6500. Additionally, pure adhesive failure was

observed when the pull-off test was performed. There was a reduction in the dry cohesive strength by 1% LOF 6500 of 284.9 psi to adhesive strength of 157.2 psi. Also, PG 64-22 with no LOF 6500, showed after moisture conditioning, an adhesive strength of 150.7 psi. Moreover, for PG 76-22M a mixed mode of failure was observed and after moisture conditioning its adhesive strengths with and without LOF 6500 were 238.1 psi and 234.6 psi respectively.

3.4.11 Effects of Sasobit ® and Adhere LOF 6500 on Adhesive Strengths of Asphalt Binders

The lowest adhesive strengths were observed for both asphalt binders when Sasobit® and LOF 6500 were mixed together. Adhesive failure was observed in the case of PG 64-22 after moisture conditioning and pull-off test and a mixed mode of failure was observed for PG 76-22M. The adhesive strength for PG 64-22 with the absence of additives was 130.2 psi from 150.7 psi and for PG 76-22M, with the absence of additives, the adhesive strength was 142.7 psi from 238.1 psi.

3.4.12 Healing of Damaged Samples

Two out of the four conditioned samples were checked for adhesive strength, and the rest of the two samples were heated dry at 64°C for 24 h to investigate whether there would be any healing or recovering of strength. Depicted in Table 3-1, PG 64-22 damaged samples recovered almost 100% dry cohesive strengths in all the cases. The recovery was less than 90% in the case of PG 76-22 M, except 1% LOF 6500 additive. In all the four cases of PG 64-22 and PG 76-22M, the failure mode was found to be cohesive, indicating that with high temperature of the drying of the samples, moisture damage can be healed.

3.4.13 Conclusions on Pull-Off Test on Conditioned Samples

Various moisture conditioning methods were investigated (Wasdiuddin and Saltibus, 2010; Wasiuddin et al., 2011b) to achieve pure adhesive failure or stripping of an asphalt film. Moreover, in producing adhesive failure in this study, the simple procedure followed was effective in that regard. Based on the moisture conditioning procedure, it was observed that PG 64-22 original, with 1% LOF 6500 and with 1% LOF 6500 plus Sasobit®, revealed adhesive failure; whereas, a mixed mode of failure was produced by PG 64-22 plus Sasobit®. Moroever, adhesive failure was exhibited only in the original samples of PG 76-22M. For 1% LOF 6500 and 1% LOF 6500 plus 2% Sasobit®, a mixed mode of failure was observed; whereas, for 2% Sasobit® cohesive failure was observed. Therefore, it is an indication that 1% LOF 6500 was not effective in resisting moisture damage as opposed to Sasobit® which changed the mode of failure to mixed or cohesive but did not necessarily increase the strength. Heating the samples at 64°C for 24 h in dry condition caused healing of the adhesive failure to occur based on the moisture conditioning followed in this study. The strength recovery was near 100% of the dry cohesive strength for PG 64-22 with and with the absence of additives, while the recovery for PG 76-22M with and without additive was relatively smaller.

3.5 Cohesive and Adhesive Strengths from Surface Free Energy Measurements: Surface Free Energy (SFE) Method

In Wasiuddin and Saltibus (2010), and Wasiuddin et al., (2011a, 2011b) SFE of a solid (or liquid) is defined as the work that is required to increase a unit area of surface of the solid under vacuum. As a consequence, the free energy of cohesion is the work that is done by that of a unit force acting along the surface of an asphalt binder at a right angle

of any line of a unit length against a cohesive force in order to create two interfaces from one (i.e. asphalt binder) under vacuum. The free energy of adhesion, therefore, is the free energy required in order to create two interfaces from one interface that consists of two different phases in contact (aggregate and asphalt binder in this case).

According to Good (1992), the SFE of an asphalt binder is mainly composed of an apolar component (also termed the Lifshiz-van der Waals component) and an acid-base component, shown in the equation:

$$\Gamma = \Gamma^{LW} + \Gamma^{AB} \qquad \textbf{Eq. 3-4}$$

where, Γ = SFE of the asphalt binder, Γ^{LW} = Lifshitz-van der Waals component of SFE, and Γ^{AB} = Acid-Base component of the SFE. Moreover, based on Good's postulation (Good, 1992), the acid-base term can be decomposed that of a Lewis acidic surface parameter and a Lewis basic parameter shown by:

$$\Gamma^{AB} = 2\sqrt{\Gamma^{+}\Gamma^{-}} \qquad \textbf{Eq. 3-5}$$

where, Γ^{+}= Lewis acid component of the surface interaction, and Γ^{-} = Lewis base component of the surface interaction. In this study, dynamic contact angles for various liquids were employed in the evaluation of the SFE components. In order to measure the advancing contact angles, the Sessile Drop method was employed.

3.5.1 Advancing Contact Angle from Sessile Drop Method (SDM)

Wasiuddin and Saltibus (2010), Wasiuddin et al., (2011a, 2011b) used an optical contact angle analyzer called "OCA 15" Plus from Future Digital Scientific Corporation to measure the advancing contact angle of a liquid on an asphalt film or on a polished aggregate surface. While the release of a liquid was made at the rate of 0.33μl/s to a final drop size of 8μl/s, the dynamic contact angle of a liquid drop was thus measured

(Figure 3-5). For measurements and analysis of the data, the software SCA 20 obtained from Future Digital Scientific Corporation was used.

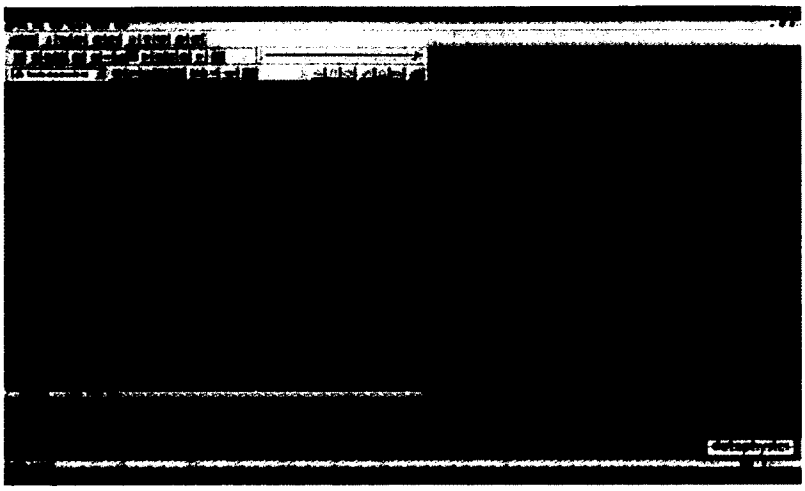

Figure 3-5: Advancing contact angle from sessile drop (Wasiuddin and Saltibus, 2010).

3.5.2 Calculation of SFE from Dynamic Contact Angle

According to Wasiuddin and Saltibus (2010), Young's equation based on an energy balance of a liquid drop (in this case, liquid solvent) spreading on a flat solid (asphalt binder in this case) in the horizontal direction, can be utilized to evaluate the SFE characteristics which is associated with cohesion. This equation is expounded by (Good, 1992):

$$\Gamma_{SV} = \Gamma_{SL} + \Gamma_{LV} Cos\theta_{SL} \qquad \textbf{Eq. 3-6}$$

where, θ_{SL}= Contact angle made between the solid and liquid measured through the liquid, Γ_{SV} = SFE of solid in vacuum, Γ_{SL}= SFE of solid in liquid, Γ_{LV} = SFE of liquid in vacuum.

To evaluate the surface free energy of adhesion, Dupre's equation can be utilized, which represents the energy that is required to create two interfaces from two different

phases that is in contact with a third medium (Good, 1992). The equation is written as (Wasiuddin and Saltibus, 2010):

$$\Delta G_{12}^{a} = \Gamma_1 + \Gamma_2 - \Gamma_{12}, \qquad \textbf{Eq. 3-7}$$

where, ΔG_{12}^{a} = Free energy of adhesion, Γ_1= SFE of phase 1 (in this case-asphalt binder or aggregate), Γ_2= SFE of phase 2 (in this case-liquid solvent), and Γ_{12} = Interfacial SFE of phase 1 and phase 2. With the assumption that the equilibrium film pressure is negligible for both the asphalt binder and the aggregate, Young's and Durpre's equation can be combined with the postulate of Good in order to obtain the Young-Dupre equation (Good, 1992). As mentioned in the review of literature, the Young-Dupre equation can be detailed as shown in Equation 3-8:

$$(1 + cos\theta)\Gamma_L = 2\left(\sqrt{\Gamma_S^{LW}\Gamma_L^{LW}} + \sqrt{\Gamma_S^{+}\Gamma_L^{-}} + \sqrt{\Gamma_S^{-}\Gamma_L^{+}}\right) \qquad \textbf{Eq. 3-8}$$

where, $\Gamma_L^{LW}, \Gamma_L^{-}, \Gamma_L^{+}$= liquid solvent SFE components, $\Gamma_S^{LW}, \Gamma_S^{-}, \Gamma_S^{+}$ = asphalt binder or aggregate and θ = Contact angle. Based on the equation, the three unknowns ($\Gamma_S^{LW}, \Gamma_S^{-}, \Gamma_S^{+}$) represents the SFE components of an asphalt binder or aggregate. The dynamic contact angles are to be measured with a minimum of three various liquid solvents in order to obtain these unknowns. For the liquid solvents, the SFE characteristics must be known beforehand. Therefore, three liquid solvents, namely, water, formamide and diiodomethane were used due to their relatively large SFE, their immiscibility with asphalt binder, and differing SFE components (Cheng et al., 2002).

3.5.3 Calculation of Free Energy of Adhesion from SFE

ΔG^A , the free energy of adhesion, has two components which are called "the Lifshitz-van der Waals" or "non-polar part of adhesion" and an "acid-base component". The acid-base is also termed the "polar part of adhesion". The non-polar and polar adhesion between an asphalt binder and an aggregate are given by Equation 3-9:

$$\Delta G^A = \Delta G^{aLW} + \Delta G^{aAB} = 2\left(\sqrt{\Gamma_S^{LW}\Gamma_L^{LW}} + \sqrt{\Gamma_S^{+}\Gamma_L^{-}} + \sqrt{\Gamma_S^{-}\Gamma_L^{+}}\right) \quad \textbf{Eq. 3-9}$$

where, ΔG^A = Free energy of adhesion, ΔG^{aLW}= Non-Polar or Lifshitz-van der Waals part of adhesion, ΔG^{aAB} = Acid-base or polar part of adhesion, $\Gamma_L^{LW}, \Gamma_L^{-}, \Gamma_L^{+}$= SFE components of asphalt binder, and $\Gamma_S^{LW}, \Gamma_S^{+}, \Gamma_S^{-}$= SFE components of aggregate. Moreover, in order to compute the adhesion of asphalt binder with aggregates in water, Equation 3-10 was used, and subscripts 1, 2 and 3 signify the asphalt binder, aggregate, and water, respectively. Two phases of the material are apt to bind together when the value of free energy of adhesion is positive. The more positive the value is, the higher will be the bonding strength. This is shown by Equation 3-10:

$$\begin{aligned} Adhesion = \Big(& 2\Gamma_3^{LW} + 4\sqrt{\Gamma_3^{+}\Gamma_3^{-}} - 2\sqrt{\Gamma_1^{LW}\Gamma_3^{LW}} - 2\sqrt{\Gamma_1^{+}\Gamma_1^{-}} \\ & - 2\sqrt{\Gamma_1^{-}\Gamma_3^{+}} - 2\sqrt{\Gamma_2^{LW}\Gamma_3^{LW}} - 2\sqrt{\Gamma_2^{+}\Gamma_3^{-}} \\ & - 2\sqrt{\Gamma_2^{-}\Gamma_3^{+}} + 2\sqrt{\Gamma_1^{LW}\Gamma_2^{LW}} - 2\sqrt{\Gamma_1^{+}\Gamma_2^{-}} \\ & - 2\sqrt{\Gamma_1^{-}\Gamma_2^{+}}\Big) \end{aligned} \quad \textbf{Eq. 3-10}$$

where, $\Gamma_1^{LW}, \Gamma_1^-, \Gamma_1^+$= SFE components of asphalt binder, $\Gamma_2^{LW}, \Gamma_2^+, \Gamma_2^-$= SFE components of aggregate, and $\Gamma_3^{LW}, \Gamma_3^+, \Gamma_3^-$= SFE components of water.

3.5.4 Preparation of Samples

The preparation of asphalt samples on glass plates was done in the same manner as discussed earlier (Wasiuddin and Saltibus, 2010; Wasiuddin et al., 2011b). Polishing was conducted for aggregate samples with the use of 600 and 1200 grit size papers with the model Alpha-Beta Polisher, manufactured by Buehler, Lake Bluff, IL. Additionally, water was used to aid in the polishing. Buehler polishing-cloths, in the range of 3-0.02 μm was used for micro-polishing. The cloths (BUEHLER, Lake Bluff, IL) utilized were as follows: ULTRA-PAD: 3 μm (for the removal of particle), TEXMET 2000: 3 μm (used for profile flattening), TRIDENT: 1 μm (for polishing), and MICROCLOTH: 0.02 μm (used for finishing). A non-aqueous lubricant (propylene glycol) was used to perform the polishing with no particulate abrasives. The specimens were rinsed with ethyl alcohol in order to remove loose material, after each stage of the polishing (Cardenas et al. 2011).

3.5.5 Surface Free Energy of Asphalt Binders

Wasiuddin and Saltibus (2010), observed as shown in Table 3-2 that the total SFE of PG 64-22 is 20.4 ergs/cm^2; whereas for PG 76-22M, it is 15.2 ergs/cm^2. It is from the non-polar SFE component (Γ^{LW}) that the major contributions of these energies are derived. For PG 76-22M, the acid-base component is a few times higher than that of PG 64-22, even though the total SFE and non-polar SFE of PG 64-22 are higher than PG 76-22M. The importance of these energy components are to be reflected in dry and wet adhesive strengths and in the cohesive strength. An increase of the total SFE of PG 64-22 to 22.5 and 30.2 ergs/cm^2 was observed by 1% LOF 6500 and 2% Sasobit®,

respectively. The total SFE was increased to 33.4 ergs/cm^2 when these two are applied together. For PG 76-22M a similar pattern was observed, except when 1% LOF 6500 and 2% Sasobit® were together applied. The total SFE of PG 76-22M, then resulted in 16.2 ergs/cm^2. Generally, it was observed that the base component (Γ^-) of SFE for both of the binders increased by these additives. Wasiuddin et al. (2007a; 2007b; 2008) also observed a similar pattern of the increasing of the base component by similar additives.

3.5.6 SFE of Aggregates and Glass Plates

The total SFE of novaculite, limestone and glass plates were 52.6, 51.1, and 49.4 ergs/cm^2, respectively, as depicted in Table 3-2. Despite the similarity of the SFE values, the corresponding non-polar SFE values were 45.4, 25.1, and 35.9 ergs/cm^2. Moreover, the polar SFE values were found to be 7.2, 25.9, and 13.5 ergs/cm^2. As expected, the base SFE component of limestone (Γ^-) was much higher than that of novaculite (75.5 and 40.7 ergs/cm^2), respectively.

Table 3-2: Surface free energy.

Asphalt	Total SFE in(ergs/cm^2, Γ^L)	Non Polar SFE(ergs/cm^2, Γ^{LW})	Acid SFE (ergs/cm^2, Γ^+)	Base SFE (ergs/cm^2, Γ^-)	Acid-Base or Polar SFE(ergs/cm^2, Γ^{AB})
PG64-22	20.4	20.1	0.01	2.0	0.3
PG64-22+ 1% LOF 6500	22.5	21.8	0.1	2.5	0.8
PG64-22+ 2% Sasobit®	30.2	26.8	0.9	3.1	3.4
PG64-22 + 2%Sasobit + 1% LOF 6500	33.4	29.2	1.0	4.4	4.3

Table 3-2: Surface free energy (Continued).

Asphalt	Total SFE in(ergs/cm^2, Γ^L)	Non Polar SFE(ergs/cm^2, Γ^{LW})	Acid SFE (ergs/cm^2, Γ^+)	Base SFE (ergs/cm^2, Γ^-)	Acid-Base or Polar SFE(ergs/cm^2, Γ^{AB})
PG76-22M	15.2	13.1	0.6	1 8	2.1
PG76-22M +1% LOF 6500	29.6	27.4	0.7	1.8	2.2
PG76-22M + 2% Sasobit®	29.3	26.8	0.7	2.2	2.4
PG76-22M + 2% Sasobit® + 1%LOF 6500	16.2	14.1	0.4	2.5	2.1
Novaculite	52.6	45.4	0.3	40.7	7.2
Limestone	51.1	25.1	2.2	75.5	25.9
Glass plate	49.4	35.9	2.1	21.6	13.5

3.5.7 Dry Cohesive Strengths of Asphalt Binders From SFE Measurements

For PG 64-22 and PG 76-22M the cohesive strengths or free energy of cohesion are 40.8 and 30.4 ergs/cm^2 respectively, as depicted in Table 3-3. Additionally, the cohesive strengths of both of these asphalt binders was increased with the use of 1% LOF 6500, 2% Sasobit® and a combination of these two additives.

Table 3-3: Cohesive and adhesive strength.

Asphalt	Cohesive Strength (ergs/cm^2)	Adhesive Strength with Novaculite in (ergs/cm^2)	Adhesive Strength with Limestone in (ergs/cm^2)	Adhesive Strength with Glass Plate in (ergs/cm^2)
PG64-22	40.8	63.4 (18.7)	51.1 (-10.3)	58.9 (29.6)
PG64-22 + 1% LOF 6500	45.0	67.7 (18.4)	55.6 (-10.3)	62.7 (28.9)

Table 3-3: Cohesive and adhesive strength (Continued).

Asphalt	Cohesive Strength (ergs/cm^2)	Adhesive Strength with Novaculite in (ergs/cm^2)	Adhesive Strength with Limestone in (ergs/cm^2)	Adhesive Strength with Glass Plate in (ergs/cm^2)
PG64-22+ 2% Sasobit®	60.4	84.0 (20.9)	73.8 (-6.0)	76.1 (28.4)
PG64-22 + 2% Sasobit® + 1% LOF 6500	66.9	88.1 (18.8)	78.1 (-7.9)	80.3 (26.4)
PG76-22M	30.4	60.2 (17.6)	53.7 (-5.6)	54.5 (27.4)
PG76-22M + 1% LOF 6500	59.3	82.7 (24.5)	70.9 (-3.9)	74.4 (31.7)
PG76-22M + 2% Sasobit®	58.5	81.9 (22.9)	70.5 (-5.1)	74.0 (30.5)
PG76-22M + 2% Sasobit® + 1%LOF 6500	32.3	60.9 (15.8)	53.9 (-7.8)	55.8 (26.2)

*Values in ( ) are taken in the presence of water.

3.5.8 Comparison of Dry Cohesive Strengths from Pull-Off Test and SFE Measurements

For PG 64-22 and PG 76-22M, the dry pull-off strengths (dry cohesive strengths) from the PATTI were 1.964 and 2.067 MPa, respectively. However, the free energy of cohesion (called the dry adhesive strengths) from the SFE measurements were 40.8 and 30.4 ergs/cm^2.

G*/sinδ (G* - complex shear modulus, δ - phase angle) as it is known, gives an indication of stiffness against rutting of PG 76-22M, was much higher than that of PG 64-22. The G*/sinδ values of PG 64-22 and PG 76-22M varied greatly at 70°C; whereas, the values were comparable at lower temperatures for instance at 34°C (Table 3-4). From the pull-off test, the dry cohesive strength obtained where PG 76-22M showed slightly higher cohesive strength than that of PG 64-22 can be justified. However, what

cannot be justified, is that PG 64-22 yielded higher cohesive strength than that of PG 76-22M as obtained from the SFE measurements. In Table 3-3, it is observed that cohesive strengths obtained from SFE measurements show that the additives increased the cohesive strengths. G*/sinδ values also increased with the addition of 2% Sasobit® at a temperature of 34°C. However, all the additives and their combination reduced the dry cohesive strengths of both asphalt binders from the cohesive strengths obtained from the pull-off test. (Wasiuddin and Saltibus, 2010; Wasiuddin et al., 2011a, 2011b)

Table 3-4: G*/Sinδ results.

G*/Sinδ in kPa		
Temperature	Average at 34°C	Average at 70° C
PG64-22	227.85	1.43
PG76-22M	247.9	4.32
PG6422M+2%Sasobit®	618.0	
PG76-22M+2%Sasobit®	473.9	

3.5.9 Dry Adhesive Strengths from SFE Measurements

From the SFE measurements, the dry adhesive strengths or the free energy of adhesion obtained between PG 64-22 with and without additives and novaculite reflected higher values than that of limestone. As depicted in Table 3-3, for PG 76-22M, a similar trend is noted. Table 3-2 also shows the dry adhesive strengths of the asphalt binders with the presence and without the presence of additives. Limestone, as can be observed, has better dry adhesive strength with PG 76-22M than with PG 64-22. This was not so with novaculite which reflects higher adhesive strength with PG 64-22 than PG 76-22M. The pull-off test samples was observed not to fail in adhesive mode in dry condition and therefore, dry adhesive strengths (free energy of adhesion) that were acquired from SFE measurements were not able to be justified.

3.5.10 Wet Adhesive Strengths from SFE Measurements

For limestone, as is depicted in Table 3-3, the wet adhesive strengths were negative which suggests that spontaneous stripping of asphalt binder will occur. Novaculite is less moisture susceptible than limestone, as the wet adhesive strengths of the former are positive. Furthermore, among the three materials, the glass plate was the best performer. The worst performer, as depicted in Table 3-3, was when 1% LOF 6500 and 2% Sasobit® were applied together.

3.5.11 Comparison of Wet Adhesive Strengths from Pull-Off Test and SFE Measurements

From the SFE measurements, (Wasiuddin and Saltibus, 2010) the wet adhesive strengths of the glass plates were 29.6 and 27.4 ergs/cm^2, respectively, as compared to the wet adhesive strengths obtained from the pull-off test (1.039 and 1.642 MPa, respectively). The application of both 2% Sasobit® and 1% LOF 6500 together, generated the lowest wet adhesive strengths as both methods indicate. The corresponding values obtained from the pull-off tests were 0.898 and 0.984 MPa, respectively . However, in the case of the SFE measurements, the values obtained,were 26.4 and 26.2 ergs/cm^2, respectively, for PG 64-22 having both additives and PG 76-22M having both additives as well.

3.6 Conclusions

The following conclusions based on the tests performed in this study were arrived at by Wasiuddin and Saltibus, (2010); Wasiuddin et al., (2011a, 2011b):

- A lot of moisture sensitivity test methods are available and AASHTO T283 is used by most of the agencies. A critical review of the literature

indicates that AASHTO T 283 does not necessarily explain the mechanisms of moisture induced damage or the stripping of asphalt binder.

- The literature review on moisture damage mechanisms and theories indicated that the surface free energy method is the most promising one due to its approach for fundamental properties of materials, its theoretical interest, modeling approach and its applications to other pavement damages such as fatigue and healing.
- A moisture conditioning procedure has been developed and proposed that comprises mainly of heating the asphalt coated substrate at 64°C inside the oven in submerged condition. The proposed conditioning procedure was able to develop purely adhesive failure in most cases.

Based on the adhesive failure achieved, a new mechanism on moisture damage has been proposed: Under submerged conditions at pavement service temperatures, water develops randomly distributed micro- and macro- scale cylindrical holes on asphalt film within reasonable time period that penetrates up the asphalt-substrate interface and starts replacing asphalt film from the substrate surface and adhesive failure or stripping is observed. The first process will be called dewetting of the asphalt film from the substrate and the second process will be called spreading of moisture on substrate.

Based on the adhesive failure procedure and the mechanism involved, the researchers also proposed a moisture damage theory for asphalt mixes: It was therefore proposed by the researchers that there should be a two-step process which involved the adhesive failure or stripping in an asphalt-aggregate system: (1) That asphalt film dewets

from the aggregate which forms randomly distributed holes in the asphalt film in water at pavement service temperatures followed by (2) the spreading of water on aggregate in the process replacing asphalt films. The dewetting of the asphalt film from that of the aggregate will be a function of the dewetting coefficient, P, which can be described as the additional pressure that is derived from capillary force. Moreover, the spreading of water on the aggregate surface is to be dependent on the spreading coefficient, S. This parameter, S, can be defined in terms of the reduction in surface free energy on losing the asphalt-aggregate surface which will then form new water-aggregate and asphalt-water interface. Therefore, the higher the values of P and S (coefficients), the higher would be the moisture susceptibility.

- The dry cohesive strengths from pull-off test of PG 64-22 and PG 76-22M were 1.964 and 2.067 MPa, respectively which is very close. Dry cohesive strength of asphalt binders using pull-off test indicate that adding 2% Sasobit® or 1% LOF 6500 or combination of these two additives reduces the cohesive strengths of both the asphalt binders used in this study. The reduction can be as much as 50.0% as has been observed for PG 76-22M with both the additives. The cohesive strengths obtained from SFE measurements indicate that PG 64-22 has higher cohesive strength (free energy of cohesion) than that of PG 76-22M. Also, addition of additives increases the cohesive strengths of asphalt binders according to SFE measurements.
- The researchers investigated different moisture conditioning methods to achieve pure adhesive failure or stripping of asphalt film. Finally, the

simple procedure followed in this study was effective in producing adhesive failure. With this moisture conditioning procedure it was observed that PG 64-22 original, with 1% LOF 6500 and with 1% LOF 6500 plus Sasobit® exhibits adhesive failure while PG 64-22 plus Sasobit® produces mixed mode of failure. For PG 76-22M, only original samples (without additives) exhibited adhesive failure. Mixed mode of failure was observed for 1% LOF 6500 and 1% LOF 6500 plus Sasobit® while cohesive failure was observed for Sasobit®. This indicates that 1% LOF 6500 is not effective for moisture resistance while Sasobit® changes the mode of failure to mixed or cohesive but not necessarily increasing strength.

- The adhesive strengths (free energy of adhesion) obtained from SFE measurements were compared with that of pull-off test. The results do not necessarily correlate well except that both the methods (pull-off and SFE) indicate that combination of 2% Sasobit® and 1% LOF 6500 increases moisture susceptibility.
- Besides cohesive and adhesive strengths, SFE measurements indicated that addition of additives used in this study increased the base component of SFE. Also, it indicated that limestone is much more basic than novaculite. The base SFE components of limestone and novaculite are 75.5 ergs/cm^2 and 40.7 ergs/cm^2, respectively.

- Overall, pull-off test was found useful to predict adhesive failure or stripping and SFE method can be useful to measure the dewetting parameter, P and spreading co-efficient, S as proposed in this study for moisture susceptibility analyses.

CHAPTER 4

DEWETTING OF APSHALT BINDER ON GLASS SUBSTRATE

4.1 Background and Objectives

To understand the dewetting phenomenon observed in the previous chapter, nucleation and growth of dewetted holes were recorded and characterized under microscopic setup under submerged water condition. It was observed in this chapter that dewetting, reported in Chapter 3, occurs under an air bubble in the submerged asphalt film. The parameters that were varied to understand and characterize dewetting are specified in the following objectives:

- To observe under an air bubble (that forms spontaneously in the submerged water condition), the moisture damage in three performance grade (PG) asphalt binder films (PG 58-28, PG 64-22, and PG 76-22M), in the form of the dewetting mechanism on glass plate at various temperature ranges.
- To observe the effects that additives may have on the dewetting process of the asphalt films on the glass plate substrates.

4.2 Methodology and Experimentation

Three performance graded asphalt binders were used in the experiments, namely PG 58-28, PG 64-22, and PG 76-22M binder (Table 4-1-Test Matrix). Additives were added to investigate the effects that the modified asphalt binders would have on the

dewetting mechanism. Dewetting temperature range, thickness, and curing conditions are described in Table 4-1.

Table 4-1: Test matrix for glass plate samples.

Figure	Asphalt	Temperature (°C)	Thickness (μm)	Curing Condition
4-4	PG64-22	Ambient to 40	94.78	Oven Cured
4-5	PG64-22	Ambient to 40	94.50	Oven Cured
4-6	PG64-22	Ambient to 40	94.50	Oven Cured
4-8	PG64-22	Ambient to 50	102.36	Oven Cured
4-9	PG64-22	Ambient to 50	86.61	Oven Cured
4-11	PG64-22	Ambient to 60	78.74	Oven Cured
4-12	PG58-28	Ambient to 40	125.98	Oven Cured
4-14	PG58-28	Ambient to 50	141.73	Oven Cured
4-15	PG58-28	Ambient to 50	165.35	Oven Cured
4-16	PG58-28	Ambient to 60	102.36	Oven Cured
4-17	PG76-22M	Ambient to 40(Increased to 50)	130.71	Oven Cured
4-18	PG76-22M	Ambient to 40 (Increased to 50)	78.74	Oven Cured
4-19	PG76-22	Ambient to 50	114.83	Oven Cured
4-20	PG 76-22	Ambient to 50	149.61	Oven Cured
4-21	PG58-28 + 1% LOF 6500	Ambient to 50	67.71	Ambient Cured
4-22	PG76-22 + 1% LOF 6500	Ambient to 50	102.36	Ambient Cured
4-23	PG58-28	Ambient to 50	75.59	Ambient Cured
4-24	PG64-22 + 2% Sasobit®	Ambient to 60	110.24	Ambient Cured
4-25	PG58-28 + 1% LOF 6500	Ambient to 50	118.11	Ambient Cured

4.2.1 Test Matrix Used for Testing

Many trial samples were used for developing the test procedure and for the development of the software. A final set of samples are reported in this dissertation that consisted of the test matrix as seen in Table 4-1. For PG 64-22, six samples were used

with three different temperatures increases, ambient to 40, 50, and 60°C. For PG 58-28, four samples were used at ambient to 40, 50, and 60 °C. For PG 76-22M, four samples were used at ambient to 50°C.

As this chapter is used to report the characterization of the dewetting phenomenon of asphalt films, many variables were used in the test matrix including oven cured or ambient cured, anti-strip additives and warm mix additive, as can be seen in Table 4-1.

4.2.2 Procedure Used in Sample Preparation

The procedure used in this study is described below:

1. Glass plates (measuring 2 in. x 2 in. x ¼ in. thick) were cleansed in soap water and heated for 15 minutes at 163 °C. Tape (3M Company, USA) (~0.13 mm thick) was used on two opposite ends of the glass plates to control the thickness of the asphalt, and as a result, the final area was reduced to 2.5 cm x 5.08 cm.
2. The glass plate (PILKINGTON, Toledo, OH; melting point, > 1100°C, Specific gravity, 2.45) specimens were then heated for approximately 1 h while the asphalts were heated for approximately 45 min at a temperature of 163°C.
3. The asphalt was applied on the glass plate with the help of a silicone mold (TA Instruments, New Castle, DE; Gilson Company, Inc., Lewis Center, OH). (The asphalt film thickness was approximated by the gravimetric technique. Upon curing, the excess asphalt was cleansed carefully with solvent (Kleane Strip Paint Thinner).
4. The asphalt samples were then cured for 75 min in the oven at 60°C before being placed in the desiccators and are called "pre-cured" or "oven cured" samples in

this study. Some samples were not cured and placed directly in the desiccators after being prepared. These samples hereafter are called "ambient cured".

5. All specimens, before testing, were left in ambient temperature for 24 h.

4.2.3 Testing Procedure

To generate the necessary temperature for the water, a hotplate was used. A small pyrex container was placed at a preferred level to accommodate at least 4 mm of water above the specimen surface to reduce the loss of accuracy that can take place when there is too much diffracted light when a high level of water is present. As the water was being heated, a slight amount of water was added at specified time intervals to control the height of the water. The temperature was taken after pouring and also at other times to assess the temperature increase. When necessary, the camera was slightly adjusted. A light microscope from Amscope® (Irvine, California), model MD 400E, was used in conjunction with a desktop computer for taking snapshots of the frames as the experiment was being conducted. The frames were taken at 10 s intervals until completion. The microscope was calibrated with a 1 mm scale rule at 40 X, which was supplied by the microscope's manufacturer. The calibration ruled out the effect of water above the sample. Figure 4-1 (a) shows the experimental setup for the dewetting of asphalt binder in submerged water condition, and Figure 4-1 (b) shows a typical asphalt sample used for testing.

(a)

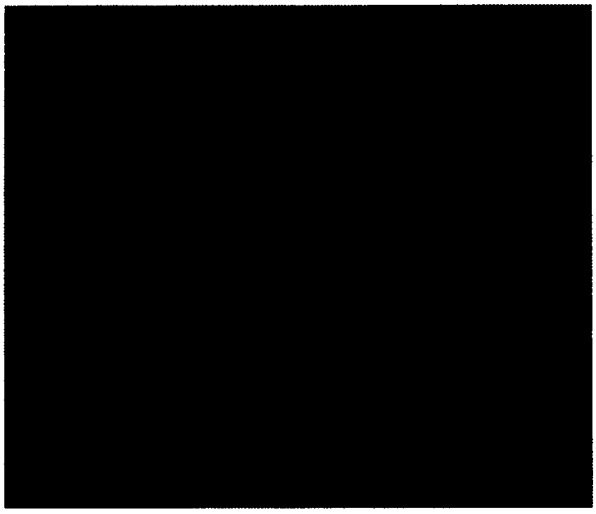

(b)

Figure 4-1: (a) Experimental setup for the dewetting of asphalt binder in submerged water condition for glass plate analysis, **(b)** Typical asphalt sample used for testing .

4.3 Adoption of an Image Analysis Program (NIV Builder 2012)

To aid in the analysis of the dewetting of asphalt film on both the glass plate surface and aggregate (Chapter 5), an industrial software was adopted named (National Instruments Vision Builder AI 2012 (NIVB) which includes an image analysis program. The program was used to calculate the area of the hole as it expands.

4.4 Spreading Experiment of Bitumen Used in Floatation Industry

Due to a heterogeneous surface which is not perfectly smooth, there exist, possibly, trapped air pockets in the film or at nucleation sites. Additionally, dust on asphalt surfaces can serve as nucleation sites. The spreading of bitumen has been investigated in the past and still continues to be, especially in the floatation industry (Lelinki et al., 2004). To examine bitumen (not the same as asphalts used in the pavement industry) film transfer from a quartz surface to an air bubble, Lelinki et al. (2004) used toluene-extracted White rocks bitumen (approximately 1 mm thick) diluted with 10% kerosene by weight. The quartz specimen was placed upside down on two supports placed in a glass cell in alkaline (NaOH) solution. A bubble of 2.5 to 3.5 mm was induced in the bitumen. It was observed that as the bitumen spread on the air/water interface, three possible layers of the bitumen could be formed (Figure 4-2).

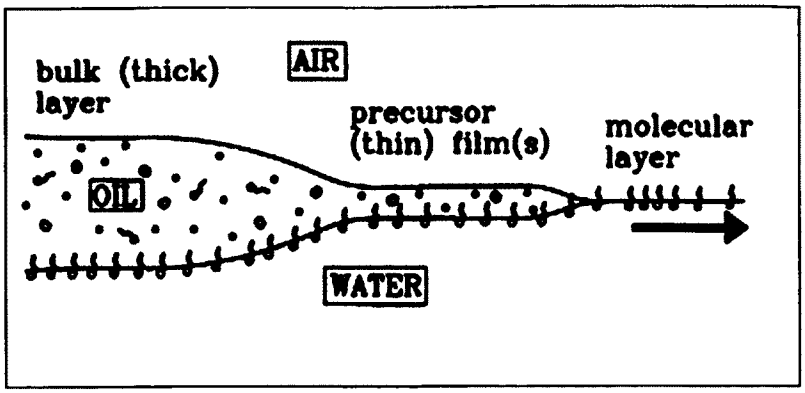

Figure 4-2: Schematic of possible films formed by the bitumen during its spreading over the water surface. Reprinted with permission. Darius Lelinski, Jaroslaw Drelich, Jan D. Miller and Jan Hupka, 2004. Rate of Bitumen Film Transfer from a Quartz Surface to an Air Bubble as Observed by Optical Microscopy. Canadian Journal of Chemical Engineering, 82.

Areal velocity, linear velocity, and surface coverage at varying temperatures were some of the parameters that were investigated in Lelinki et al. (2004). At high temperatures (50°C– 60°C), bitumen film transfer was found to be more efficient as opposed to that of room temperature. Moreover, the activation energies for the bulk layer were reported to vary from 66 to123 kJ/mol. For the precursor film (the layer next to the molecular layer (Figure 4-2) it was found to be 105 kJ/mol.

4.5 Asphalt Pavement Related Moisture Damage and Dewetting

In investigating the surface energies and adhesion properties in asphalt-aggregate systems, Thelen (1958) calculated the free energy change as asphalt spreads on water and was found to be 16 ergs/cm^2 while he found that the free energy change for the spreading of asphalt at room temperature and humidity over a stone surface was 33 ergs/cm^2. Thelen (1958) have also highlighted that even though the destruction of asphalt films on stone by water can take place under a variety of conditions by many

mechanisms, the most likely occurs where there is a discontinuity in the film as a result of a line of contact with water, asphalt, and that of stone. Additionally, blister formation was reported after the asphalt from the stone surface has covered a drop of water and burst afterwards leaving what is called a "pit". Thelen (1958) noted that dust on the aggregates does have a tendency to trap air, which can enhance stripping by providing channels at the interface. He observed that although in practice the importance of such a phenomenon is not known, theoretically it can be significant. It was noted that there is a high probability that air is trapped at the interface between an adherent and a solid substrate not excluding asphalt and aggregate (Thelen, 1958). If that is the case, the analysis and theory put forward by Slavchov et al. (2005) can be significant although the trapped air may not have a distinct shape to that of a gas bubble. Moreover, Fromm (1974) presented two mechanisms of stripping: spontaneous emulsification and pull back (the spreading of the asphalt on the air/water interface). This moisture damage process was highlighted in a report by Brown et al. (1972). Field and Fang (1967), in conducting the static immersion test, recognized the stripping left under an air bubble on the stone surface and the spreading of asphalt on air bubble from the glass plate. This observation, the authors attribute to stripping of asphalt in the asphalt mix in the pavement. Moreover, in conducting experiments on non-solvent induced dewetting of thin polymer films (nanometer range), Xu et al. (2007) investigated dewetting of polymer films and observed that the process of non-solvent-induced dewetting was prominently different from other dewetting processes.

The authors proposed that the formation of holes could occur as the water molecules penetrate into the polymer film, and after that the capillary force drives the

formation of holes. They additionally note that the capillary force must be strong enough that it is able to drive the process of hole formation. In this present study, the aim was to attempt to measure the dewetting of the asphalt from the substrate (glass plate, and aggregate) under the base of the air bubble as it dewets. As has been noted, quantitative studies have been undertaken to measure the spreading properties of the bitumen in the floatation industry.

4.6 Results and Discussion

In this study, dewetting of an asphalt film inside an air bubble attached to the asphalt film surface under water submerged condition was analyzed. Figure 4-3 (a) below shows an air bubble attached to an asphalt film surface submerged in water, while Figure 4-3 (b) shows the stages of asphalt dewetting.

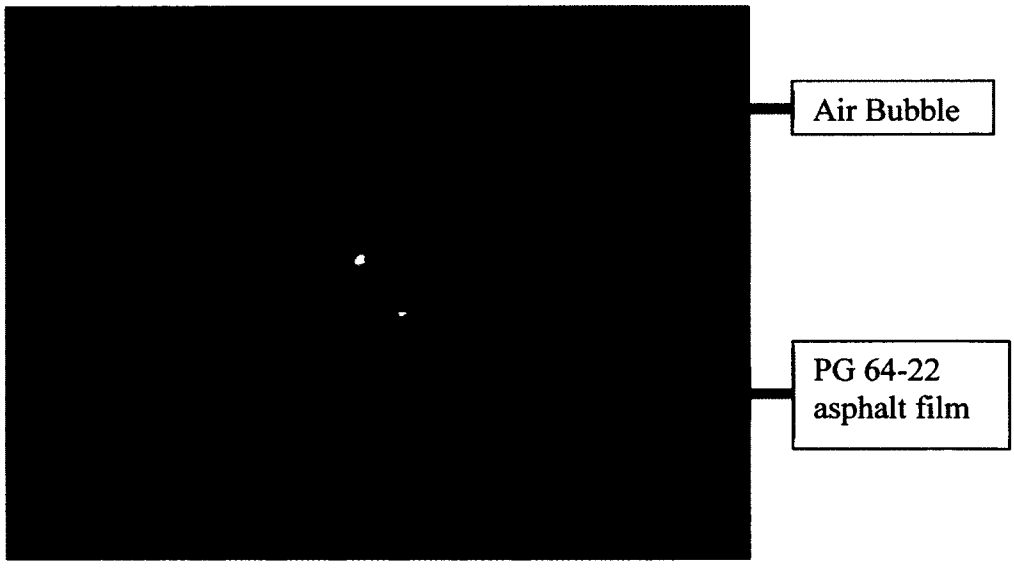

(a)

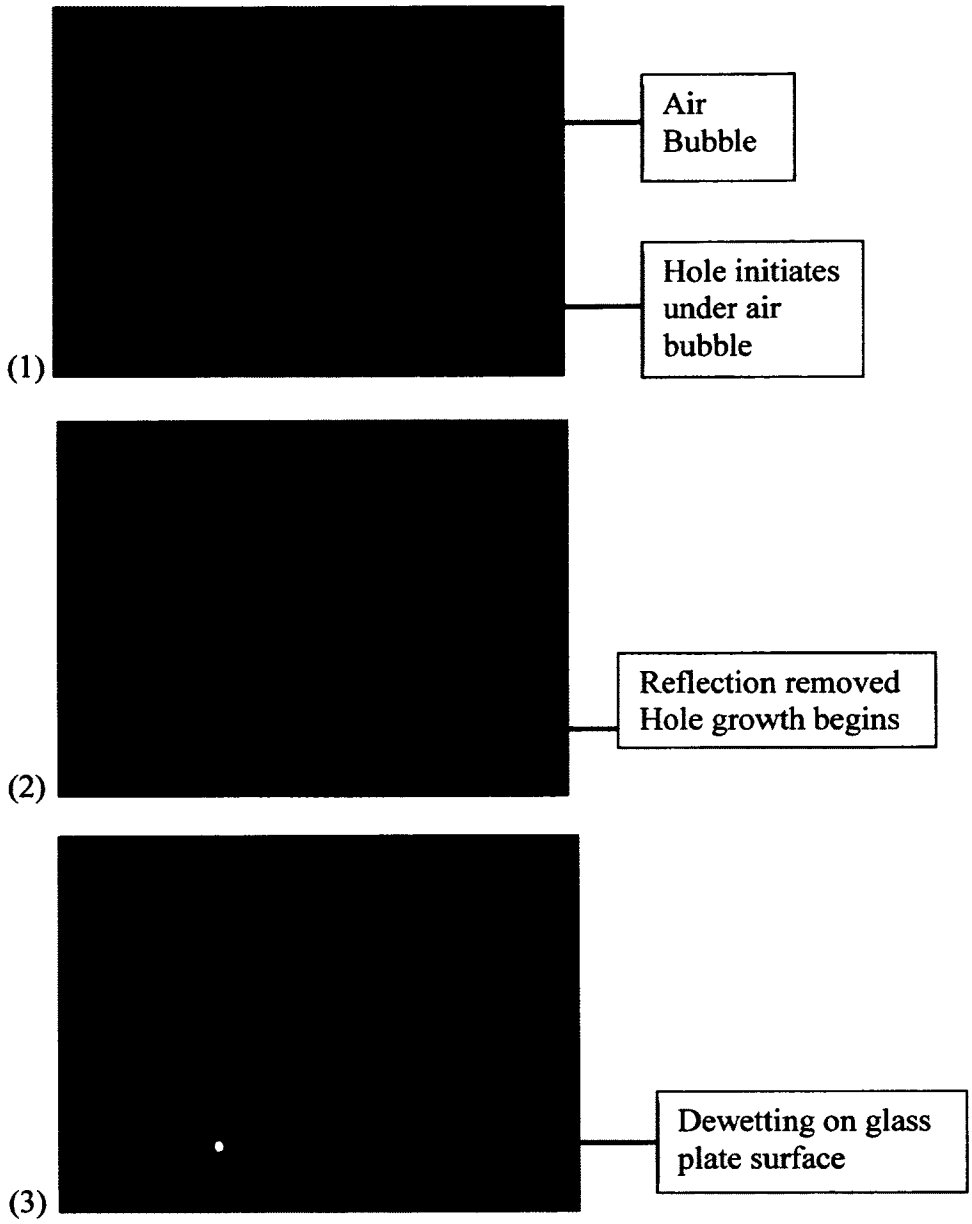

(b)

Figure 4-3: (a) Air bubble on the surface of an asphalt film (PG 64-22) submerged in water. The asphalt film is prepared on a glass plate **(b)** Stages of asphalt dewetting.

4.6.1 Brief Description of Nucleation and Growth of a Hole

(1) As has already been discussed, trapped air pockets possibly exist in the film or at nucleation sites due to a film surface that is heterogeneous and not perfectly

smooth. After the air bubble was located, it was observed to grow in size. The light which is housed below the stage of the microscope is turned on and left on for the duration of the experiment. After time elapses, dewetting initiated from the top of the asphalt film which was observed by the camera to be reddish in color (Figure 4.3 (b)). This reddish color signified that it was fully dewetted and that the layer of film that remained allowed for light to pass through.

(2) The light source was turned off and the reflection in the camera was no longer visible. Only the reddish color was now visible.

(3) As the hole began to expand, the reddish color slowly disappeared making way for the light to appear fully through the hole. The hole began to grow and the radius growth vs. time was generally in the form of a logarithmic pattern.

4.6.2 PG 64-22 Asphalt (Oven Cured) Samples

In this study, air bubbles were allowed to be generated or to be attached to the surface of the asphalt film on their own and the dewetting occurred spontaneously, depending on time and temperature. Most bubbles were estimated to be in the micrometer range (less than 1 mm). The glass plate samples were moved as needed in the water as the temperature increased in an effort to locate a bubble. Table 4-1 shows the testing temperature ranges and thicknesses of oven cured and ambient cured samplesused in the dewetting experiments. Figures 4-4 to 4-6 presents dewetting of three PG 64-22 asphalt samples of approximately similar thicknesses.

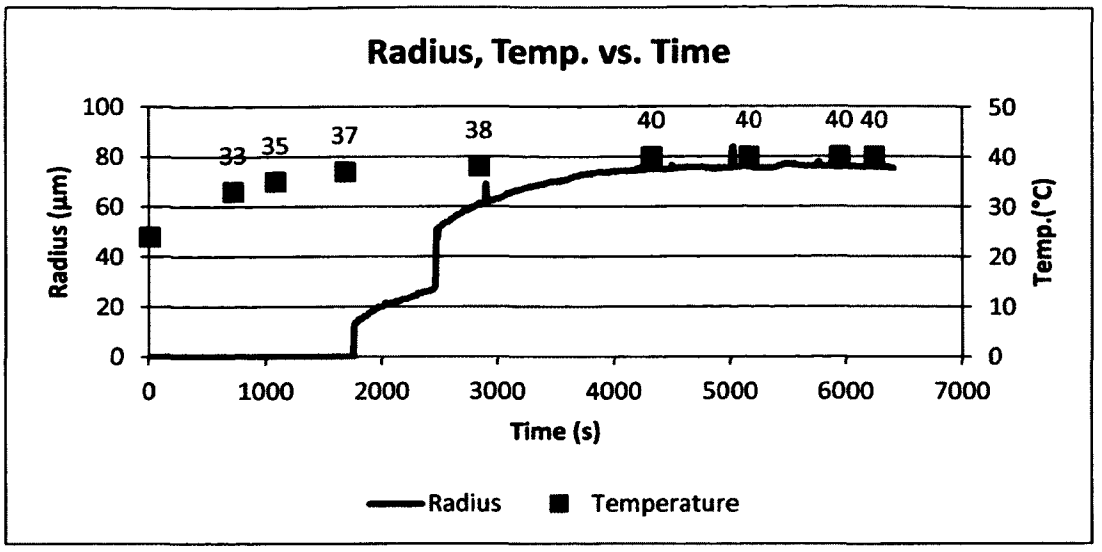

Figure 4-4: Dewetted radius and temperature vs. time of PG 64-22 asphalt on glass plate of a temperature increase from ambient to 40°C in submerged water condition.

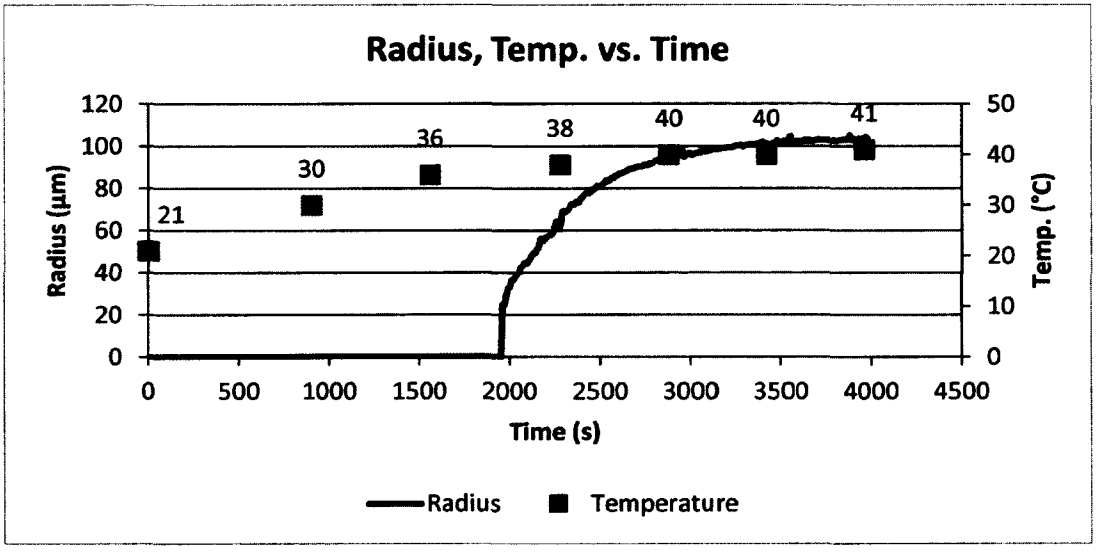

Figure 4-5: Dewetted radius and temperature vs. time of PG 64-22 asphalt on glass plate of a temperature increase from ambient to 40°C in submerged water condition.

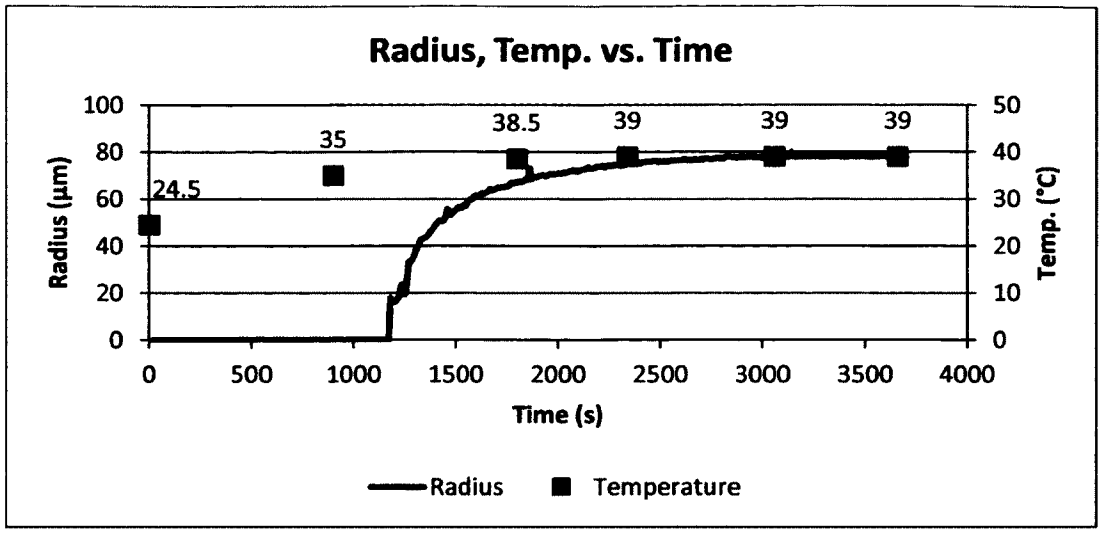

Figure 4-6: Dewetted radius and temperature vs. time of PG 64-22 asphalt on glass plate of a temperature increase from ambient to 40°C in submerged water condition.

Although these samples were pre-cured in an oven at 60°C for 75 min before placing in ambient temperature for 24 h (minimum 18 h), the asphalt film surface may not be totally homogenenous in nature. In Figure 4-4, the jump in the dewetting pattern was the result of the first hole merging into another faster growing hole within the close proximity of the second (See Appendix, Figure C-1). The dewetting began at a temperature above 35°C. The same was observed in Figure 4-5 and Figure 4-6. From these observations, it can be said that dewetting and rupture of the asphalt film from the film surface at the base of the air bubble down to a certain portion within the asphalt film could have already occured. The three films, were approximated in thicknesses of about 94.78, 94.50, and 94.50 µm, respectively. As asphalt is dark due to its chemical composition and cannot be properly captured by the optical stage microscope, initial stages of dewetting from the surface of the film to the time the asphalt actually started dewetting from the glass plate surface would be difficult to observe. Nonetheless, that time difference should not be long concidering these film thicknesses. Another key

observation made in Figure 4-4 to Figure 4-6 is that the time dewetting initiates was different for all three samples.

Contributing factors may very well include, the size of the bubble at the time of dewetting and the size of the defect that may be at the surface or possibly below the surface of the asphalt film. The water level above the glass plate samples was kept to approximately 5 mm. If there were multiple air pockets in the film at a particular nucleation site, they would coaggulate and give rise to the growth of an air bubble. Moreover, at atmospheric pressure polymers take up some amounts of gas, accumulating in specific areas where the material is less dense (Jacobs et al. 1998).

Therefore, this is highly possible in the case of asphalt films.Upon observing some specimens with the eyes rather than that of the attached video (after removing the sample from its submerged condition), there appeared to be three films present (Figure 4-7). Each film layer in sequence had multipe dewetted holes in the micrometer range. In some cases, only one thin film was present and attached to the glass substrate. The thinnest layer was attached to the glass plate (that which was very light in texture could very well be the closest in measurement to that of a monolayer, as was observed by Lelinki et al. (2004) where bitumen from the Whiterocks spreads on the bubble surface). In a few cases this layer was absent especially when the major hole is very small. The next layer is somewhat light brown in texture, followed by a third layer. Layer 1 is the layer attached to the glass plate and layer 3 would be two layers above it. An approximation of this phenomenon (layer patterns) is dipicted in the Figure 4-7.

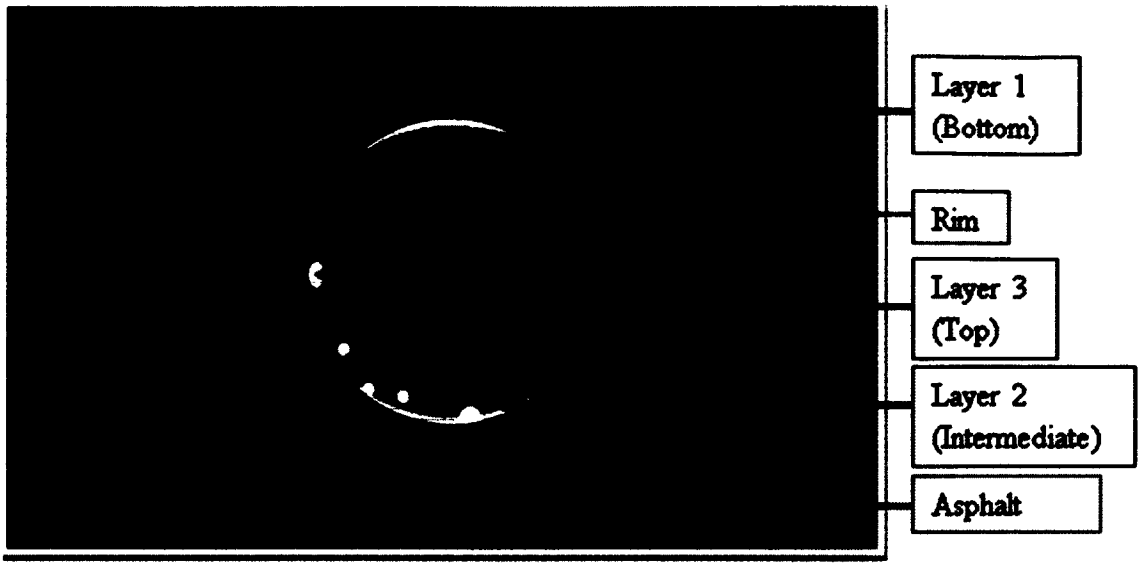

Figure 4-7: Approximate plan view of a typical arrangement of the three films that are left after nucleation and growth of hole has occurred.

The three layers may very well be related to the bulk layer, the precusor film and that of the monolayer disscussed by Lelinki et al. (2004).This phenomena could not have been possibly picked up by the camera for two reasons: the sensitivity and power of the camera and also due to the fact that the dewetting is taking place under water even though the accuracy that is lost under water is very little based on the water level (~ 5 mm). Xu et al. (2007) also observed the coalesce of holes in nonsolvent induced dewetting of polymers. In all three graphs, the hole grow exponentially. As asphalt is a viscoelastic material the radius growth of a hole with respect to time can quite possibly be followed by the dewetting models presented for viscoelastic polymers (Brochard-Wyart et al., 1997; Vilmin and Raphaël, 2006). In most dewetting experiments presented in the literature, epecially viscoelastic polymer films, the dewetted film was collected into a rim as it dewetted from the surface, (hydrophillic or hydrophic). In the present experiment, this rim can only be realized based on the thickness of film in the micrometer range and

that of the bubble height. Upon removal of the samples from their submerged condition in water, this rim was quite visible. Again, it must be noted that the base of the dewetted hole, or the space in which the air bubble was located, was smaller than the top of the hole which corresponded to that of the rim. Also, the smaller the diameter of the hole that was dewetted, the more cylindrical the hole would be. The former was due to capillary forces and the latter was due to viscous dissipation.

Next, the dewetting of PG 64-22 asphalt film at ambient temperature to 50°C is investigated. In Figure 4-8, the graph has a peculiar shape.

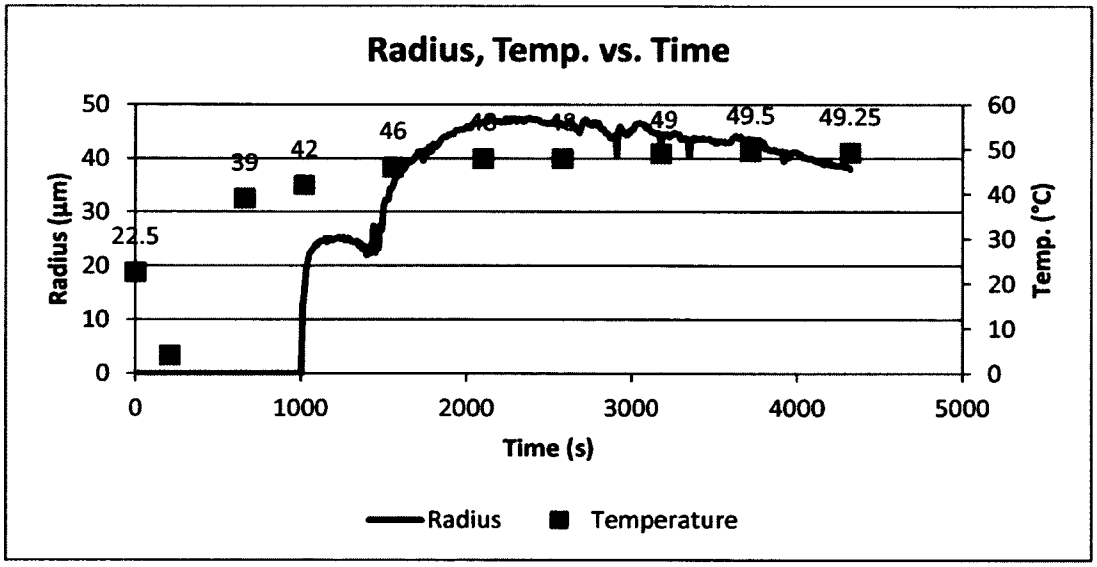

Figure 4-8: Dewetted radius vs. time of PG 64-22 asphalt on glass plate of a temperature increase from ambient to 50°C in submerged water condition.

The first section on the graph represents a dewetting hole as it grows, but within a short space of time, this hole began diminishing in size and as it did so, another hole adjacent to it began to open. As the first hole closed, at a certain point, it was approximately merged in the second hole for analysis. An exponential growth of the hole was visible where it grew relatively rapidly as the temperature increased from 46°C,

remaining relatively constant for some time and then decreased slightly until the end of the experiment. In this scenario, especially the first hole, what is called "healing of asphalt" may have taken place. Based on an equation derived by Sharma (1993)(Czarnecki et al., 2005) with modifications to the critical thickness equation, $e_c = 2\kappa^{-1}\sin\left(\frac{\theta_E}{2}\right)$ for macroscopic liquid films, Czarnecki et al. (2005) point out in their investigation of bitumen films, in Athabasca and other oil sands, that whenever a hole is formed in a film that is thicker than the critical thickness (when there is no solution for the Young-Laplace equation), the hole will eventually heal itself and the film, therefore, will remain stable.

In Figure 4-9 (PG 64-22 Asphalt, ambient to 50°C), there are two holes being dewetted, the main one being the largest of the two.

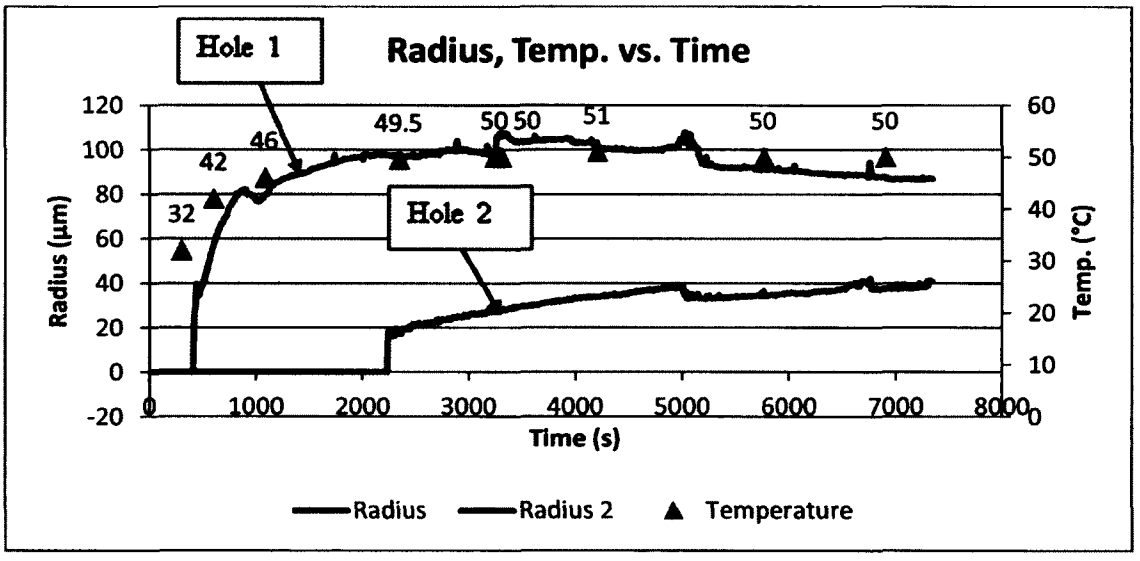

Figure 4-9: Dewetted radius and temperature vs. time of PG 64-22 asphalt on glass plate of a temperature increase from ambient to 50°C in submerged water condition (hole 1 and hole 2).

On the one hand, dewetting of hole 1 occured just above 32°C, following the exponential growth with the initial dewetting taking place very quickly. From 5000 s onward hole 1 appears to want to heal even at a constant temperature of 50°C. On the contrary other hand, for the second hole, dewetting initiated rather late, as compared to hole 1. It increased slowly and steadily and toward the end appears to become constant. The early part of the graph increased linearly with time. It must be noted that approximately the same time that elapsed, approximately 5000 s there was a drop in the curve for the larger hole while the smaller hole continues to grow. Nonetheless, within the region of 7000 s, both holes were growing at a constant rate. Figure 4-10 shows the second hole as it begins to dewet in reference to the first hole.

Figure 4-10: Initiation of the second hole that will dewet while the first hole has grown excessively; location is at 1900 s after start of experiment.

In order to evaluate the effect of higher temperatures, some samples were heated from ambient to approximately 60°C. The highest temperature recorded in Figure 4-11 is 65°C.

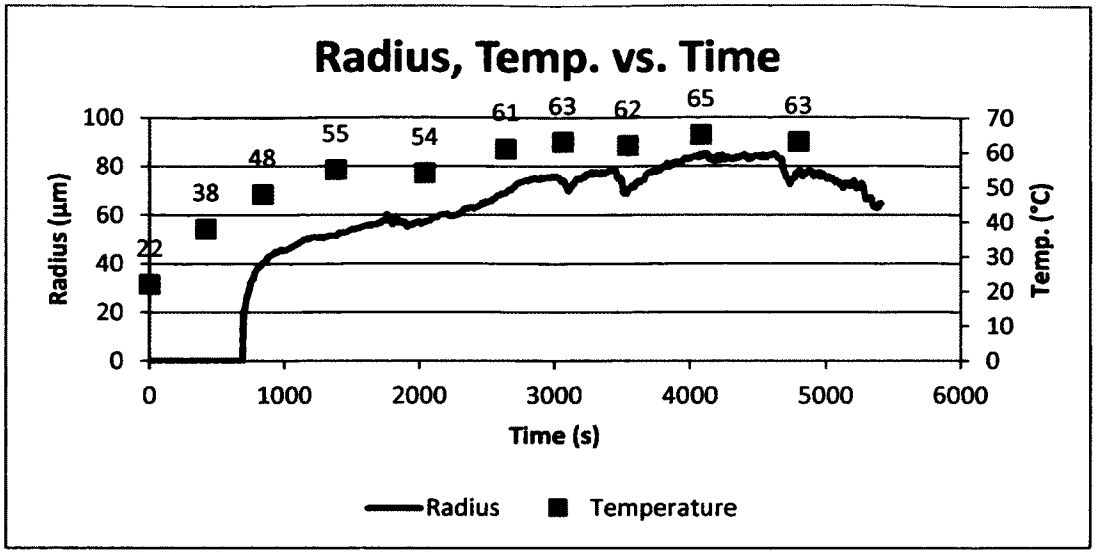

Figure 4-11: Dewetted radius and temperature vs. time of PG 64-22 asphalt on glass plate of a temperature increase from ambient to 60°C in submerged water condition.

The hole initiated and grew at just above 38°C, and the radius grew from approximately 40 to 70 μm in a linear pattern. From 63°C, the hole appeared unstable as it decreaseed slightly twice, increased steadily and finally decreased. From 4800 s at 63°C, the hole began to heal even at such a high temperature.

In general, the holes grow exponentially at the beginning then grow linearly, and finally, very slowly reach equilibrium. From the three samples tested at ambient to 40°C, dewetting of PG 64-22 took place relatively undisturbed, for a long time duration except in Figure 4-4 and then arrived at an asymptote. In case of dewetting of PG 64-22 from ambient to 50°C sample, the graph tended to the asymptote in a shorter time span, even though dewetting began at different stages. Clearly, temperature has a significant role in dewetting of pre-cured PG 64-22 asphalt.

4.6.3 PG 58-28 Asphalt (Oven Cured) Samples

The dewetting of PG 58-28 asphalt binder having a viscosity less than that of the previously investigated asphalt, PG 64-22, was next investigated. Figure 4-12 shows that the rate of radius growth was high, right off the inception of the hole.

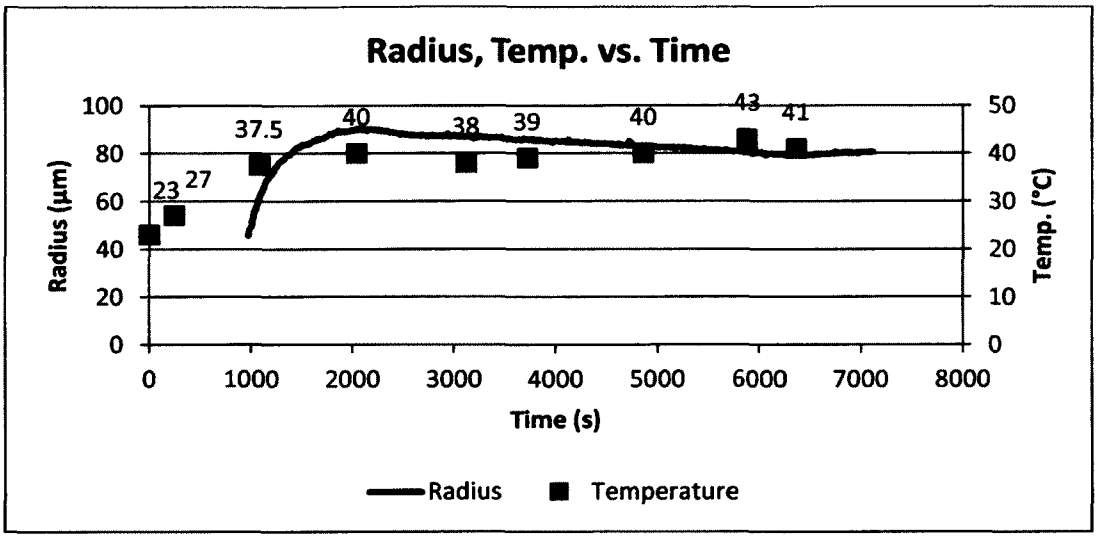

Figure 4-12: Dewetted radius and temperature vs. time of PG 58-28 asphalt on glass plate of a temperature increase from ambient to 40°C in submerged water condition.

A peak radius was attained at approximately 40°C and then, the radius decreased slightly over time, and remained constant at approximately 80 µm for the latter part of the observation. It must be highlighted that the growth of this specific hole was from the onset two holes in close proximity being merged, and then expanding to give rise to a larger hole as is shown in Figure 4-13.

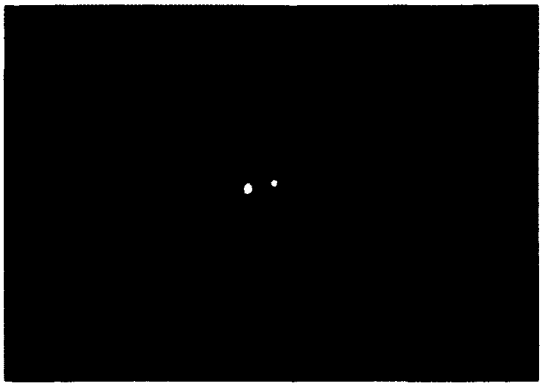

(a) Location is at 970 s after start of experiment

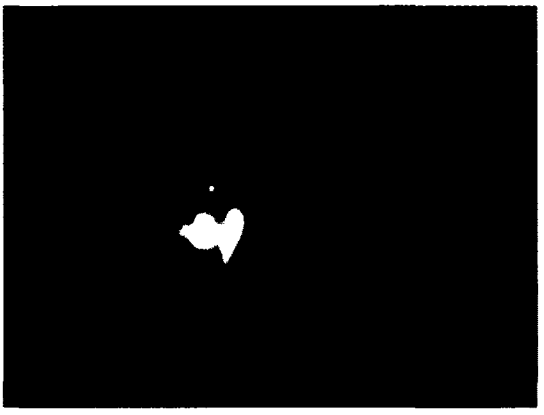

(b) Location is at 1150 s after start of experiment

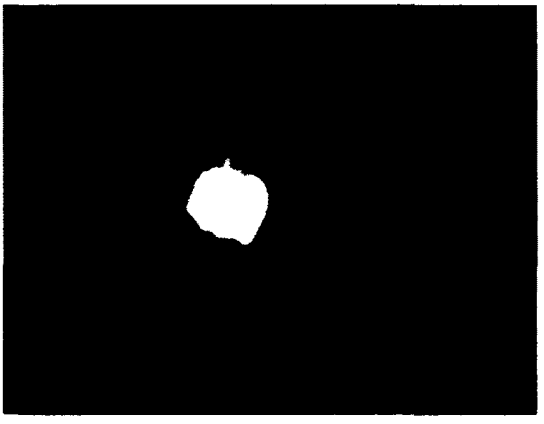

(c) Location is at 1310 s after start of experiment

Figure 4-13: Stages of the dewetting of holes via merging and expanding (a) Location is at 970 s after start of experiment, (b) Location is at 1150 s after start of experiment, (c) Location is at 1310 s after start of experiment.

In Figure 4-14 dewetting of the hole started relatively late, over 2000 s at a temperature higher than that of 47°C, and making its way to an approximate constant growth early, remaining there within the vicinity of about 50°C.

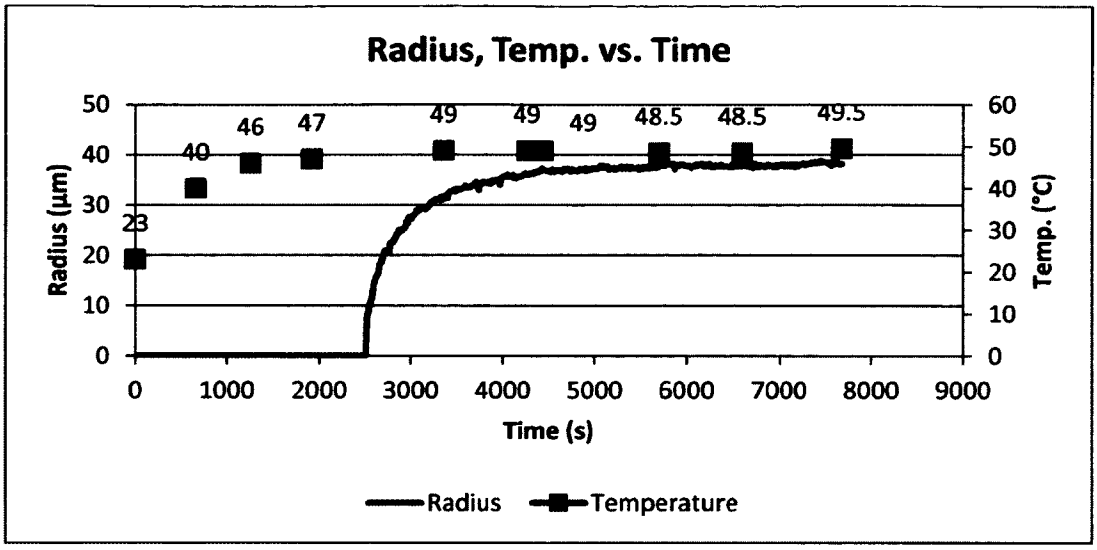

Figure 4-14: Dewetted radius and temperature vs. time of PG 58-28 asphalt on glass plate of a temperature increase from ambient to 50°C in submerged water condition.

It should be pointed out that this dewetted hole may be on or within the periphery of the circumference of the bubble base. In this particular case, the growth in that region may be slightly different from one being dewetted from under the bubble cap. The shape of the graph resembles that of the hole growth found in the last two dewetting curves for the dewetting of PG 64-22 at a temperature range from ambient to 40°C. For approximately 4000 s, films remained relatively constant. A similar temperature increase was presented in the next analysis.

For Figure 4-15, at a temperature increase from that of ambient to 50°C, two holes were analyzed.

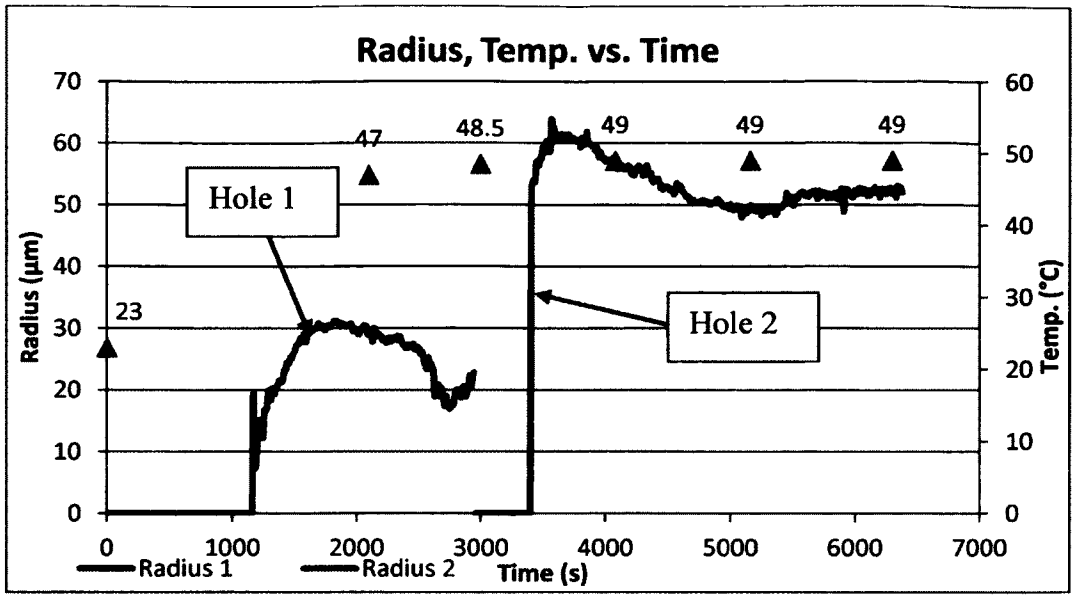

Figure 4-15: Dewetted radius and temperature vs. time of PG 58-28 asphalt on glass plate of a temperature increase from ambient to 50°C in submerged water condition (hole 1 and hole 2).

For the first hole, the rate of growth of the radius was linear in the first section of the graph and then decreases to approximately 22 μm. The second hole being investigated was observed at the time of initiation of about 53 μm. With the passage of time the radius of this hole gradually decreased and remained constant within the temperature of 49°C water bath.

In Figure 4-16, however, at ambient to 60°C, we noted the rate of growth of the radius was relatively linear, increased to a peak from where there was a fast rate of healing as it is evident that the radius dropped very sharply.

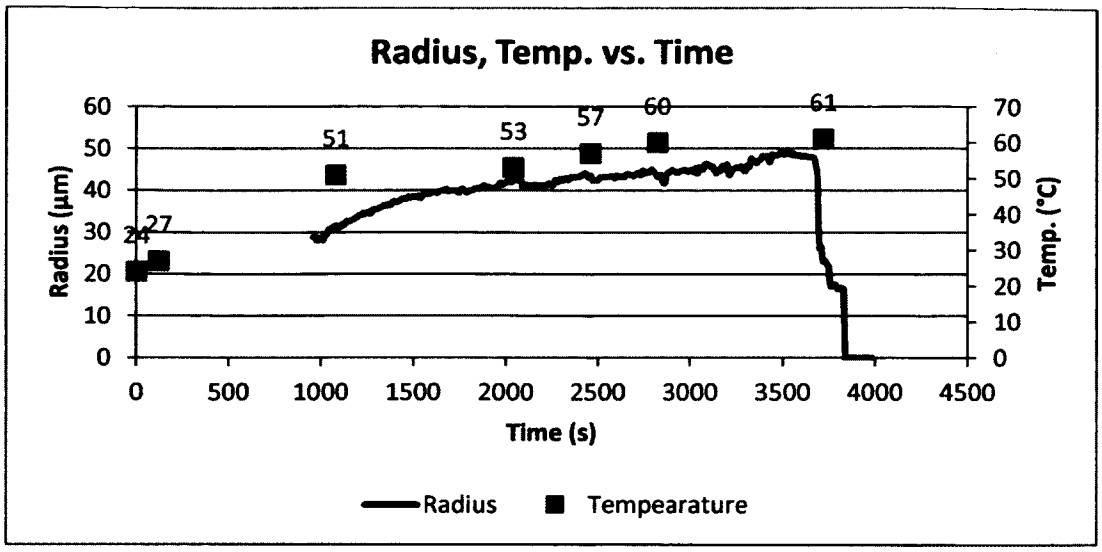

Figure 4-16: Dewetted radius and temperature vs. time of PG 58-28 asphalt on glass plate of a temperature increase from ambient to 60°C in submerged water condition.

With the last specimen (Figure 4-16), at ambient to 60°C, it is interesting to note that at such a high temperature, when PG 58-28 asphalt film was submerged in water subjected to moisture damage, the dewetted hole could possibly be healed, but not necessarily at a temperature range of ambient to 40°C and 50°C for the two holes observed. This observation suggests that in submerged condition and up to 60°C subsurface temperature, PG 58-28 asphalt being attacked by moisture damage can heal itself.

4.6.4 PG 76-22M Asphalt (Oven Cured) Samples

Although the temperature range of the experiment in Figure 4-17 (5200 s after the start of experiment) and Figure 4-18 (increase to 50°C 8530 s after start of experiment) was initially set for ambient to 40°C, observation showed that after a long time period, there was no sign of dewetting and as a result, both sets of experiments had their temperature increased to 50°C.

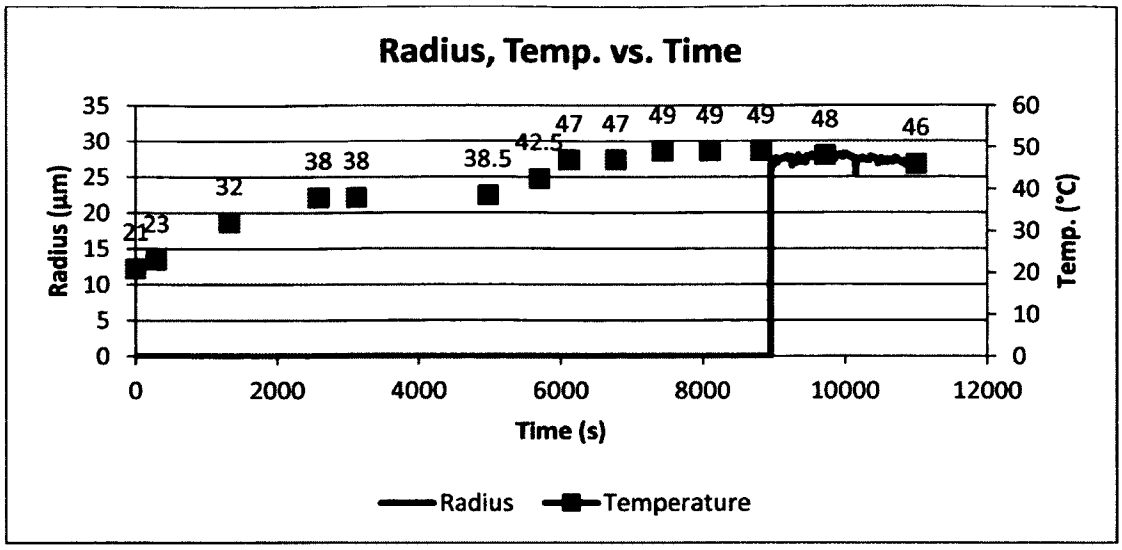

Figure 4-17: Dewetted radius and temperature vs. time of PG 76-22M asphalt on glass plate at a temperature increase from ambient to 40°C (increased to 50°C) in submerged water condition.

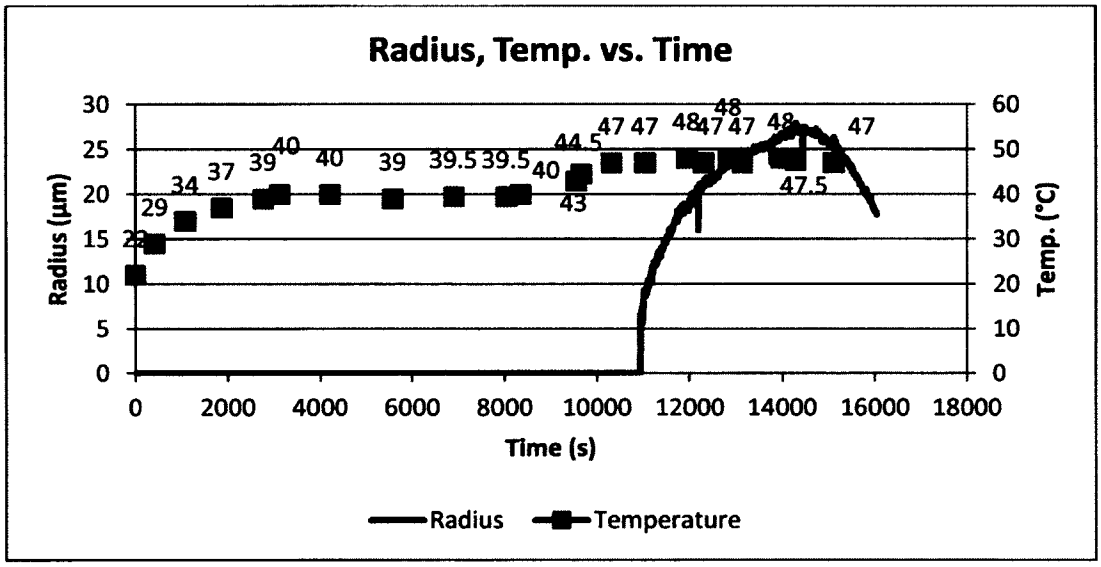

Figure 4-18: Dewetted radius and temperature vs. time of PG 76-22M asphalt on glass plate at a temperature increase from ambient to 40°C (increased to 50°C) in submerged water condition.

In Figure 4-17, the PG 76-22M film began to dewet after the temperature reached approximately 50°C, remained constant for a time, then decreased slightly. That temperature rise was significant to moisture damage of the film as the viscosity of the PG 76-22M film would be reduced making it more susceptible to damage. At 40°C in submerged condition of the pavement, PG 76-22M asphalt film can remain relatively unharmed. In contrast to the constant growth of the hole in Figure 4-17, there was found in Figure 4-18, a fast rate of the dewetting of PG 76-22M, arriving at a maximum radius and then healing was observed. In both curves, the dewetting began at a minimum of 47°C, even though the behavior of dewetting of the independent holes on each samples were different. As PG 76-22M is much more viscous than the two above investigated asphalts (PG 64-22 and PG 58-28), it would be deemed necessary that the more viscous a liquid film, the more the driving force (capillarity) would be required to drive the retraction of the film, even capillarity.

Moreover, in Figure 4-19, the graph tends to exhibit a linear motion with radius against time, arriving at a peak height, growing slightly constant from that time onwards and is now tending to heal from approximately 45 μm to 30 μm which is very slow. The high viscosity of the asphalt can, therefore, have a major impact on healing. As is observed in the two previous analyses, a similar feature is observed in this current graph, where the breakup of this specimen initiates at a minimum of 47°C.

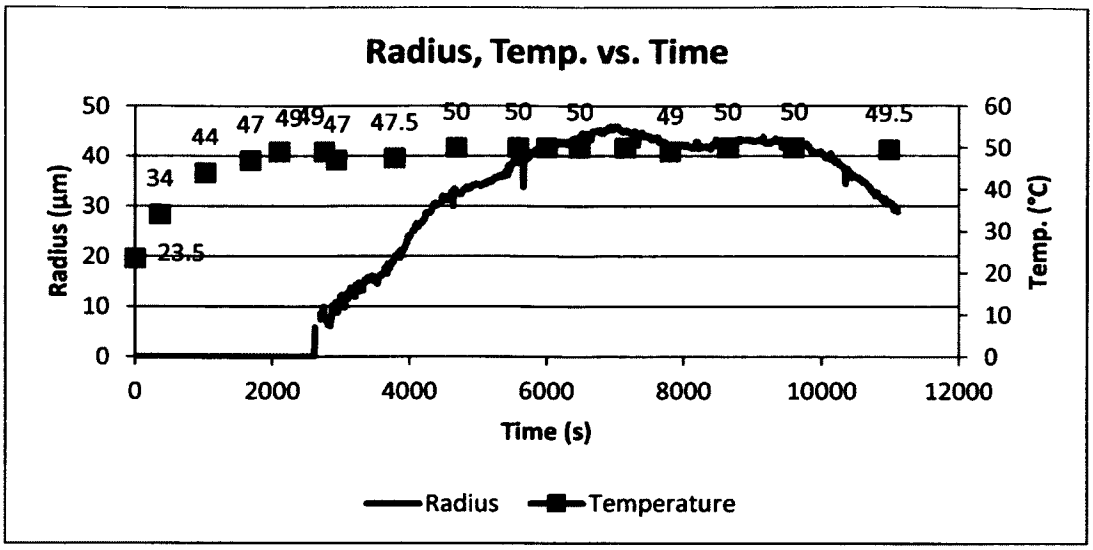

Figure 4-19: Dewetted radius and temperature vs. time of PG 76-22M on glass plate at a temperature increase from ambient to 50°C in submerged water condition.

In Figure 4-20 (oven cured) the breaking up of the film was observed in PG 76-22M. Two holes were being dewetted in the neighborhood of each other at a temperature increase from ambient to 50°C. Concerning the first hole, the graph took on an almost exponential form, decreasing over a period of time and finally healing from about 5430 s from inception. It can be noted that after a minimum of 47°C, dewetting began. The second hole which began to form and grow did this from about 5040 s and lean more toward an exponential growth rather than a linear pattern as was found by Redon et al. (1991) for a film of PDMS (polydimethylsiloxane) deposited on a fluorinated wafer. Finally, wetting or healing of the PG 76-22M asphalt binder was observed rather rapidly. It must be realized that although the dewetting was under the same bubble cap in the PG 76-22M asphalt film sample, definitely the dewetting patterns may vary which, as previously mentioned, could be attributed to the size of the air/water

interface (air bubble), and the causes of the disturbances such as the type of defect, thermal fluctuation or fluctuations in the film thickness or surface.

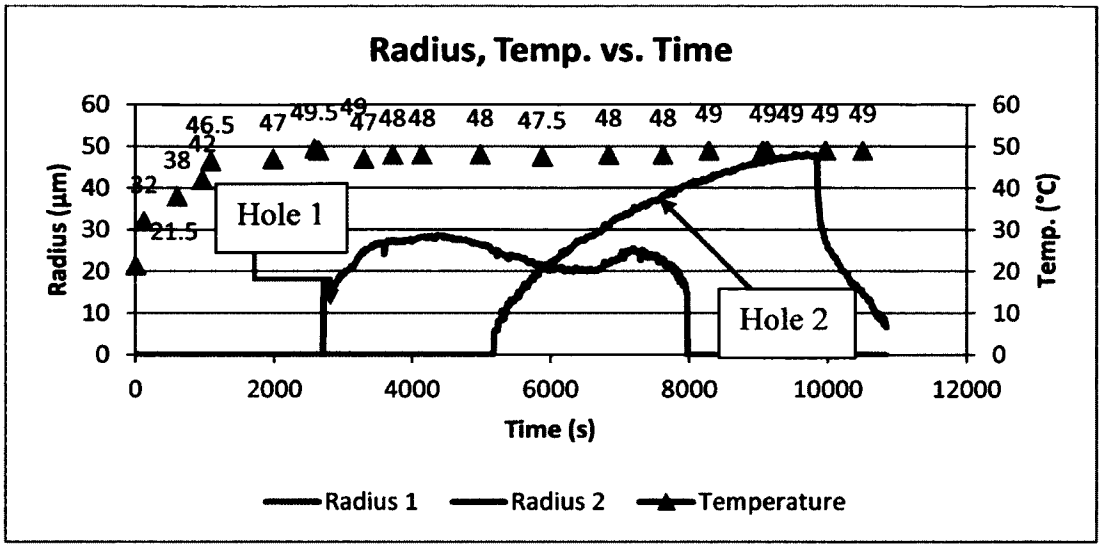

Figure 4-20: Dewetted radius and temperature vs. time of PG 76-22M asphalt on glass plate at a temperature increase from ambient to 50°C in submerged water condition.

4.6.5 PG 58-28 + 1% LOF 6500 Asphalt (Ambient Cured) Samples

In the following experiments, after preparation, the asphalt samples were placed in desiccators being allowed to cure in room temperature before testing as opposed to the previous samples which were allowed to cure in the oven for some time before being allowed to cure at room temperature. One percent additive, namely Adhere LOF 6500, was added to PG 58-28 and the dewetting trend is depicted in Figure 4-21. A rapid growth was in the rate of change of the radius, but no sooner did the radius arrive at a peak of approximately 100 µm, there was a steady decline in the closing of the hole over a reasonably long time period. As Adhere LOF 6500 additive primarily serves to enhance the wetting characteristics of the asphalt film on the aggregate, this behavior could reflect

that function strongly, as the hole was reduced and finally closed in the process. Healing, therefore is effected in the process by the additive.

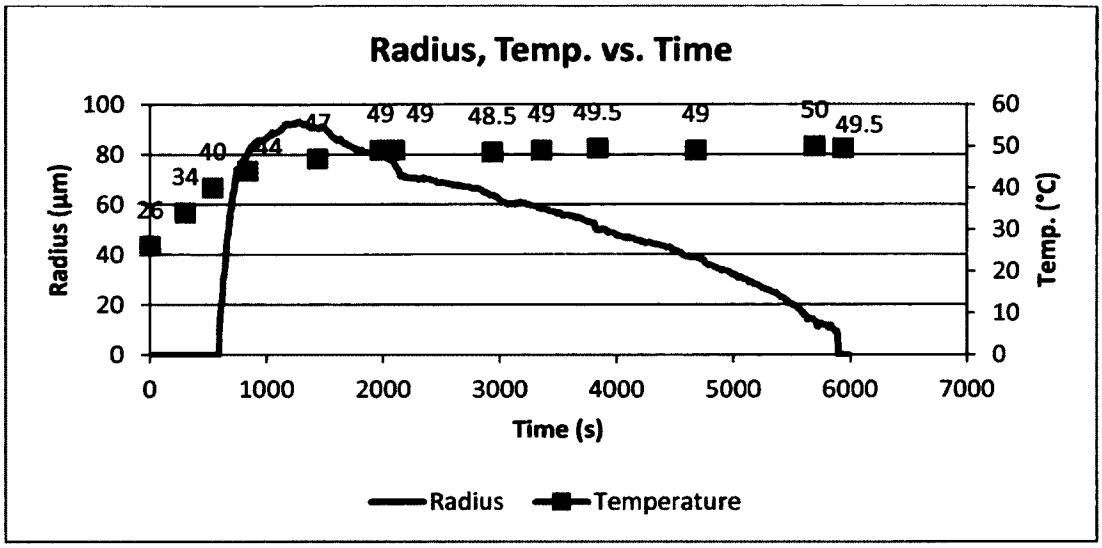

Figure 4-21: Dewetted radius and temperature vs. time of PG 58-28 asphalt + 1% Adhere LOF 6500 on glass plate at a temperature increase from ambient to 50°C in submerged water condition.

4.6.6 PG 76-22M + 1% Adhere LOF 6500 Asphalt (Ambient Cured) Samples

In Figure 4-22, (approximately 2 holes in close proximity) the rate of hole growth was fast. The holes reduced and closed although not totally in the same area and then re-emerged at a very fast rate and having 40 µm as a lower bound for the radius in the constant region of the latter part of the experiment. Although there was healing in PG 58-28 + 1% Adhere LOF 6500 asphalt from ambient to 50°C, there was no healing as observed in PG 76-22M + 1% Adhere LOF 6500 asphalt from ambient to 50°C. Therefore, it must be noted that the 1% Adhere LOF 6500 additive may not have had a considerable impact on the behavior of PG 76-22M due to its high

viscoelastic properties. Comparing the behavior of ambient cured asphalt 58-28 + 1% Adhere LOF 6500, from ambient to 50°C to Figure 4-13, it was noticed that no healing took place in the neat binder, yet there was healing taking place in PG 58-28 + 1% Adhere LOF 6500.

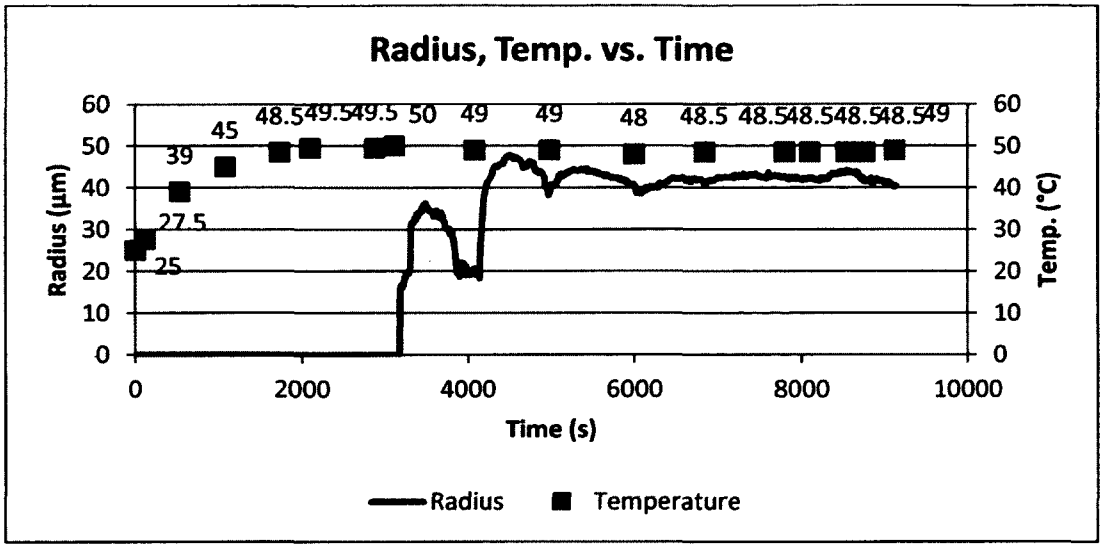

Figure 4-22: Dewetted radius and temperature vs. time of 76-22M asphalt + 1% Adhere LOF 6500 on glass plate of a temperature increase from ambient to 50°C in submerged water condition.

4.6.7 PG 58-28 Asphalt (Ambient Cured) Sample

In Figure 4-23, there was also healing taking place. It is interesting to note that although this PG 58-28 asphalt does not contain anti-strip additives, there was a significant reduction in the radius of the hole.

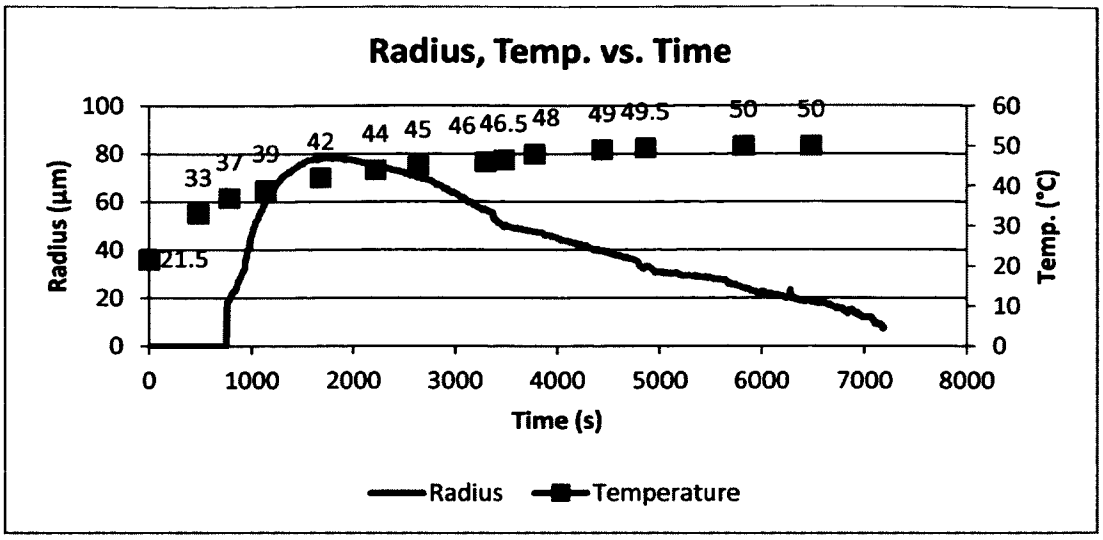

Figure 4-23: Dewetted radius and temperature vs. time of PG 58-28 asphalt on glass plate at a temperature increase from ambient to 50°C in submerged water condition.

4.6.8 PG 64-22 + 2% Sasobit® (Ambient Cured) Sample

In Figure 4-24, two holes were being dewetted in the asphalt film. An additive of 2% Sasobit® (warm mix additive) was added to the binder. Dewetting seemed to take place at a minimum temperature of 57°C for the first hole, and the hole closed within 2440 s, not before remaining constant for some time. The second hole dewetted with a growth with that which approximates a linear function. There was a slight decrease in radius, but afterwards, it continued its growth rather slowly. Owing to the fact that there was a wax based additive present, this could have attributed to the slow rate of change of radius with time even at a relatively high temperature.

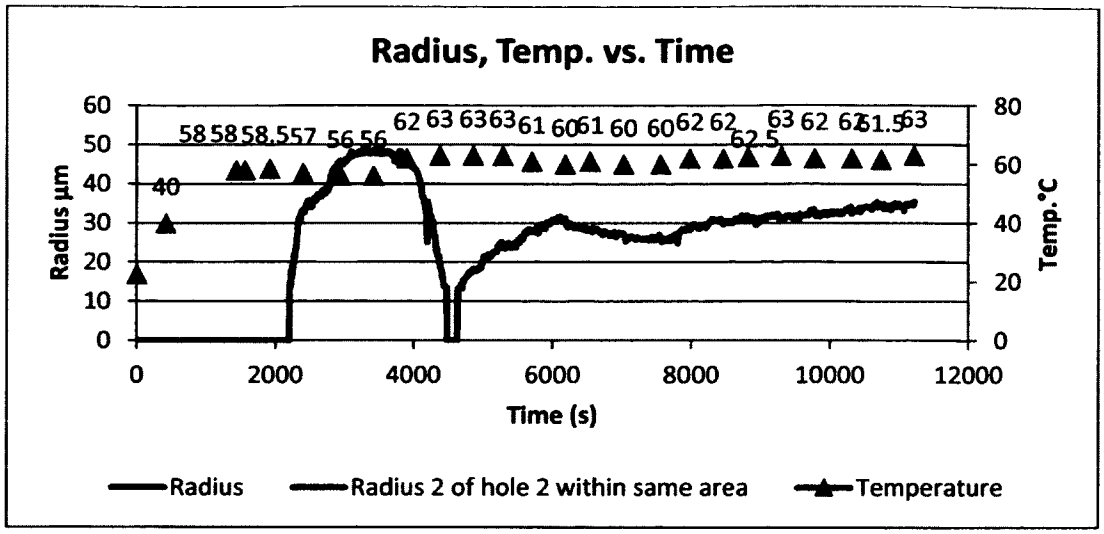

Figure 4-24: Dewetted radius and temperature vs. time of PG 64-22 asphalt + 2% Sasobit® on glass plate of a temperature increase from ambient to 60°C in submerged water condition.

4.6.9 PG 58-28 + 1% Adhere LOF 6500 (Ambient Cured)

Figure 4-25 shows the dewetting of two holes for PG 58-28 + 1% Adhere LOF 6500 at ambient to 50°C. At 4000 s, the first hole healed, leaving the second hole unhealed. There was a fast rate of dewetting from a minimum of 40°C. From a peak radius of about 105 µm, hole growth ceased, and a gradual decline in the radius with respect to time was thereby observed.

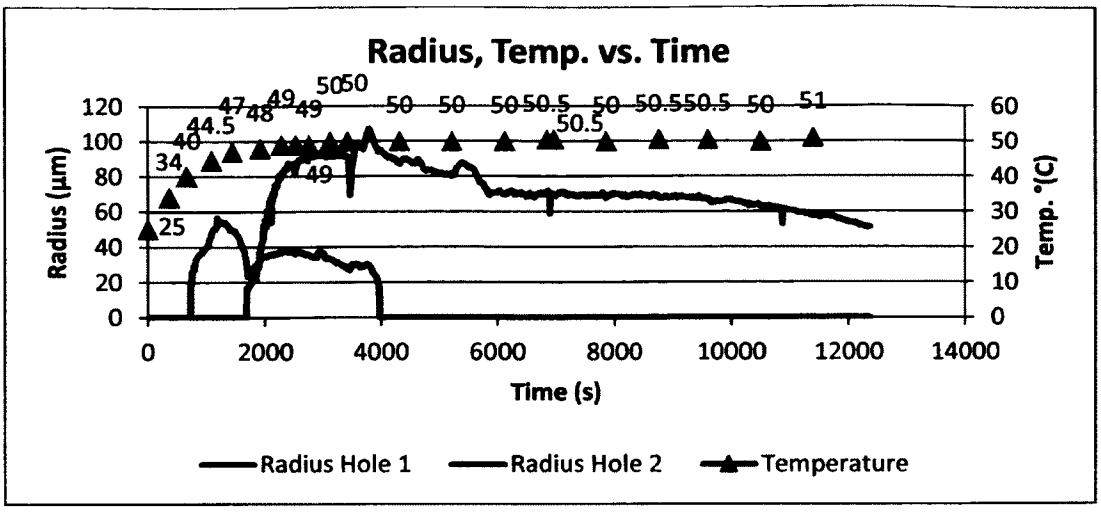

Figure 4-25: Dewetted radius and temperature vs. time of PG 58-28 asphalt + 1% Adhere LOF 6500 on glass plate of a temperature increase from ambient to 50°C in submerged water condition (hole 1 and hole 2).

4.7 Conclusions

There are many reasons why dewetting of a film on a substrate occurs. Two main types of dewetting include spinodal dewetting and nucleation and growth of a hole. Trapped air bubbles also cause the rupture of films. Moisture damage has been a major cause of distress in asphaltic pavements. A study of rupture and dewetting of asphalt film (PG 64-22, PG 76-22M, PG 58-28) and a combination of these with additives was undertaken with glass plate substrate. The observations for dewetting on glass plates show:

1) Dewetting/rupture of asphalt films occured at low temperature ranges on both glass plates and aggregate surfaces, even less than 40°C.
2) Most dewetting (radius growth) patterns follow that of an exponential growth.
3) Asphalt film will readily spread up an air/water interface. In that process, the asphalt dewets under the vicinity of an air bubble.

4) In the dewetting of some holes on glass substrate, the films do not completely dewet, leaving three layer films behind, varying in shades. Sometimes, one single film is left. Within that layer, more dewetted holes are visible. These dewetted holes within can be caused by coagulation of the air inside the film.
5) Many of the asphalt samples that were left for an extended period of time, exhibited signs of dewetting. Moreover, for some samples with 1% Adhere LOF anti-strip additive, healing was observed.
6) Based on the average thicknesses of the asphalt on glass plate, rupture occurs via nucleation and growth of a hole. It can occur via capillary forces, and as proposed by Xu et al. (2007) could be responsible for driving of the opening of the holes.

CHAPTER 5

DEWETTING OF ASPHALT BINDER ON AGGREGATE SUBSTRATE

5.1 Background and Objectives

To understand the dewetting phenomena observed in chapter 3, nucleation and growth of dewetting holes were characterized under microscopic setup under submerged water conditions. The parameters that were varied to understand and characterize dewetting on an aggregate surface are specified in the following objectives:

- To observe and measure under an air bubble, the moisture damage in two performance asphalt binder films (PG 58-28, PG 64-22) in the form of the dewetting mechanism on aggregate substrate in submerged water conditions at various temperature ranges.
- To investigate the effects of additives on the dewetting process of the asphalt films on the aggregate substrates.
- To evaluate the effects of water type and pH on the dewetting process.

5.2 Methodology and Experimentation

Two performance graded asphalt binders were used in the experiments, namely, PG 64-22, and PG 58-28 binder. Additives were put in to investigate the effects that the modified asphalt binders would have on the dewetting mechanism.

Although many aggregates and asphalt types were used in the trial experiments for this study, the final results presented are from the samples that allowed data to be taken.

5.2.1 Procedure Used in Sample Preparations

The procedure used in this study is described below:

1. For the aggregate specimens, ½ in. gravel (Standard Gravel, Eagle Mills, Bearden, AR) consisting mainly of silicon and oxygen, based on SEM analysis was used in the experiment with the exception of one limestone aggregate sample. The aggregates were left to soak for 1 h and then washed thoroughly.

2. The aggregates were then placed in the oven to dry at a temperature of 163°C for 24 h (18 h minimum).

3. Approximately 1% asphalt by weight of heated aggregate (163°C) was placed in 1 lb aggregate and mixed for 4 min thoroughly before putting away in desiccators.

4. A small pyrex container was placed at a preferred level which was to accommodate at least 4 mm depth of water above the specimen surface to reduce the loss of accuracy that can take place when there is too much diffracted light when a high level of water is present. Induced air in water (in some of the experiments) was created by shaking the experimental water in a container. This was an attempt to facilitate the entrapment of air in the water to increase the possibility of the air bubble initiating on aggregate surface to measure dewetting.

5. To generate the necessary temperature for the water, a hotplate (Corning hot plate scholar 170) was used for that purpose. Similar to the methodology in Chapter 4, as the water was being heated, a slight amount of water was added at specified time intervals to control the height of the water. The temperature was thereby measured after pouring and also at other times to assess the temperature increase. When necessary, the camera was slightly adjusted as mentioned previously in Chapter 4.

The stereoscope, model SM-4T (Amscope®, California) microscope was calibrated with a 1 mm scale rule at 80 X magnification as opposed to 40 X as used in the previous Chapter for glass plate samples. This microscope was purchased from Amscope®. As the light microscope was not helpful to analyze aggregate samples, the stereoscope (model SM-4T) was utilized. Moreover, 1-1.5% asphalt by weight of aggregate was found to produce mix with reasonable film thicknesses. The thickness of the stone specimens was estimated by measuring a cross section of an aggregate with the stereomicroscope in four locations and taking the average. A grinder was utilized to make a full cross sectional cut with the aid of a mechanical bench. Figure 5-1 shows the experimental setup for the dewetting of asphalt binder in submerged water condition for aggregate analysis.

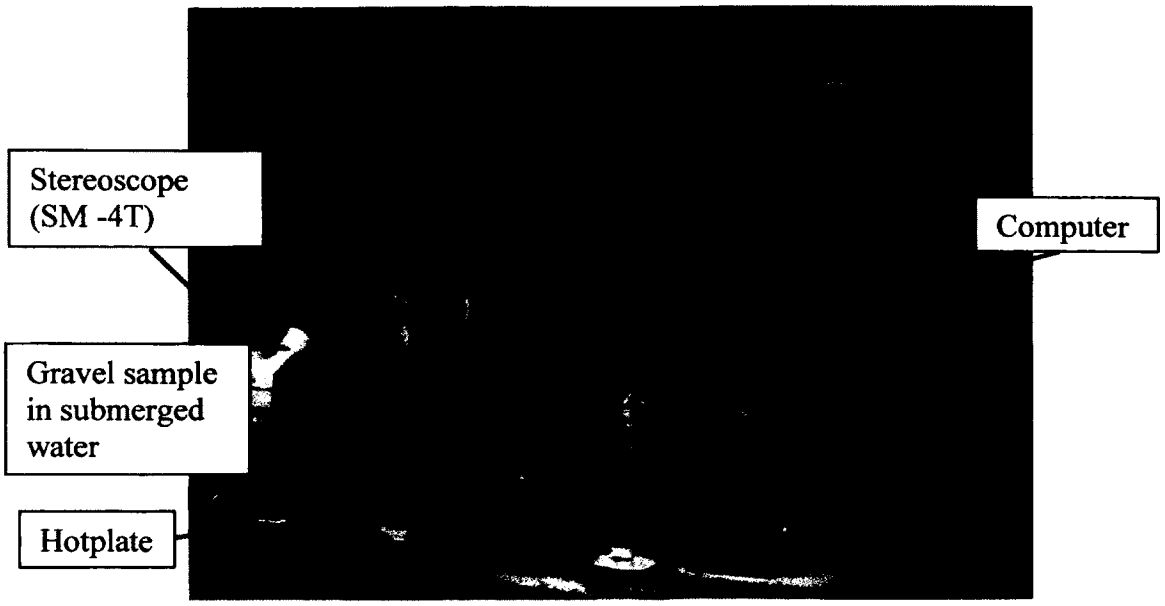

Figure 5-1: Experimental setup for the dewetting of asphalt binder in submerged water condition for aggregate analysis.

Two asphalt binders (PG 64-22, PG 58-28) were used in this study to observe dewetting characteristics but it was very difficult to come up with a quantitative test procedure to differentiate binders based on moisture susceptibility with the analysis of one dwetted hole.

5.3 General Characteristics of Dewetting of Asphalt Film on Aggregate Surface

In many of the aggregate experiments, it should be noted, though mentioned earlier, that the rupture of the asphalt film and growth of a hole was not cited since its earliest inception as the microscope was moved across the aggregate surface to capture a site and to analyze its growth. Many air pockets may have existed at the interface between aggregate and asphalt film, or the air pockets may have resided in the film structure itself. In the process, these air pockets may coagulate upon being heated and then giving birth to an air bubble which grows. The air pockets indicated the non-

homogeneity of asphalt films as they coat the aggregate and a case for incomplete wetting of the film on the aggregate, causing moisture susceptibility. The phenomenon that is being observed with the moisture damage of the asphalt on aggregate closely follows the theory presented earlier by Slavchov et al. (2005). Their case was built for nano-bubbles present at the interface being responsible for film rupture, even though in presenting their model the film (water) thickness was in the nano scale region where long and short range forces dominate. As in the case for the dewetting observed on glass plate, depending on the size of the bubble base, there was a removal of asphalt from the surface of the film as time elapsed. Then the dewetting of the minor holes occured which depended again on the size of the rupture. Table 5-1 shows the various test conditions and samples used in the dewetting experiments.

Table 5-1: Test conditions and samples used in the dewetting experiments.

Asphalt Type	Stone	Temperature °C	App. Water level (mm)	Water	pH	Average Asphalt Thickness (μm)	Figure
PG 64-22	Gravel	Ambient to 40	11	Deionized	6.7	36.54	5-2
PG64-22	Gravel	Ambient to 50	5	Deionized	6.0	57.51	5-3
PG64-22	Gravel	Ambient to 60	6	Deionized	6.2	25.80	5-4
PG64-22	Limes-tone	Directly in 40	5	Deionized	6.2	18.83	5-5
PG64-22	Gravel	Directly in 50	5	Deionized	6.2	14.76	5-6
PG58-28*	Gravel	Directly in 60	6	Deionized	6.3	21.13	5-7
PG64-22*	Gravel	Ambient to 40	4	Tap water	7.8	16.81	5-8
PG64-22* Hole 1&2	Gravel	Ambient to 50	6	Tap water	7.9	31.22	5-9
PG64-22*	Gravel	Ambient to 60	5	Tap water	7.8	21.29	5-10
PG64-22*	Gravel	Directly in 40	4	Tap water	7.9	23.88	5-11

*Induced air in water to generate greater possibility of bubble attachment on aggregate
Temperatures are rounded to the nearest ten whole number on graphs.

5.4 Results and Discussion (PG 64-22, PG 58-28 Asphalt)

It must be noted that for the microscopic observation of asphalt aggregate samples, the hole that is being measured in the stone specimen, is not the actual hole size. The actual hole size was observed upon draining the water from the container and taking a much closer look via the camera and microscope.

The radius growth of a hole and temperature, as a function of time, can be seen in Figure 5-2 (a), the radius growth after specified times (c and d), and the actual rim after the drainage of water from the experiment.

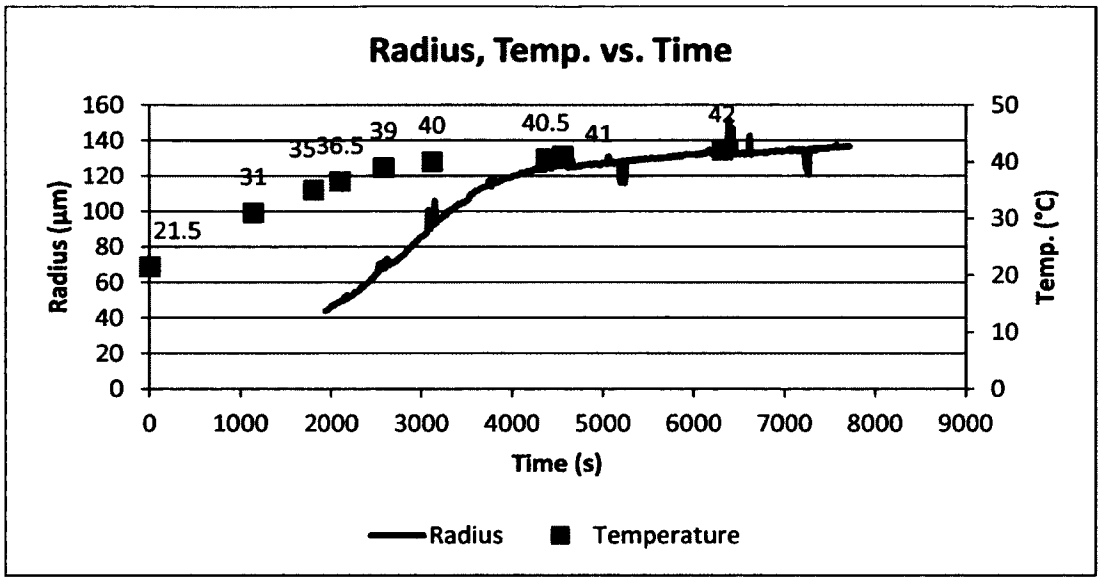

(a)

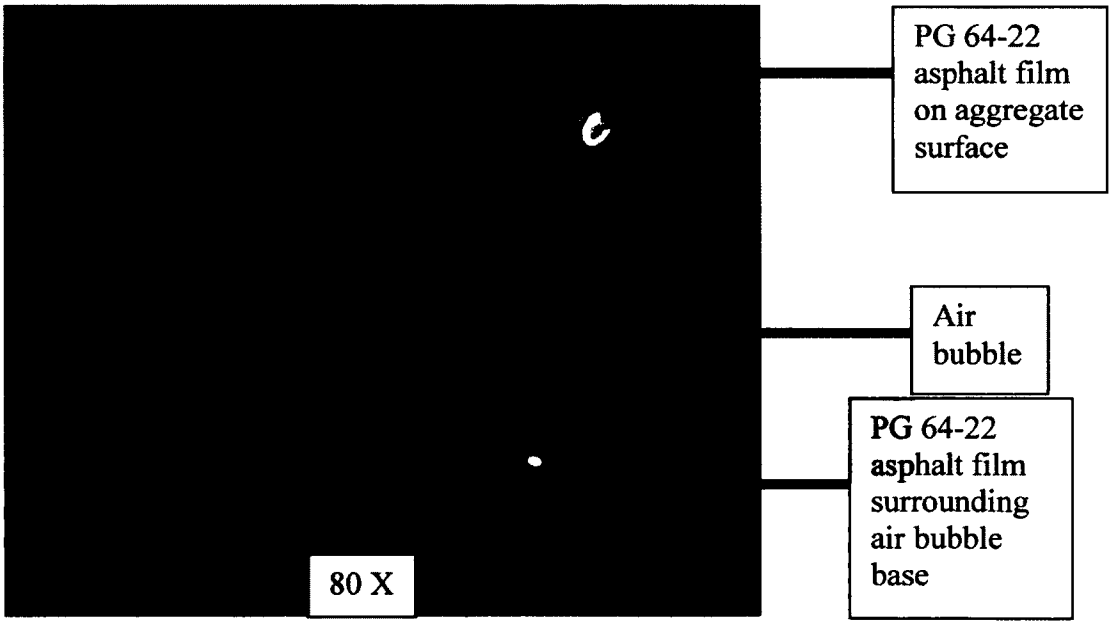

(b)

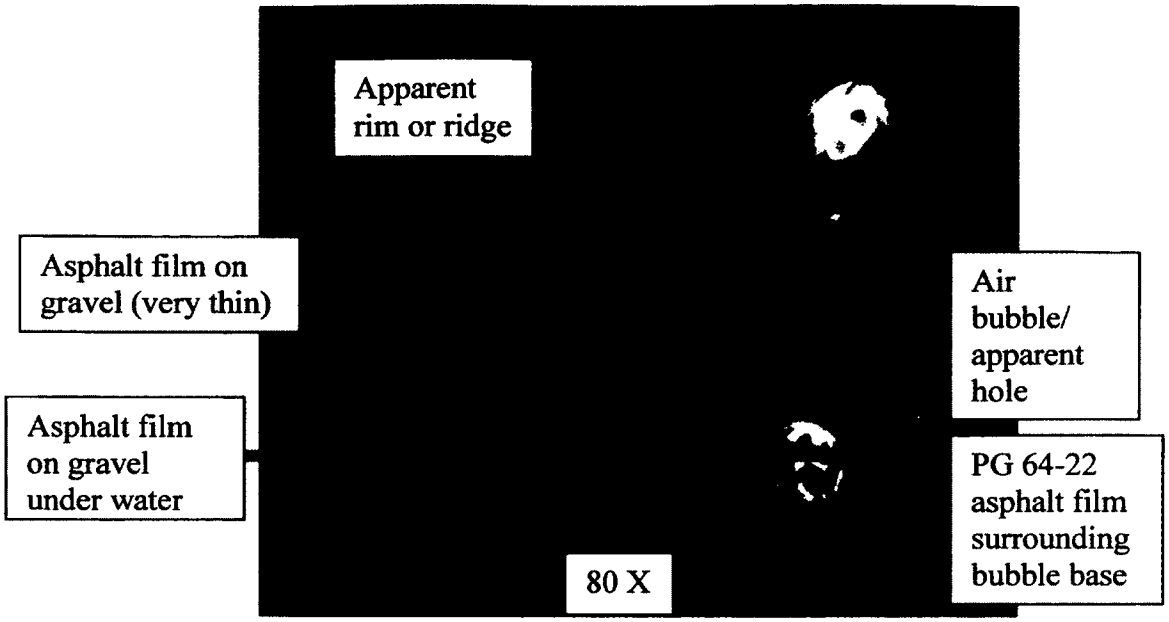

(c)

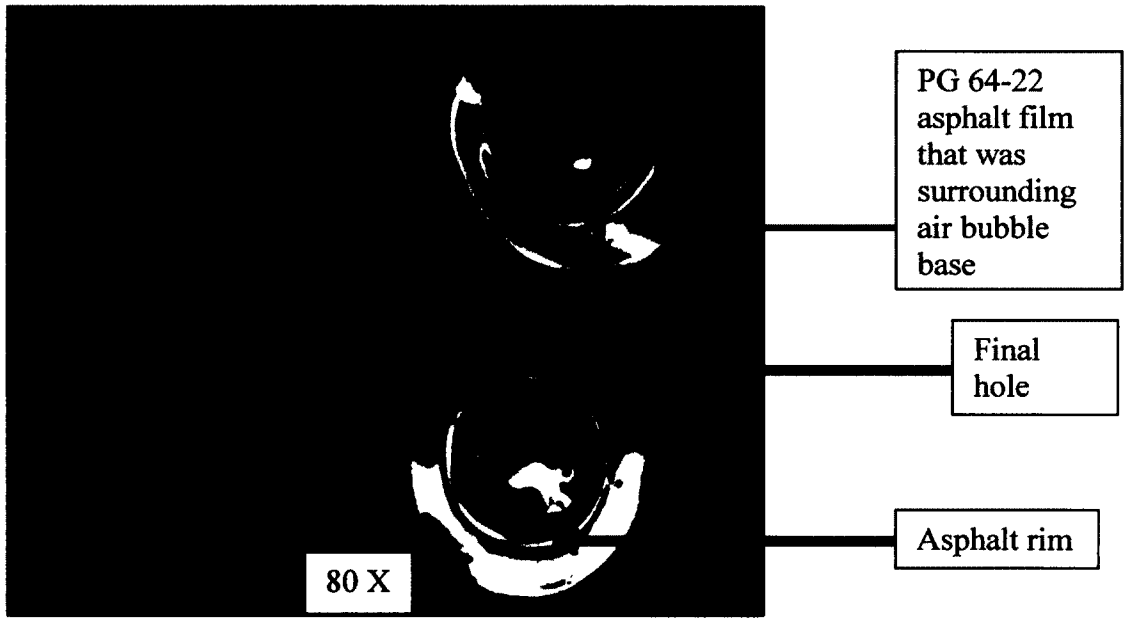

(d)

Figure 5-2: **(a)** Dewetted radius and temperature vs. time of PG 64-22 asphalt on ½ in. gravel of a temperature increase from ambient to 40°C in submerged water condition, **(b)**, Approximately 2860 s after start of experiment, **(c)** Approximately 7730 s after start of experiment, **(d)** Final hole with rim after the completion of the experiment in the absence of water.

Due to the shape of the bubble base, the expanding hole that was measured was at the aggregate/asphalt/air vapor interface. The "apparent ridge or rim" (Figure 5-2 (d)), as recorded from the top of the system by the camera, was a layer of asphalt within the vicinity of the bubble base and the rim produced after the drainage of water from the experiment. It should be noted that the actual hole, (Figure 5-2 (d)), after drainage is larger than the hole that is depicted in Figure 5-2 (c), under the microscope in submerged water condition. This "apparent ridge or rim" resembles the precursor film as mentioned in Lelinki et al. (2004) and this film is clearly seen in Figure 5-4 (e and f) as the sample is being drained. Therefore, the bulk of the asphalt that dewets formed the rim. This visible hole after drainage is the actual hole on the aggregate surface. In most cases, it was observed that there was a very thin layer of asphalt which remained attached to the mineral aggregate. Its thickness may possibly be in the nanometer range or even less. As there was a challenge in getting some specimens with air bubbles at the aggregate surface in the right geometric conditions for analysis, additional air was induced in the water used for some of the experiments. However, on the sides of the aggregates, many bubbles were present, and in some cases, these bubbles were larger in size than those on the top surface of the aggregate. It has been cited in the literature (Read and Whiteoak, 2003) that the average theoretical film thickness of aggregates in the asphalt pavement would be in the range of 5 μm to 15 μm. This theoretical film thickness range would suggest that the asphalt film thickness was on the boundary of the nanometer scale, although another recent study showed that low theoretical film thicknesses in asphalt may not be the case and that the film thickness is much greater than that range (Elseifi et al., 2008). It was evident that for the aggregate film thicknesses greater than that range, moisture damage

occured. For moisture damage to occur, it was proposed (Lottman et al., 1969) that water forces its way into voids or pathways in the mix and displaces asphalt.

To this end, dewetting, therefore, can serve as a mechanism that contributes to moisture damage by facilitating openings in the film. In Figure 5-2 (a), PG 64-22 on ½ in. gravel in water, the hole grew linearly with temperature, and increased at a slow rate for approximately almost 3600 s. The change in the hole growth from a fast radius growth to a slow one may be attributed to the rim at the base of the air bubble in which the removed asphalt from the hole accumulated as the hole dewetted. Brochard-Wyart et al. (1997) reported that when a mature rim is built, the hole is fully formed. The theory is presented (Brochard-Wyart et al.,1997):

1) The driving force, S, or the spreading coefficient measured per unit length of the rim.
2) The resisting force due to friction k lV, where,

$$k = \frac{\eta_0}{a} \qquad \textbf{Eq. 5-1}$$

a, a monomer friction coefficient that is related to extrapolation length

$$k = \frac{\eta_0}{b} \qquad \textbf{Eq. 5-2}$$

where, b is called the hydrodynamic extrapolation length, which is defined theoretically by:

$$b = a\left(\frac{N^3}{N_e^2}\right) \qquad \textbf{Eq. 5-3}$$

where, a is monomer size, N is the polymerization index of the polymer, N_e the threshold of entanglements, l = width of the fully developed rim defined by:

$$l = (Re)^{\frac{1}{2}} \qquad \textbf{Eq. 5-4}$$

where, R = radius of the hole, e = the film thickness and V= velocity of rim on the solid substrate, in our case gravel. Substituting $l = (Re)^{\frac{1}{2}}$ into klV yields:

$$\dot{R}(Re)^{\frac{1}{2}} = \frac{S}{\eta}, \qquad \textbf{Eq. 5-5}$$

further giving rise to:

$$R^{\frac{3}{2}} = \frac{S}{\eta}\frac{b}{e^{1/2}}t \qquad \textbf{Eq. 5-6}$$

where, η = viscosity of the liquid, t= time, $\dot{R}$= radius velocity.

A critical radius is thus defined as $R_c^{'}$, the onset of the rim formation. It is noted that above this critical radius, the dewetting enters a classical viscous phase, allowing the liquid of the hole to collect into the rim. The researchers also indicated that the velocity of the rim reduces as the driving force is constant, adding that the friction increases with the size of the rim. This radius growth law as a function of time strongly favors the behavior of the Figure 5-2 (a) as it leaves the linear phase merging into the near constant latter phase depicting very slow growth.

Figure 5-2 (b and c) shows the dewetting of the asphalt on gravel at approximately 2860 s and 7730 s, respectively from the start of the experiment while Figure 5-2 (d) presents the final hole after removal of water from the container. Figure 5-3 (a) presents a similar behavior to that of Figure 5-2 (a). Just above 3600 s, the growth of the radius appeared to be stabilizing.

It appeared that the friction of the rim as the hole formed would also contribute to the constant growth of the hole in Figure 5-3 (a). It was observed in both the cases that the growth of the hole, the growth of the air bubble and the spreading of asphalt on the surface of the air bubble initiated at low temperatures. Also in Figure 5-3 (a) it was

observed that there was no healing in the fully formed hole as was noted by the other glass plate samples in the previous chapter. Figure 5-3 (b and c) shows the dewetting of the asphalt on the gravel at approximately 460 s and 8150 s, respectively, from the start of the experiment. Figure 5-3 (d) depicts the final hole and rim after drainage of water.

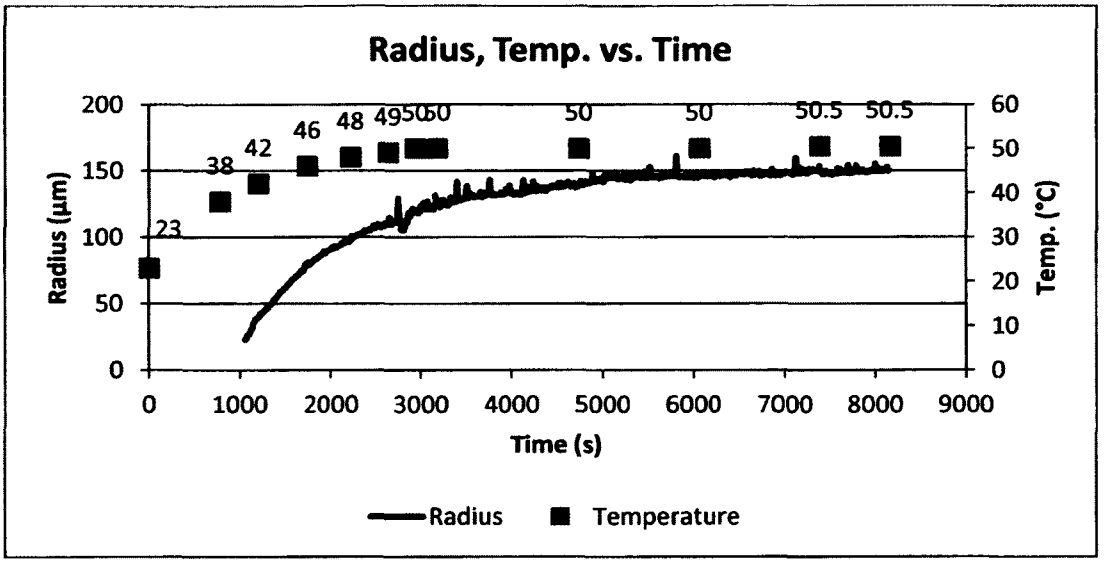

(a)

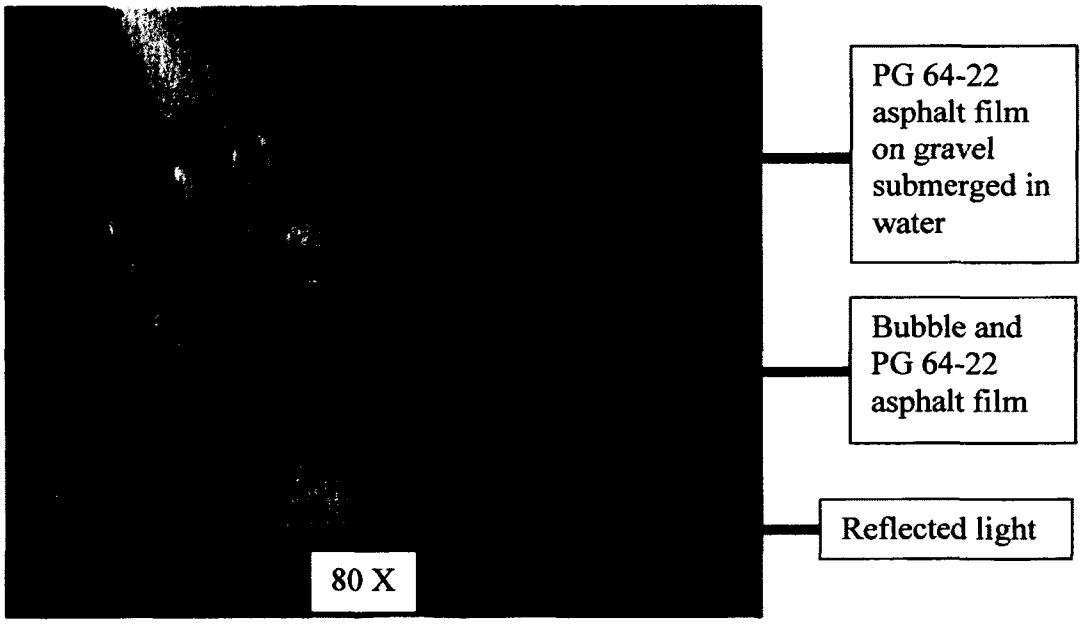

(b)

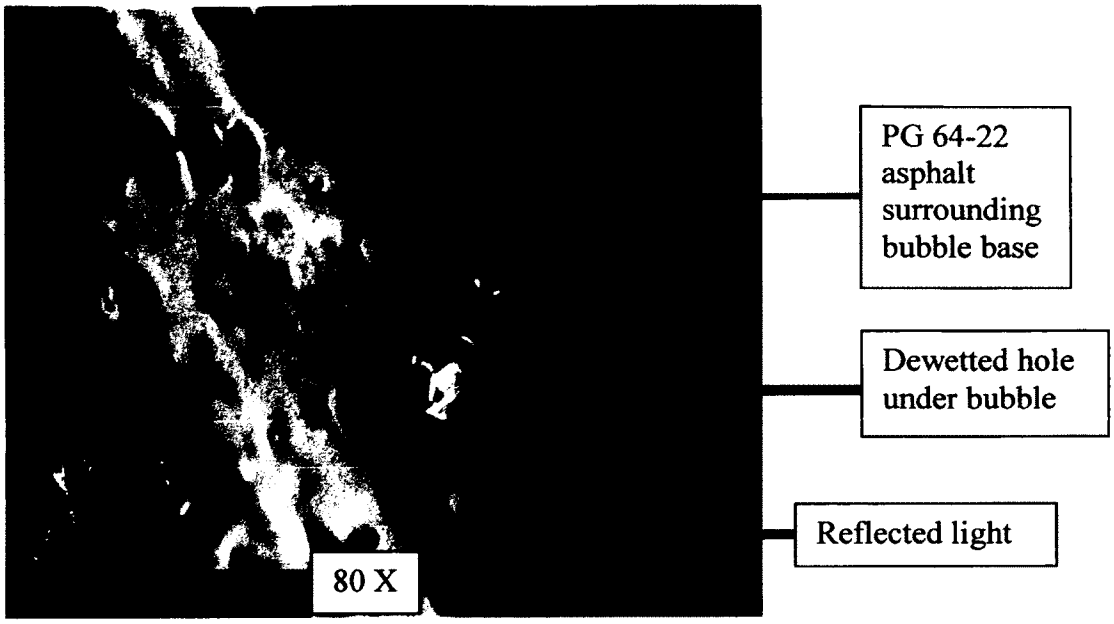

(c)

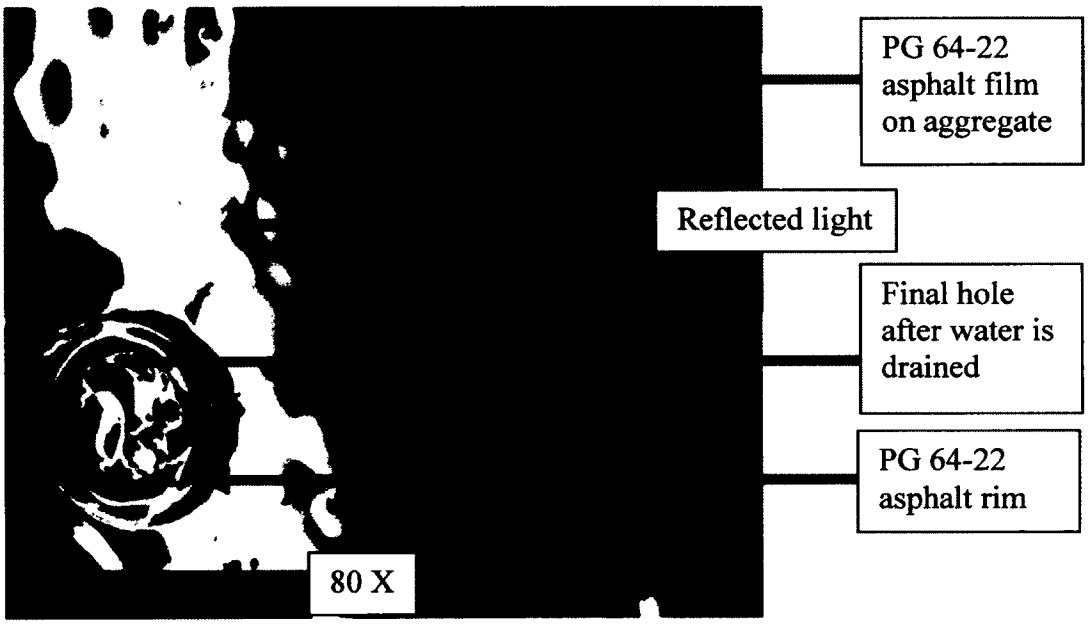

(d)

Figure 5-3: (a) Dewetted radius and temperature vs. time of PG 64-22 asphalt on ½ in. gravel at a temperature increase from ambient to 50°C in submerged water condition, **(b)** Approximately 460 s after start of experiment, **(c)** Approximately 8150 s after start of experiment, **(d)** Final hole with rim after completion of the experiment in the absence of water.

The dewetting curve for the temperature increased from ambient to 60°C is shown in Figure 5-4 (a). The hole grew as temperature increased from ambient to 60°C at a constant speed. The relatively very slow growth of the hole from that point indicates the possible resistance of the velocity of the rim due to friction. The breakup in the graph represents the inability of the software to capture a reading of the picture frames due to the vapor that was captured by the camera as the water temperature was being increased to 60°C temperature.

Figure 5-4 (b and c) shows the dewetting of the asphalt on the gravel at approximately 50 s and 7760 s, respectively, from the start of the experiment. Figure 5-4(d) depicts the final hole and rim after drainage of water. To demonstrate the relative difference between the apparent hole in Figure 5-4 (a) and the actual hole formed after water drainage, Figure 5-4 (e) shows the sample at the end of the experiment and the draining of the water at different time intervals. The mature rim that was hidden by the layer of asphalt surrounding the air bubble base is now clearly visible.

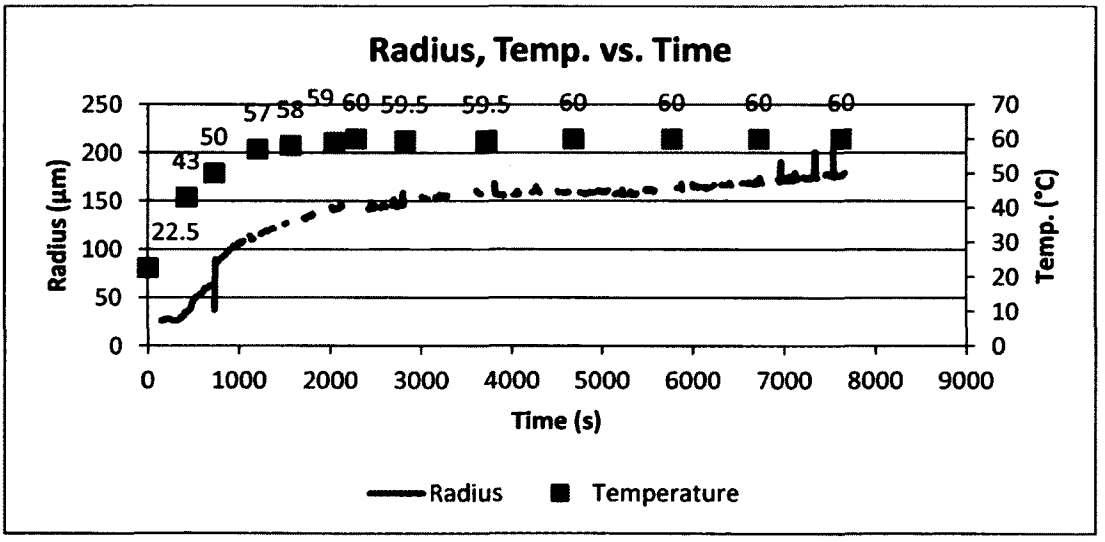

(a)

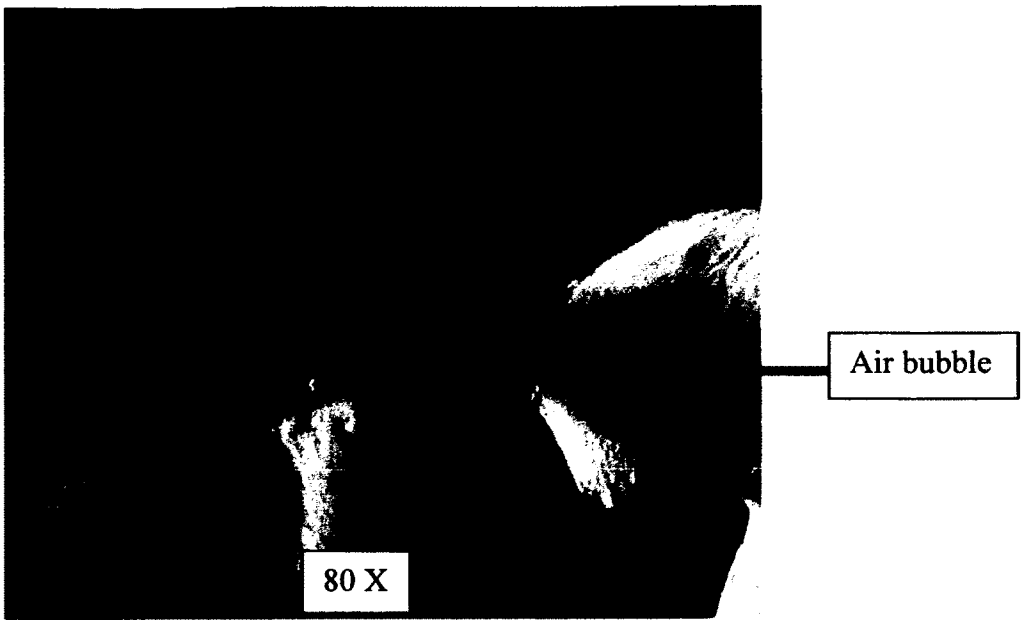
Air bubble
80 X

(b)

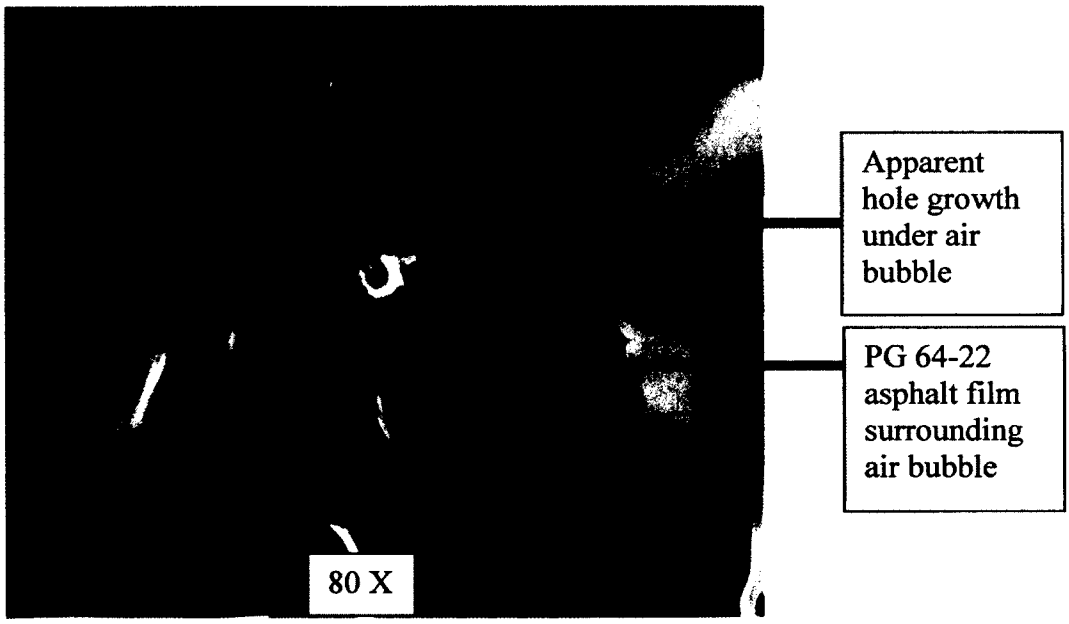
Apparent hole growth under air bubble
PG 64-22 asphalt film surrounding air bubble
80 X

(c)

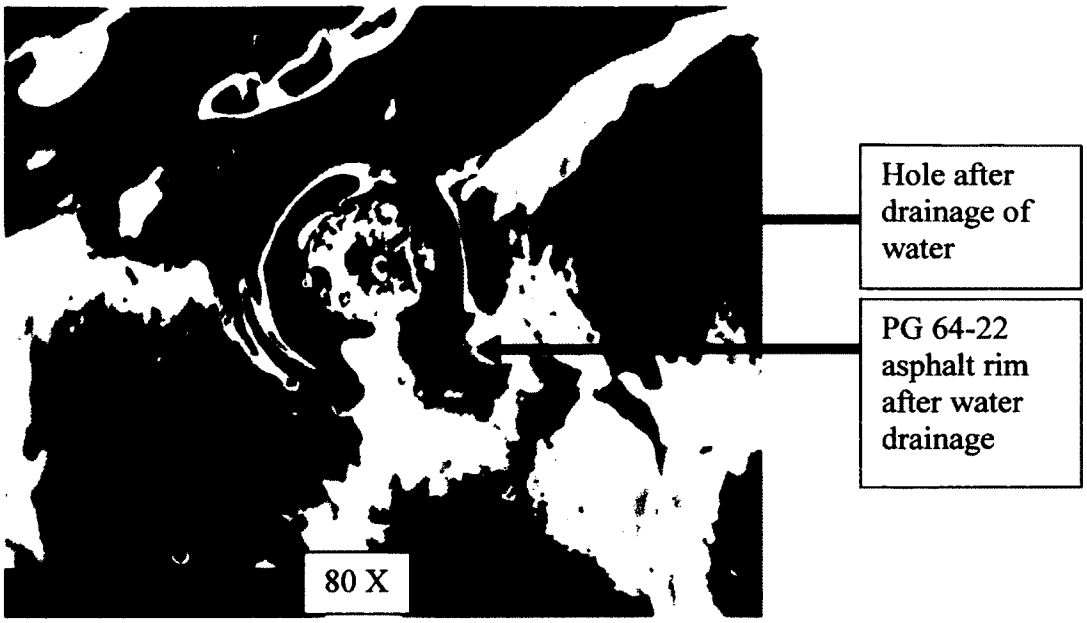

(d)

Specimen submerged

(1)

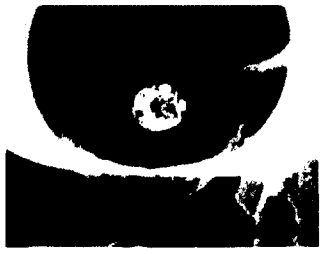

Removal of water

(2)

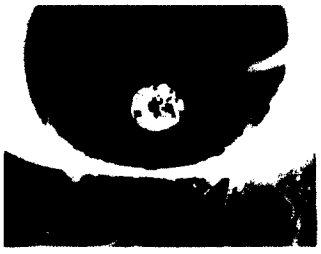

After 1 min 9 s

(3)

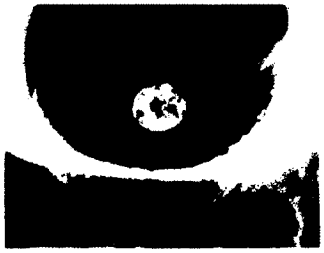

After 1 min 19 s

(4)

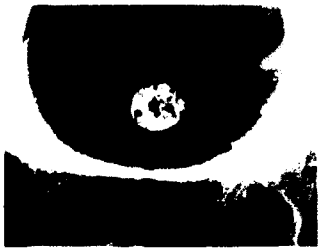

After 1 min 30 s

(5)

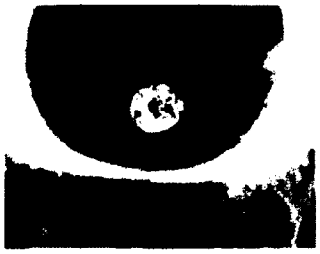

After 1 min 43 s

(6)

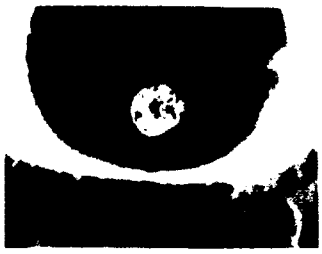

After 1 min 59 s

(7)

After 2 min 24 s

(8)

After 5 min 24 s

(9)

After 8 min 51 seconds

(10)

(e)

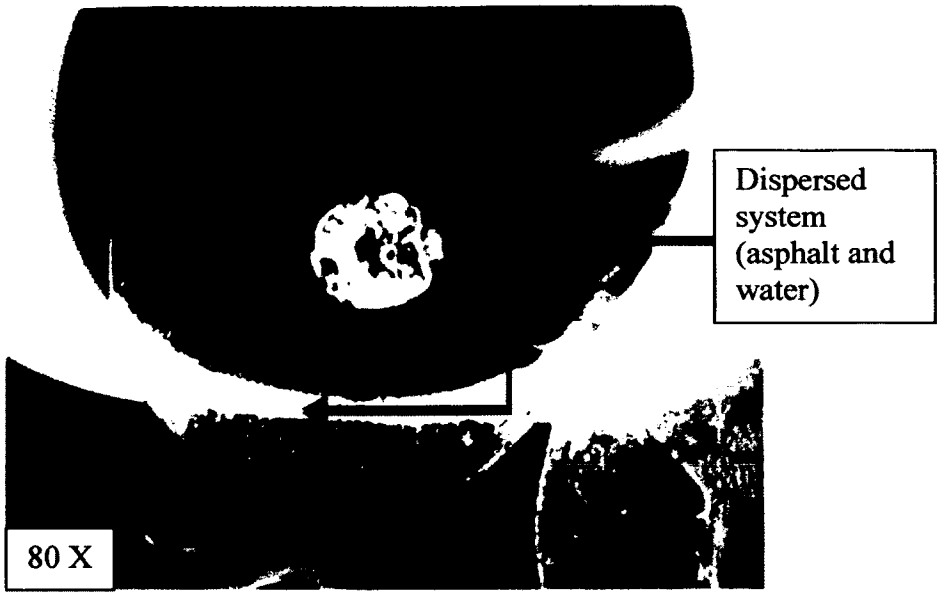

(f)

Figure 5-4: (a) Dewetted radius and temperature vs. time of PG 64-22 asphalt on ½ in. gravel of a temperature increase from ambient to 60°C in submerged water condition, **(b)** Approximately 50 s after start of experiment, **(c)** Approximately 7660 s after start of experiment, **(d)** Final hole with rim after the completion of the experiment in the absence of water, **(e)** Stages of actual rim consolidation as water is being removed of PG 64-22 sample from ambient to 60°C specimen, **(f)** Dispersed system (No. 2).

In Figure 5-5 (a) PG 64-22 asphalt with a ½ in. limestone aggregate (Martin Marietta, Hatton Quarry, Cove, AR) substrate was placed directly in 40 °C water. Despite being placed at that direct temperature (not at ambient to 40°C), the curve tends to the same behavior as that of the previous samples. From approximately 3000 to 5000 s, there was a slow growth followed by a slow decline in radius growth up to about 8000 s. Figure 5-5 (b and c) shows the dewetting of the PG 64-22 asphalt binder on the ½ in. limestone at approximately 460 s and 9610 s, respectively, from the start of the experiment. In this instance, even though the time difference was quite large (9150 s), the apparent hole growth was not significant.

Figure 5-5 (d) depicts the final hole and rim after drainage of water used in the experiment and it is much larger than that viewed while submerged in water.

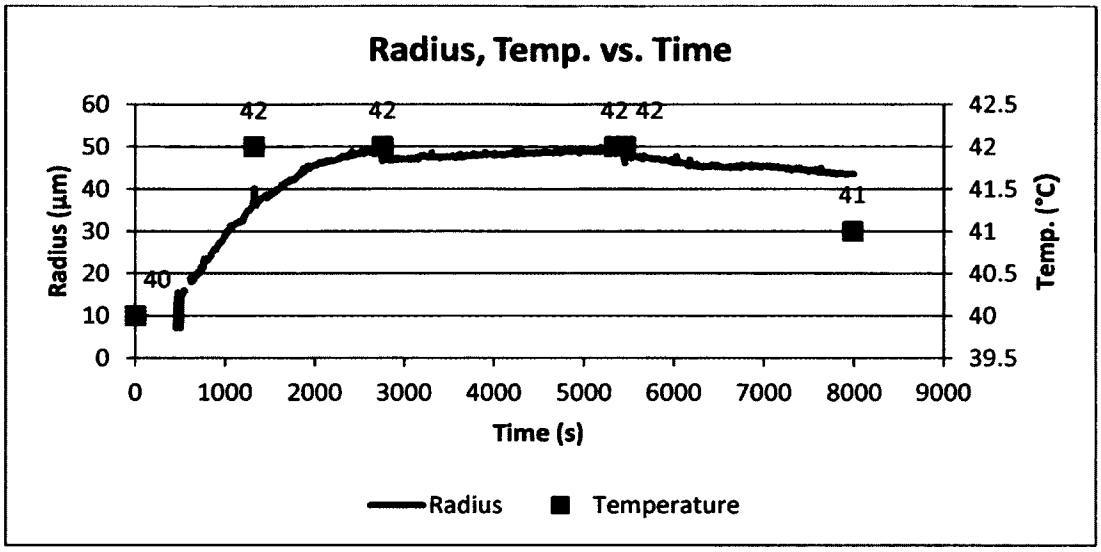

(a)

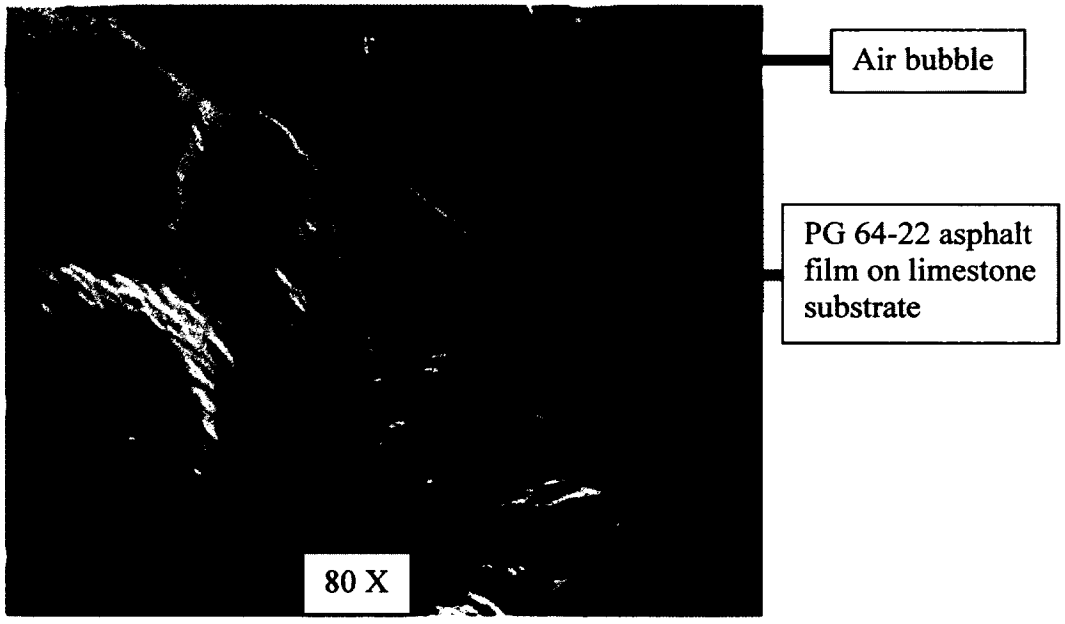

(b)

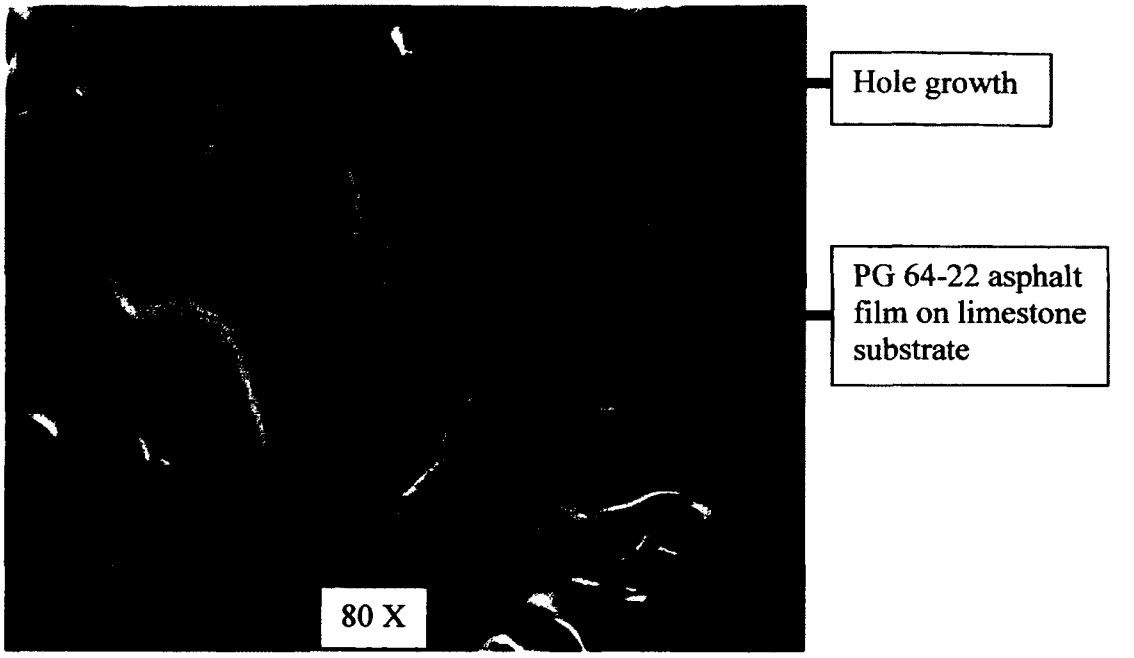

(c)

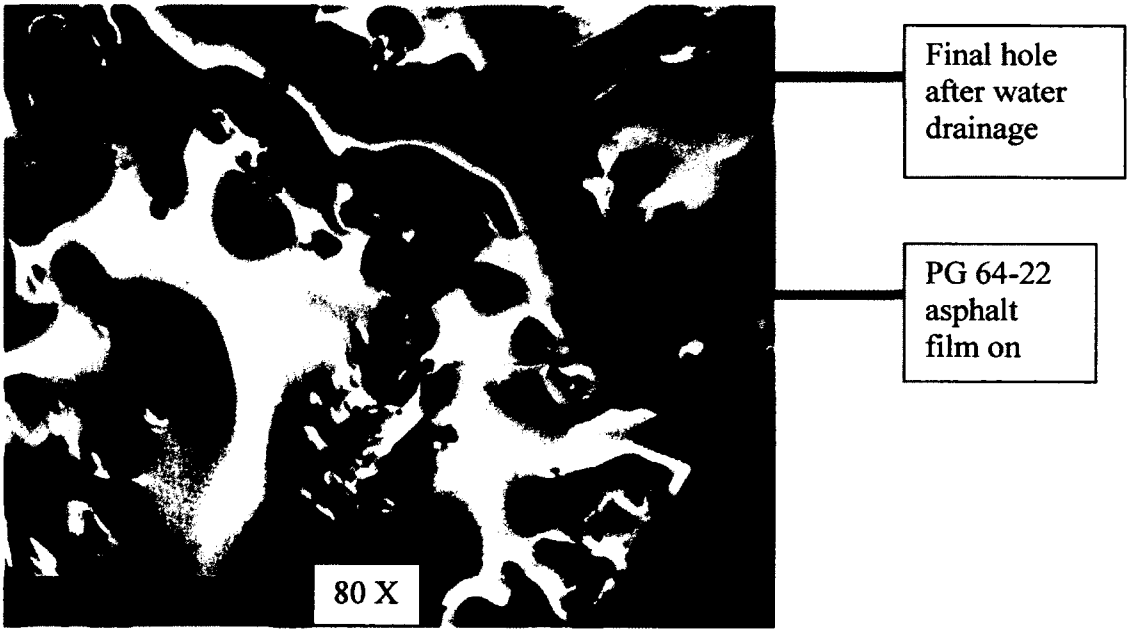

(d)

Figure 5-5: (a) Dewetted radius and temperature vs. time of PG 64-22 asphalt on ½ in. limestone placed in water bath at 40°C, **(b)** Approximately 460 s from start of experiment, **(c)** Approximately 9610 s from start of experiment, **(d)** Final hole with rim after the completion of the experiment in the absence of water.

In Figure 5-6, PG 64-22 asphalt dewetting results were extracted for the sample on gravel placed directly in 50°C. For this apparent growth, the hole tended to be linear up to approximately 7000 s. Onwards, the rate of radius growth leveled off, increased slightly, leveled off and repeated the same toward the end of the experiment as opposed to leveling out at a specific range. Figure 5-6 (b and c) shows the dewetting of the PG 64-22 asphalt on the ½ in. gravel at approximately 940 s and 12942 s, respectively, from the start of the experiment. Despite the long time duration of this experiment, no healing of the hole took place. Figure 5-6 (d) depicts the final hole and rim after drainage of the water at the end of the experiment.

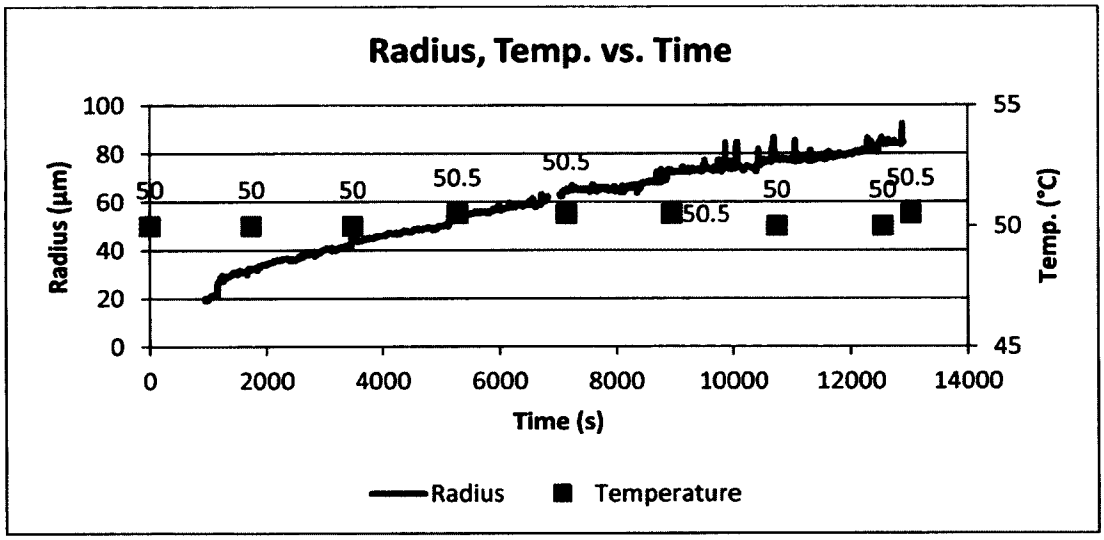

(a)

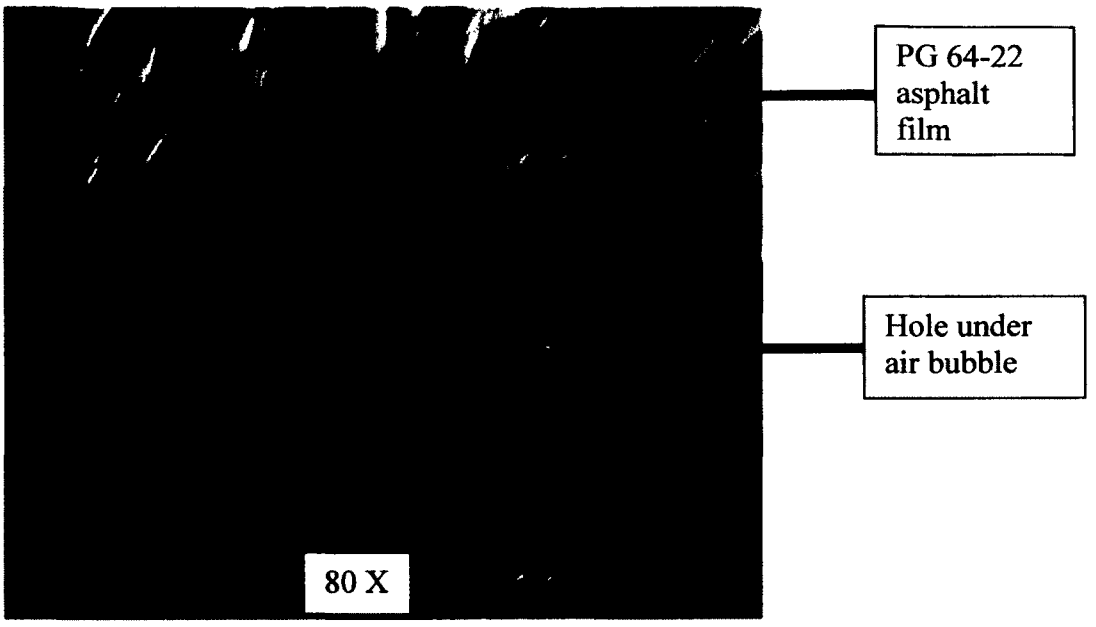
PG 64-22 asphalt film
Hole under air bubble
80 X

(b)

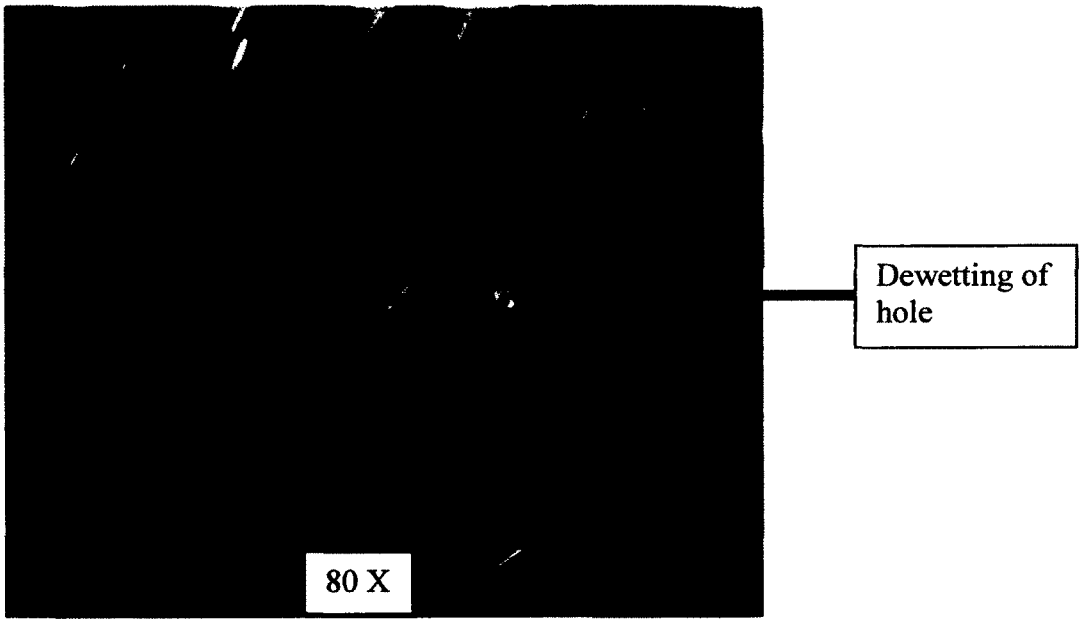
Dewetting of hole
80 X

(c)

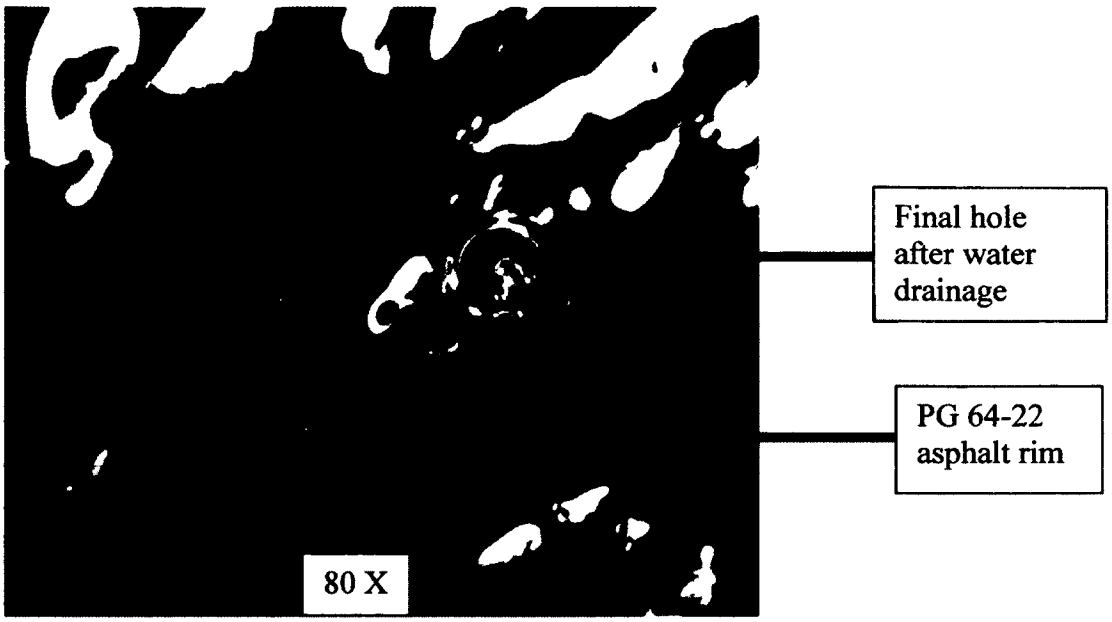

(d)

Figure 5-6: (a) Dewetted radius and temperature vs. time of PG 64-22 asphalt on ½ in. gravel placed in water bath at 50°C, **(b)** Approximately 940 s after start of experiment, **(c)**: End of experiment, approximately 12942 s after the start of the experiment, **(d)** Final hole with rim after the completion of the experiment in the absence of water.

In Figure 5-7, the ½ in. gravel used in the experiment is coated with another asphalt PG 58-28. Overall, a similar trend was observed with PG 58-28 asphalt dewetting on gravel when placed directly in submerged water condition at 60°C as that of the graph in Figure 5-6. Redon et al. (1994), in investigating the dewetting of a different polymer, PDMS (polydimethylsiloxane) film with thickness in the microscopic range observed that the radius (R) of a hole grows linearly with time over a large time scale. It should be noted that although these are two different polymer films on two different substrates (silanized silicon wafers), in various conditions, one in submerged water condition and the other in ambient, the relation appears to be similar. Figure 5-7 (b and c) shows the dewetting of the PG 58-22 asphalt on the ½ in. gravel at approximately 645 s and 7465 s

respectively from the start of the experiment. The final dewetted hole and the rim after drainage of the water at the end of the experiment is shown in Figure 5-7 (d). From this picture, it can be observed that the hole may have been completely dewetted leaving the aggregate surface exposed. A combination of parameters such as high temperature and low viscosity of PG 64-22 could have been the factors contributing to complete asphalt film dewetting from gravel.

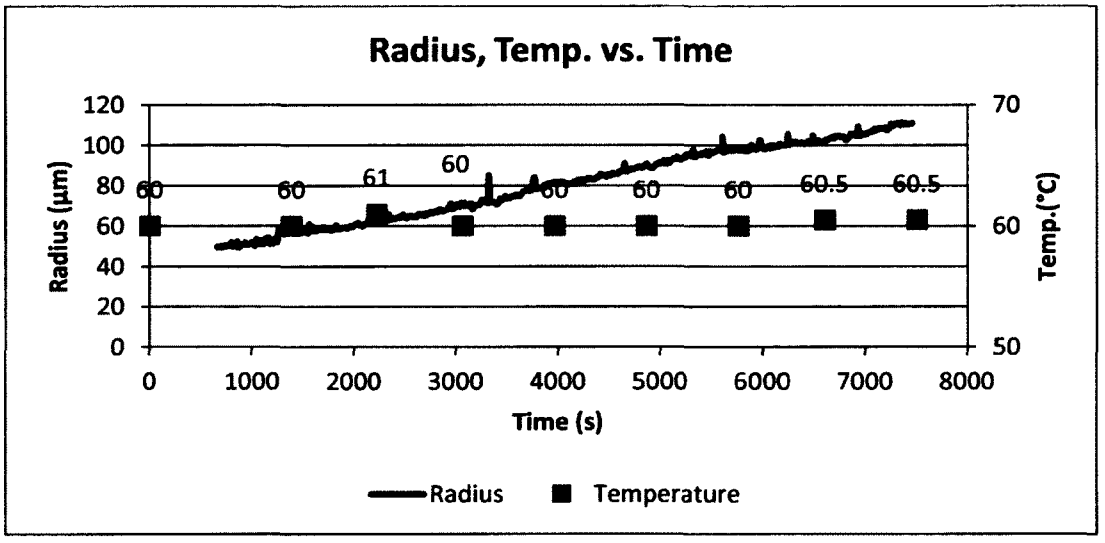

(a)


PG 64-22
asphalt film
Hole under air
bubble
80 X

(b)

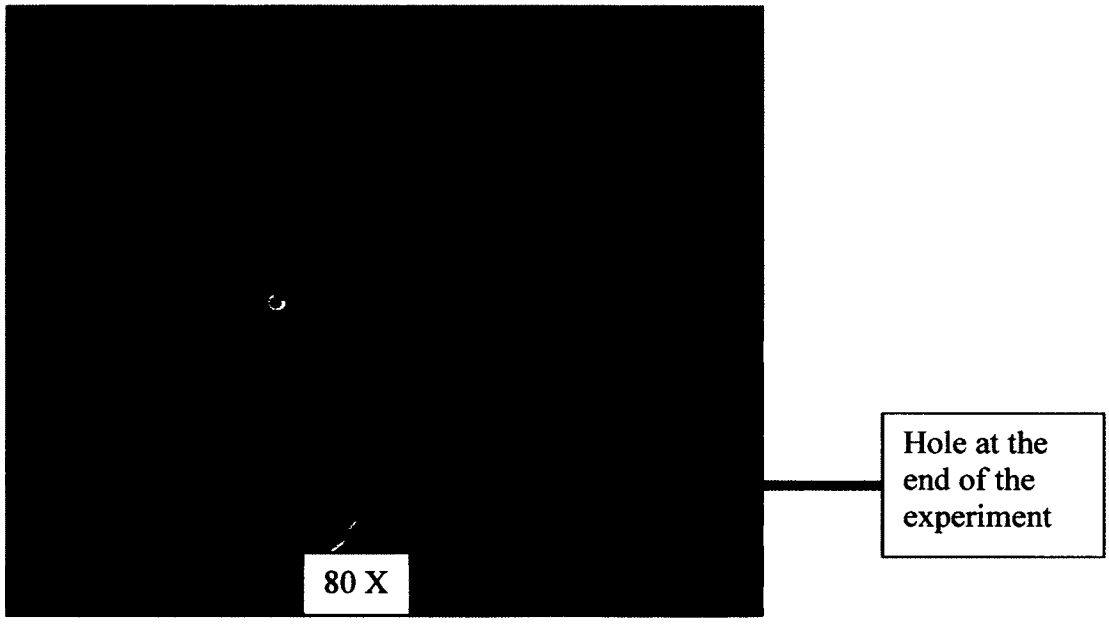
Hole at the
end of the
experiment
80 X

(c)

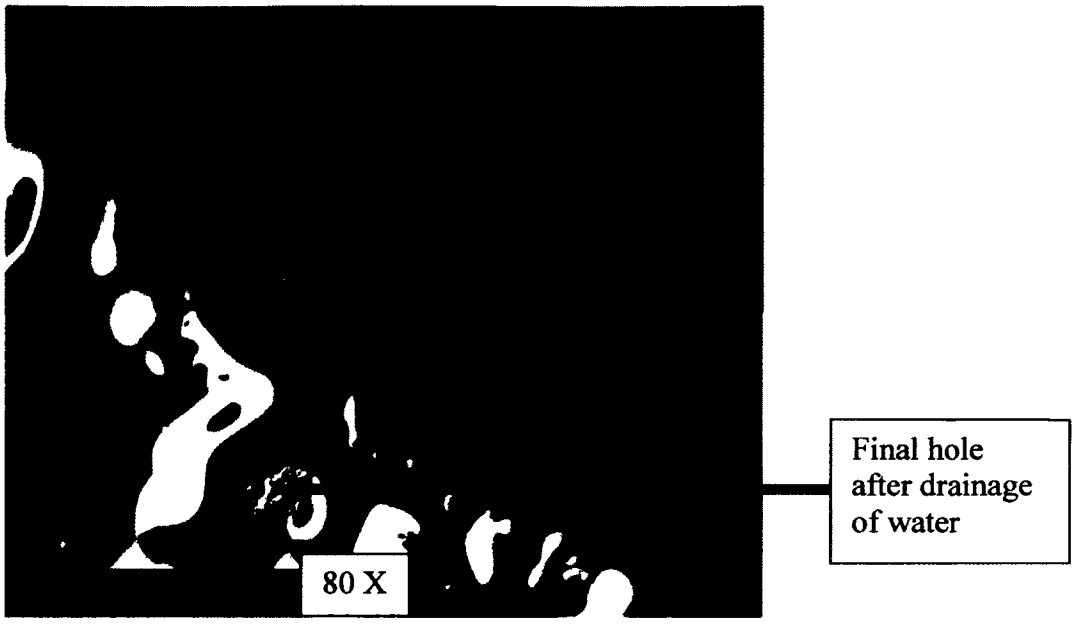

(d)

Figure 5-7: (a) Dewetted radius and temperature vs. time of PG 58-28 asphalt on ½ in. gravel placed in water bath at 60°C, **(b)** Approximately 645 s after start of experiment, **(c)** Approximately 7465 s after start of experiment, **(d)** Final hole and rim after the completion of the experiment in the absence of water.

In Figure 5-8 (a), even at low temperature, dewetting of the asphalt film was already taking place. Within the temperature range of ambient to 40°C, the expansion of the hole followed the behavior of most of the dewetted holes whenever the initial temperature was at the ambient. From observation, this film thickness having a thickness of about 16.81 μm, higher than the average asphalt thicknesses, 5μm-15μm (Read and White, 2003), can be damaged by moisture very easily even at a low temperature. From 40 μm, the radius increased to 86 μm and continued with time and then increased steadily and leveled out again retaining a radius of approximately 40 μm before finally leveling out. Figure 5-8 (b and c) shows the dewetting of the PG 64-22 asphalt on the ½ in. gravel at approximately 2027 s and 9237 s, respectively, from the start of the experiment.

Figure 5-8 (d) shows in expanded view the hole and rim after drainage of the water at the end of the experiment.

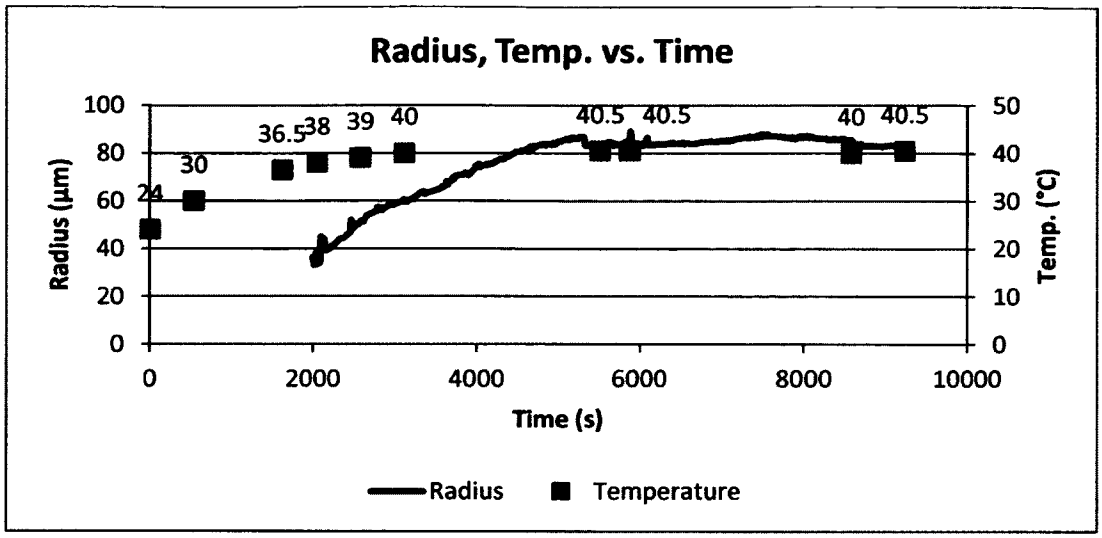

(a)

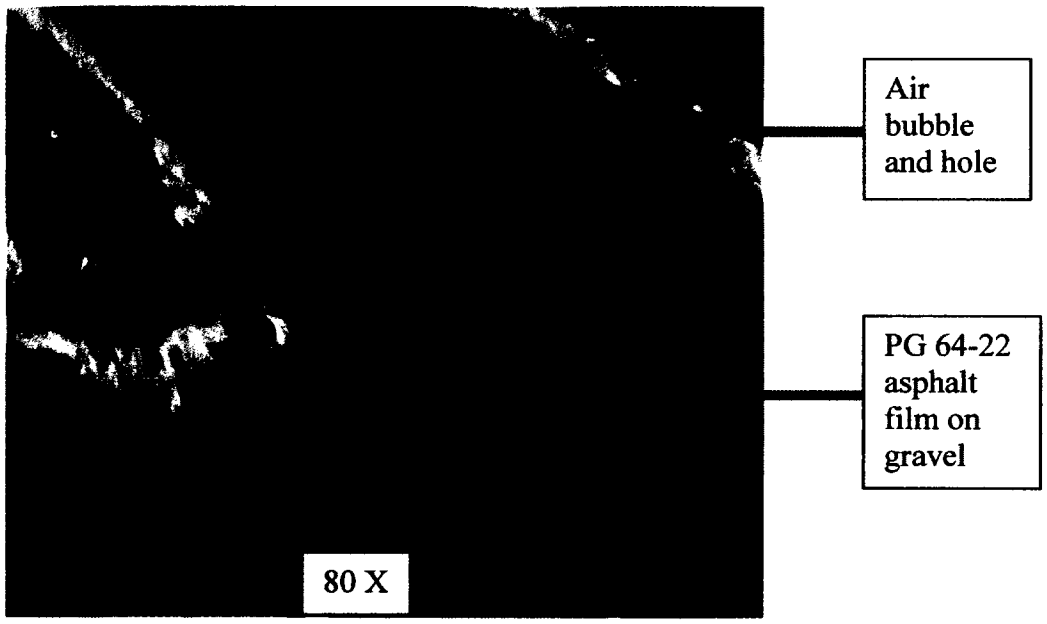

(b)

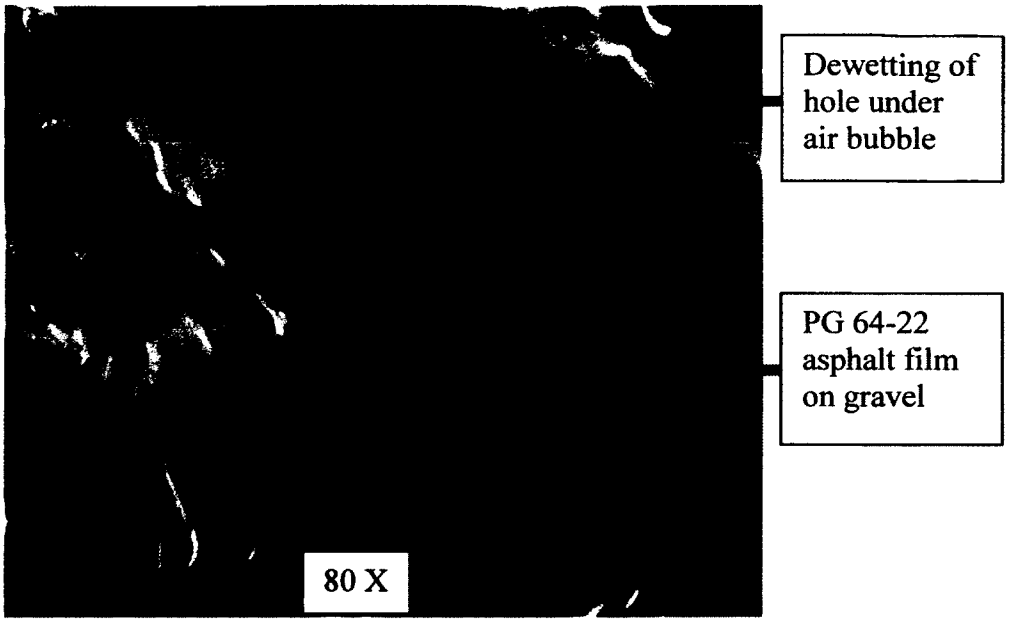

(c)

(d)

Figure 5-8: (a) Dewetted radius and temperature vs. time of PG 64-22 asphalt on ½ in. gravel of a temperature increase from ambient to 40°C in submerged water condition, **(b)** Approximately 2027 s after start of experiment, **(c)** Approximately 9237 s after start of experiment, **(d)** Final hole with rim after the completion of the experiment in the absence of water.

Rather than analyzing one hole as was done in the previous experiments, two holes have been analyzed in Figure 5-9. It was observed that the holes grow linearly up to a certain point in the experiment, as toward the end of the experiment the behavior of the system under investigation would not allow for proper measurement. The second hole, a few seconds after initiating, expanded greatly. Coagulation of air bubbles within the film could be the cause for that rapid change. Although two separate holes, the growths ran parallel to each other intersecting at 3680 s and changing behavior from that point onwards. Figure 5-9 (b and c) shows the dewetting of the PG 64-22 asphalt on the ½ in. gravel at approximately 2027 s and 9237 s, respectively, from the start of the experiment. The depiction of the final hole and rim after drainage of the water at the end of the experiment is seen in Figure (d). From this microscopic image, it is observed that the PG 64-22 asphalt thin film on the aggregate substrate has not been completely dewetted as a residue layer was preserved.

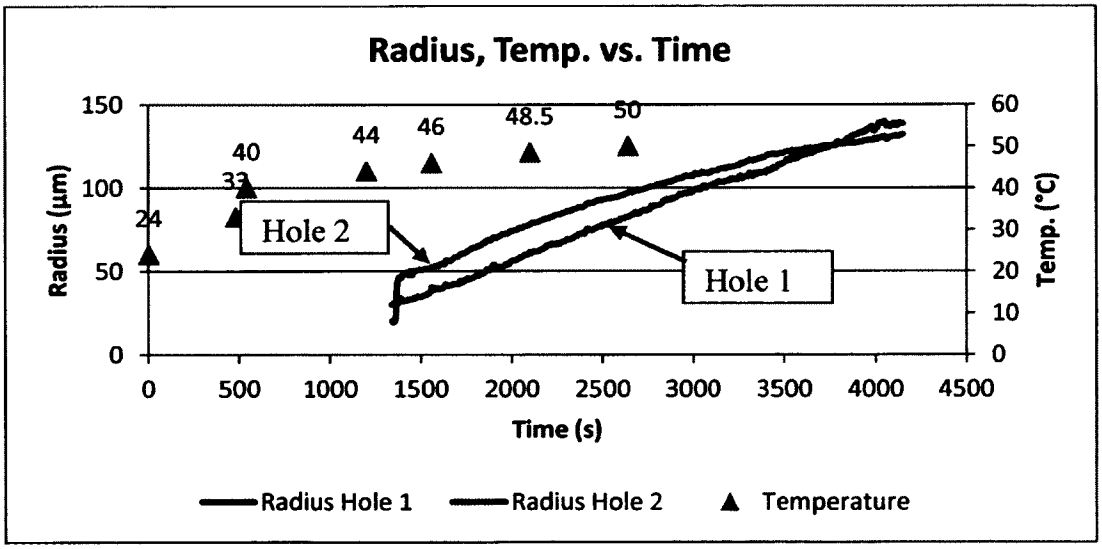

(a)

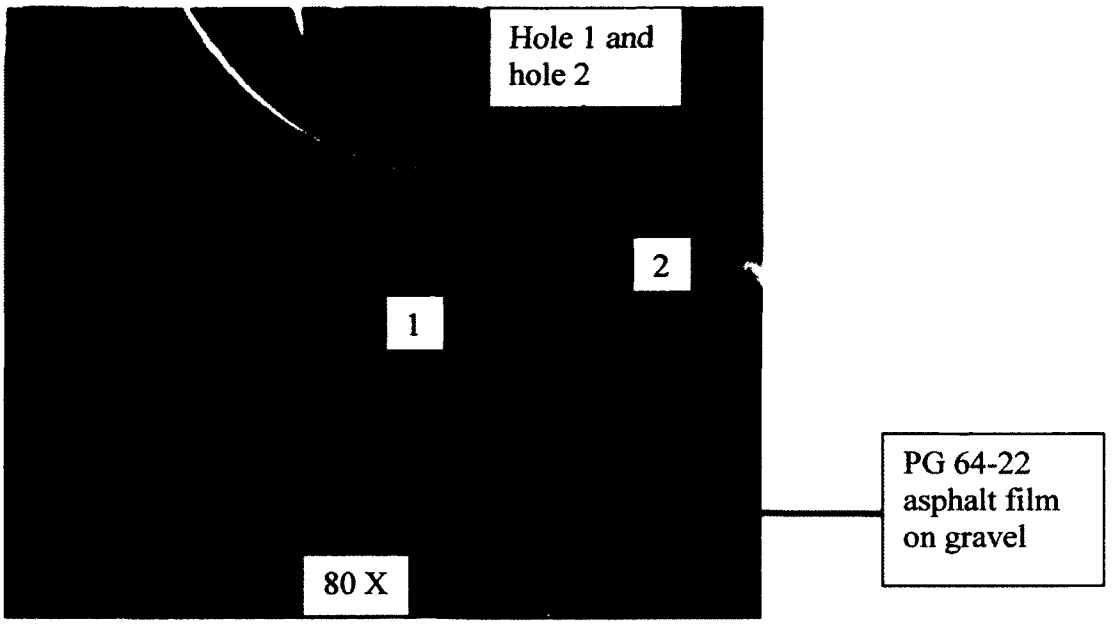
Hole 1 and
hole 2
2
1
80 X
PG 64-22
asphalt film
on gravel

(b)

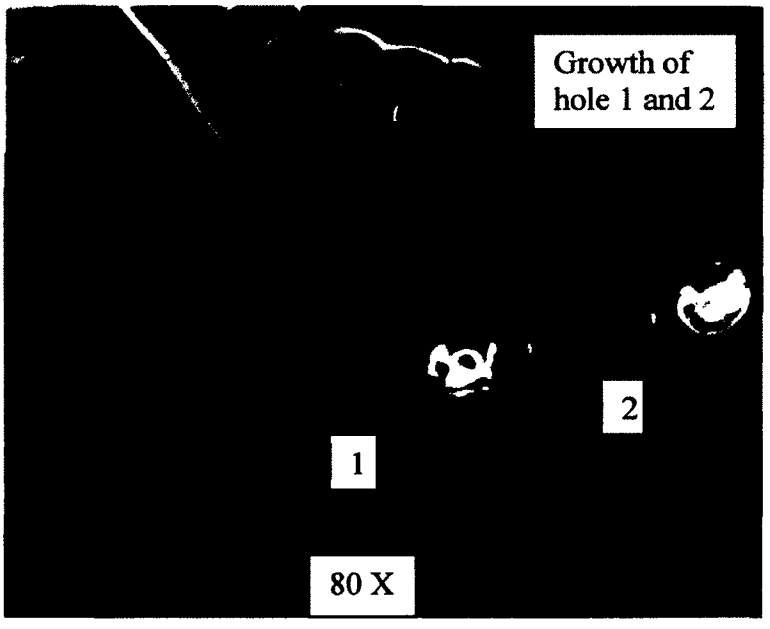
Growth of
hole 1 and 2
2
1
80 X

(c)

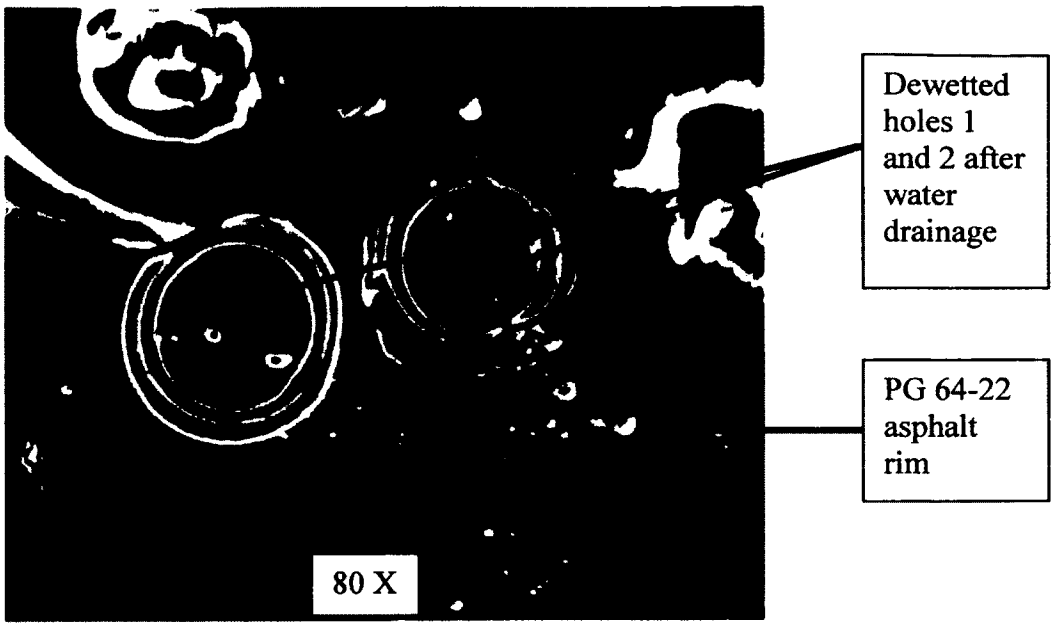

(d)

Figure 5-9: (a) Dewetted radius and temperature vs. time of PG 64-22 asphalt on ½ in. gravel of a temperature increase from ambient to 50°C in submerged water condition **(b)** Approximately 1459 s after start of experiment (hole 1 and hole 2), **(c)** Approximately 4009 s after start of experiment, **(d)** Final hole with rim after the completion of the experiment in the absence of water.

At a temperature increase from ambient to 60°C, the hole growth in Figure 5-10 was mostly linear, moving at a fast pace up to 2171 s approximately, and reducing its speed from there as dewetting continues to be undertaken in a linear pattern. Figure 5-10 (b and c) shows the dewetting of the PG 64-22 asphalt on the ½ in. gravel at approximately 871 s and 4891 s, respectively, from the start of the experiment. It must be realized that the growth pattern of the hole does not resemble that of an exponential growth than those of the other samples whose experiments began from ambient temperature. The depiction of the final hole and rim after drainage of the water at the end of the experiment is seen in (d). As observed in the previous experiments, asphalt was seen to not dewet completely on the substrate leaving behind a very thin residual film on

the aggregate possibly measuring in the sub micrometer range leaving some parts of the aggregate visible. The film substrate of aggregate (gravel), even though relatively smoother than limestone, is not smooth on the micrometer scale and, therefore, can retain this thin residual film. Given time, these relatively thin films can dewet via spinodal decomposition. Also as can be seen in Figure 5-10 (d), the asphalt rim was properly formed. Moisture damage, therefore, in pavements, can occur in the micrometer range based on these observations thus far with trapped moisture in the film or interface.

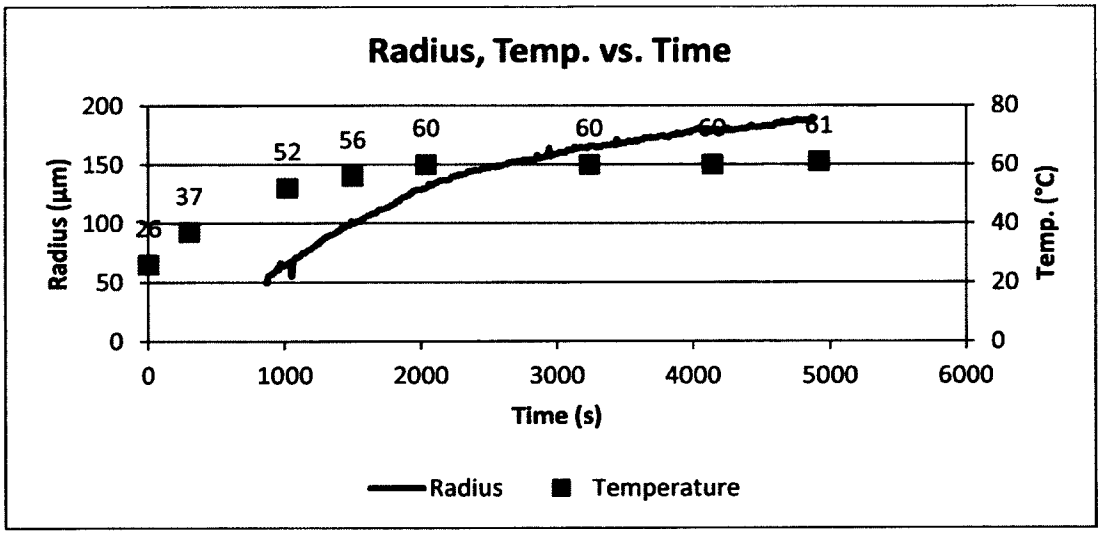

(a)

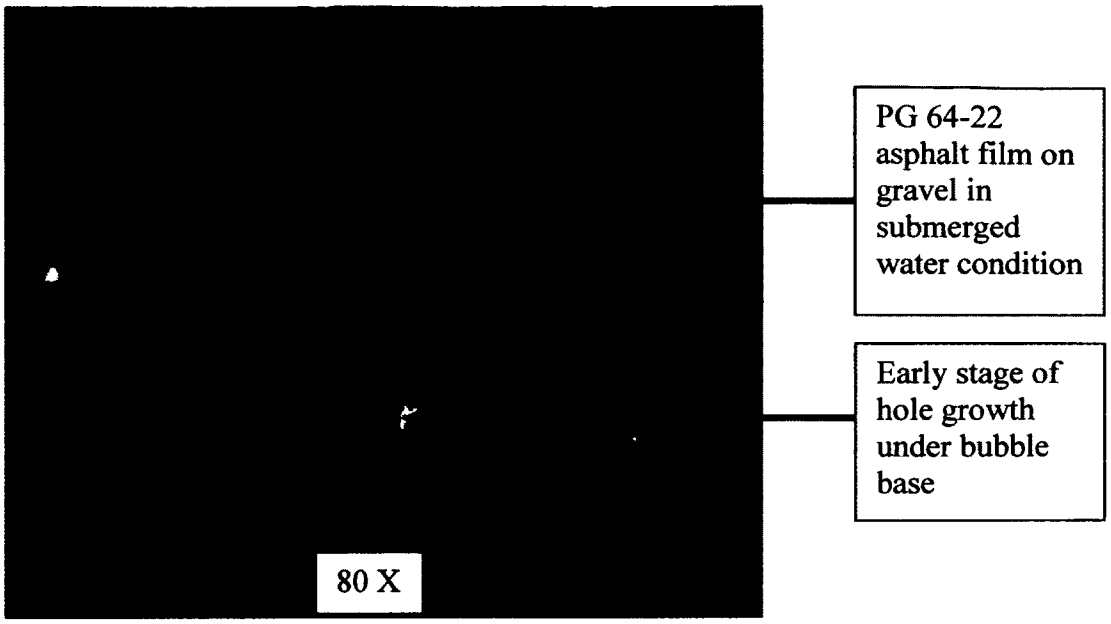
PG 64-22 asphalt film on gravel in submerged water condition
Early stage of hole growth under bubble base
80 X

(b)

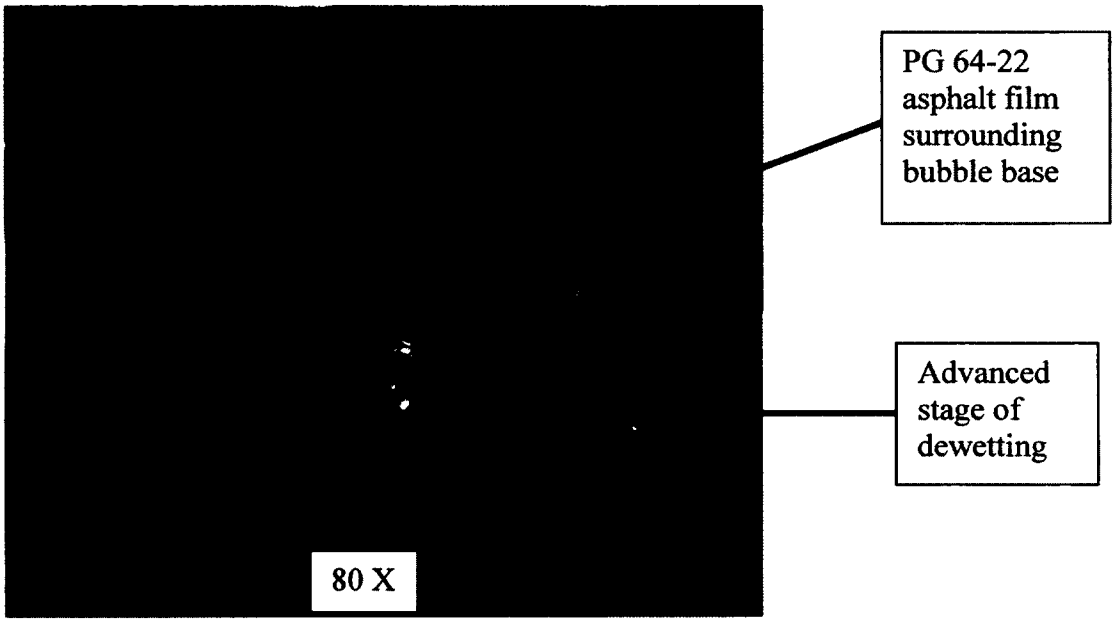
PG 64-22 asphalt film surrounding bubble base
Advanced stage of dewetting
80 X

(c)

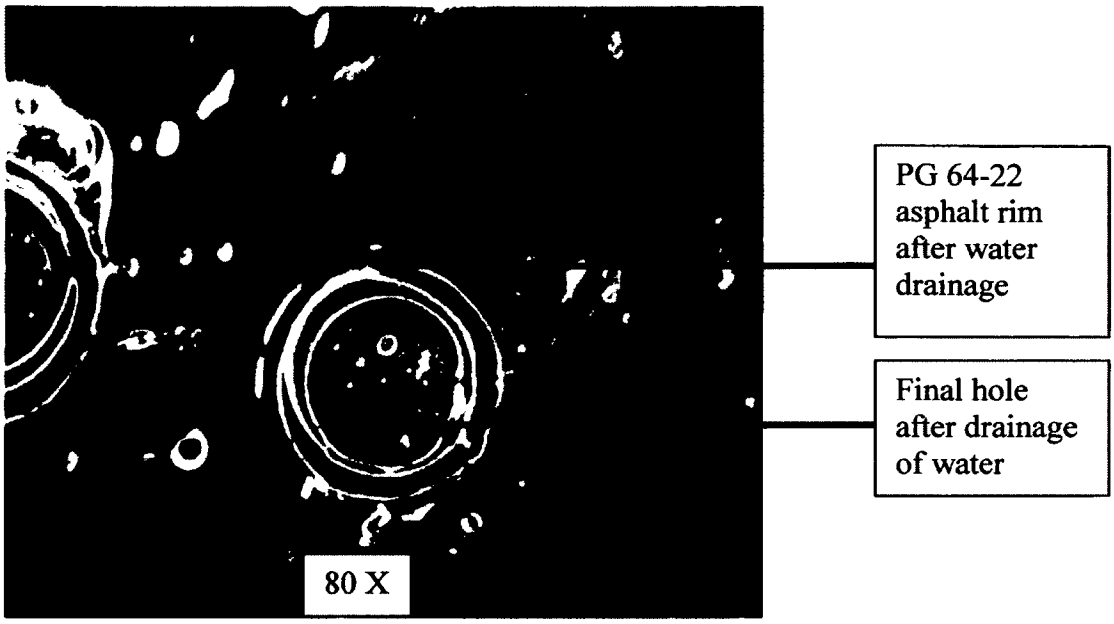

(d)

Figure 5-10: (a) Dewetted radius and temperature vs. time of PG 64-22 on ½ in. gravel of a temperature increase from ambient to 60°C in submerged water condition, **(b)** Approximately 871 s after start of experiment, **(c)** Approximately 4891 s after start of experiment, **(d)** Final hole with rim after the completion of the experiment in the absence of water.

As seen in Figure 5-11, the aggregate with film was placed directly in warm water at 40°C. The rate at which the hole grew was linear for the entire experiment, though occurring very slowly. This rupture was not captured in the earliest stages of hole formation.

Figure 5-11 (b and c) shows the dewetting of the PG 64-22 asphalt on the ½ in. gravel at approximately 2254 s and 9284 s respectively, from the start of the experiment. It must be realized that the growth pattern of the hole does not resemble that of an exponential growth as those of the other samples, whose water conditioning temperature increased from ambient temperature. The depiction of the final hole and rim after drainage of the water at the end of the experiment is seen in Figure 5-11 (d). Moreover,

observations in Figure 5-11 (d) show that after water drainage at the end of the experiment, the aggregate surface was clearly visible with the rim surrounding the hole. The film was totally dewetted even though the average film thickness of 23.88 μm is slightly thicker than that of other aggregate samples. Moisture damage, hence, can therefore occur at low temperatures in asphalt films within the pavement in a submerged water condition.

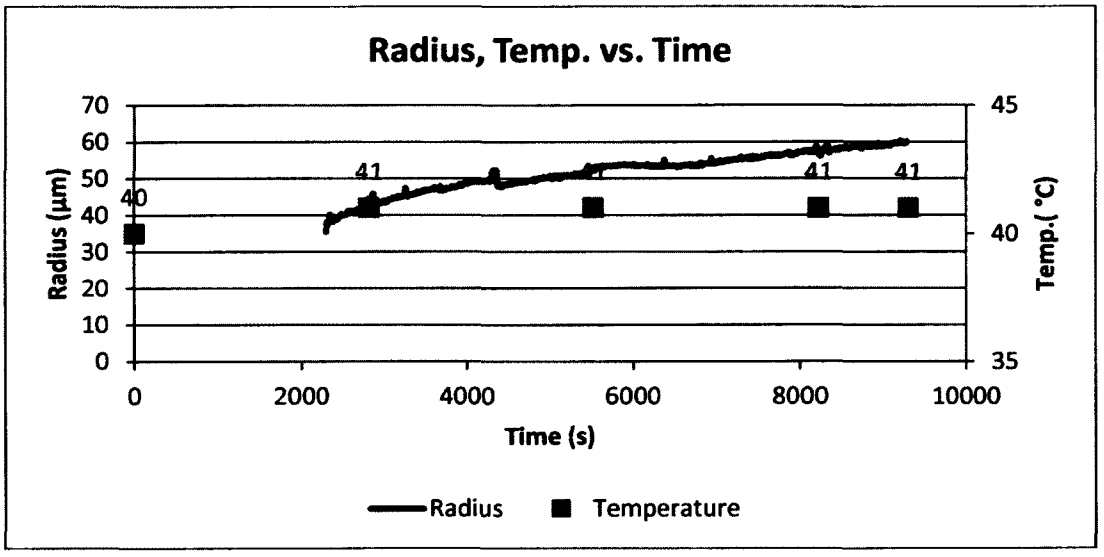

(a)

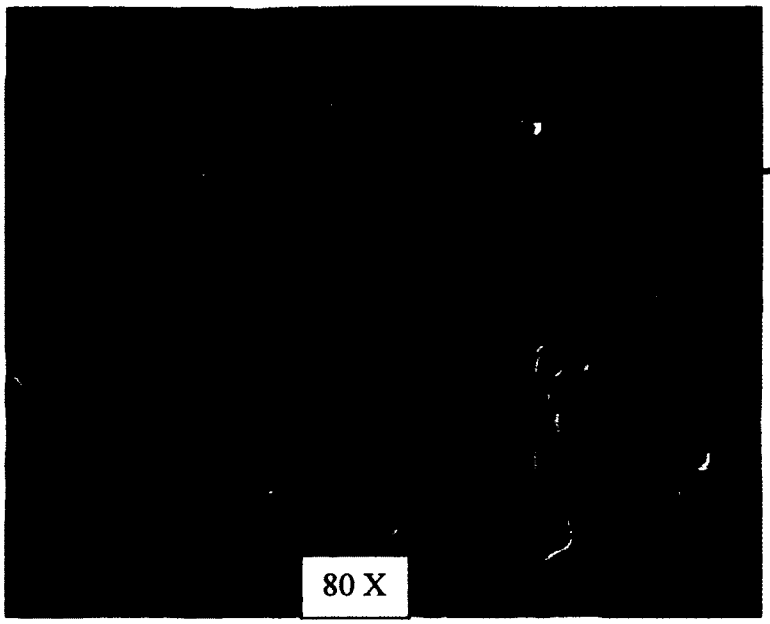
Early stage of dewetting under air bubble
80 X

(b)

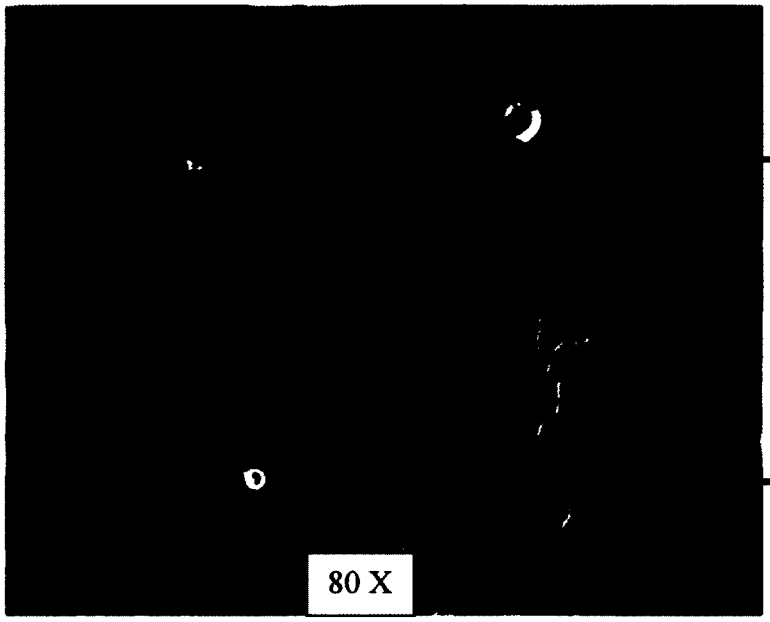
Dewetting of hole under air bubble
PG 64-22 asphalt film on gravel
80 X

(c)

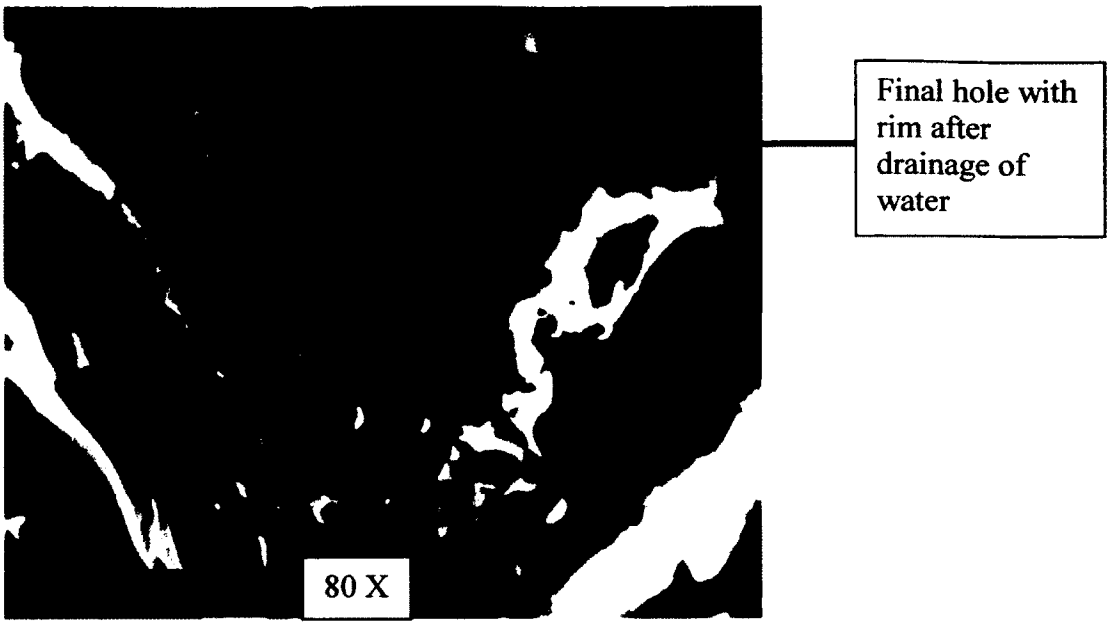

(d)

Figure 5-11: (a) Dewetted radius and temperature vs. time of PG 64-22 on ½ in. gravel placed in water bath at 40°C **(b)** Approximately 2254 (s) after start of experiment, **(c)** Approximately 9284 (s) after start of experiment, **(d)** Final hole with rim after the completion of the experiment in the absence of water.

5.5 Effect of Water Type and pH on Dewetting

The contact angle of a wetting film on substrate is a fundamental characteristic of wetting. The dynamic contact angle has been observed to alter more rapidly at a lower pH value than at higher pH values (Basu et al.,1996).

Interactions between solid surfaces and liquid media that contain dissolved ions such as water, are most notably important in the explanation of moisture damage in asphalt mixes (Kumar and Anand, 2012). Moreover, in conducting experiments of hydrocarbon film rupture on mineral surfaces, Francisca et al. (2003) observed that the film tended to break at a faster rate when the wetting fluid used was a water-detergent rather than when it is deionized water or isopropyl alcohol.

Two different types of media were used to test all samples in this experiment: water (ionized) and deionized water to assess the effects on the dewetting and moisture damage of asphalt films on aggregate surface (Table 5-1). The dewetting patterns of the first three aggregate specimens in deionized water (Ambient to 40°C, Ambient to 50°C, and Ambient to 60°C; pH 6.7, 6.0, 6.2 respectively) were very similar despite the maximum temperature attained. For tap water, subjected to the same temperature increase, and pH 7.8, 7.9, and 7.8, respectively, the radius growth behaved relatively linearly within the first 4000 s of the experiments. In 40°C water conditioning (deionized and ionized), the dewetting of asphalt film on limestone was compared to dewetting on gravel. Subjected to a minimum of 7000 s of radius growth, in deionized water and pH of 6.2, the apparent hole radius remained constant and then decreased slightly toward the end of the experiment with the temperature increasing to 42°C. In tap water at 40°C, also increasing to 41°C, the hole continued to dewet relatively slowly for the entire experiment. At a temperature of 50°C in deionized water at pH of 6.2, the radius growth rate was linear throughout except toward the latter end when it became constant.
PG 58-28 was observed to dewet on gravel in deionized water at a temperature of approximately 60°C. In comparing the growth to the previous analysis of PG 64-22 at 50°C, the rate of radius growth was slower for the PG 58-28 asphalt film.

5.6 Conclusions

As is the case for the dewetting of asphalt films on glass plates, there are many reasons why dewetting of a film on a substrate occurs. Two main types of dewetting include spinodal dewetting and nucleation and growth of a hole. Trapped air bubbles also cause the rupture of films. Moisture damage has been a major cause of distress in

asphaltic pavements. A study of rupture and dewetting of asphalt films (PG 64-22, PG 58-28) was undertaken with aggregate substrates. The observations of dewetting as it pertain to aggregate substrate shows:

1) Dewetting and rupture of asphalt films occur at low temperature ranges on aggregate surfaces, even less than 40°C.
2) Most dewetting patterns follow that of an exponential growth.
3) Asphalt film will readily spread up an air/water interface. During that process, asphalt dewets at the base of an air bubble.
4) For most of the aggregate specimens, a very thin layer of the asphalt was observed to remain on the surface after dewetting.
5) Healing on a large scale of the asphalt binder in the aggregate samples was not observed.
6) For the aggregates, what begins off as a minute rupture, grows into a macroscopic hole leaving behind a solid rim which remains after the drainage of water from the experiment.
7) The water environment, including ions and pH may have an influence on the dewetting of asphalt films.

CHAPTER 6

DEVELOPMENT OF A TEST METHOD TO TEST MOISTURE DAMAGE AND DEWETTING

6.1 Background and Objectives

Chapters 3 and 4, and 5 helped understand and characterize the dewetting as well as the moisture damage mechanism of the asphalt film. However, it was not possible to quantify the effects of all possible variables (e.g. additives, pH and asphalt binders), by analyzing one singular dewetting hole. Therefore, in this chapter, a macro-scale dewetting analysis procedure was developed that considers all the holes in the sample. The objectives of this study are as follows:

- To estimate by experimentation the critical film thickness for asphalt films related to moisture damage in the field.
- To evaluate the effects of film thickness on dewetting.
- To evaluate the effects of polymer on dewetting.
- To evaluate the effects of anti-strip additives on dewetting of asphalt films.
- To evaluate the effects of additive dosages (0%, 0.25%, 1%, 2%) on dewetting.
- To evaluate the effects of pH on dewetting of asphalt films.

6.2 Development of a Unique Test Procedure and Analysis

For the development of a test method, three performance grade (PG) asphalt binders (PG 58-28, PG 64-22, and PG 76-22M) and two anti-strip additives (Adhere HP Plus, Adhere LOF 6500) from Arr Maz Custom Chemicals, Inc., were used. Varying percentages of anti-strip additive, film thicknesses and pH were used in this test method to investigate the effects that the modified asphalt binders would have on the dewetting mechanism. The test matrix for this test method can be seen in Appendix D, Table D-1. Many other trial experiments were performed to assess the causes of the dewetting which was predominantly caused by the air bubbles. Other exploratory studies were used to characterize the dewetting mechanism as discussed in the previous Chapters.

6.2.1 Procedure Used in Sample Preparations

Figure 6-1 (a) shows typical sample preparation, experimental setup for testing, and data collection while (b) shows the detailed experimental setup for collection of data for analysis.

1. Glass plates (measuring 2 in. x 2 in. x ¼ in. thick) were cleansed in detergent water, followed by tap water and heated for 15 min at 163°C to produce a relatively clean surface. Kapton (5 mil) high temperature tape was utilized on two opposite ends of the glass plates to control the thickness of the asphalt film, and as a result, the final area was reduced in most cases to 2.5 cm x 5.08 cm. The thickness after testing was also approximated by the gravimetric technique, where the asphalt density was approximated at 1 g/cm^3.
2. The glass plate specimens were then heated for approximately 1 h while the asphalts were heated for approximately 45 min at a temperature of 163°C.

3. The asphalt was applied on the glass plate with the help of a silicone mold purchased from TA Instruments, New Castle, DE; Gilson Company Inc., Lewis Center, OH.

   The samples were placed directly in the desiccators after being prepared. Each specimen before testing was left in ambient temperature for a minimum of 18 h. Upon curing, the excess asphalt was cleansed carefully with solvent.

4. After curing, the samples, generally placed by twos were placed in ambient water and the temperature was increased from ambient to approximately 50°C by placing the container with the samples on top of the hotplate.
5. Before testing, 0.01 grams of particles, aggregates (gravel) (See Appendix G for SEM analysis) retained on # 100 sieve size, were spread in a random pattern on the asphalt film area of 2.5 cm x 5.08 cm.
6. Before adding the particles, photos were taken, against the light source by the camera also after the particles were added.
7. After 2 h of testing, the samples were removed from the bath and the dewetted holes were captured with the use of a camera
8. After testing, the pictures were analyzed, with the National Instruments Vision Builder AI 2012 software, (Austin, TX). For all analyzed specimens, an indentation of 2 mm from all four edges of the asphalt film were made to assess the hole area and dewetted hole area distribution caused via moisture damage.

The camera was placed on a solid platform, at approximately 9.7 cm from the glass plate specimen (Figure 6-1b). A light source was placed in front of the glass plate specimen and measured about 8 cm from the back of the glass plate. For measurement calibration of the software, a 10 mm (1 cm) rule was placed parallel to the glass plate samples. It must be noted that every sample tested was calibrated for accuracy although the distances of the experimental set-up were approximately the same.

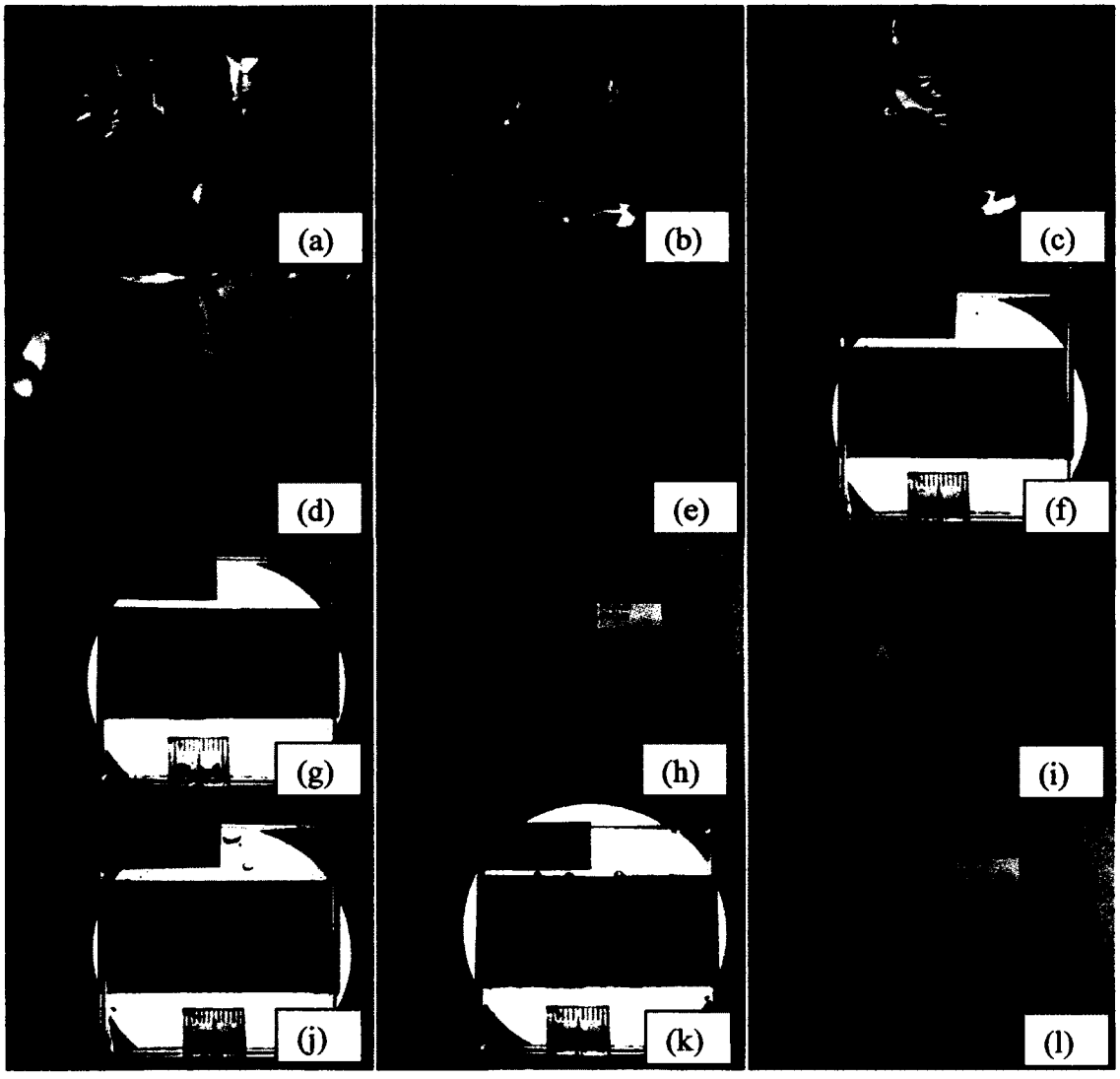

[a]

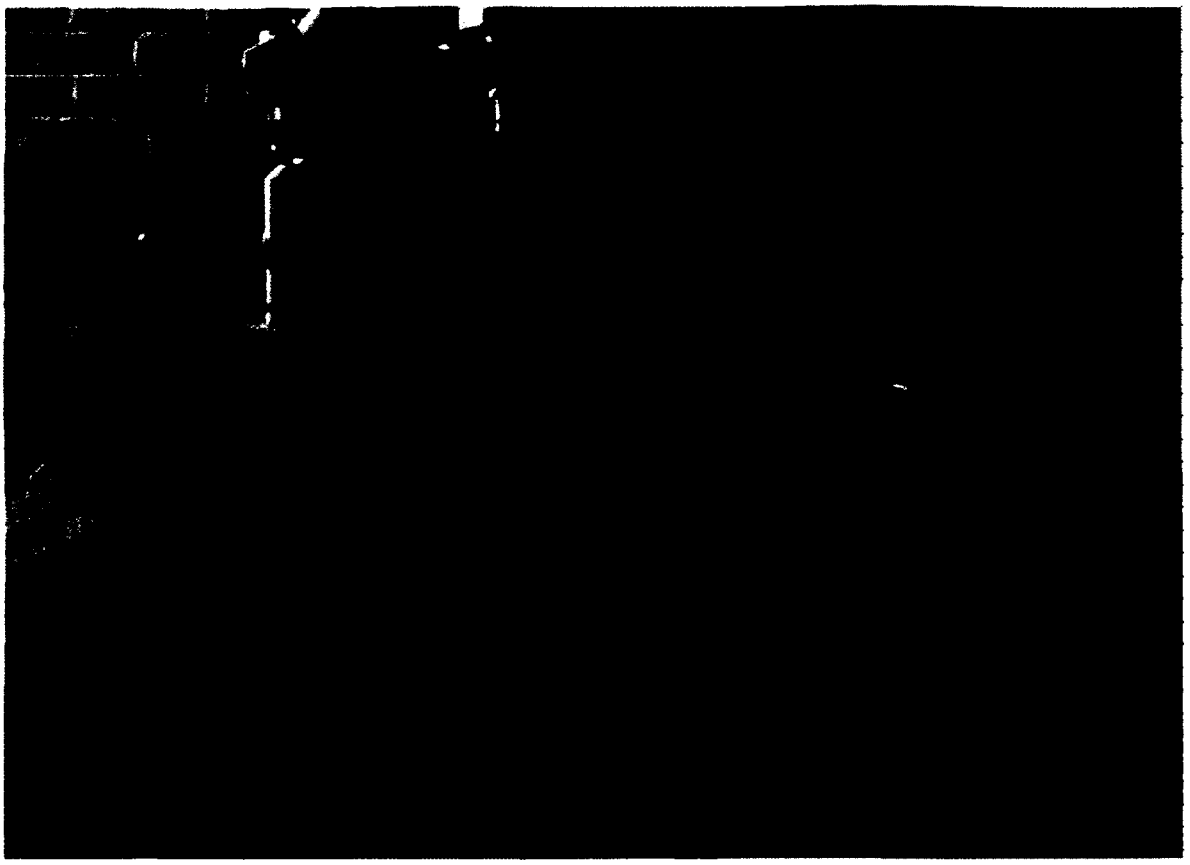

[b]

Figure 6-1:[a]Sample Preparation and Testing: **(a)** Asphalt getting ready to be poured; (b) Asphalt being poured on glass plate surface; **(c)** Asphalt film created with the use of a mold; **(d)** Asphalt sample complete; **(e)** Asphalt samples placed in desiccators; **[(f)** and **(g)]** Asphalt samples placed before light source and picture taken before testing; **(h)** #100 gravel randomly distributed on asphalt samples; **(i)**Samples submerged in water in pyrex placed on hot plate; **[(j)** and **(k)]** Asphalt samples placed before light source and picture taken after testing; **(l)** Tested samples **[b]** Experimental setup with camera, base, glass plate sample, calibration scale and light source.

Figure 6-2 shows an enlarged dewetted area of PG 64-22 + 1% Adhere LOF 6500 sample. Moreover, Figure 6-3 shows a microscopic image of the dewetting of a PG 64-22 + 1% Adhere HP Plus sample submerged in water (Ambient to 50°C).

It must be noted that the SM-4T microscope from Amscope® (Irvin, CA) with light was focused on some asphalt samples, particularly those of the neat binders

connected to the computer to assess the growth of the holes within specific intervals of the two hour duration of the experiment. However, it was found that the dewetting of these specimens was affected by the light and, as a result, these samples were not used in the analysis. These samples are included in the Appendix D, Table D-1.

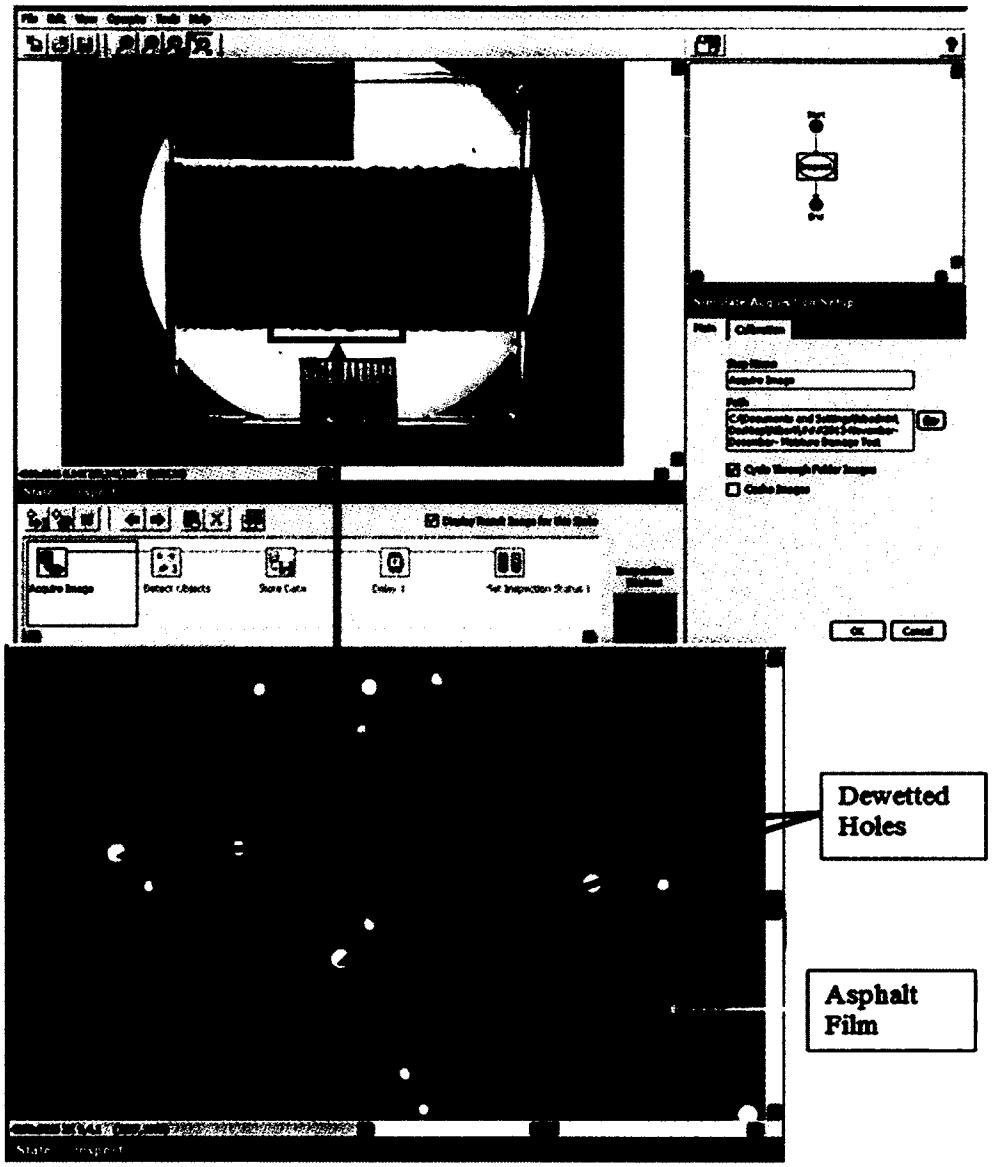

Figure 6-2: PG 64-22 + 1% Adhere LOF 6500 dewetted sample.

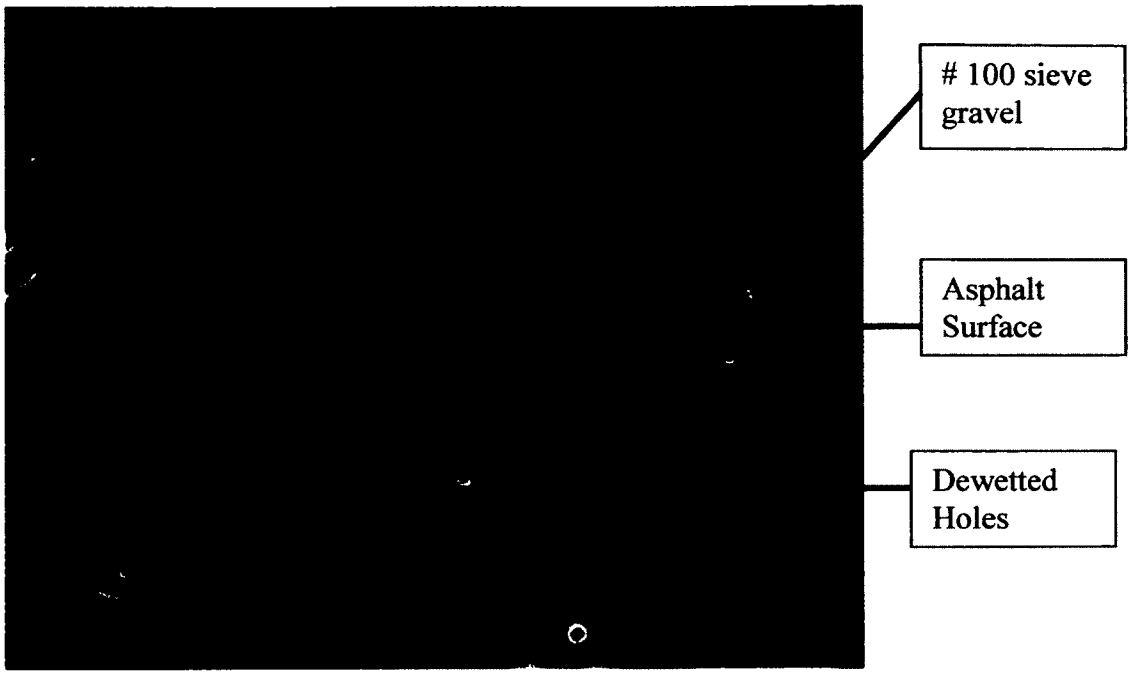

Figure 6-3: Microscopic Image PG 64-22 + 1% Adhere HP Plus submerged in water (Ambient to 50°C) for 2 h.

6.3 Results and Discussion

6.3.1 Effects of Film Thickness on Dewetting of Asphalt Films

The thickness of a film (polymer or otherwise) is one of the most important critical parameters for the dewetting of thin polymer films and vary for various polymers. In the typical hot mix asphalt pavement, a theoretical asphalt film thickness is used in the mix design which ranges from approximately 5 μm to 15 μm (Read and Whiteoak, 2003). Read and Whiteoak (2003) asserted that the aggregate and filler are coated with this typical thickness through the mixing process. Kandhal et al. (1998) concluded that an average minimum thickness of 8 μm is to be recommended to ensure mix durability. A recent publication has questioned the validity of this thickness range (Elseifi et al., 2008), however, recognizing that most asphalt film thicknesses are mastic thicknesses and

greater than that of the range previously mentioned. Kandhal et al. (1996) agrees with the more recent study by expounding how much validity can be ascribed to a film thickness, obtained by simply dividing the aggregate surface area (received from its gradation) by the effective asphalt content. Chadbourn et al. (1999) asserted that asphalt film thickness is one of the main elements as it pertains to the durability and moisture susceptibility of an asphalt mixture. Image analysis was used to observe and analyze film thickness distribution in a typical hot mix asphalt mix (Elseifi et al., 2008).

In Figure 6-4 (Elseifi et al., 2008), it may be observed that up to 500 μm film thickness, the occurrence in the asphalt samples had a minimum threshold of 6%. Therefore, it shows the importance of the designed film thicknesses in the field particularly to resist against moisture damage which continues to plague HMA pavements in the United States and elsewhere. The film thicknesses prepared for the moisture damage and dewetting analysis in this study were allowed to vary within this region but not exceeding 500 μm.

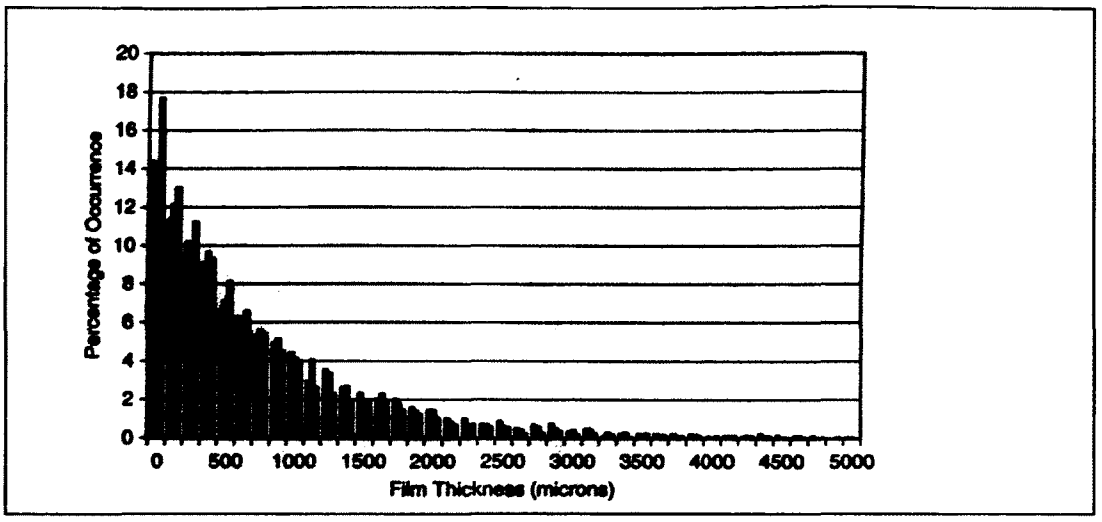

Figure 6-4: Film thickness distribution in asphalt mixes based on digital image analysis (Elseifi, et al. 2008). Printed with permission. Reproduced with permission. M.Elseifi, I.Al-Qadi, S.-Hsien Yang, and S. Carpenter, 2008. Validity of Asphalt Binder Film Thickness Concept in Hot-Mix Asphalt. *Transportation Research Record: Journal of the Transportation Research Board,* No. 2057, [Adapted] Figure 5, p. 41, Washington, D.C., 2008.

Moreover, an understanding of the critical dewetting film thickness is of paramount importance. As a result, an effort was put forth to measure experimentally the critical film thicknesses of asphalts PG 58-28, PG 64-22, and PG 76-22M based on the total number of dewetting holes per sample based on 12 samples per asphalt type.

From the plot in Figure 6-5 (a), the critical film thickness for PG 58-28 was within the range of approximately 299 μm. This film thickness had a total dewetting of 10 holes. Below this range and as the asphalt film tends to 118 μm, the dewetted holes increased significantly. For PG 64-22 asphalt film, the graph exhibited a critical thickness within the range of 307 μm to 339 μm with the total number of dewetted holes at 3 and 13, respectively, although at 307 μm, 46 holes dewetted and at 315 μm 16 holes dewetted. The average thickness within these four thickness ranges was 315 μm together with an average number of dewetted holes at 10. Although there was a difference in

viscosity between PG 58-28 and PG 64-22 asphalt, it should be noted that the approximate critical thickness is relatively the same for both. The third binder that will be analyzed herein is the polymer modified binder, PG 76-22M. It must be noted that within a film thickness range of 228 μm, the dewetted holes present in the PG 76-22M asphalt are less than the other two unmodified asphalt binders used in the experiment. Within a range of 315 μm to 407 μm, the minimum number of dewetted holes were 3 at 315 μm, and the maximum was 16 at 354μm. Based on the observations, it was fair to estimate the critical film thickness for PG 76-22M at 315 μm. Although polymer modified, the critical thickness was within the range of the critical thickness for both unmodified asphalts. Therefore, based on these experiments, this finding suggests that asphalt film thickness plays a most critical role in the durability of asphalts in hot mix asphalts as it pertains to pavement withstanding moisture damage and distresses such as raveling and rutting.

The correlation coefficients are depicted in Figure 6-5 (b). The strongest correlation was reflected in the PG 64-22 asphalt binder (0.924) which showed that the moisture damage of this asphalt was strongly affected by its film thickness. However, based on critical values of the correlation coefficient for significance level α, the values for PG 58-28 and PG 64-22, asphalt binders were significant (Wheeler, 1988). At a 90% confidence level, the computed coefficient (0.697, 0.515) was higher than a critical value (0.497) based on the number of samples. At this 90% confidence level, the results show that for all three film thicknesses, the number of dewetted holes is a function of the film thickness. The PG 58-28 did not reflect such a strong correlation as PG 64-22 asphalt but nonetheless, the correlation between dewetting and film thickness was relatively strong. The least correlation was found to be in PG 76-22M. Within the vicinity of 200μm film

thickness, less dewetting was reflected in PG 76-22M asphalt as opposed to that of PG 58-28 and PG 64-22 asphalt. Generally, it was observed based on the correlations that moisture damage was directly correlated to film thickness particularly for the PG64-22 asphalt binder.

According to Czarnecki et al. (2005), the critical film thickness depends on the substrate's wettability and on the initial hole size. The critical thickness is given by Czarnecki et al. (2005) as was acknowledged was derived by Sharma (1993):

$$h = r_m ln\left(\frac{2\sin\theta}{r_m(1+\cos\theta)}\sqrt{\frac{\gamma}{\rho g}}\right) \qquad \textbf{Eq. 6-1}$$

where r_m is the minimum radius of the hole, γ is the interfacial tension of the asphalt -water interface, ρ is the density difference between water and asphalt, g is the acceleration due to gravity, and θ is the contact angle of the asphalt film on the substrate.

Based on the interfacial tension of PG 58-28 (Miknis et al. 2005), the above equation was used, which included the minimum radius of three actual holes from the experiments, where the contact angles span from within the range of approximately 0-180 degrees. The value for ρ used in the equation was 0.01 g/cm^3 (ρ water is 1g/cm^3, ρ asphalt is 0.99 g/cm^3) and g was taken as 9.8 m/s^2. In Figure 6-5 (c), it was observed that r = 0.01 mm will dewet completely below a film thickness of 0.1 mm. Based on the theory, a film with a hole of radius of r = 0.05 mm will dewet completely for a contact angle up to 70°. The largest hole on the graph, r = 0.1 mm will dewet in a film below a PG 58-28 film thickness of 0.75 mm. Therefore, at 10°, approximately all PG 58-28 asphalt films will dewet at a film thickness of 0.3 mm. The theoretical dewetting film thickness model appeared to reflect the film thickness found experimentally.

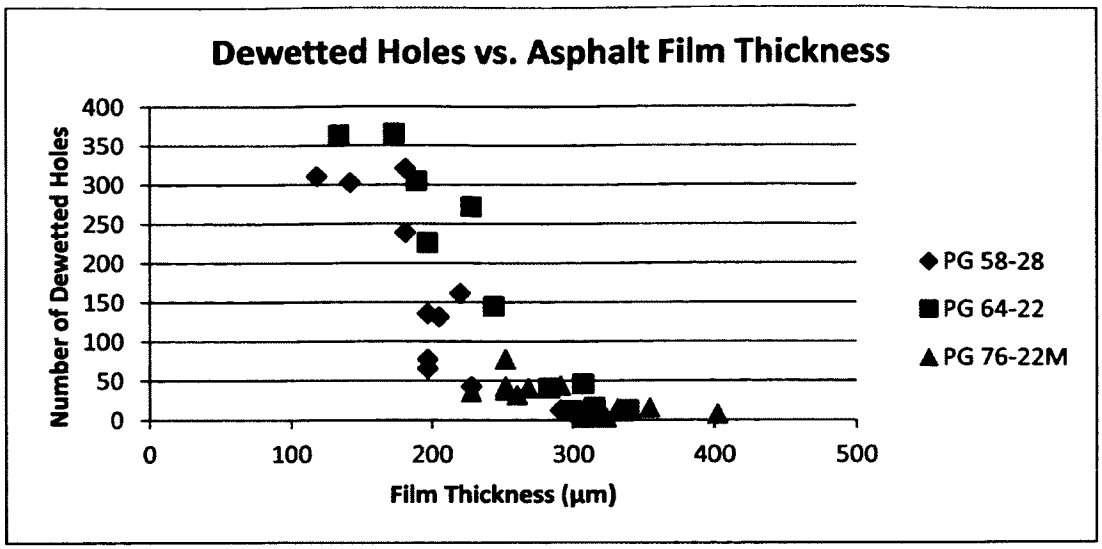
Dewetted Holes vs. Asphalt Film Thickness
Number of Dewetted Holes
400
350
300
250
200
150
100
50
0
0
100
200
300
400
500
Film Thickness (µm)
PG 58-28
PG 64-22
PG 76-22M

(a)

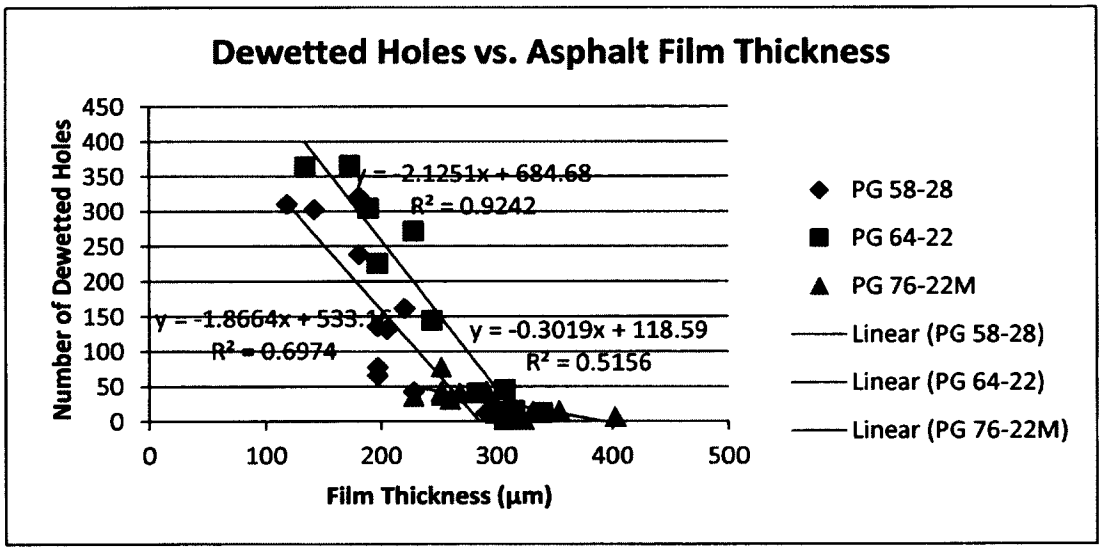
Dewetted Holes vs. Asphalt Film Thickness
Number of Dewetted Holes
450
400
350
300
250
200
150
100
50
0
0
100
200
300
400
500
Film Thickness (µm)
y = -2.1251x + 684.68
R² = 0.9242
y = -1.8664x + 533.1
R² = 0.6974
y = -0.3019x + 118.59
R² = 0.5156
PG 58-28
PG 64-22
PG 76-22M
Linear (PG 58-28)
Linear (PG 64-22)
Linear (PG 76-22M)

(b)

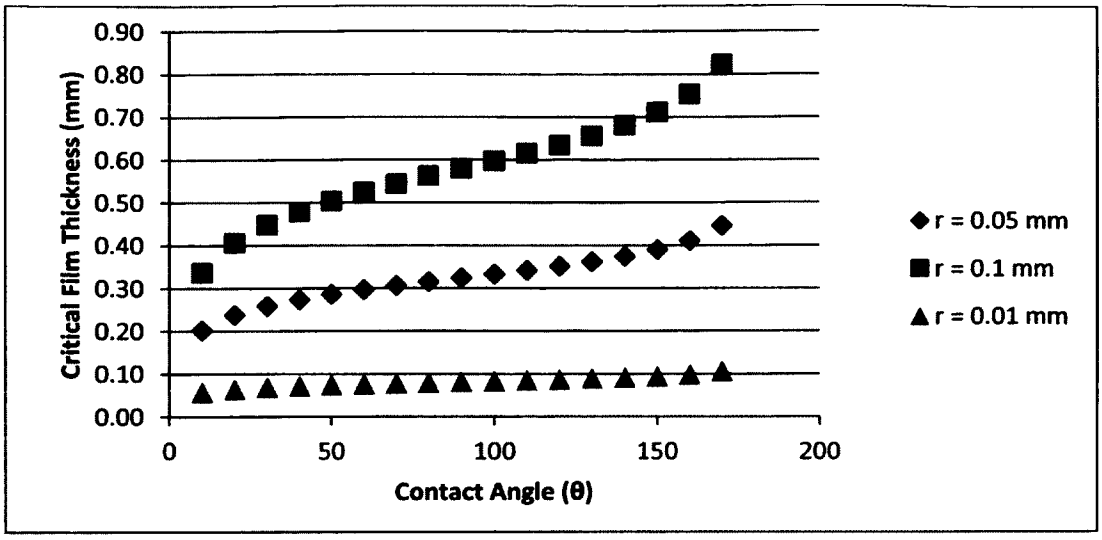

(c)

Figure 6-5: (a) Effects of film thickness on the dewetting of three asphalt binders: (PG 58-28, PG 64-22, and PG 76-22M), **(b)** Correlation of total dewetted holes and film thickness: (PG 58-28, PG64-22, and PG 76-22M), **(c)** Critical asphalt film thicknesses for various dewetted hole radii based on asphalt/water interfacial tension (γ = 26.8 dyn/cm: PG 58-28, e = 220 μm).

6.3.2 Effects of Polymer on Dewetting of Asphalt Films

Polymer added in asphalt binders should serve to enhance the HMA mix and guard against premature pavement failure such as rutting, raveling and moisture damage. One reason for this enhancement can be reflected in a study conducted by Wekumbura et al. (2007). Wekumbura et al. performed the interrupted shear test on polymer modified asphalts based on the theory of the presence of a three dimensional network structure in polymer modified asphalt. Wekumbura et al. concluded, based on the shear test, that at the disturbance or destruction of this network by the shear flow, the structure, with time can reform, imparting the ability to self-heal. Albritton et al. (1999) concluded that all the modifiers used in their study were out-performing the control section, results being

reflected from roadway rutting and rutting in the APA. In evaluating the effects of moisture damage in polymer modified asphalts namely, styrene-butadiene and styrene-butadiene-styrene, SB and SBS, respectively, Tarefder and Zaman (2010) concluded that under wet conditions, neat binders were more prone to moisture damage than the polymer modified binders investigated in their studies. Additionally, it was reported that for both polymer modifications, 3% SB and 3% SBS, were observed to be the optimum to maximize the adhesion and cohesion forces of asphalts in wet conditions. This allows for a reduction in moisture induced damage for both polymer modified asphalt systems (SB and SBS). Kandil et al. (2007) also found that polymer modified asphalt binders retained a higher tensile strength with the use of the indirect tensile test after moisture conditioning. In conclusion, Kandil et al. (2007) suggests that PMA (polymer modified asphalts) would have better performance than pavements constructed with conventional binders if subjected to moisture damage. Moreover, Kim et al. (2003) in investigating fracture toughness of polymer-modified asphalts subjected to low temperatures observed that PMA (polymer modified asphalt) concrete in their studies had a higher resistance to low temperature damage when compared to normal asphalts. Moreover, the polymer modified asphalt performed better than normal asphalt concrete with the absence of fracture at lower temperatures (-10°C and below).

In the current experiment, the same 36 samples used to estimate critical thickness were tested and analyzed, 12 for each of the binder type under investigation (PG 58-28, PG 64-22, and PG 76-22M). The results were based on the sum of the total dewetted areas and are depicted in Figure 6-6. As it was generally expected, PG 76-22M performed better than the other two unmodified asphalt binders. Its total dewetted area was 4.15

mm^2, as compared to PG 58-28 and PG 64-22 binder, which had a total dewetted area of 24.69 mm^2, and 31.45 mm^2, respectively. It must be noted that although PG 64-22 had an average thickness of 0.251 mm, the total amount of dewetting was approximately 1.27 times that of PG 58-28 binder. This finding is contrary to what should be generally expected as PG 58-28 is less viscous than that of PG 64-22 asphalt binder.

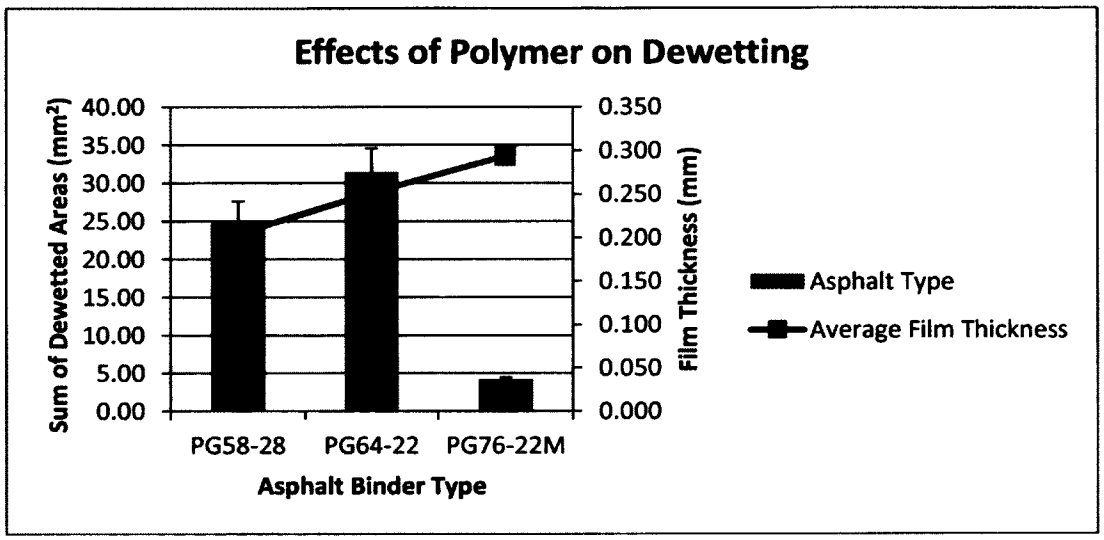

Figure 6-6: Effects of polymer on dewetting of asphalt binders: (PG 58-28, PG 64-22, and PG 76-22M).

6.3.3 Effects of Additives on Dewetting of Asphalt Films

Six samples, taken from the three sets of twelve that were prepared to check for the effects of polymer on dewetting, were prepared and tested for each asphalt binder (PG 58-28, PG 64-22, and PG 76-22M). Six samples for the asphalt binder with various percentages (1%, 2% and 0.5%) of anti-strip additives were prepared to assess the effects of chemical additives on the dewetting of asphalt films in submerged water condition. All samples were placed in 200 mL volume of water in a container on a hotplate and the temperature of the water was allowed to be raised from ambient to 50°C. After two h, the

hot plate was turned off. The samples were removed and photographs were taken for analysis.

Specifically to avert or lessen moisture damage in asphalt pavements, anti-strip additives are added to the binder to help in that regard. The liquid anti-strip additives come in different forms such as amine, phosphate esters or hydrated lime (Harnish, 2010). Anderson et al. (1982), in carrying out experiments on determining the effects of antistrip additives on the properties of asphalt cement, concluded that antistrip additives can have an effect on the physical properties of the asphalt cement. Additionally, it was noted that the aging characteristics and temperature susceptibility of the asphalt can be affected. Moreover, Anderson et al. (1982) noted that various asphalts are affected differently by different anti-strip additives.

An extensive study was conducted in some VDOT (Virginia Department of Transportation) districts of Virginia by Maupin (1997) assessing field cores from asphalt pavements with hydrated lime and six types of chemical additives. Maupin (1997) noted that while the use of additives appeared to help, stripping still took place for no understandable reasons and pointed out that there is difficulty that exists for long term evaluation of its effectiveness. Maupin (1997) further continued that to correctly forecast the performance 100% of the time, no single test has been found, and in that area, still more work is required. Based on the extensive research conducted, Maupin (1997) concluded that in many sites considerable stripping was identified. Maupin (1997) also concluded that in comparing the performance of hydrated lime to that of chemical anti-stripping additives, no superiority was found of the former over the latter.

6.3.4 Average Film Thicknesses of Samples Used in Dewetting Experiments

Figure 6-7 (a) shows the average film thickness used in assessing the dewetted area when 1% additive (Adhere HP Plus, Adhere LOF 6500) was added to the three neat asphalts under investigation, whereas Figure 6-7 (b) shows the average film thicknesses used in assessing the dewetted area when 1% additive (Adhere HP Plus and Adhere LOF 6500) was added to the neat asphalts, at an approximate pH of 10.

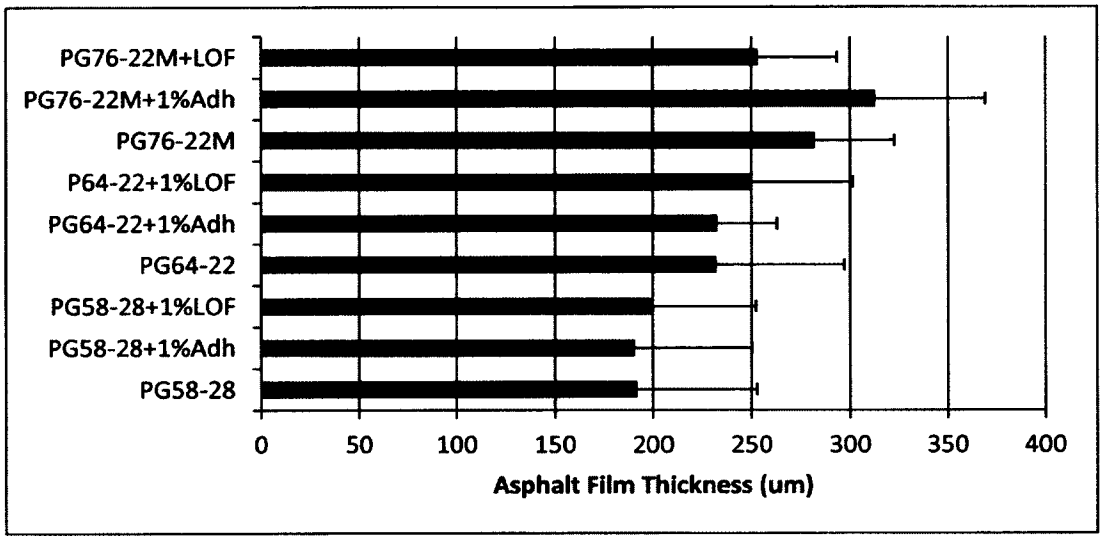

(a)

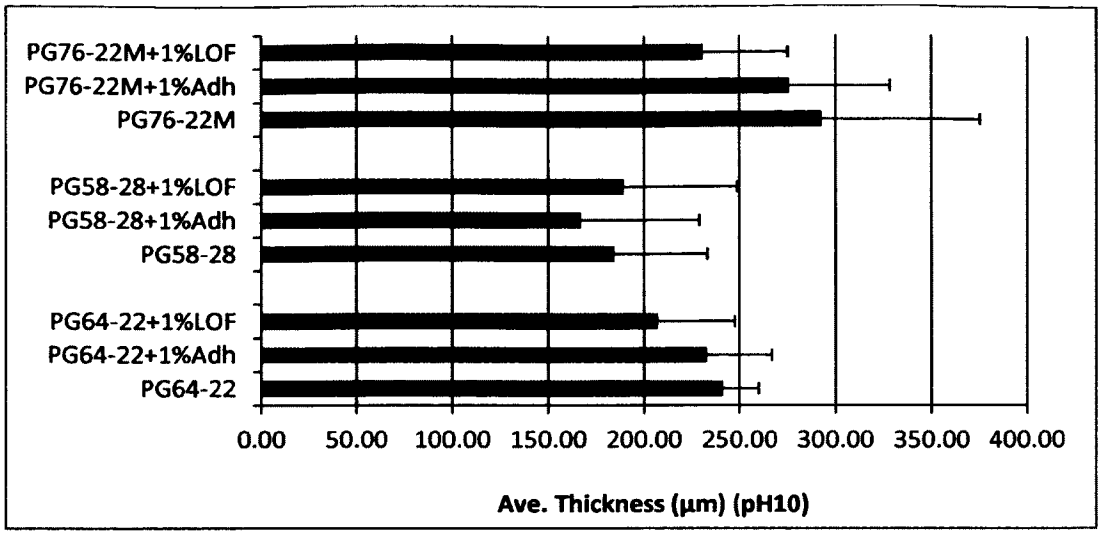

(b)

Figure 6-7: (a) Average film thicknesses used in assessing the dewetted area when 1% additive (Adhere HP Plus and Adhere LOF 6500) is added to the neat asphalts (PG 58-28, PG 64-22, and PG 76-22M), **(b)** Average film thicknesses used in assessing the dewetted area when 1% additive (Adhere HP Plus and Adhere LOF 6500) is added to the neat asphalts (PG 58-28, PG 64-22, and PG 76-22M)(pH10).

6.3.5 Effects of 1% Adhere HP Plus on Dewetting of Asphalt Films

From Figure 6-8, based on the test method and the approximate range of film thicknesses of the three asphalts that were modified with 1% Adhere HP Plus, two had more damage in terms of dewetting than that of their neat asphalts counterparts, namely PG 64-22 and PG 76-22M asphalt. Although the average film thickness for PG 58-28 + 1% Adhere HP Plus and PG 64-22 + 1% Adhere HP Plus were 190.50 µm and 232.7 µm, respectively, PG 64-22 asphalt had a higher amount of dewetting, (1.9 times the amount of dewetting), 15.52 mm^2 for the former and 28.76 mm^2 for the latter. For PG 58-28 + 1% Adhere HP Plus, the damage decreased approximately 26% when compared to that of PG 58-28 and for PG 64-22 + 1% Adhere HP Plus, the damage increased by 27.8% compared to PG 64-22 asphalt. Although the total dewetted areas for

PG 76-22M + 1% Adhere HP Plus was less than that of PG 64-22 + 1% Adhere HP Plus asphalt, 28.76 mm^2; nonetheless, it was 2.6 times the total damage as compared to PG 76-22M asphalt. The viscosity of Adhere HP Plus based on the suppliers MSDS is approximately 180 ± 10 centipoise (cps) at a temperature of 77°F and falls below 100 cps as temperature arrives at 110°F, (RoadScience, Tulsa, OK). The penetration viscosity for PG 64-22 at 77°F was found to be 4.17 E + 09 cps (Lolly, 2013). As the temperature increased from ambient to 50°C, the Adhere HP Plus additive may have had an effect of reducing the viscosity of the PG 64-22 and PG 76-22M asphalt binders giving rise to more accumulated damage per set. Anderson et al. (1982) noted that generally adding additives to asphalt tends to soften it.

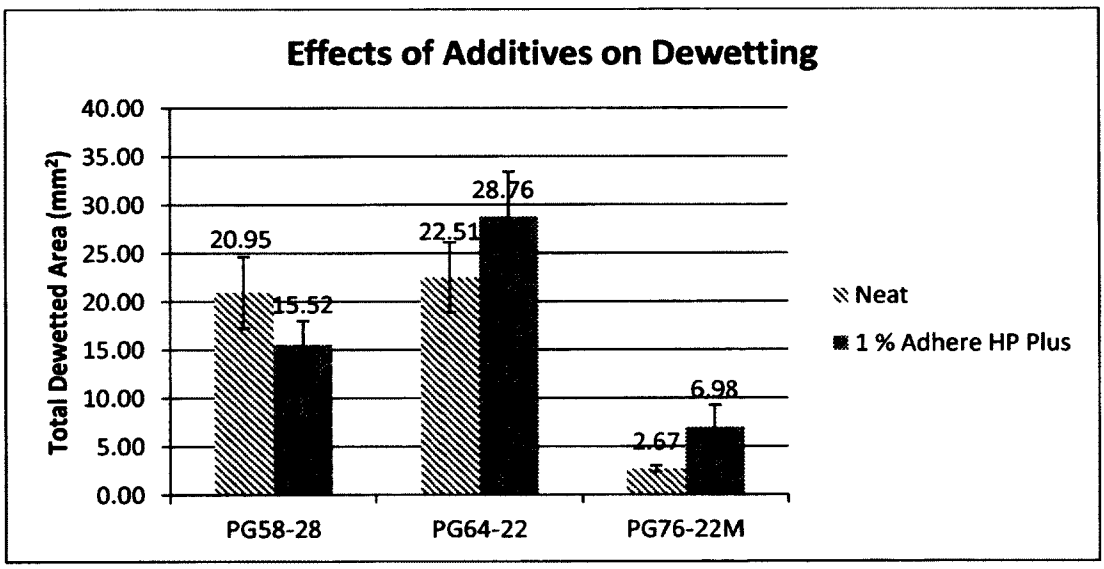

Figure 6-8: The effects of 1% Adhere HP Plus on the dewetting of asphalt films subjected to moisture damage.

6.3.6 Effects of 1% Adhere LOF 6500 on Dewetting of Asphalt Films

For the same set of three asphalt binders, PG 58-28, PG 64-22 and PG 76-22M, 1% Adhere LOF 6500 was added to check for its effect on the dewetting behavior on these asphalts (Figure 6-9). For the PG 76-22M asphalt binder, with the addition of 1% Adhere LOF 6500, there was an increase in dewetting. As in the previous section, a similar trend (increase in dewetting) was observed for PG 76-22M with the addition of 1% Adhere HP Plus. A 1.7 fold increase in dewetting was observed with the addition of the 1% LOF 6500 additives. The total dewetting was relatively the same for PG76-22M + 1% LOF 6500 and PG 76-22M + 1% Adhere HP Plus, a difference of 2.48 mm^2.

However, there was a significant reduction in dewetting for the PG 58-28 in particular and PG 64-22 asphalts with the addition of 1% Adhere LOF 6500. The reduction in dewetting for PG 58-28 + 1% Adhere LOF 6500 was 70.1%. The reduction recorded for PG 64-22 asphalt is 45.3%. For the two unmodified polymer asphalt binders, the research suggested that the binders modified with 1% Adhere LOF 6500 performs better than asphalt mixes in the field with 1% Adhere HP Plus as the cumulative damage was reduced.

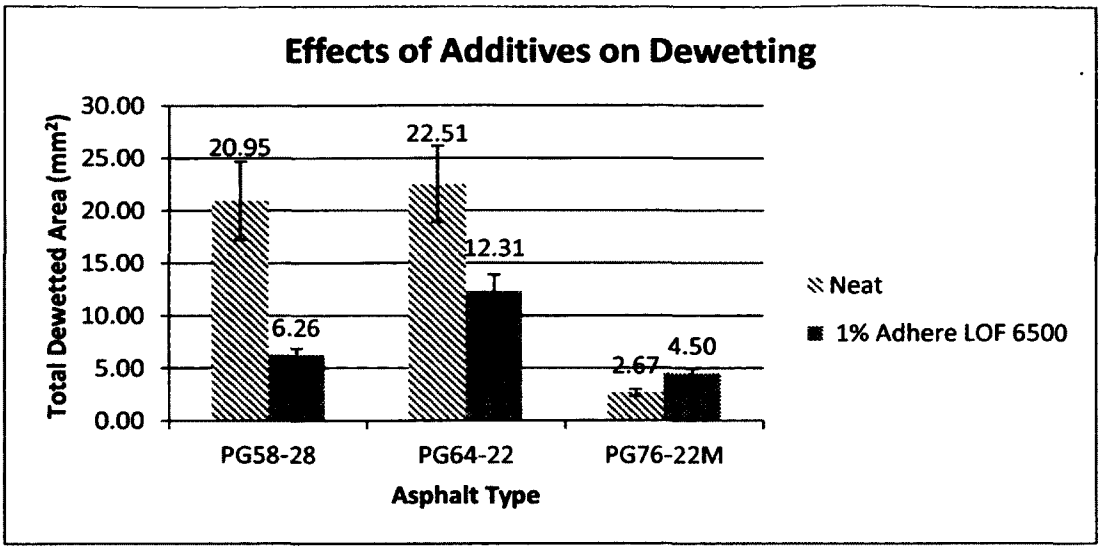

Figure 6-9: The effects of 1% Adhere LOF 6500 on the dewetting of asphalt films subjected to moisture damage.

In conducting tests to check on the effects of prolonged heating on asphalt binder and mixes with two additives including LOF 6500, Tayebali et al. (2005) observed that anti-strip additive content was found to decrease considerably when exposed to extended heating periods. Specifically, it was concluded by Tayebali et al. (2005) that the measured anti-strip additive content for asphalt binders was practically zero after 24 to 48 h of heating extensively while for the asphalt mixes came within the reach of zero after being subjected to 6 to 12 h of heating. Moreover, Tayebali et al. (2005) assert that it was neither apparent nor possible based on the study results to conclude the effect, if any, would the loss of anti-strip additives have on the sensitivity of moisture of mixes in the event the loss occurs after the mix production bearing in mind that the specific dosage was utilized during production. Additionally, there have also been concerns about chemical anti-strip additives not being heat stable (Tarrer, 1996). Rahim (2010) concluded based on ITS (Indirect Tensile Strength Test), on compacted asphalt samples

that for two liquid anti-strip additives which include Adhere LOF 6500, a peak dosage of 0.5% to 0.75% was observed based on performance. Based on the Lottman test, all antistrip additives, which also included hydrated lime, improved hot mix asphalt resistance to moisture-damage (Rahim, 2010).

6.3.7 Effects of Additional Additive Percentages (0.25% and 2%) on Dewetting of Asphalt Films

The amount of chemical additives added to asphalts is important and, in turn, determines whether the modified asphalt or mix will behave as it is designed to in its ability to reduce moisture damage in the field. Anderson et al. (1982) concluded that the anti-strip additives when added to a specific asphalt, there is a particular "demand" for that asphalt. Based on this asphalt additive relationship, Anderson et al. (1982) continues that a certain minimum or threshold percentage of anti-strip must be added to an asphalt prior to it being available to the aggregate surface, which explains the reason for different asphalts requiring different minimum anti-strip dosages. In this respect, 0.25% Adhere HP Plus and 2% Adhere HP Plus were investigated on the three binders (Figure 6-10). For the 2% Adhere HP Plus additive, PG 64-22 asphalt was not subjected to the test as only the two asphalts with extreme viscosities were analyzed.

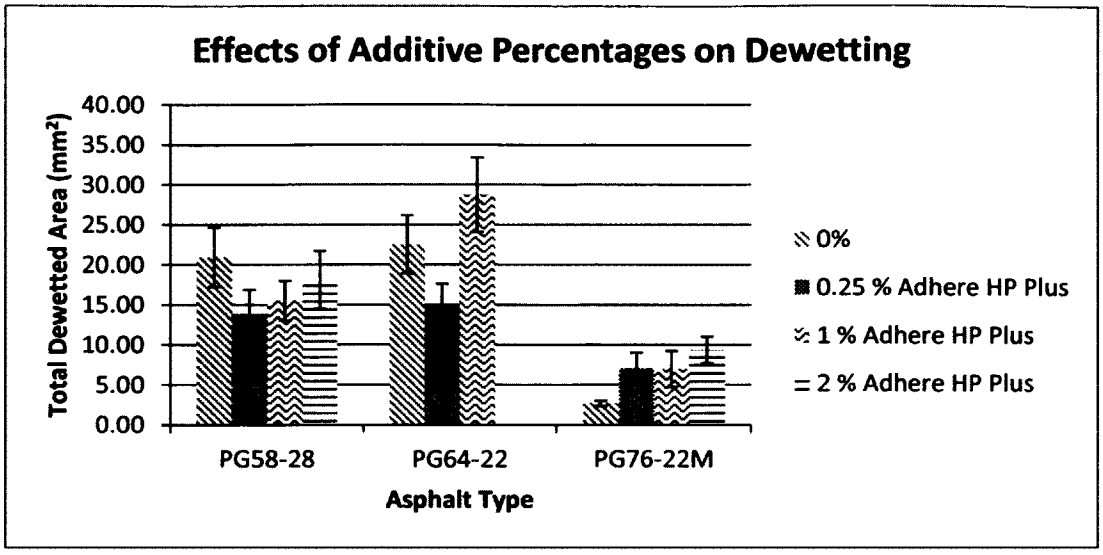

Figure 6-10: The effects of additive percentages (0%, 1%, 0.25%, and 2%) on Adhere HP Plus on the dewetting of asphalt films subjected to moisture damage.

The 2% additive did not reduce dewetting for PG 76-22M asphalt binders in terms of total dewetting as opposed to the neat binder; whereas, a slight reduction was observed for PG 58-28 asphalt by 13.5%. However, in comparing the dewetting of the 2% to the 1% additive for PG 58-28, there was a 16.8 % decrease in dewetting as compared to the 1% additive. Moreover, for PG76-22M there was a 33.8 % increase with 2% additive as opposed to the 1% additive. When the 0.25% Adhere HP Plus additive was added to asphalt PG 58-28 and PG 64-22, a reduction in the dewetting for the former was noted while an increase in dewetting in the latter when compared to the neat binders was observed. However, the total dewetting when compared to that of 1% dewetting, was reduced slightly for PG 58-28 + 1% Adhere HP Plus but remained the same in the case of PG 76-22M + 1% Adhere HP Plus. A 10.7% reduction compared to PG 58-28 + 1% Adhere HP Plus and a reduction of 48.2% as compared to PG 64-22 + 1% Adhere HP Plus asphalt binder were observed. For the PG 76-22M asphalt binder, the total area of

dewetting was approximately the same, 7.08 mm^2 for PG 76-22M + 0.25% Adhere HP Plus and 6.98 mm^2 for that of PG 76-22M + 1% Adhere HP Plus. This observation suggests that for PG 76-22M, the asphalt is not susceptible to a change in additive content for that specific range. The most effective additive percentage (Adhere HP Plus) to reduce dewetting can be noted at 0.25%. Even at this low percentage, there was an increase in dewetting for PG 76-22M asphalt.

6.3.8 Effects of Additive Percentages on Dewetting based on Total Number of Dewetted Holes

Not only was the moisture damage assessed based on the total dewetted area of asphalts with the addition of the additives (Adhere HP Plus and Adhere LOF 6500), but also the total number of dewetted holes was assessed based on the addition of 1% additives. Figure 6-11 shows the effects of 1% Adhere HP Plus and 1% Adhere LOF 6500 on the number of dewetted holes of asphalt films subjected to moisture damage. Twelve samples were utilized for neat binders for the assessment while six were used for each set of additive samples. In the case for a low film thickness range (118μm-142μm) when 1% Adhere HP Plus was added to the neat asphalt, a greater number of dewetted holes was observed as in agreement with the total dewetted area analysis. Except for one point, 118 microns film thickness, the total dewetted number of holes was approximately the same, 311 for PG 58-28 and 275 holes for PG 58-28 + 1% Adhere HP Plus, the lowest number of dewetted holes being PG 58-28 + 1% Adhere LOF 6500.

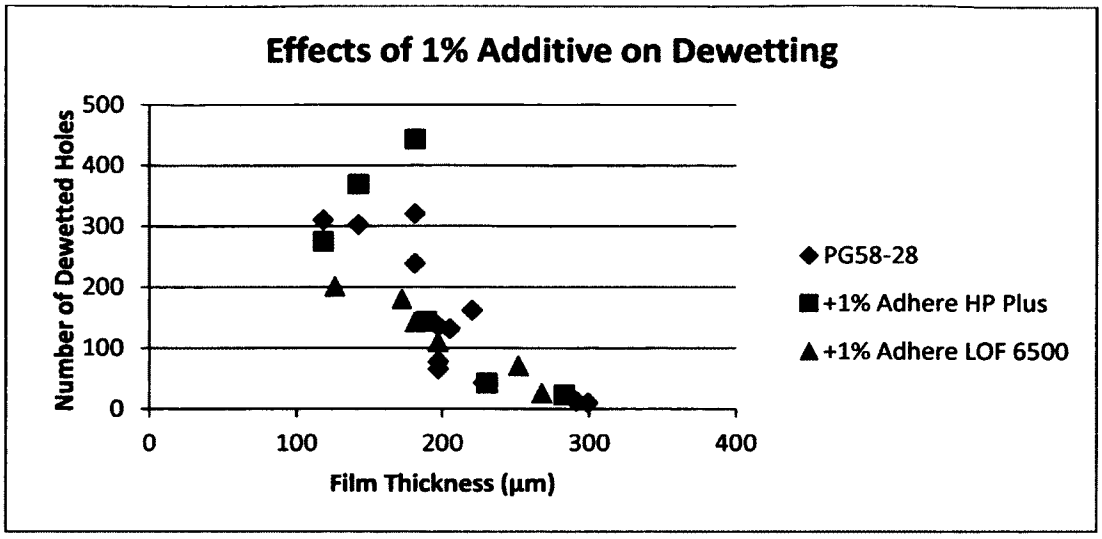

Figure 6-11: The effects of 1% additive (Adhere HP Plus and Adhere LOF 6500) on the dewetted holes of asphalt films (PG 58-28) subjected to moisture damage.

For instance, in the vicinity of 181 μm, the average dewetted holes for PG 58-28 was 280 while it was observed that there was 443 for that of 1% Adhere HP Plus. As film thickness is the most critical factor, within the film thickness range of 139 to 230 μm (0.139 to 0.230 mm), the number of dewetted holes decreased with the neat asphalt and PG 58-28 + 1% Adhere HP Plus being approximately the same. There was a strong contrast, however, when 1% Adhere LOF 6500 was added to PG 58-28 in that rather than an increase in the number of dewetted holes, a decrease was observed. Within the vicinity of 126 μm, the lowest thickness for PG 58-28 + 1% Adhere LOF 6500, 201 dewetted holes were recorded as opposed to 311 holes for PG 58-28. A very interesting observation was made within the vicinity of 197 μm. Two sets of data were recorded for PG 58-28 in terms of number of dewetted holes, 66 and 78 in the lower range and 136 and 132 in the upper range. For the asphalt with the addition of 1% Adhere LOF 6500, 110 holes were recorded for the asphalt with the addition of 1% Adhere LOF 6500. Moreover, within the vicinity of 252 μm film thickness, slightly more holes were

recorded overall for PG 58-28 + 1% Adhere LOF 6500. These results suggest that film thickness is the controlling factor and had affected the 1% Adhere LOF 6500 additive film significantly. It must be realized that as in the analysis of the critical film thickness for the neat binders, as the film thicknesses of all binders are increased to approximately 300 μm, the total number of dewetted holes per samples are tending to zero. Therefore, even as 1% additives are added, both Adhere HP Plus and Adhere LOF 6500 seem to obey that critical film thickness rule in this experiment.

Figure 6-12 shows the effects on the dewetted number of holes when 1% Adhere HP Plus and 1% Adhere LOF 6500 was added to PG 64-22 asphalt binder. Within the approximate vicinity of 173 μm, there was a greater number of holes observed for the PG 64-22 as compared to the other two additive added asphalts. Within a film thickness range of 197 to 244 μm, all three asphalt types appeared to reflect the same dewetting behavior, only with one PG 64-22 + 1% Adhere HP Plus sample recording 121 holes. Moreover, within a film thickness range of 291 and 339 μm, the total dewetted number of holes for dewetting has been reduced significantly for the neat asphalt tending to zero. This reduction in the total number of dewetted holes is not necessarily the case for PG 64-22 + 1% Adhere HP Plus and PG 64-22 + 1% Adhere LOF 6500, particularly for the latter as even within the film thickness of 315 μm, 83 holes were recorded. These results suggest that the critical film thickness range for PG 64-22 with the addition of both additives in this research may go beyond 300 μm. Concerning the two asphalt binders (PG58-28 and PG 64-22) at a low average film thickness of 126 μm, 364 holes were recorded for PG 64-22 and 311 holes for PG 58-28, although approximately the same in number. PG 58-28 asphalt, although lowest in viscosity, appeared to be performing

slightly better that PG 64-22 as reflected in the total dewetted area analysis (Figure 6-11 and 6-12).

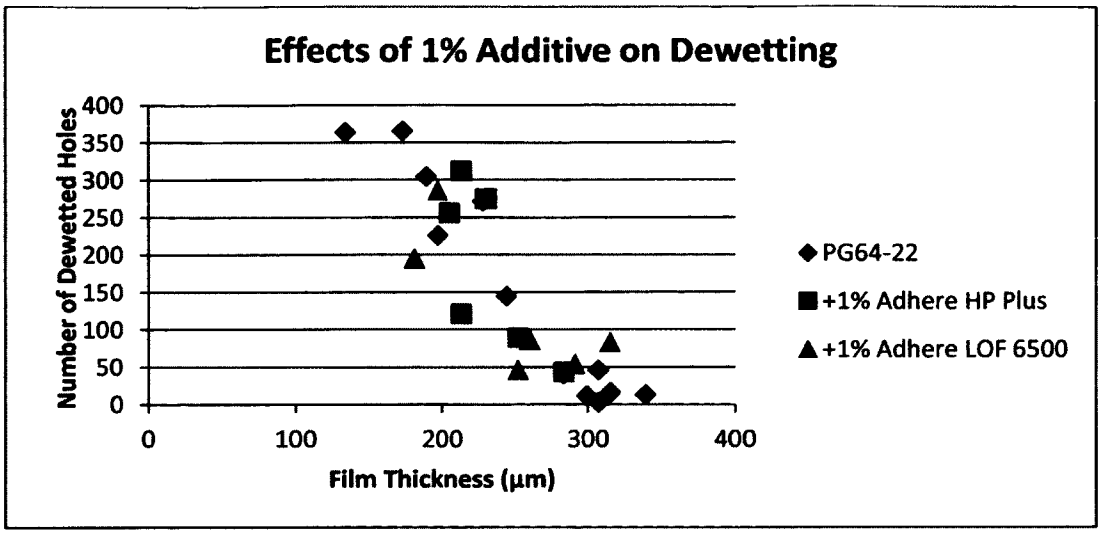

Figure 6-12: The effects of 1% additive (Adhere HP Plus and Adhere LOF 6500) on the dewetted holes of asphalt films subjected to moisture damage.

Figure 6-13 shows the effects of 1% additive (Adhere HP Plus and Adhere LOF 6500) on the number of dewetted holes as compared to PG 76-22M. Generally, except for one sample, the number of dewetted holes was less than and equal to 104. Between a film thickness range of 205 and 291 µm, and in the vicinity of 291 µm the total number of holes for PG 76-22M + 1% Adhere HP Plus and PG 76-22M + 1% Adhere LOF 6500 was more than that of PG 76-22M neat binder. Particularly, is this comparison the case for the latter as within that range more holes were visible. Nevertheless, in that range and within the vicinity of 260 µm film thickness, fewer holes were recorded for PG 76-22M + 1% Adhere LOF 6500. As the film thickness increased (307-402 µm), the dewetting in both asphalt additives decreased, the limiting value being that of 39. Within that film thickness range, all films, particularly PG 76-22 M and PG 76-22M + 1% Adhere HP Plus, had their total number of dewetted holes fast approaching to zero. Again, the

additives seem to be agreeing with a critical film thickness within this thickness range. In investigating field asphalt film thickness and the performance of HMA, Li et al. (2009) concluded that the field data and the experimental laboratory results related that asphalt film thickness is a major factor affecting the rutting performance for asphalt mixtures. Therefore, this conclusion shows the significance of the film thickness as it pertains to the durability of asphalt pavements to help in its resistance to premature pavement failure.

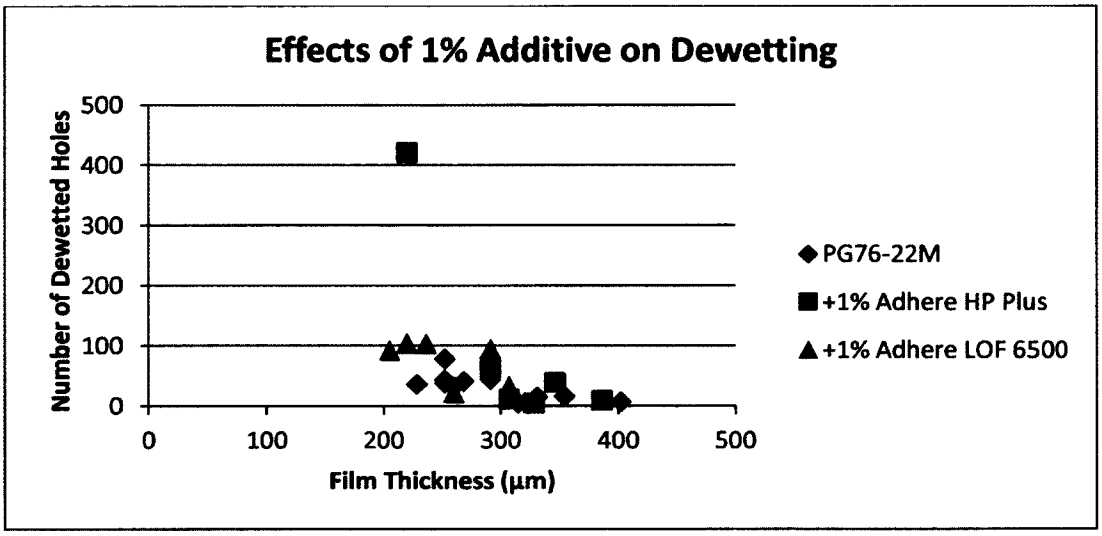

Figure 6-13: The effects of 1% additive (Adhere HP Plus and Adhere LOF 6500) on the dewetted holes of PG 76-22M asphalt films subjected to moisture damage.

6.3.9 Effects of Additive 2% Adhere HP Plus on Dewetting of Asphalt Films

Figure 6-14 shows the effects of 2% Adhere HP Plus on PG58-28 asphalt on the number of dewetted holes when subjected to moisture damage. Within the approximate vicinity of 118 µm, PG 58-28 + 2% Adhere HP Plus performed the worst with an average number of dewetted holes at 446. However, within the vicinity of 181 µm, PG 58-28 + 2% Adhere HP Plus performed better than that of the neat asphalt or

PG 58-28 + 1% Adhere HP Plus. Yet, at 236 μm film thickness, all three asphalts performed relatively the same with the total dewetted holes being approximately the same. It must be noted that as film thickness increases, all three types of asphalt films limited the total number of dewetted holes.

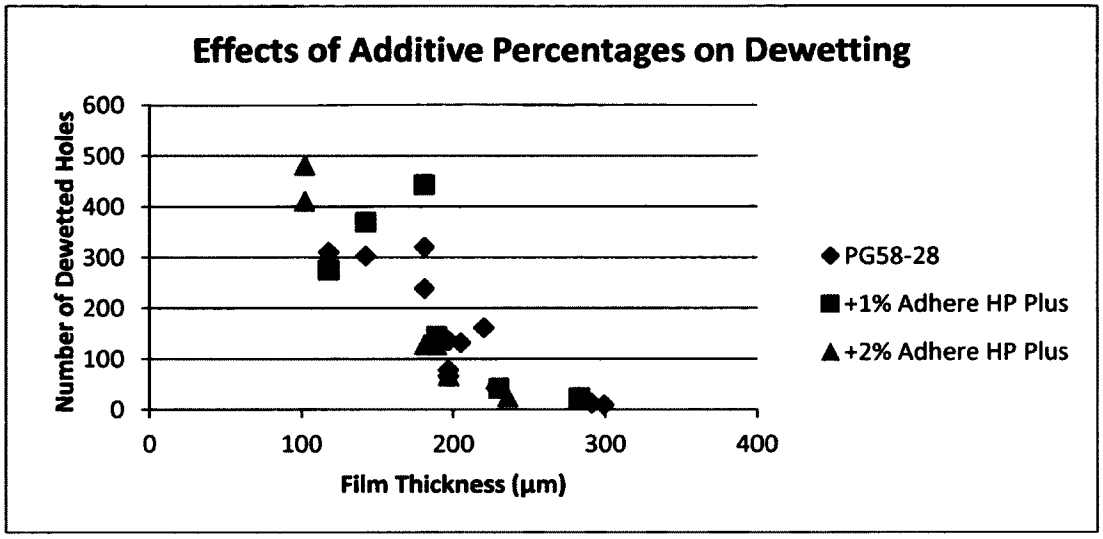

Figure 6-14: The effects of 1% and 2% additive (Adhere HP Plus) on the dewetted holes of asphalt films subjected to moisture damage.

Figure 6-15 shows the effects of 1% and 2% Adhere HP Plus on the number of dewetted holes in PG 76-22M asphalt films.Within the vicinity of 260-291 μm, two samples, PG 76-22M + 2% Adhere HP Plus exhibited a higher number of dewetted holes as compared to PG 76-22M. Moreover, within the vicinity of 307 μm, more dewetted holes were observed than that of PG76-22M asphalt film. As the film thickness increased in PG 76-22M + 2% Adhere HP Plus, the dewetting approached zero, even at 354 μm being slightly less than the neat binder. Overall, PG 76-22M + 2% Adhere HP Plus followed the film thickness rule that as film thickness increases, the dewetting tends to decrease.

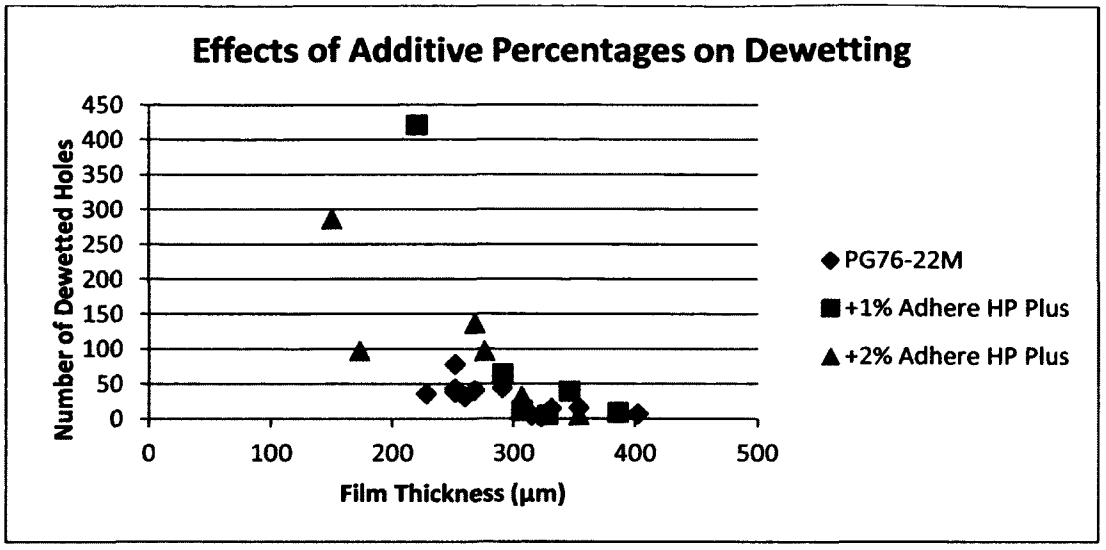

Figure 6-15: The effects of 1% and 2% additive (Adhere HP Plus) on the dewetted holes of asphalt films subjected to moisture damage.

From 307 to 402 μm, apart from 2% Adhere HP Plus, it was observed that PG 76-22M + 1% Adhere HP Plus and also that of PG 76-22M was also tending to zero which is what was to be expected. Generally, it was observed that more dewetting took place when the 2% Adhere HP Plus and 1% Adhere HP Plus was added to the polymer modified asphalt binder, PG 76-22M, being in agreement with the total dewetted area analysis.

6.3.10 Analysis of Dewetting based on Average Dewetted Area per Hole

In the previous analysis, the total dewetted area of the samples was considered. In further analyzing the dewetting of holes subjected to moisture damage, the average dewetted area per hole was examined (Figure 6-16). Generally, the effects of both additives on dewetted hole area was minimal for PG 58-28, affected by 1% Adhere HP Plus on PG 64-22 asphalt, and affected by both additives on PG 76-22M asphalt.

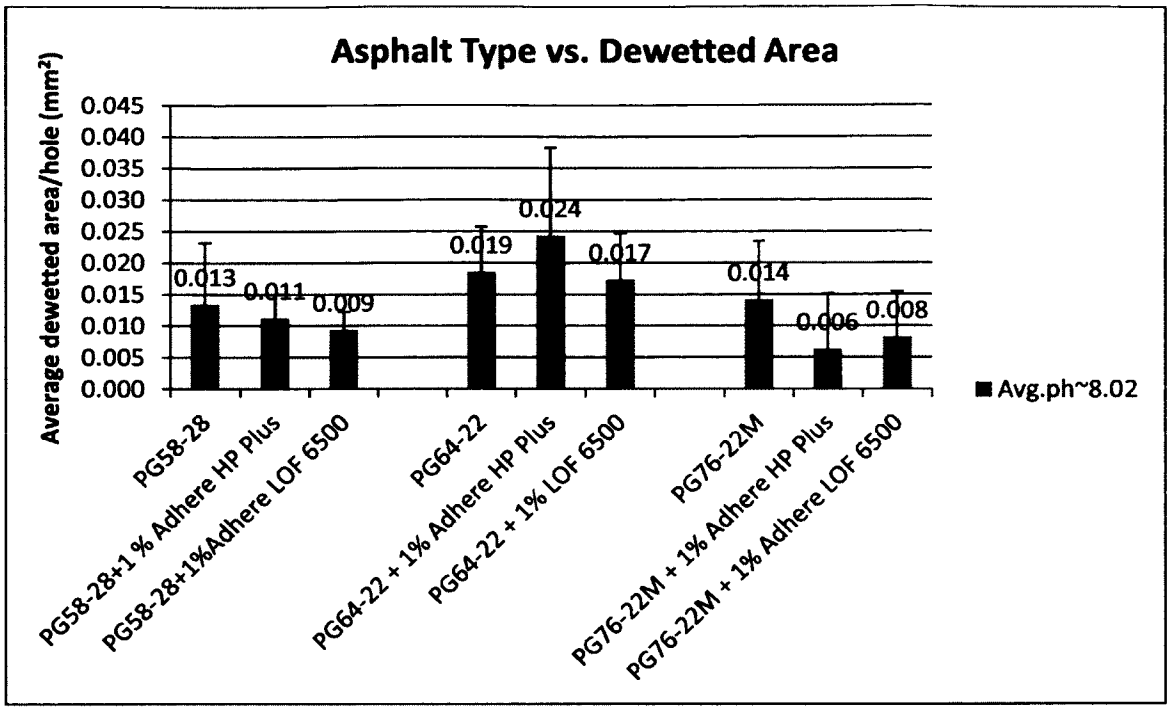

Figure 6-16: The effects of anti-stripping additives on the average dewetted area per hole in asphalt films with and without additives.

6.3.11 Effects of pH on Dewetting of Asphalt Films

All previous samples were tested at an approximate pH of 8. Figure 6-17 shows the effects of pH 10 on the total dewetted area of asphalt films, (PG58-28 and PG58-28 with 1% Adhere HP Plus and 1% Adhere LOF6500) subjected to moisture damage as compared to an average pH of 8.03.

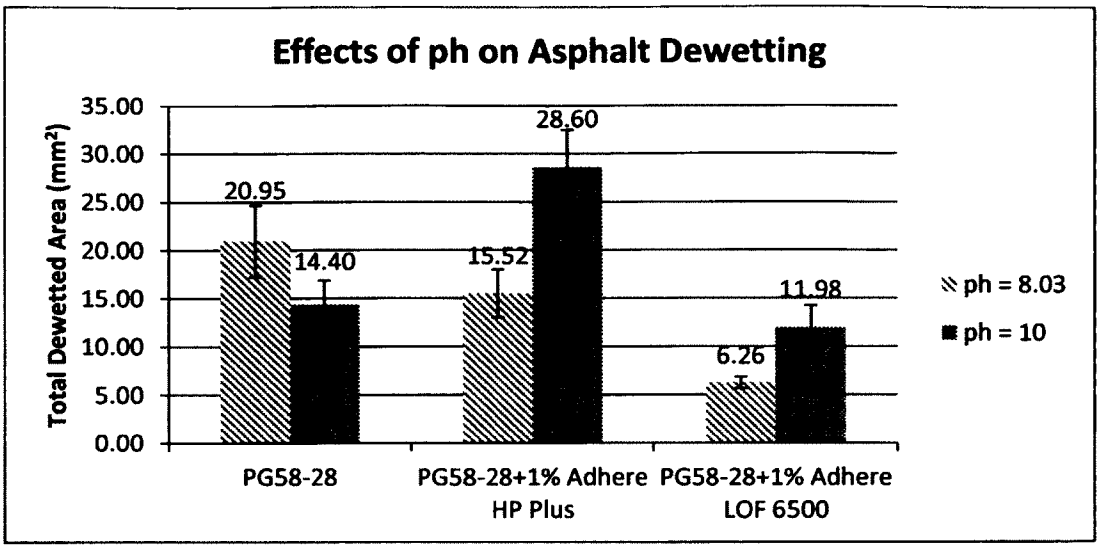

Figure 6-17: The effects of pH (~10) on the dewetted holes of asphalt films (PG 58-28 and PG 58-28 with additives) subjected to moisture damage.

The PG 58-28 asphalt films were affected by the increase in pH, resulting in a reduction of dewetting by as much as 31.2% when subjected to a pH of 10 allowing a difference of 6.55 mm^2 of total dewetted area to be recorded. For the PG58-28 + 1% Adhere LOF 6500, the total dewetted area was approximately doubled. This observation suggests that at a pH of 10, 1% Adhere LOF 6500 is susceptible to dewetting, as compared to being subjected to moisture damage at an average pH of 8.03. Moreover, at the higher pH value, PG 58-28+1% Adhere HP Plus dewetted significantly, an increase of 84.3%. Therefore, it is observed that dewetting and moisture damage is susceptible to pH shifts significantly affecting PG 58-28 + 1% Adhere HP Plus asphalt films.

Figure 6-18 shows the effects of pH 10 on the dewetted holes of asphalt films (PG 64-22 and PG 64-22 +1% Adhere HP Plus and 1% Adhere LOF 6500) subjected to moisture damage. A significant decrease of 81.9% in the total dewetted area for PG 64-22

at pH of 10 was observed compared to the total dewetted area at pH of 8.02 where the reduction in dewetting at pH 10 was significantly reduced.

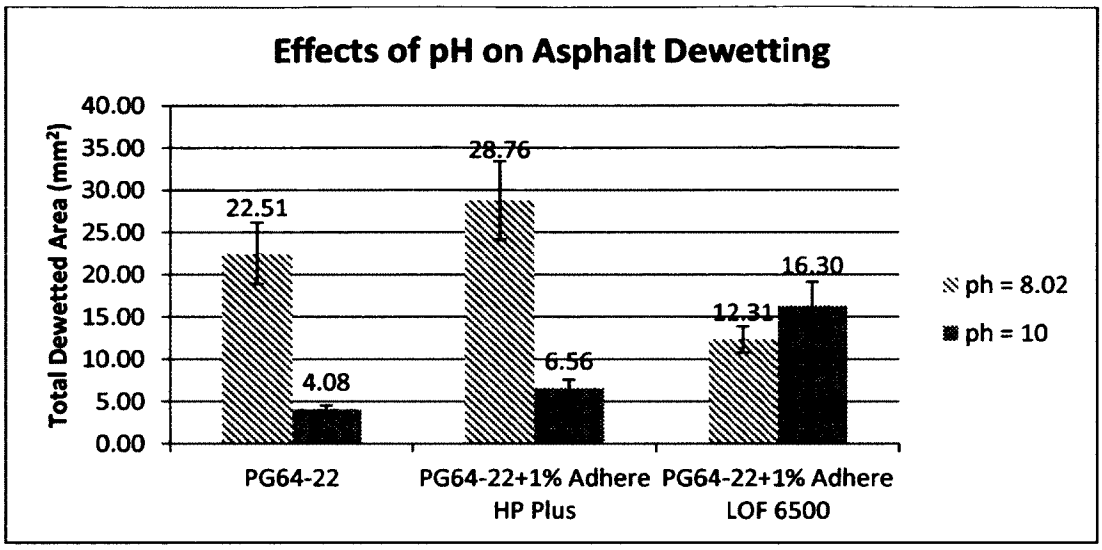

Figure 6-18: The effects of pH (~10) on the dewetted holes of asphalt films (PG 64-22 and PG 64-22 with additives) subjected to moisture damage.

In this case, although the viscosity of PG 64-22 is higher than that of PG 58-28, at a pH of 10 much more dewetting is observed for the latter than that of the former. There was a significant difference observed in the behavior of the two additives when added to PG 64-22 asphalt. At pH 10, a notable reduction in dewetting occurred by as much as 77.2% for PG 64-22 + 1% Adhere HP Plus. That was not the case with PG 64-22 + 1% Adhere LOF 6500. At pH 10, an increase of 32.4% dewetting was observed. For both asphalts, PG 58-28 and PG 64-22, 1% Adhere LOF 6500 increased the dewetting of the films while 1% Adhere HP Plus appeared to be helping in both asphalts much more evident in PG 64-22 asphalt binder.

Thus far, for these two unmodified asphalt binders (no polymer), it was shown that changes in pH do have an effect on moisture damage in asphalt pavements which agrees with Tarrer (1996).

The polymer modified binder was also subjected to such treatment in an effort to assess its behavior. Figure 6-19 shows the effects of pH (~10) on the dewetted holes of asphalt films (PG76-22M and 1% Adhere HP Plus and 1% Adhere LOF 6500) subjected to moisture damage.

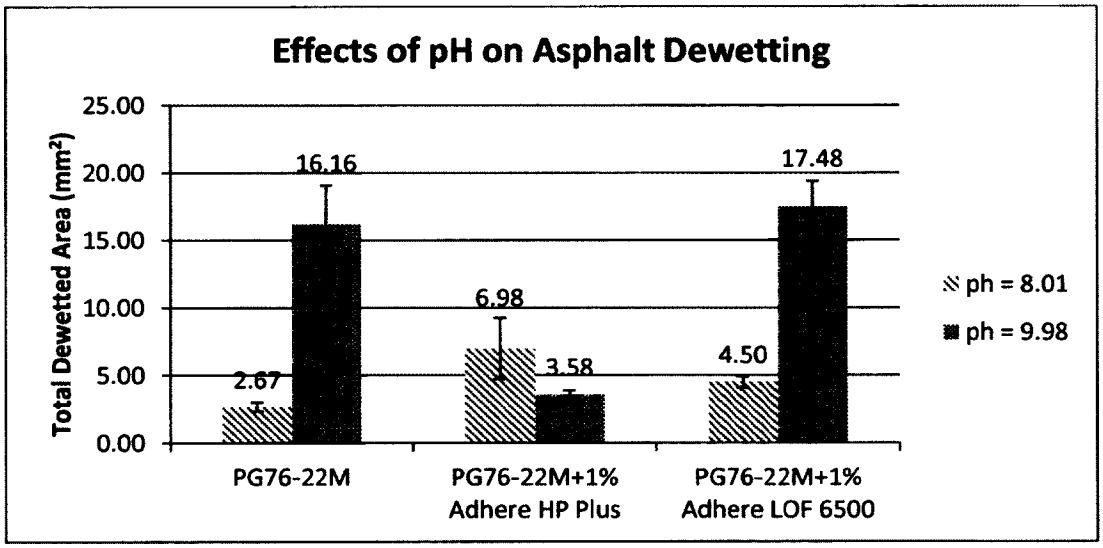

Figure 6-19: The effects of pH (~10) on the dewetted holes of asphalt films (PG 76-22M and PG 76-22M +1% Adhere HP Plus and 1% Adhere LOF 6500) subjected to moisture damage.

The results suggest that pH shifts had a very strong influence on the polymer modified asphalt (PG 76-22M), with and without additive. For PG 76-22M, the total dewetted area was approximately 6 times more at an average pH of 9.98 than when subjected to an average pH of 8.01. This observation suggests that PG 76-22M asphalt is very susceptible to pH shifts, especially at high pH. Moreover, the difference in the total

dewetted area of PG 76-22M + 1% Adhere LOF 6500, to that of the neat binder at a pH of 8.01, is 7.6%. From the lower pH PG 76-22M + 1% Adhere LOF 6500 the total area of dewetting increased by 74.3% for the higher pH. Therefore, it was observed that in all asphalts there was consistent behavior when 1% additive Adhere LOF 6500, was added most significantly affecting PG 76-22M. At an average pH of 9.98, there was a reduction of 48.7% dewetted area for PG 76-22M + 1% Adhere HP Plus as opposed to that of the influence of 8.01. This behavior was consistent with the other two asphalts which implies that the additive (1% Adhere HP Plus) performance on these three asphalts, most significantly on the PG 58-28 and PG 64-22 asphalts, helped reduce the dewetting or moisture damage at an average pH of 10 as opposed to these asphalts being exposed to a lower pH of approximately 8.

The average dewetted area per hole was also analyzed and is shown in Figure 6-20 to understand the effects of the dewetted area per hole of both additives at high pH. Overall, for all three asphalts, the effects of both additives on the dewetted area per hole were not that significant.

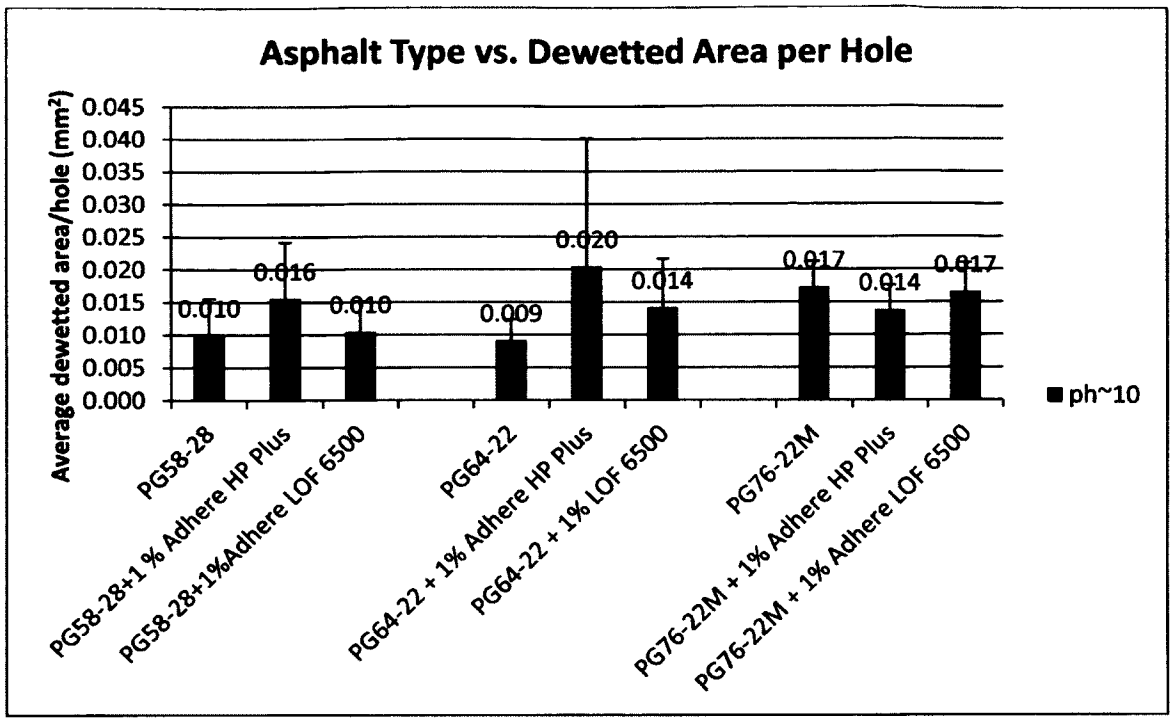

Figure 6-20: The effects of pH (~10) on the average dewetted area per hole of asphalt films (PG 76-22M and PG 76-22M with additives) subjected to moisture damage.

The total dewetted area for PG 58-28, PG 64-22, and PG 76-22M asphalts, together with 1% Adhere HP Plus and 1% Adhere LOF 6500 at pH 10 was analyzed and the results are reflected in Figure 6-21. For PG 58-28 asphalt, with the addition of 1% Adhere HP Plus, there was an increase in the total dewetted area. An increase in 49.7% dewetted area was observed in comparison to PG 58-28 asphalt. However, although not significant, a reduction of 16.8% in total dewetting was observed under the influence of 1% Adhere LOF 6500. Moreover, that was not the case reflected in the dewetting of PG 64-22 asphalt with and without additives. A 60.8% increase was observed in dewetting for 1% Adhere HP Plus while an even more significant increase in total dewetting was recorded for that of PG 64-22 + 1% LOF 6500 asphalt. This observation indicates that 1% Adhere LOF 6500 performed consistently as in the case of total dewetted area for that

asphalt in an average pH of 8. Additionally, 1% Adhere HP Plus performed consistently when added to PG 58-28 asphalt is also the case of pH 8. However, that was not the case with PG 76-22M, polymer modified asphalt.

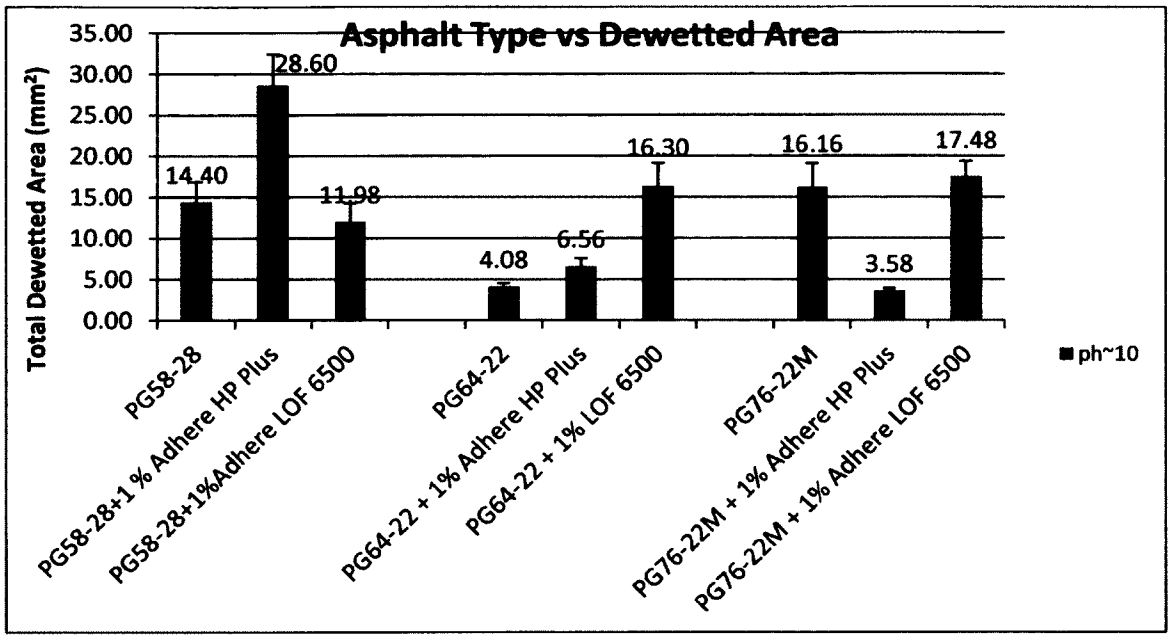

Figure 6-21: The total dewetted area for three asphalts with and without additives (pH 10).

At high pH, 1% Adhere HP Plus appeared to help the dewetting of PG 76-22M greatly. There was 77.8% reduction in dewetting compared to the PG 76-22M. There was almost no change observed when 1% Adhere LOF 6500 was added to the polymer modified binder. The percentage difference recorded in the total dewetted area was 8.2%, approximately. These observations show that for the three asphalts tested, PG 58-28, PG 64-22, and PG 76-22M, with the addition of the two additives, Adhere HP Plus, and Adhere LOF 6500, are susceptible to pH shifts and do agrees with the literature (Tarrer,1996).

6.4 Conclusions

The final dewetting-based moisture damage test protocol that was developed and followed in this study is given as follows. Asphalt film samples on glass were prepared. After curing, 0.01 grams of aggregates (gravel) retained on a #100 sieve size was spread over the asphalt film surface (~2.5 x 5.08 cm). Samples were tested in submerged water condition at ambient to 50°C. After 2 h, photographs were taken for analysis with the National Vision Builder AI 2012 software. The analysis procedure is fully quantitative. Moreover, the total dewetted area of holes, the number of dewetted holes, hole distribution etc. can be quantitatively analyzed with the use of this procedure.

Effects of film thickness on dewetting of asphalt films

1. The critical film thickness for PG 58-28, PG 64-22, and PG 76-22M was estimated experimentally and was found to be 300 μm. The critical film thickness is the minimum thickness above which very few holes, tending to zero, was observed. This critical film thickness indicates a possible threshold for field asphalt film thickness in the pavement mix.

Effects of polymer on dewetting

2. Polymer in PG 76-22M asphalt binder do aid in reducing dewetting and, as a result, moisture damage in asphalt pavements.

Effects of 1% Adhere HP Plus

3. When added to the three asphalts, 1% Adhere HP Plus, reduced dewetting in PG 58-28 asphalt but increase in dewetting was observed for PG 64-22 and PG 76-22M binder

Effects of 1% Adhere LOF 6500

4. 1% Adhere LOF 6500 reduced dewetting significantly for PG 58-28, particularly and that of PG 64-22, with reductions as high as 70.1% for the former and 45.3% for the latter. However, that was not the case for PG 76-22M asphalt where an increase in dewetting was observed.

Effects of additional additive percentages (0.25% and 2%) on dewetting

5. For PG 58-28 asphalt films, all additive rates decreased dewetting. For PG 64-22 , 0.25% Adhere HP Plus showed optimum performance. Dewetting decreased with the addition of 0.25% Adhere HP Plus while it increased with the addition of 1% Adhere HP Plus.
6. For PG 76-22M, all additive rates (below and above 1%) increased dewetting, which suggests that polymer in the absence of additives performs relatively well in the process reducing moisture damage. Additionally, for PG 76-22M, with and without additives, the dewetting was significantly lower as compared to the other two asphalt binders (PG 58-28 and PG 64-22) with and without additives. Therefore, this finding indicates that polymer helps in the reduction of dewetting.
7. The 2% Adhere HP Plus reduced dewetting slightly for PG 58-28 asphalt, but increased dewetting for PG 76-22M asphalt significantly.

Effects of additive percentages on dewetting based on total number of dewetted holes

8. For PG 58-28, PG 64-22, PG 76-22M, with and without both additives, (1% Adhere HP Plus, 1% Adhere LOF 6500), the number of dewetted holes decreased as film thickness increased and arrived at a critical film thickness of approximately 300μm. However, PG 64-22 (with additives) reflected some

slight variations within the vicinity of this point. Generally, very few dewetted holes were observed when this film thickness exceeded the critical film thickness.

Effect of adding 2% Adhere HP Plus on dewetting of asphalts

9. 2% Adhere HP Plus helped with the reduction of number of dewetted holes for PG 58-28, but holes generally increased when 2% Adhere HP Plus was added to PG 76-22M.

Analysis of dewetting based on average dewetted area per hole

10. For the average dewetted area per hole, both 1% additives helped reduce the dewetted area per hole for both PG 58-28 and PG 76-22M asphalts while only PG 64-22 + 1% Adhere LOF 6500 reduced dewetting for PG 64-22.

Effects of pH on dewetting

11. pH had an effect on total dewetted area for all asphalt types, together with their respective 1% Additives (Adhere HP Plus, Adhere LOF 6500). For both neat asphalt binders (PG 58-28, PG 64-22), without polymer, pH of 10 decreased dewetting while for the polymer modifiedcases, dewetting was increased.
12. At high pH, for all three asphalts, dewetting was increased for 1% Adhere LOF 6500, significantly for PG 76-22M. Moreover, PG 58-28 + 1% Adhere HP Plus showed a significant increase in total dewetted area for high pH. However, there was a decrease in dewetting for the other two asphalts.

Effects of pH (10) on average dewetted area per hole

13. Overall, for all three asphalts, the effects of both additives (1% Adhere HP Plus and 1% Adhere LOF 6500) on the dewetted area per hole were not that significant.

Effects of pH (10) on total dewetted area

14. In comparing PG 58-28 and PG 64-22 asphalts with and without additives (1% Adhere HP Plus + 1% Adhere LOF 6500), pH 10 had a greater effect on the former than the latter, in terms of total dewetted area, for both neat binder and when 1% Adhere HP Plus was added. While 1% Adhere 6500 decreased dewetting for PG 58-28, it increased dewetting significantly for PG 64-22, and slightly for PG 64-22+1% LOF 6500. The 1% Adhere HP Plus additive significantly reduced dewetting for PG 76-22M. Generally, there was observed an increase in dewetting for both additives in PG 64-22 in pH 10. The research results suggest that 1% Adhere HP Plus additive appears to help reduce moisture damage via dewetting for PG 76-22M at pH (10).

CHAPTER 7

VALIDATION OF THE DEWETTING-BASED MOISTURE SUSCEPTIBLE TEST METHOD WITH A MODIFIED BOIL TEST

7.1 Background and Objectives

Almost all the state agencies use AASHTO T283 (Indirect Tensile Strength Test) as the moisture susceptibility test. Due to its limitations and disadvantages as discussed in the literature review, this study will employ a modified boil test (Modified ASTM D3625) to validate the uniquely developed dewetting based moisture susceptibility test method.

As discussed in the literature review, the boil test has been used by some state highway agencies and researchers as a screening tool. There exists a possibility for bias as has been shown on the part of researchers in assessing the results of the moisture susceptible boil test. The boil test is also referred to as a severe test as the aggregates are boiled to a temperature of 100°C. In this modified boil test, the aggregates were not subjected to such a high temperature but rather 82°C to be comparable with the newly developed dewetting based moisture susceptibility test. Additionally, the moisture damage mechanism is expected to be similar for the boil test and uniquely developed dewetting test method.

Therefore the objective of this study is:

To validate the unique test method and analysis by comparison with the modified boil test. Five students were utilized in conducting the assessment of the modified boil test to reduce the level of bias that may be associated with this test.

7.2 Methodology and Experimentation

A modified ASTM D3625 test was used in this study. For this test, approximately 1 lb of aggregates (gravel) were mixed with 1% asphalt by weight in case of PG 58-28 and PG 64-22 asphalt binder and 1.5% by asphalt weight for PG 76-22M. As PG 76-22M binder is more viscous than that of the other two binders, to ensure thin film coating on much of the aggregates as possible, 1.5% was used. In the coating of the aggregates, 0% additive, 1% Adhere HP Plus by asphalt weight, and 1% Adhere LOF 6500 by asphalt weight was used for each asphalt type (Table 7-1). Fifty grams of asphalt coated aggregates was placed in a 1000 mL beaker, with the water level being placed at 500 ml before the coated aggregates were placed in it. A hot plate was used to heat up the submerged aggregates from ambient to 82°C, which took approximately 35-45 min. As soon as water arrived at the aforementioned temperature, the sample was removed from the hot plate.

Table 7-1: Asphalt test matrix for asphalts used.

Asphalt Type	Aggregate Amount (g)	No Additive Dosage (%)	Adhere HP Plus Dosage (%)	Adhere LOF 6500 Dosage (%)
PG 58-28	50	0	1	1
PG 64-22	50	0	1	1
PG 76-22M	50	0	1	1

The water surface was cleansed, and the remaining water with the coated aggregates was allowed to cool to room temperature. After reaching the room temperature, the water was decanted and poured into a plastic container for observation. Five students were called to assess the damage and scored accordingly to limit the biasness that may accompany the visual assessment of this test, as has been mentioned in other literature.

The samples were scored in two directions, 1-Horizontal, which reflects the effects of additives on any binder and, 2- Vertical direction which reflects the effects of different asphalts (with and without additives) as seen in Figures 7-1 to 7-3. The ratings were 1, 2, 3 and the key was based on the level of dewetting of the asphalt film on the aggregate as follows:

1-Worst (performance)

2-Moderate (performance)

3-Best (performance).

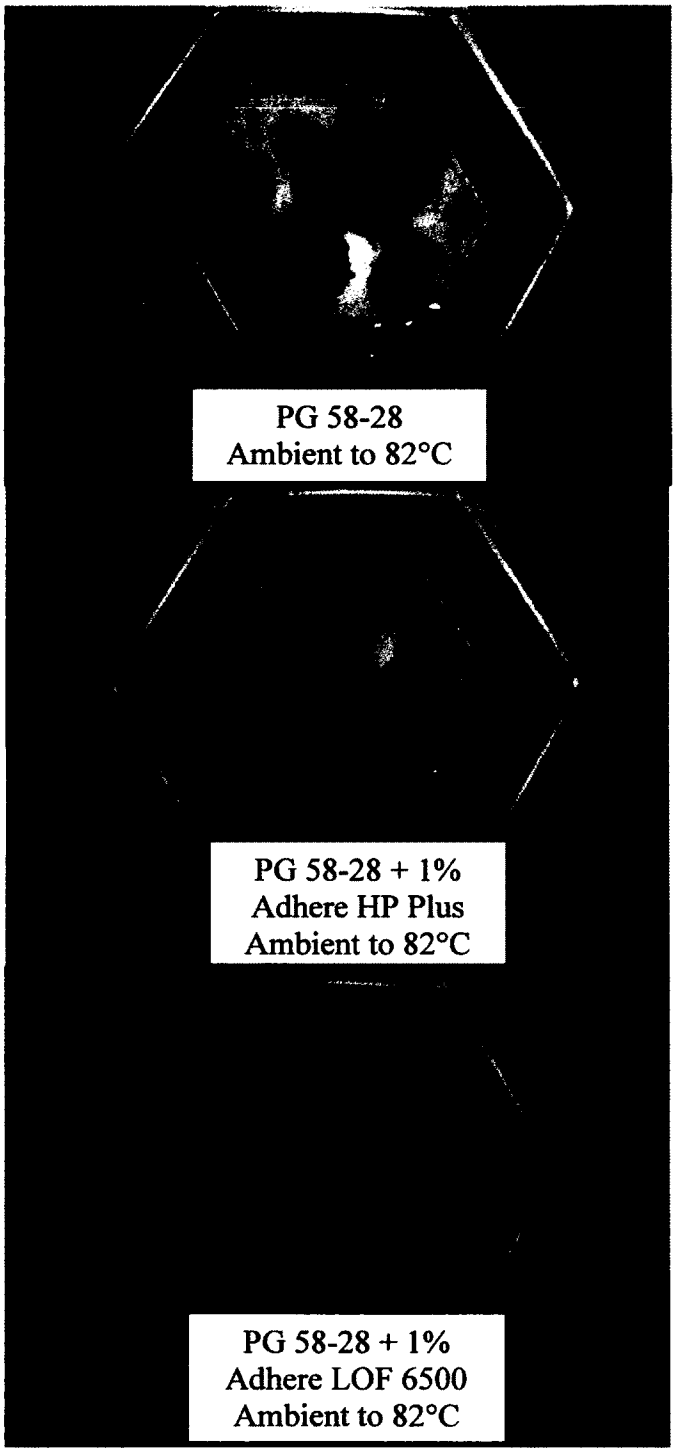

Figure 7-1: Stripping/dewetting of asphalt samples (PG 58-28, PG 58-28 + 1% Adhere HP Plus, PG 58-28 + 1% Adhere LOF 6500) after modified ASTM D 3625 test.

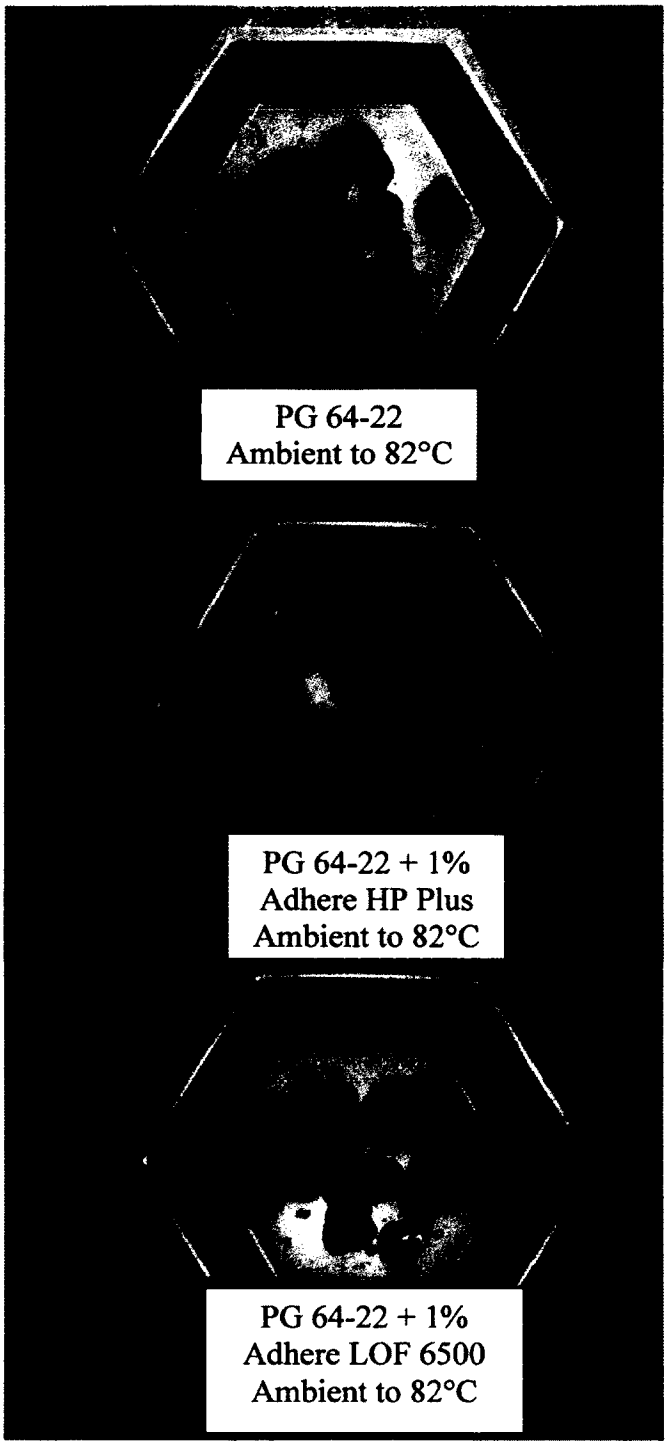

Figure 7-2: Stripping/dewetting of asphalt samples (PG 64-22, PG 64-22 + 1% Adhere HP Plus, PG 64-22 + 1% Adhere LOF 6500) after modified ASTM D 3625 test.

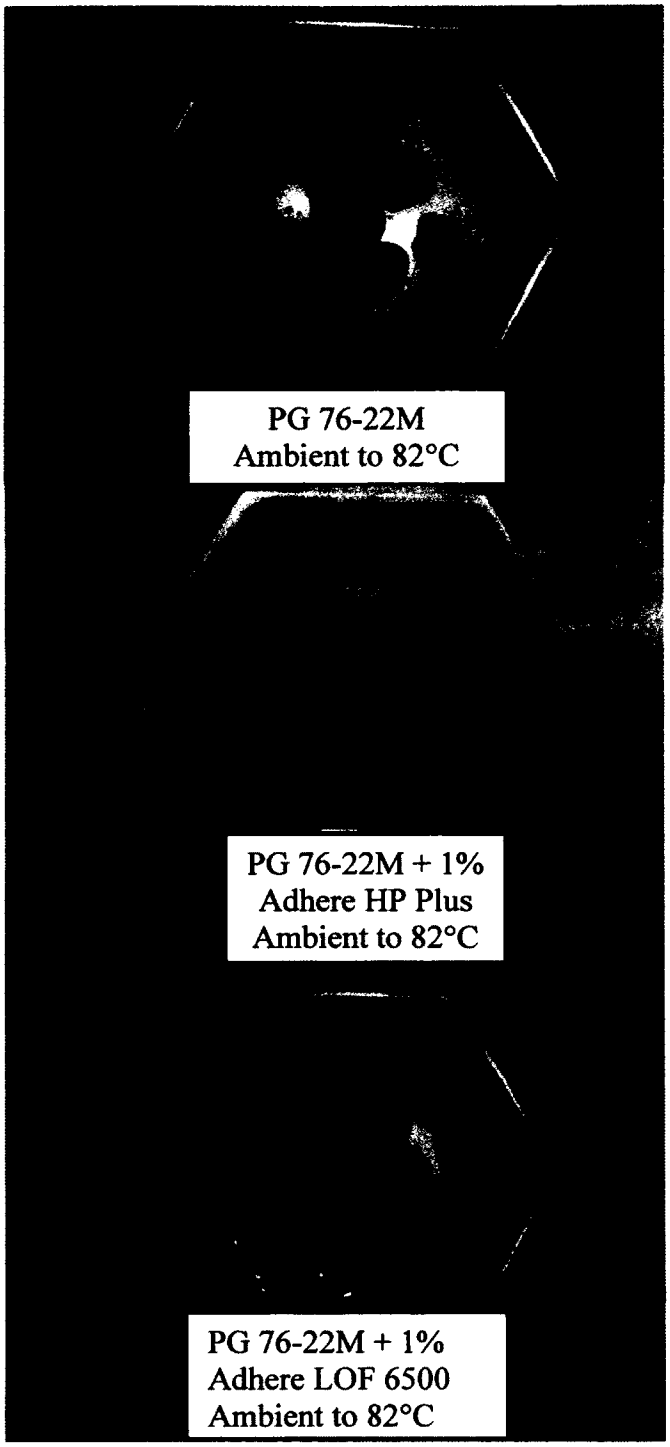

Figure 7-3: Stripping/dewetting of asphalt samples (PG 76-22M, PG 76-22 M + 1% Adhere HP Plus, PG 76-22M + 1% Adhere LOF 6500) after modified ASTM D 3625 test.

7.3 Results and Discussion

The average pH, 8.3, was similar to that used in the glass plate dewetting test. The results were compared to check the correlation between the two methods: The modified boil test and the dewetting based method.

Before discussing the results, the analysis process followed by various researchers is as it pertains to the boil test will be reviewed. Kennedy et al. (1984) indicates that dramatically different results can be obtained with boiling water type (distilled and tap water) for the Texas Boiling Test (Tex-530-C), and also related that similar effects were reported by officials of the Alabama Department of Transportation. Therefore, Kennedy et al. (1984) utilized distilled water in their test. Kennedy et al. concluded that in comparing the boil test to other test results have been shown to not always be consistent; that is they do not correlate well, and Kennedy et al. advise that the evaluation of field performance be long term in order to determine which test or tests would accurately predict field performance. Additionally, Kennedy et al. (1984) found that in the event that the component of a mixture is altered, the mixture should be re-examined as the stripping is dependent on asphalt and aggregate and due to the effectiveness of anti-stripping additives appearing to be aggregate and asphalt dependent. Kiggundu and Roberts (1988) in assessing the success/failure of methods used to predict the stripping propensity in the performance of bituminous pavement mixtures concluded that the boil test registered success at 57.9%, noting that the results obtained do not determine the superiority of a test method against the other as they were not assessed on a common set of material. Also, Kiggundu and Roberts (1988) noted that although the success/ failure pattern can be evaluated, it is not totally deterministic, as stripping action does not occur by a single

factor. It can be noted that this observation is why in the past decades, many tests have been developed in an effort to adequately assess the moisture of bituminous mixtures. Additionally, Cross et al. (2001) noted that Kennedy and Ping (1991) observed that the boiling water test supported chemical anti-strip additives when compared to hydrated lime as opposed to the AASHTO T 283, supporting instead, the hydrated lime than that of the anti-strip additives.

The damage ratings of the modified boil test were correlated with the dewetted area of the asphalt films on the glass plates. A "Best" rating, would signify the least amount of total dewetting of the asphalt film from that of the gravel aggregate. The "Worst" rating would represent the samples with the least overall film retention on the aggregate surface while "Moderate" would represent a fair retention of the asphalt film on the aggregate.

Figure 7-4 shows the distribution of ratings by all observers of the modified boil test in terms of film dewetting on PG 64-22 asphalt with and without additives. Table 7-2 shows the boil test score (horizontal direction) and dewetting results for PG 64-22 with and without additives.

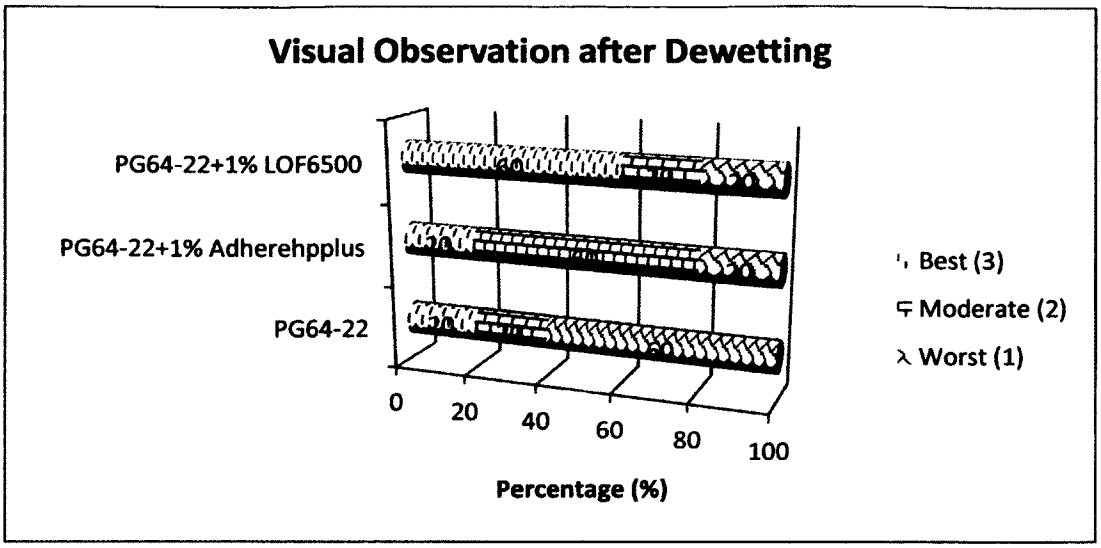

Figure 7-4: Distribution of ratings by all observers of the modified boil test in terms of film dewetting on PG 64-22 asphalt with and without additives.

Based on the observations in Table 7-2, PG 64-22 asphalt appears to be the worst performer with an average rating of 1.6. This result does not correlate well with the total dewetted area on the glass plate which shows PG 64-22 to perform better than PG 64-22 + 1% Adhere HP Plus. PG 64-22 + 1% Adhere LOF 6500 received a score of 2.4 in the boil test which strongly agrees with the dewetting results based on total area where it performed the best. PG 64-22 + 1% Adhere HP Plus was observed to perform moderately in the visual observation but was the worst performer as based on the total dewetted area.

Table 7-2: Boil test scores (horizontal direction) and dewetting results for PG 64-22 with and without additives.

Asphalt Aggregate	Boil Test Score	Dewetting (mm^2)	
		Total Area	
PG 64-22	1.6	22.51	Fig. 6-8
PG 64-22 + 1% Adhere HP Plus	2	28.76	Fig. 6-8
PG 64-22 + 1% LOF 6500	2.4	12.31	Fig. 6-9

Figure 7-5 shows the distribution of ratings by all observers of the modified boil test in terms of film dewetting on PG 58-28 asphalt with and without additives. Table 7-3 shows the boil test scores (horizontal direction) and dewetting results for PG 58-28 with and without and additives. In assessing the PG 58-28 + 1% Adhere LOF 6500 asphalt, it performed the best as is reflected in the former binder PG 64-22 + 1% Adhere LOF6500. Moreover, there was a direct correlation with the boil test score and the total dewetting area for this analysis.

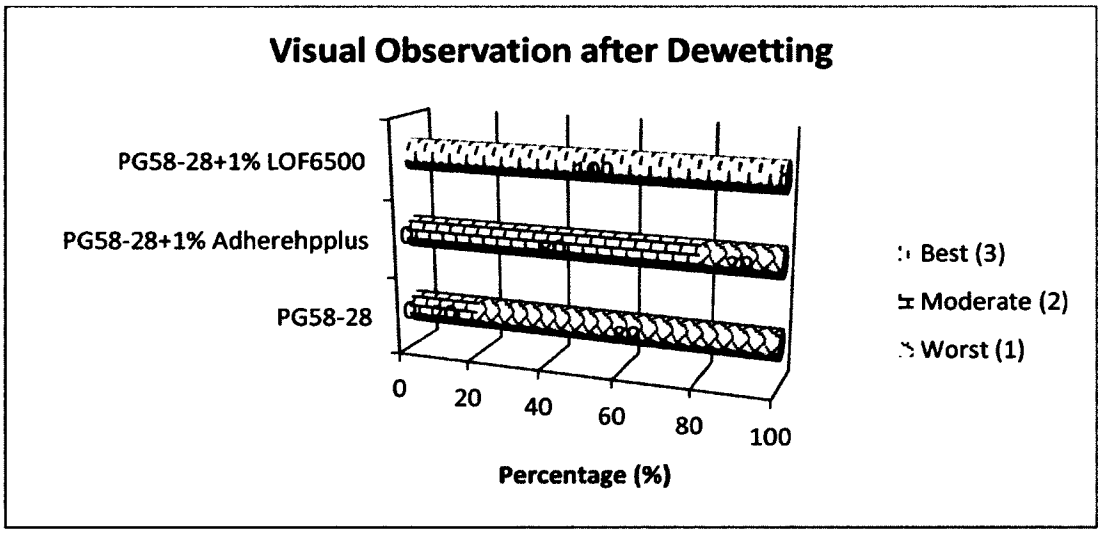

Figure 7-5: Distribution of ratings by all observers of the modified boil test in terms of film dewetting on PG 58-28 asphalt with and without additives.

Comparing the average boil test scores with the glass plate analysis (Table 7-3), the same results are reflected, which suggests a relatively strong correlation between the two different tests. The visual observations showed that PG 58-28 + 1% Adhere performed moderate with a boil test score of 1.8, which also agrees strongly with the total dewetted area results. As PG 58-28 was observed to perform the worst in the modified boil test with a test score of 1.2, it performed the worst in the total dewetting experiments in the glass plate analysis giving rise to a strong correlation. Therefore, it can be

concluded that the two test methods correlated relatively well as it pertains to moisture damage.

Table 7-3: Boil Test scores (horizontal direction) and dewetting results for PG58-28 with and without additives.

Asphalt Aggregate	Boil Test Score	Dewetting (mm^2)	
		Total Area	
PG 58-28	1.2	20.95	Fig. 6-8
PG 58-28 + 1% Adhere HP Plus	1.8	15.52	Fig. 6-8
PG 64-22 + 1% LOF 6500	3	6.26	Fig. 6-9

Figure 7-6 shows distribution of ratings by all observers of the modified boil test in terms of film dewetting on PG 76-22M asphalt with and without additives. Table 7-4 Boil Test scores (horizontal direction) and Dewetting results for PG76-22M with and without additives.

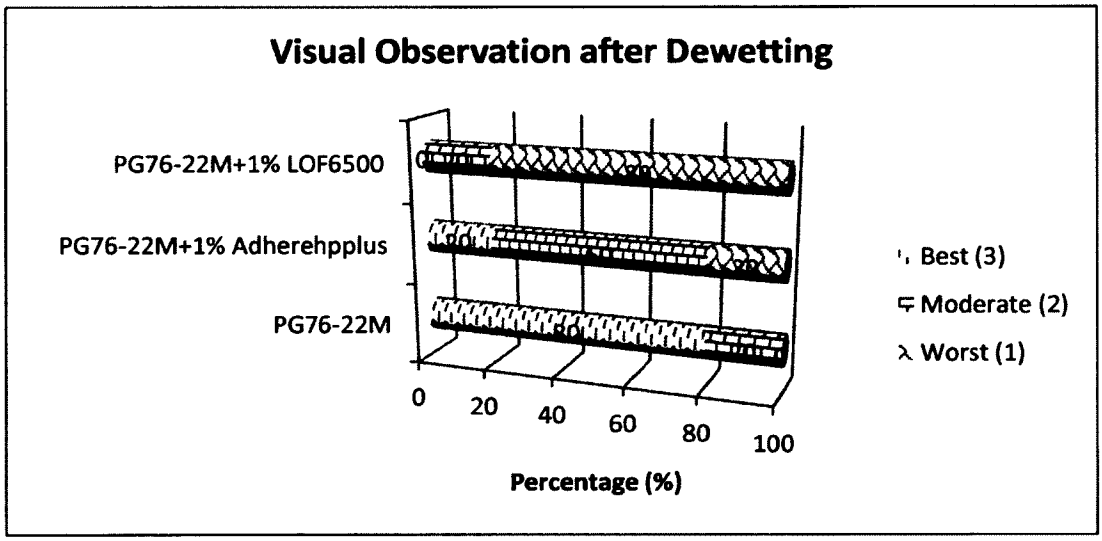

Figure 7-6: Distribution of ratings by all observers of the modified boil test in terms of film dewetting on PG 76-22M asphalt with and without additives.

A strong relation was observed for PG 76-22M asphalt (boil test score 2.67) and total dewetted area (Table 7-4). For total dewetted area, the PG 76-22M asphalt had the

least dewetted area (2.67 mm^2), than compared to when the additives were added. Although for the total dewetted area, PG 76-22M + 1% Adhere HP Plus performed slightly worse than PG 76-22M + 1% Adhere LOF 6500, for the modified boil test, it performed moderately, with a boil test score of 2. These results show that for the total dewetted area analysis, there was a relatively fair correlation with PG 76-22M asphalts with and without additives and the modified boil test.

Table 7-4: Boil Test scores (horizontal direction) and dewetting results for PG 76-22M with and without additives.

Asphalt Aggregate	Boil Test Score	Dewetting (mm^2)	
		Total Area	
PG 76-22M	2.8	2.67	Fig. 6-8
PG 76-22 + 1% Adhere HP Plus	2	6.98	Fig. 6-8
PG 76-22M + 1% LOF 6500	1.2	4.50	Fig. 6-9

The asphalt coated aggregate mixes were additionally assessed vertically, meaning that the three neat asphalts were compared with neat asphalts, and the three asphalts with their respective anti-strip additives were compared with each other.

Figure 7-7 shows the distribution of ratings by all observers of the modified boil test in terms of film dewetting among the three neat asphalts.

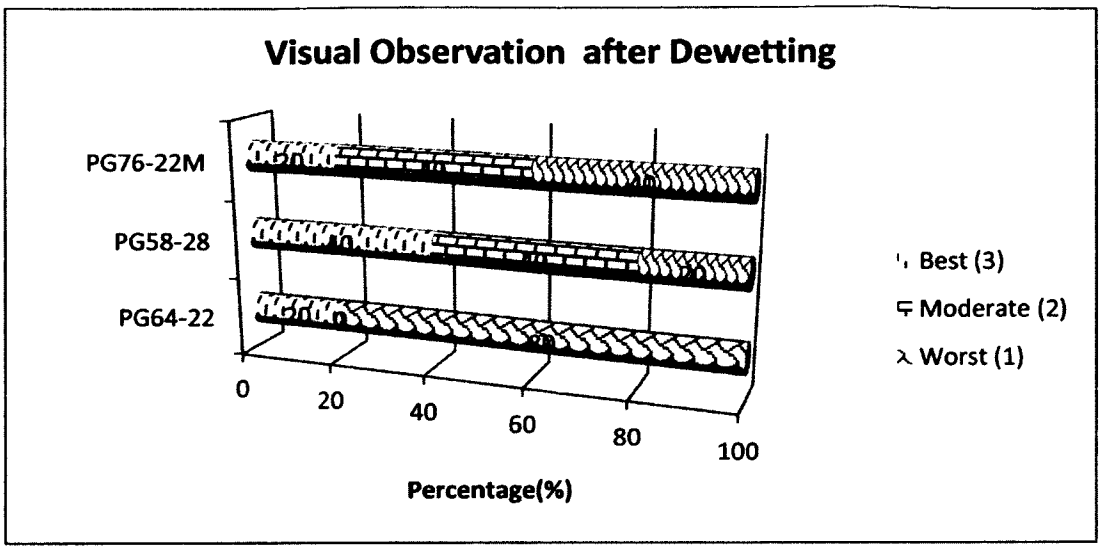

Figure 7-7: Distribution of ratings by all observers of the modified boil test in terms of film dewetting among the three neat asphalts.

Table 7-5 shows the boil test scores (vertical direction) and dewetting results for neat asphalts. Based on the modified boil test results, Table 7-5, PG 64-22 asphalt binder performed the worse among all three neat asphalts with a boil test score of 1.4.

Table 7-5: Boil test scores (vertical direction) and dewetting results for neat asphalts.

Asphalt Aggregate	Boil Test Score	Dewetting (mm^2)	
		Total Area	
PG 76-22M	1.8	2.67	Fig. 6-8
PG 58-28	2.2	20.95	Fig. 6-8
PG 64-22	1.4	22.51	Fig. 6-8

This result agrees, though not strongly, with the dewetting of asphalt films on glass plates. The correlation was not that strong for the best performer which was PG 58-28 asphalt as opposed to the total dewetted area results which showed PG 58-28 to be the intermediate performer. The total dewetted area analysis showed that PG 76-22M

asphalt performed the best, but in the modified boil test, it performed moderately with a test score of 1.8.

Figure 7-8 shows the distribution of ratings by all observers of the modified boil test in terms of film dewetting and retention on three asphalts with 1% Adhere HP Plus.

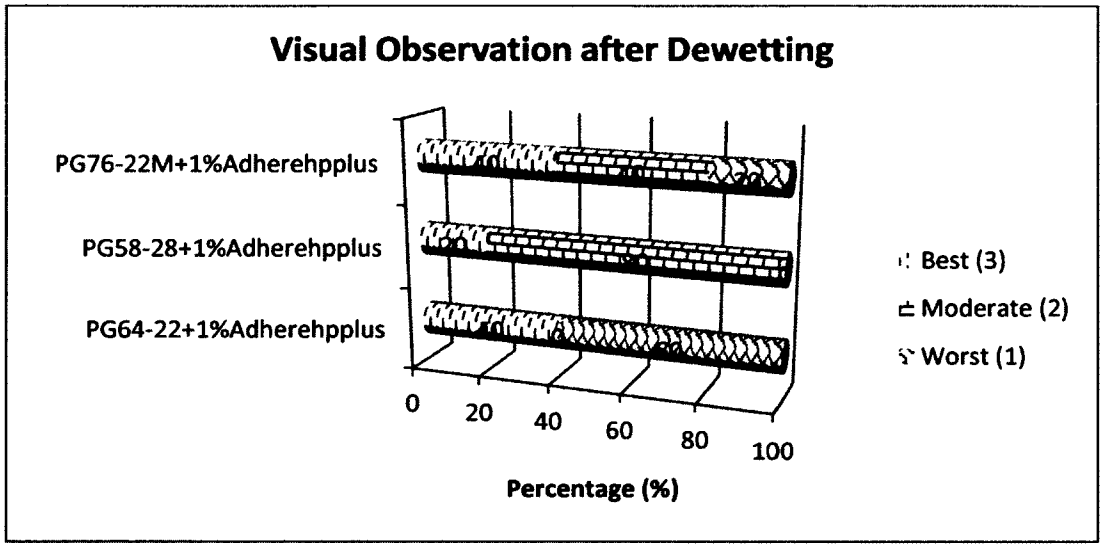

Figure 7-8: Distribution of ratings by all observers of the modified boil test in terms of film dewetting and retention on three asphalts with 1% Adhere HP Plus.

Table 7-6 shows the boil test scores (vertical direction) and dewetting results for 1% Adhere HP Plus added asphalts. From Table 7-6, the worst performer of the asphalts with the additives was observed to be PG 64-22 + 1% Adhere HP plus, with a test score of 1.8 which correlates well with the worst performer in the total hole dewetting analysis. Based on a boil test score of 2.2, PG 58-28 + 1% Adhere HP Plus performed moderately which agrees strongly with the total dewetted area analysis, (15.52 mm^2). However, PG 76-22M + 1% Adhere HP Plus also received a 2.2 test score, which tends to moderate performance, performed the best in the total dewetted area results. The test score as mentioned earlier (2.2), being exactly the same as for PG 58-28 + 1% Adhere HP Plus,

tends to a moderate performance. In that regard, little correlation exists between the two analyses.

Table 7-6: Boil Test scores (vertical direction) and dewetting results for 1% AdhereHPPlus added asphalts.

Asphalt Aggregate	Boil Test Score	Dewetting (mm^2)	
		Total Area	
PG 76-22+1% Adhere HP Plus	2.2	6.98	Fig. 6-8
PG 58-28+1% Adhere HP Plus	2.2	15.52	Fig. 6-8
PG 64-22+1% Adhere HP Plus	1.8	28.76	Fig. 6-8

Figure 7-9 shows distribution of ratings by all observers of the modified boil test in terms of film dewetting and retention on three asphalts + 1% Adhere LOF 6500.

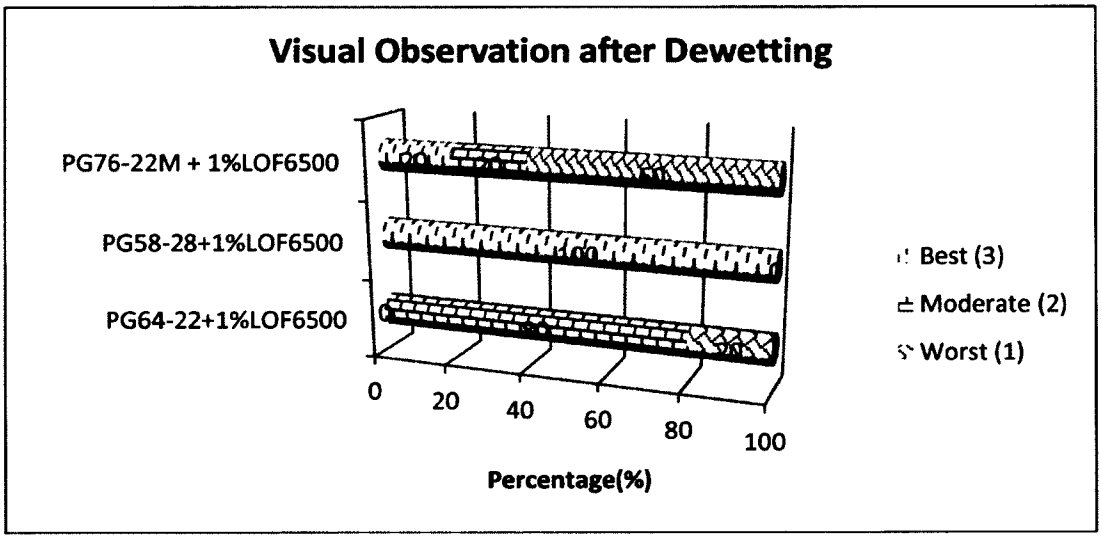

Figure 7-9: Distribution of ratings by all observers of the modified boil test in terms of film dewetting and retention on three asphalts + 1% Adhere LOF 6500.

Table 7-7 shows the boil test scores (vertical direction) and dewetting results for 1% Adhere LOF 6500 added asphalts. Based on the modified boil test scores in Table 7-7, the best performer was observed to be PG 58-28 + 1% LOF 6500, with a boil

test score of 3, whereas in the total dewetted area analysis, PG 76-22M + 1% LOF 6500 asphalt performed the best.

Table 7-7: Boil Test scores (vertical direction) and dewetting results for 1% Adhere LOF 6500 added asphalts.

Asphalt Aggregate	Boil Test Score	Dewetting (mm^2)	
		Total Area	
PG 76-22M + 1% LOF 6500	1.6	4.50	Fig. 6-9
PG 58-28 + 1% LOF 6500	3	6.26	Fig. 6-9
PG 64-22 + 1% LOF 6500	1.8	12.31	Fig. 6-9

PG 64-22 + 1% Adhere LOF 6500 with a boil test score of 1.8, was observed to perform more near moderate than the other two asphalts. This correlation did not agree well when compared with the total dewetted area analysis, as it performed the worse among the three additives. In the total dewetted area analysis, the difference between the worst performer (PG 64-22 + 1% LOF 6500) and the best performer (PG 76-22M + 1% Adhere LOF 6500) was 7.81 mm^2.

Generally, it can be concluded that some sections of the results of the dewetted area analysis correlated well with the modified boil test results while other aspects did not.

7.4 Conclusions

A modified ASTM (3625) boil test was correlated with the total dewetting area analysis. Generally, rankings agreed relatively well for the horizontal analysis for PG 58-28, PG 58-28 + 1% Adhere HP Plus and PG 58-28 + 1% Adhere LOF 6500. Moreover, the boil test rankings agreed fairly well to that of the 1% Adhere HP Plus additives and the three asphalt binders when compared vertically. However, in the other sections of the boil test, there was only fair agreement (33.3%) and in other aspects, no agreement (66.7%) at all.

CHAPTER 8

HOLE DISTRIBUTION IN ASPHALT FILMS AFTER THE DEWETTING OF ASPHALT FILMS

8.1 Background and Objectives

To further understand the dewetting phenomena within the asphalt films, the hole distribution in the film was analyzed based on the pattern and on the area density within the film. Therefore, the objectives of this study were to analyze the distribution of the dewetted holes in some of the dewetted asphalt films with approximately the same film thickness, pH, asphalt type, polymer modified asphalt, and the additives used previously in Chapter 6.

8.2 Results and Discussion

Table 8-1 gives the asphalt type, the thickness of the film and the pH of the samples analyzed for hole distribution.

Table 8-1: Asphalt film thicknesses (e) and pH.

Asphalt Type	Thickness (e) mm	pH
PG58-28	0.205	10
PG64-22	0.236	10
PG76-22M	0.197	10
PG 58-28 + 1% LOF6500	0.126	8.1
PG 58-28 + 1% LOF 6500	0.119	10
PG 64-22 + 1% LOF 6500	0.181	8.1
PG 64-22 + 1% LOF 6500	0.189	10
PG 76-22M + 1% LOF 6500	0.291	8

Table 8-1: Asphalt film thicknesses (e) and pH (Continued).

Asphalt Type	Thickness (e) mm	pH
PG76-22M + 1% LOF6500	0.283	10
PG 58-28 + 0% Additive	0.165	8
PG 58-28 + 1% Adhere HP Plus	0.189	8
PG58-28 + 2% Adhere HP Plus	0.181	7.9
PG 58-28 + 0.5% Adhere HP Plus	0.189	8.2
PG64-22	0.205	7.7
PG76-22M	0.213	8
PG58-28	0.157	8.1

First, the dewetted holes were numbered from North to South by the NI Vision Builder 2012 software (Austin, TX) and can be seen below in Figure 8-1.

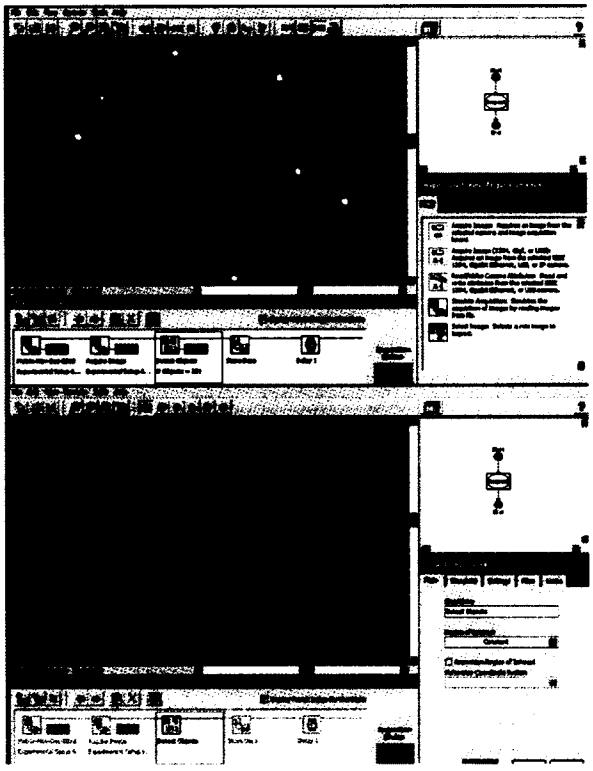

Figure 8-1: A typical PG 64-22 sample (damaged at pH 10) for hole numbering and distribution by software.

In Figure 8-2, the dewetting hole density is compared among the three asphalts PG58-28, PG64-22 and PG76-22M at a high pH, 10, for analysis. As has been mentioned earlier, the pH in asphalt pavements can climb as high as 10. At an average film thickness of 0.213 mm, the two lower viscosity asphalts have most of their area density distributions less than 0.20 mm^2, 99.2% for PG58-28 asphalt and 95. 97% for PG 64-22 asphalt.

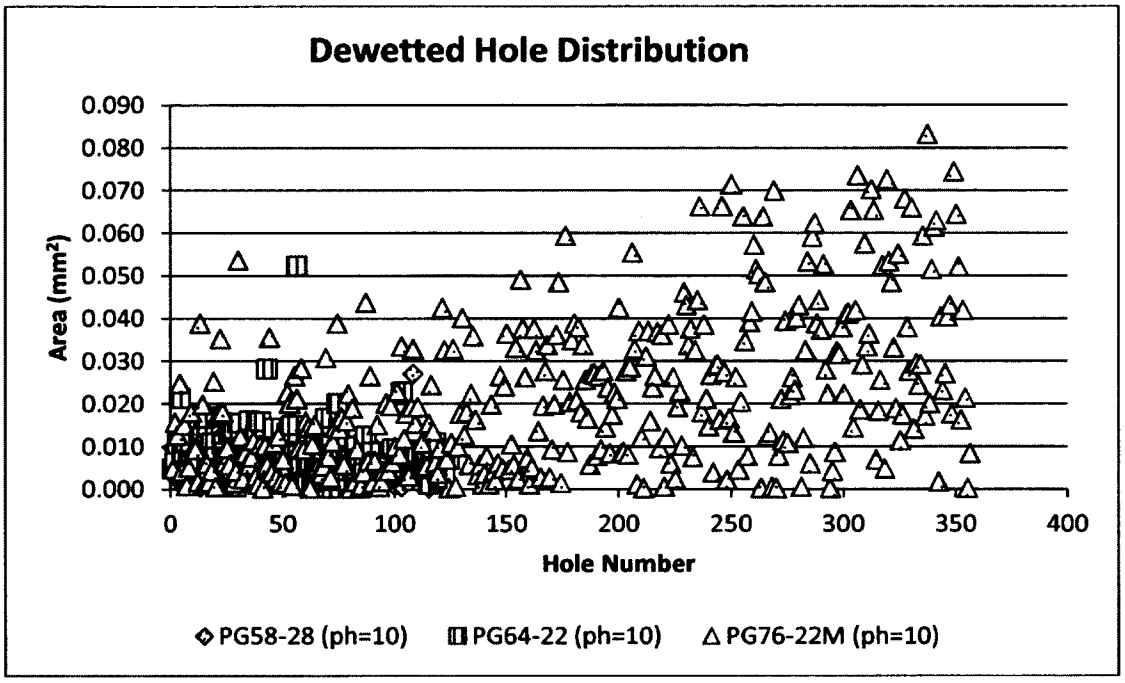

Figure 8-2: Hole and area distribution for PG 58-28, PG 64-22, and PG 76-22M at pH 10.

It was expected that for the lowest viscosity asphalt PG 58-28, the area distribution would be greater than PG 64-22 but that was not the case. It must be noted that although PG 76-22M did contain a modifier which makes the film much stiffer than the other two unmodified asphalts, the density was significantly greater and having one hole being dewetted for up to 0.083 mm^2. It can be clearly observed in this case that a

high pH does have an effect on dewetting or moisture damage on PG 76-22M asphalt binder which agrees with the literature (Tarrer, 1996).

Next, to analyze and observe the effects of pH shifts for hole and area density distribution on (PG 58-28, PG 64-22, and PG 76-22M) with Adhere 1% LOF 6500, six samples were used at approximately the same thickness at two different pH's approximately 8 and 10. For PG 58-28 + 1% Adhere LOF 6500 at pH 8.1 and pH 10, 0.126 mm and 0.119 mm was used, respectively (Figure 8-3).

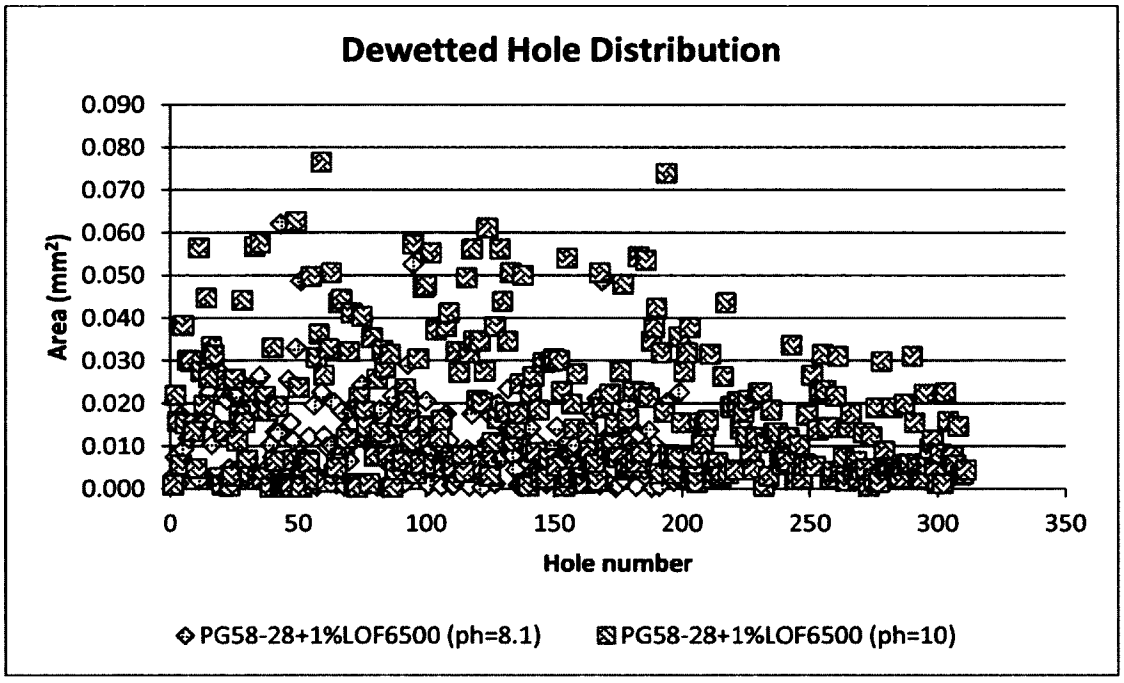

Figure 8-3: Hole and area distribution for PG 58-28 + 1% Adhere LOF 6500 samples, at pH 8.1 and 10 respectively.

There were approximately 200 dewetted holes for the samples at pH 8.1 while at pH 10, there were approximately 300. While most of the hole area distribution lay below 0.030 mm^2 at a pH of 8.1; nevertheless, approximately half of the hole distribution lay above that limit for PG 58-28 + 1% Adhere LOF 6500 subjected to pH 10. Again, it is

therefore evident that dewetting and moisture damage is susceptible to pH shifts even when additives are added to the asphalt. That is, at a lower pH in the field dewetting or moisture damage will be reduced when 1% additive Adhere LOF 6500 is added to PG 58-28 asphalt.

Figure 8-4 shows the results for PG 64-22 + 1% Adhere LOF 6500 subjected to pH 8.1 and pH 10 with thicknesses of 0.181 and 0.189 mm, respectively.

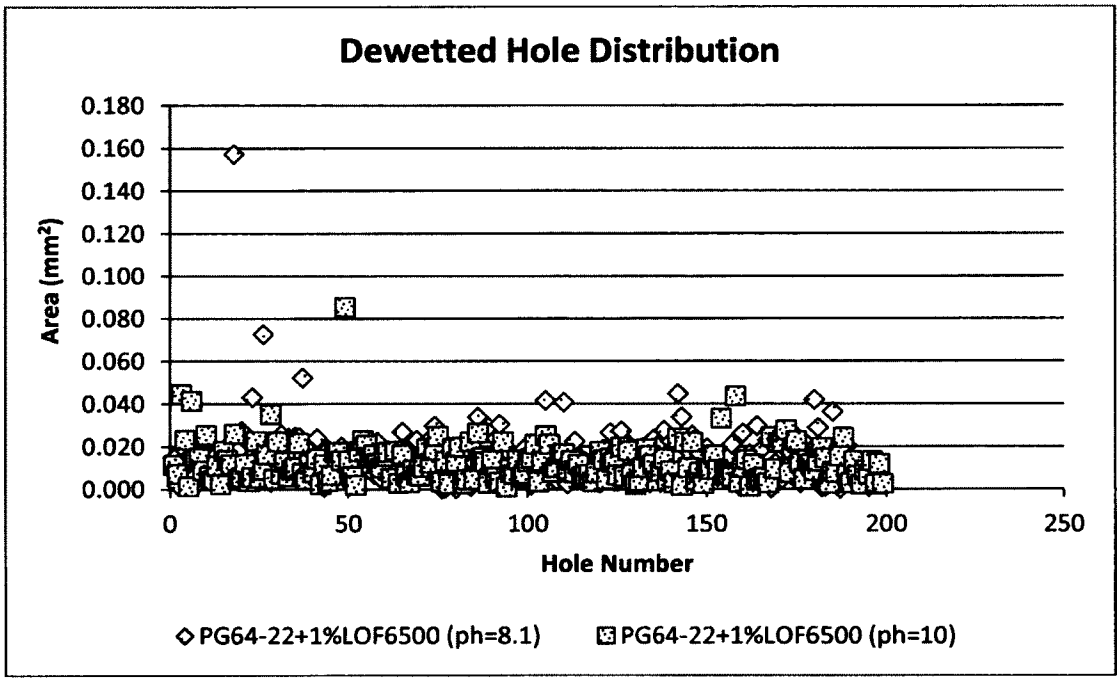

Figure 8-4: Hole and area distribution for PG 64-22 + 1% Adhere LOF 6500, at pH 8.1 and 10 respectively.

In comparing these results to PG 58-28 + 1% Adhere LOF 6500, though at lower film thicknesses, the dewetting hole areas were larger at pH 10 than for PG 64-22 + 1% Adhere LOF 6500. For PG 64-22 + 1% Adhere LOF 6500, the hole density was approximately the same for both pH's, that number being 200. The hole areas were approximately the same as well with below 0.040 mm^2 limit and below 0.020 mm^2 limit

for PG 64-22 + 1% Adhere LOF 6500 at a pH of 10. It must be noted that one hole area at the lower pH was as high as 0.157 mm^2.

Two PG 76-22 M + 1% Adhere LOF 6500 asphalt films (0.291 and 0.283 mm) were subjected to pH 8 and 10 (Figure 8-5). It must be noted that this film thicknesses were generally higher than the thicknesses of the non-polymer modified asphalt films.

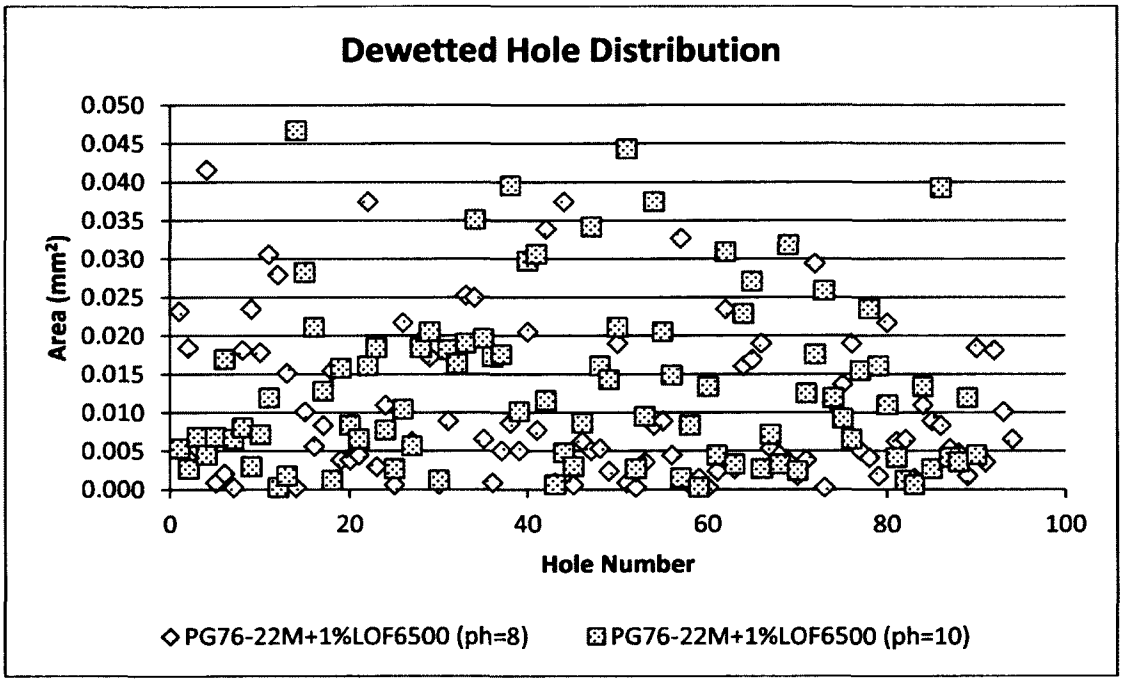

Figure 8-5: Hole and area distribution for PG 76-22M + 1% Adhere LOF 6500, at pH 8 and 10 respectively.

In comparing the dewetted holes with that of PG 58-28 + 1% Adhere LOF 6500, all dewetted hole density for the polymer modified asphalt was lower than that of 0.050 mm^2. This observation suggests that as asphalt film thickness increased, dewetting on the polymer film also decreased. The area hole density distribution was approximately the same for both PG 76-22M + 1% Adhere LOF 6500 at pH 8 and 10.

Furthermore, the effects of additive percentages, 1%, 2%, 0.25% on hole area distribution was analyzed for three PG 58-28 asphalt films (Figure 8-6).

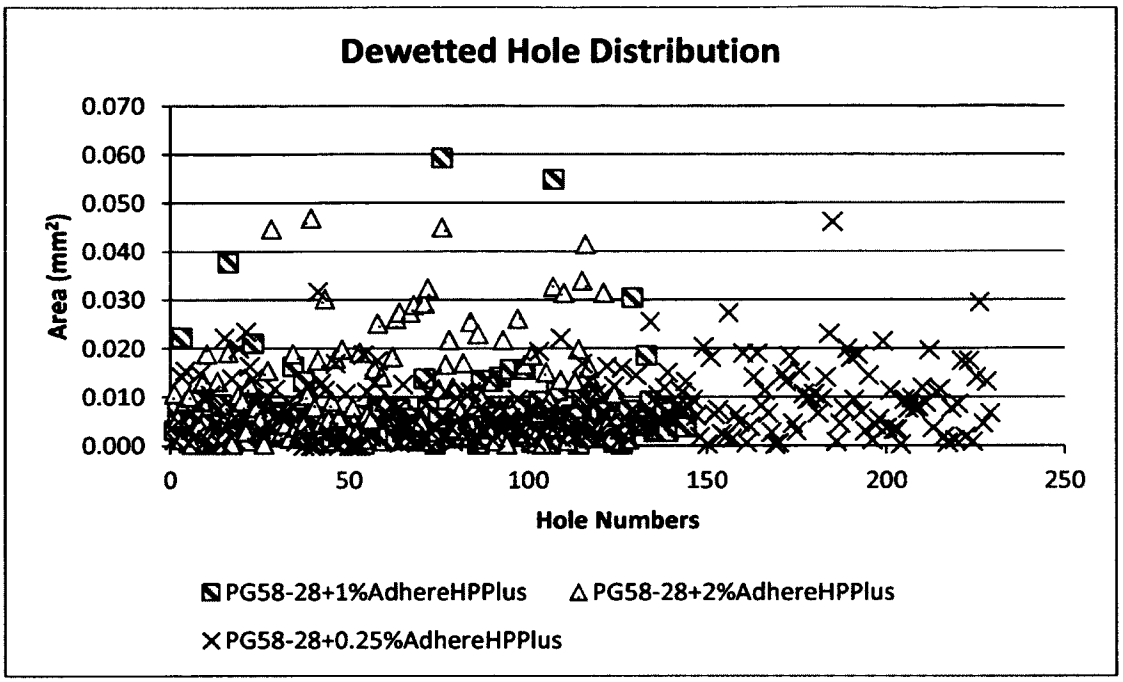

Figure 8-6: Hole and area distribution based on dewetting for various percentages of Adhere HP Plus additives on PG 58-28 asphalt.

For an average film thickness of 0.186 mm the effects of pH on the hole area distribution was analyzed. At 1% Adhere HP Plus, most of the holes fell below 0.010 mm^2 limit, approximately 88.9% though the highest hole area was near 0.059 mm^2. When 2% Adhere HP Plus was added, a dramatic change in the dewetting hole density was observed. The dewetted area of some holes increased from 0.010 mm^2 to 0.047 mm^2. There was definitely an increase in the dewetted hole areas when 2% additive was added to the asphalt. Anderson et al. (1982) pointed out that there is a certain "demand" that every asphalt type has for the anti-strip additive, suggesting that there is a certain minimum or threshold percentage of anti-strip that must be added before it can make its

way to the aggregate surface. Therefore, in applying the additives to asphalts, care must be taken to apply the right dosage as too much or too little may not have the desired effect which is to avoid loss of adhesion and loss of cohesion. Within this asphalt film thickness range, 0.25% additive was observed to increase the hole density of about 229 holes. As with 2% additive, it was similar with that of 0.25% additive whereby many dewetted holes were above the 0.010 mm^2 limit, which was true for most of the asphalt film subjected to 1% additive. For these particular film thicknesses at near normal pH, 1% Adhere HP Plus performed much better by reducing dewetting to a great extent.

Figure 8-7 shows the hole density distribution for three asphalt films, PG64-22, PG 76-22M, and PG 58-28 asphalt at the film thicknesses 220, 228, 228 μm, respectively.

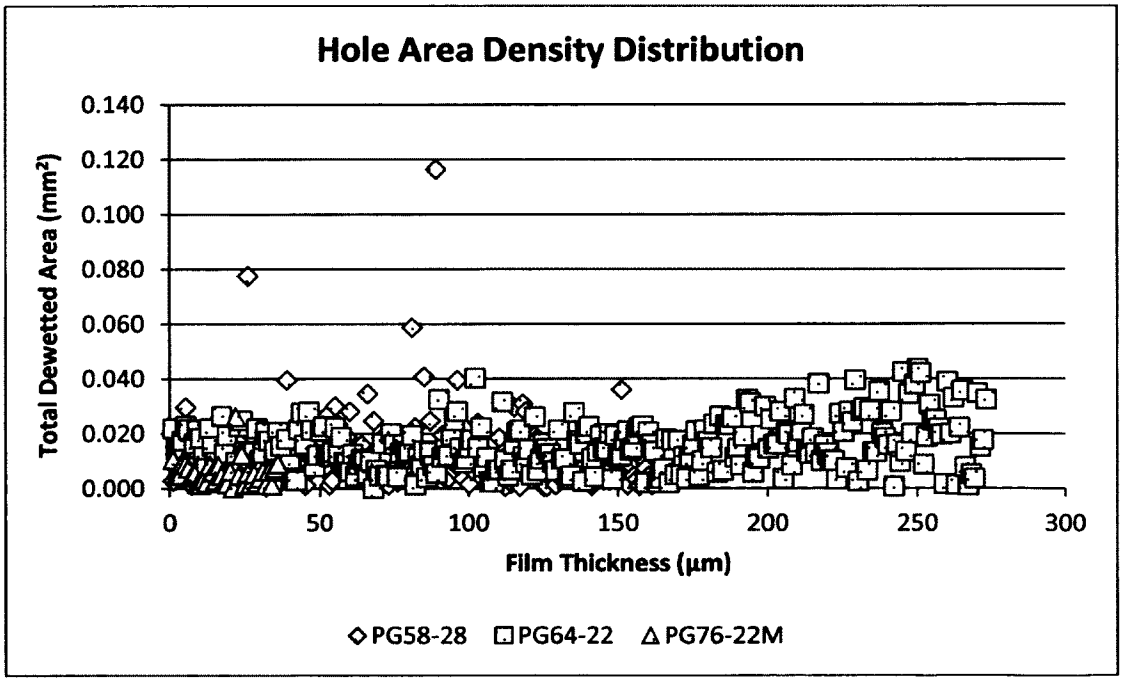

Figure 8-7: Hole and area distribution for PG 58-28, PG 64-22, PG 76-22M in water at 8.4, 8.2, and 7.9 pH respectively.

Although in this specific case, PG 58-28 asphalt film had the lowest thickness, PG 64-22 asphalt film had a higher hole density than that of PG 58-28, 272 as opposed to 162. Again, a considerable number of holes had their dewetted area less than 0.020 mm^2 with a considerable number exceeded this threshold for both PG 58-28 and PG 64-22 asphalt films while only one hole exceeds this limit for PG 76-22M asphalt. Moreover, it must be emphasized that even at similar film thicknesses, the polymer modified asphalt film appeared to be hindering dewetting which was an advantage especially to curb moisture damage in asphalt pavements. In this particular instance, probably due to its low viscosity, four holes exceeded the threshold of 0.040 mm^2 dewetted area.

8.3 Conclusions

Generally, it was observed that the distribution of the dewetted holes in the asphalt films in submerged water condition were affected by many parameters. They include film thickness, asphalt types, pH, polymer modified or non polymer modified, and anti-strip additives. These results reflect what has been discussed in the moisture damage literature that moisture damage is not caused by a single mechanism; but rather, it is influenced by a wide range of parameters, making it a complex phenomenon.

CHAPTER 9

CONCLUSIONS AND FUTURE WORK

9.1 Conclusions

At the beginning, efforts were put forth to develop a new moisture damage test in conjunction with the modified pull-off test with the use of a pneumatic adhesion tensile testing equipment (P.A.T.T.I.). Surface free energy tests were performed in an attempt to correlate pull-off adhesion (both dry and wet) to the theoretical free energy of cohesion and adhesion, respectively. However, instead of the aforementioned moisture damage test method, a novel moisture conditioning test procedure, as discussed in Chapter 3, shows the main difference among the other moisture conditioning tests afterward cited and compared, to test for stripping in asphalt. The submerged asphalt samples were placed in an oven at 64°C, allowed to be heated to that temperature, and removed within 24 h for testing, where this procedure primarily focuses on the dewetting mechanism. The phenomenon of dewetting of asphalt films was proposed as the moisture damage mechanism.

Moreover, Chapters 4, 5, 6, 7, and 8 describe the detailed investigation of the characteristics of dewetting and its analysis procedure leading to a unique dewetting-based moisture damage test procedure and analysis. Dewetting, as it was later observed via the microscope, occurs primarily under an air bubble trapped in an asphalt film. The dewetting mechanism was further investigated.

In Chapter 4, dewetting of asphalt films on glass plate substrate was observed with the use of a microscope (Chapter 5 as well), while in Chapter 5, dewetting of asphalt films on aggregates was observed in order to better understand the dewetting mechanism.

In Chapter 6, a unique dewetting –based moisture damage test and analysis procedure was developed to assess moisture damage in three asphalt films, PG58-28, PG 64-22, PG 76-22M, plus the addition of additives and the effect of pH by the dewetting phenomenon. Experimentally, the critical film thickness was estimated and as was found to be 300 μm. Furthermore, the analysis procedure of dewetting include quantitative measurements such as total dewetted hole area and average dewetted area per hole.

In Chapter 7, a modified boil test (a modified ASTM 3625) was developed in an effort to correlate this test with the results from the dewetting-based method.

In Chapter 8, the hole distribution in asphalt films after the dewetting of asphalt films was observed based on similar thicknesses, same and different asphalt types, and change in pH. Generally, it was observed that all these parameters play a very important role in the moisture damage of asphalt films.

Based on the asphalt film dewetting observations and analysis, the research suggests that dewetting plays a significant role in moisture damage in hot mix asphalt pavements.

The following general conclusions were made:

In Chapter 3:

1. The researchers investigated different moisture conditioning methods to achieve pure adhesive failure or stripping of asphalt film. Finally, the simple procedure followed in this study was effective in producing adhesive failure. With this moisture conditioning procedure it was observed that PG 64-22 original, with 1% LOF 6500 and with 1% LOF 6500 plus Sasobit® exhibits adhesive failure while PG 64-22 plus Sasobit® produces mixed mode of failure. For PG 76-22M, only original samples (without additives) exhibited adhesive failure. Mixed mode of failure was observed for 1% LOF 6500 and 1% LOF 6500 plus Sasobit® while cohesive failure was observed for Sasobit®. This indicates that 1% LOF 6500 is not effective for moisture resistance while Sasobit® changes the mode of failure to mixed or cohesive but not necessarily increasing strength.
2. The adhesive strengths (free energy of adhesion) obtained from SFE measurements were compared with that of pull-off test. The results do not necessarily correlate well except that both the methods (pull-off and SFE) indicate that combination of 2% Sasobit® and 1% LOF 6500 increases moisture susceptibility.
3. Besides cohesive and adhesive strengths, SFE measurements indicated that addition of additives used in this study increased the base component of SFE. Also, it indicated that limestone is much more basic than

novaculite. The base SFE components of limestone and novaculite are 75.5 ergs/cm^2 and 40.7 ergs/cm2, respectively. (Wasiuddin and Saltibus, 2010; Wasiuddin et al., 2011b)

Further conclusions may be made based on observations and the analysis of the results obtained in the remaining chapters:

Chapter 4 - With the aid of the microscope, the dewetting of asphalt films were observed and analyzed for one dewetted hole, the following conclusions were attained:

1. Most dewetting patterns follow that of an exponential growth.
2. In the dewetting of some holes on glass substrate, the films do not completely dewet, leaving three layer films behind, varying in shades. Sometimes, one single film is left. Within that layer, more dewetted holes are visible. This can be caused by coagulation of the air inside the film.

Chapter 5 - For the case of dewetting of asphalt films on that of the surface of the aggregate, the characteristics as observed for a single dewetted hole are as follows:

1. For most of the aggregate specimens, a very thin layer of the asphalt was observed to remain on the surface after dewetting.
2. Healing on a large scale of the asphalt binder in the aggregate samples were not observed.

Chapter 6 - The final dewetting-based moisture damage test protocol that was developed and followed in this study was given and is as follows. Asphalt samples were prepared. After curing, 0.01 grams of aggregates (gravel) retained on #100 sieve size was spread over the asphalt film surface (~2.5 x 5.08 cm). Samples were tested in submerged water condition at ambient to 50 °C. After two h, photographs were taken for analysis with the

National Vision Builder AI 2012 software. The following conclusions were arrived at when the dewetting analysis were performed for the holes in the dewetted holes in the aphalt films:

1. The critical film thickness for PG 58-28, PG 64-22, and PG 76-22M was estimated experimentally and was found to be 300 μm. The critical film thickness was the minimum thickness above which very few holes, tending to but not necessarily zero, were observed. This result indicates a possible threshold for field asphalt film thickness in the pavement mix.
2. Polymer in PG 76-22M asphalt binder does aid in reducing dewetting and as a result moisture damage in asphalt pavements.
3. For PG 76-22M, all additive rates (below and above 1%) increased dewetting, which suggests that polymer in the absence of additives performs relatively well in the process reducing moisture damage. Additionally, for PG 76-22M, with and without additives, the dewetting was significantly lower as compared to the other two asphalt binders (PG 58-28 and PG 64-22) with and without additives. Therefore, this result indicates that polymer helps in the reduction of dewetting.
4. The 2% Adhere HP Plus reduced dewetting slightly for PG 58-28 asphalt, but increased dewetting for PG 76-22M asphalt significantly.
5. For PG 58-28, PG 64-22, PG 76-22M, with and without both additives, (1% Adhere HP Plus, 1% Adhere LOF 6500), the number of dewetted holes decreased as film thickness increased and arrived at a critical film thickness of approximately 300μm. However, PG 64-22 (with additives) reflected some slight

variations within the vicinity of this point. Generally, very few dewetted holes were observed when this film thickness exceeds the critical film thickness.

6. At high pH, for all three asphalts, dewetting was increased for 1% Adhere LOF 6500, significantly for PG 76-22M. However, except for PG 58-28 + 1% Adhere HP Plus, which shows a significant increase in total dewetted area for high pH, there was a decrease in dewetting for the other two asphalts.

Chapter 7 - The correlation analysis between the modified boil test and the dewetting-based test procedure and analysis follows:

7. A strong correlation was observed overall for the horizontal analysis for PG 58-28, PG 58-28 + 1% Adhere HP Plus and PG 58-28 + 1% Adhere LOF 6500 and a fair correlation also to that of the 1% Adhere HP Plus additives and the three asphalt binders when compared vertically. However, in the other sections of the boil test, there was good correlation, and in other aspects, no correlation at all.

Chapter 8 -The analysis of the distribution of dewetted holes in selected asphalt films based on the various parameters are as follows:

8. Generally, it was observed that the distribution of the dewetted holes in the asphalt films in submerged water condition were affected by many parameters. These parameters include, film thickness, asphalt types, pH, polymer modified or non polymer modified, and anti-strip additives. This observation reflects what has been discussed in the moisture damage literature that moisture damage is not caused by a single mechanism, but rather is influenced by a wide range of parameters, making it a complex phenomenon.

9.2 Future Work

It is recommended that further research be conducted in validating the test method by conducting more tests on additional asphalt types, the use of various moisture damage additives, and other pH values (particularly lower pH) in order to observe the behavior of dewetting of asphalt films in that regard and to further substantiate the critical film thickness. Additionally, the relationship between the reactivity of the polymer, strength of the polymer with that of its molecular weight should be assessed.

APPENDIX A

APSHALT SPECIMENS DATA FOR TENSILE STRENGTH RATIO CALCULATION

Table A-1: Asphalt specimen properties.

Samples	Gmb	Pa (%)	A = Dry weight (g)	B = SSD weight (g)	C = Submerged weight (g)	Additive (%)
1	2.273	3.64	3867.5	3876.4	2175.2	0.4
2	2.281	3.3	3862.7	3869	2175.6	0.4
3	2.279	3.39	3869.3	3875.6	2177.9	0.4
4	2.265	3.98	3868.7	3876.5	2168.7	0.4
	Height (mm)	Dry Weight (g)	Gyratory Volume (cm^3)	Volume by Submersion (cm^3)	Gyratory Gmb	Gmb by Submersion
1	98	3867.5	1731.80	1701.20	2.23	2.27
2	97.5	3862.7	1722.97	1693.40	2.24	2.28
3	98	3869.3	1731.80	1697.70	2.23	2.28
4	98.3	3868.7	1737.1	1707.80	2.23	2.27
	Gyratory Air Voids (%)	Subm-ersion Air Voids (%)	Gyratory Air Voids (cm^3)	Submersion Air Voids (cm^3)	Water Absorption (%)	70% Submersion Air Voids (cm^3)
1	6.482	4.799	112.25	81.64	0.52	57.15
2	6.119	4.479	105.42	75.85	0.37	53.10
3	6.438	4.559	111.49	77.39	0.37	54.17
4	6.738	5.138	117.05	87.74	0.46	61.42
	80% Submer-sion Air Voids (cm^3)					
1	65.32					
2	60.68					
3	61.91					
4	70.19					

Gmb – Bulk specific gravity, Pa – Percentage of air voids, SSD- Surface saturated dry.

Table A-2: Results used to calculate tensile strength ratio.

Samples	Ultimate Load (lb)	Tensile Strength (psi) Dry	Tensile Strength (psi) Conditioned
1	5560		155.38
2	5220	146.63	
3	5520		154.26
4	5210	145.15	
	Dry Subset	Conditioned Subset	
Average Strength (psi)	145.89	154.82	
TSR	1.06		

Table A-3: Aggregate Blend (~3700 g).

Retained in Sieve Size	Fine Sand	Coarse Sand	Small Crushed Gravel	Coarse Crushed Gravel	
	17% (g)	18% (g)	53% (g)	12% (g)	Blend %
2"	0.00	0.00	0.00	0.00	0.00
1.5"	0.00	0.00	0.00	0.00	0.00
1"	0.00	0.00	0.00	0.00	0.00
¾"	0.00	0.00	0.00	0.00	0.00
½"	0.00	0.00	17.39	204.24	221.63
3/8"	0.00	0.00	304.51	227.92	532.43
¼"	0.00	0.00	658.23	11.47	669.70
No. 8	0.00	54.02	569.06	0.00	569.06
No. 40	62.90	338.18	278.61	0.00	278.61
No.80	79.92	213.12	70.67	0.00	70.67
No. 200	310.06	44.77	17.76	0.00	17.76
Pan	176.12	15.91	45.14	0.37	45.51
	629.00	666.00	1961.37	444.00	2405.37

APPENDIX B

PULL-OFF TEST AND SURFACE FREE ENERGY MEASUREMENT RESULTS

Table B-1: Dry cohesive strengths of PG 64-22 from pull-off test.

	Reading (psi)	Pull-Off Strength (psi)	Pull-Off Strength (MPa)	Time	Pressure (psi/sec)
PG 64-22 with No Additives					
Sample 1	61.30	305.5	2.106	32	9.55
Sample2	51.50	256.6	1.769	23	11.15
Sample 3	56.50	281.5	1.941	28	10.05
Sample 4	59.40	296.0	2.041	29	10.21
Average	57.18	284.9	1.964		
St. Dev.	4.27	21.3	0.147		
PG 64-22 with 2% Sasobit®					
Sample 1	41.60	207.1	1.428	20	10.36
Sample 2	40.30	200.6	1.38	18	11.15
Sample 3	43.70	217.6	1.500	20	10.88
Sample 4	45.40	226.1	1.559	20	11.30
Average	42.75	212.9	1.468		
St. Dev.	2.25	11.3	0.078		
PG 64-22 with 1% LOF 6500					
Sample 1	36.40	181.2	1.249	18	10.06
Sample 2	41.20	205.1	1.414	19	10.80
Sample 3	45.30	225.6	1.555	27	8.36
Sample 4	47.30	235.6	1.624	22	10.71
Average	42.55	211.9	1.461		
St. Dev.	4.82	24.1	0.166		
PG 64-22 with 2% Sasobit® and 1% LOF 6500					
Sample 1	39.70	197.6	1.363	18	10.98
Sample 2	31.30	155.7	1.074	15	10.38
Sample 3	33.10	164.7	1.136	16	10.29
Average	34.70	172.7	1.191		
St. Dev.	4.42	22.1	0.152		

Table B-2: Dry cohesive strengths of PG 76-22M from pull-off test.

PG 76-22M with No Additives					
Sample 1	60.20	300.0	2.068	28	10.71
Sample2	59.50	296.5	2.044	30	9.88
Sample 3	64.20	320.0	2.206	33	9.7
Sample 4	56.80	283.0	1.951	27	10.48
Average	60.18	299.9	2.067		
St. Dev.	3.06	15.3	0.105		
PG 76-22M with 2% Sasobit®					
Sample 1	47.80	238.1	1.642		
Sample 2	45.70	227.6	1.569		
Sample 3	40.90	203.6	1.404	19	10.72
Sample 4	40.70	202.6	1.397	18	11.26
Average	43.78	218.0	1.503		
St. Dev.	3.54	17.7	0.122		
PG 76-22M with 1% LOF 6500					
Sample 1	46.40	231.1	1.593	37	6.25
Sample 2	55.60	277.0	1.910	29	9.55
Sample 3	59.40	296.0	2.041	31	9.55
Average	53.80	268.0	1.848		
St. Dev.	6.68	33.4	0.230		
PG 76-22M with 2% Sasobit® and 1% LOF 6500					
Sample 1	31.40	156.2	1.077	15	10.41
Sample 2	31.20	155.2	1.070	18	8.62
Sample 3	27.70	137.7	0.950	16	8.61
Average	30.10	149.7	1.032		
St. Dev.	2.08	10.4	0.072		

Table B-3: Summary of dry cohesive strengths from pull-off test.

	Dry Pull-Off Strength (psi)	Dry Pull-Off Strength in (MPa)
PG 64-22	284.9	1.964
PG 64-22 + 2% Sasobit®	212.9	1.468
PG 64-22 + 1% LOF 6500	211.9	1.461
PG 64-22 + 2% Sasobit® + 1% LOF 6500	172.7	1.191
PG 76-22M		
PG 76-22M	299.9	2.067
PG 76-22M + 2% Sasobit®	218.0	1.503
PG 76-22M + 1% LOF 6500	268.0	1.848
PG 76-22M + 2% Sasobit® + 1% LOF 6500	149.7	1.032

Table B-4: Effect of film thickness on dry cohesive strengths.

	Pull-Off Strength (psi)	Pull-Off Strength (psi)
	Thin	Thick
PG 64-22 with No Additives		
Sample 1	270.5	305.5
Sample 2	198.1	256.6
Sample 3	281.0	281.5
Sample 4	228.6	296.0
Average	244.6	284.9
St. Dev.	38.4	21.3
PG 64-22 with 2% Sasobit®		
Sample 1	212.1	207.1
Sample 2	206.1	200.6
Sample 3	204.1	217.6
Sample 4	205.6	226.1
Average	207.0	212.9
St. Dev.	3.5	11.3
PG 76-22M		
Sample 1	270.5	300.0
Sample 2	246.1	296.5
Sample 3	224.1	320.0
Sample 4		283.0
Average	246.9	299.9
St. Dev.	23.2	15.3
PG 76-22M with 2% Sasobit®		
Sample 1	224.6	238.1
Sample 2	214.6	227.6
Sample 3	179.2	203.6
Sample 4	222.1	202.6
Average	210.1	218.0
St. Dev.	21.1	17.7

Table B-5: Adhesive strengths of conditioned pull-stub samples.

	Reading (psi)	Pull-Off Strength (psi)	Pull-Off Strength (MPa)	Failure Mode
PG 64-22	30.3	150.7	1.039	Adhesive
PG 64-22 with 2% Sasobit®	31.6	157.2	1.084	Adhesive
PG 64-22 with 1% LOF 6500	29.9	148.7	1.025	Mixed
PG 64-22 with 2% Sasobit® and 1% LOF 6500	26.2	130.2	0.898	Adhesive
PG 76-22M	47.8	238.1	1.642	Adhesive
PG 76-22M with 2% Sasobit®	47.1	234.6	1.617	Mixed
PG 76-22M with 1% LOF 6500	29.1	144.7	0.998	Cohesive
PG 76-22M with 2% Sasobit® and 1% LOF 6500	28.7	142.7	0.984	Mixed

Table B-6: Adhesive strengths of conditioned and oven dry pull-stub samples to check whether moisture damage samples can be healed.

	Reading (psi)	Pull-Off Strength (psi)	Pull-Off Strength (MPa)	Failure Mode (MPa)
PG 64-22	56.9	283.5	Cohesive	1.955
PG 64-22 with 2% Sasobit®	42.0	209.1	Cohesive	1.442
PG 64-22 with 1% LOF 6500	49.4	246.1	Cohesive	1.697
PG 64-22 with 2% Sasobit® and 1% LOF 6500	41.7	207.6	Cohesive	1.432
PG 76-22M	49.5	246.6	Cohesive	1.700
PG 76-22M with 2% Sasobit®	55.7	277.5	Cohesive	1.913
PG 76-22M with 1% LOF 6500	28.9	143.7	Cohesive	0.991
PG 76-22M with 2% Sasobit®and 1% LOF 6500	26.7	132.7	Cohesive	0.915

APPENDIX C

DEWETTING IMAGES OF APSHALT FILMS ON GLASS SUBSTRATE IN SUBMERGED WATER CONDITION UNDER AN AIR BUBBLE

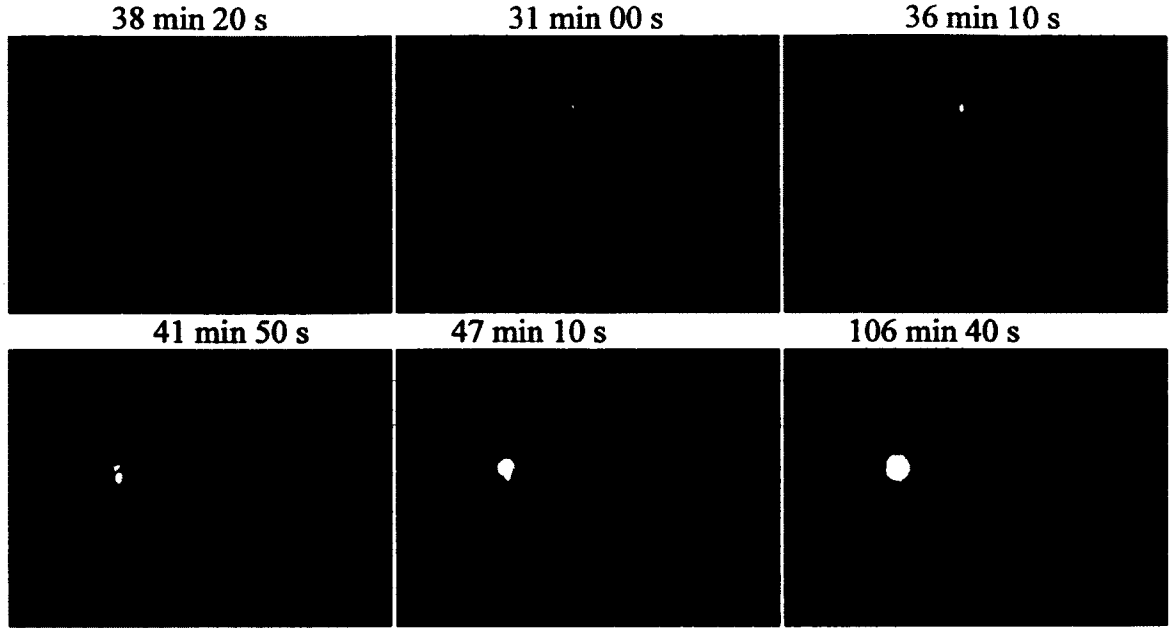

Figure C-1: Select images of hole growth from Table 4-1 (Figure 4-4).

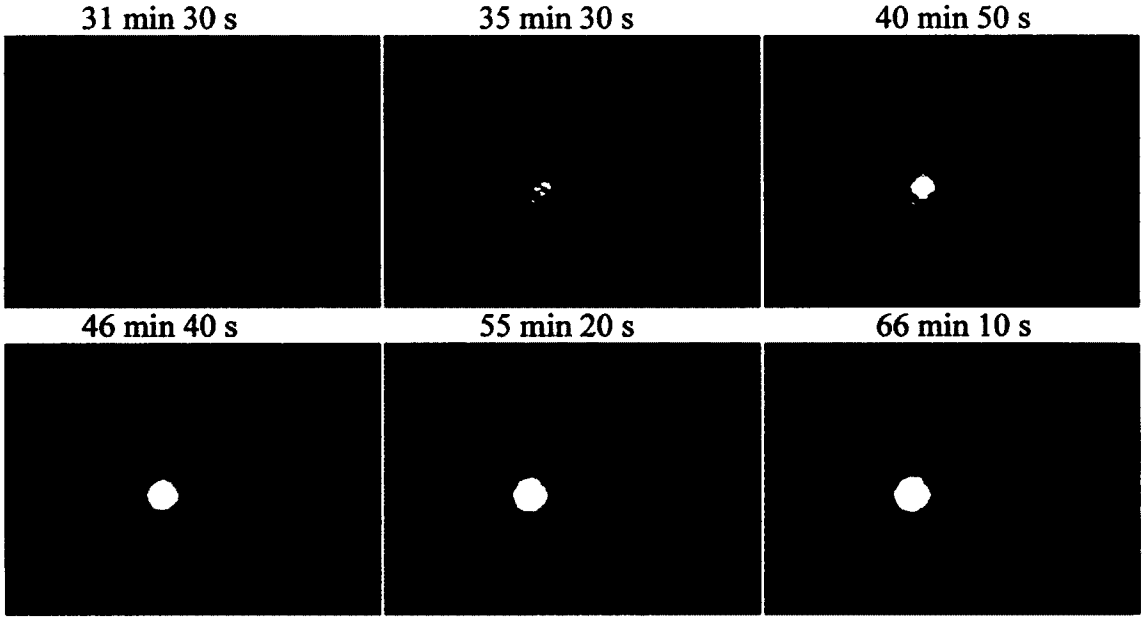

Figure C-2: Select images of hole growth from Table 4-1 (Figure 4-5).

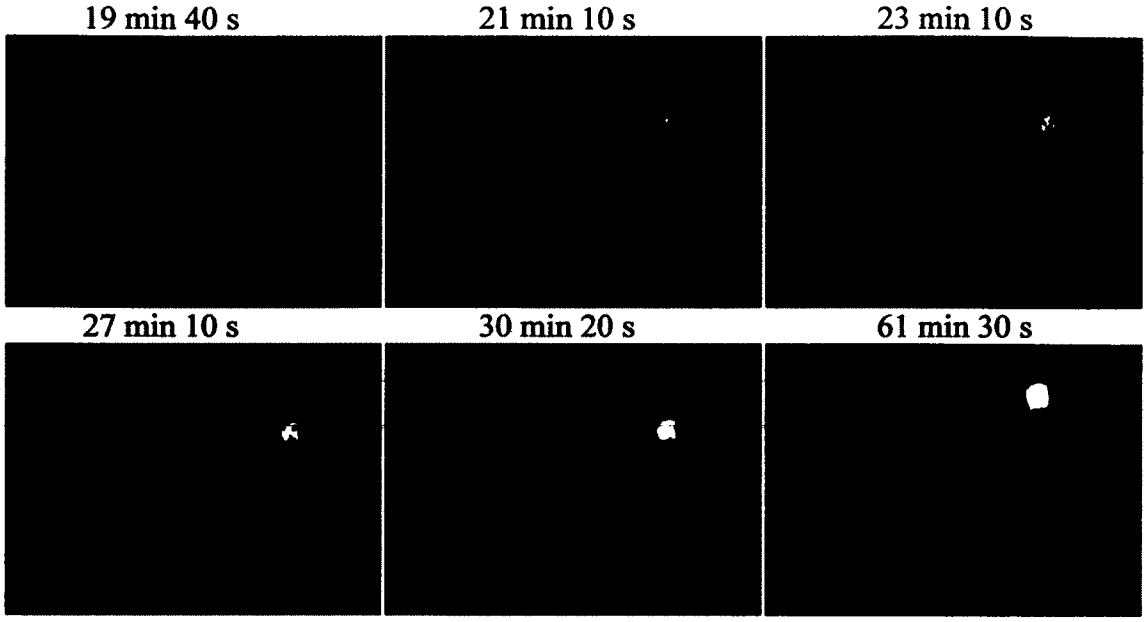

Figure C-3: Select images of hole growth from Table 4-1 (Figure 4-6).

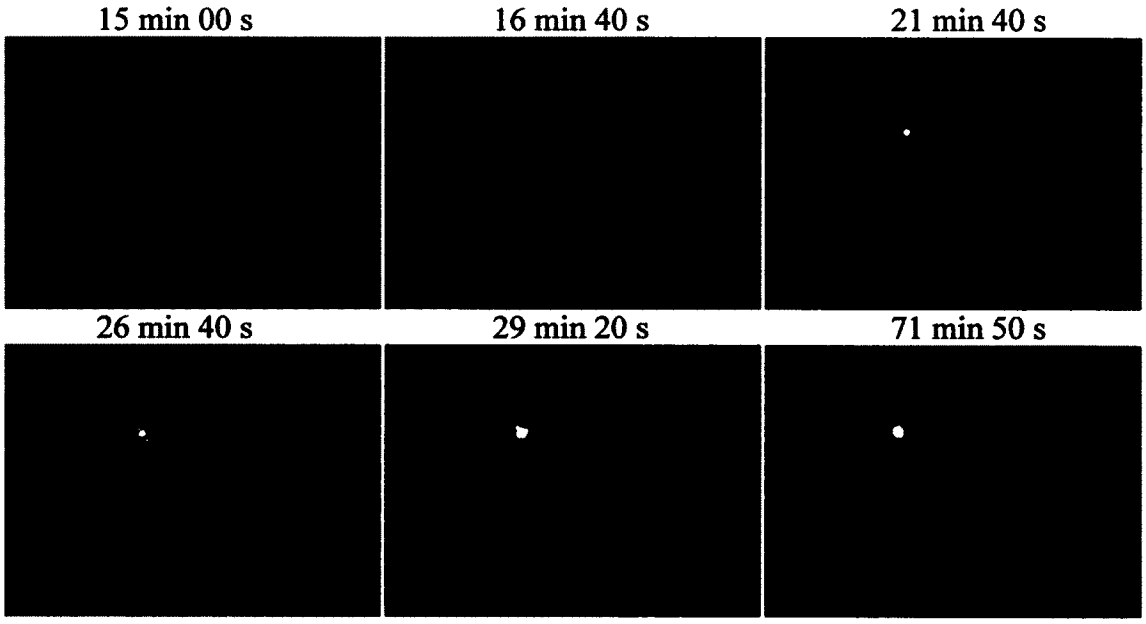

Figure C-4: Select images of hole growth from Table 4-1 (Figure 4-8).

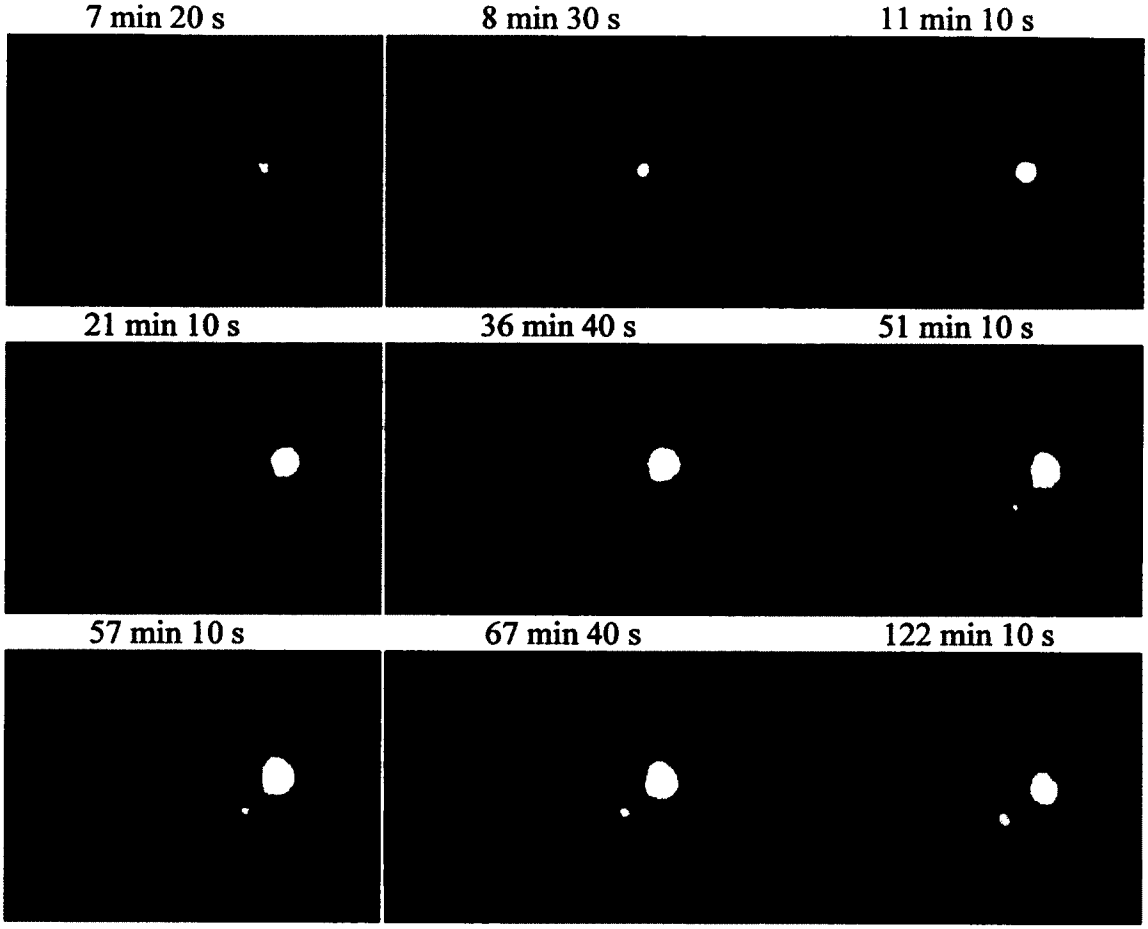

Figure C-5: Select images of hole growth from Table 4-1 (Figure 4-9).

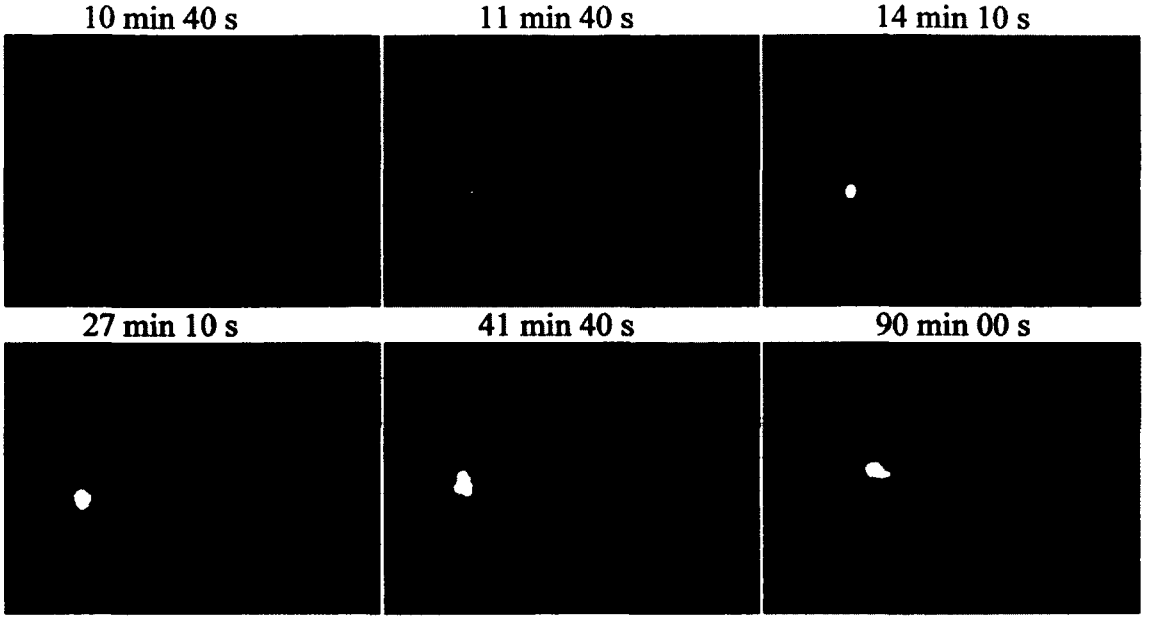

Figure C-6: Select images of hole growth from Table 4-1 (Figure 4-11).

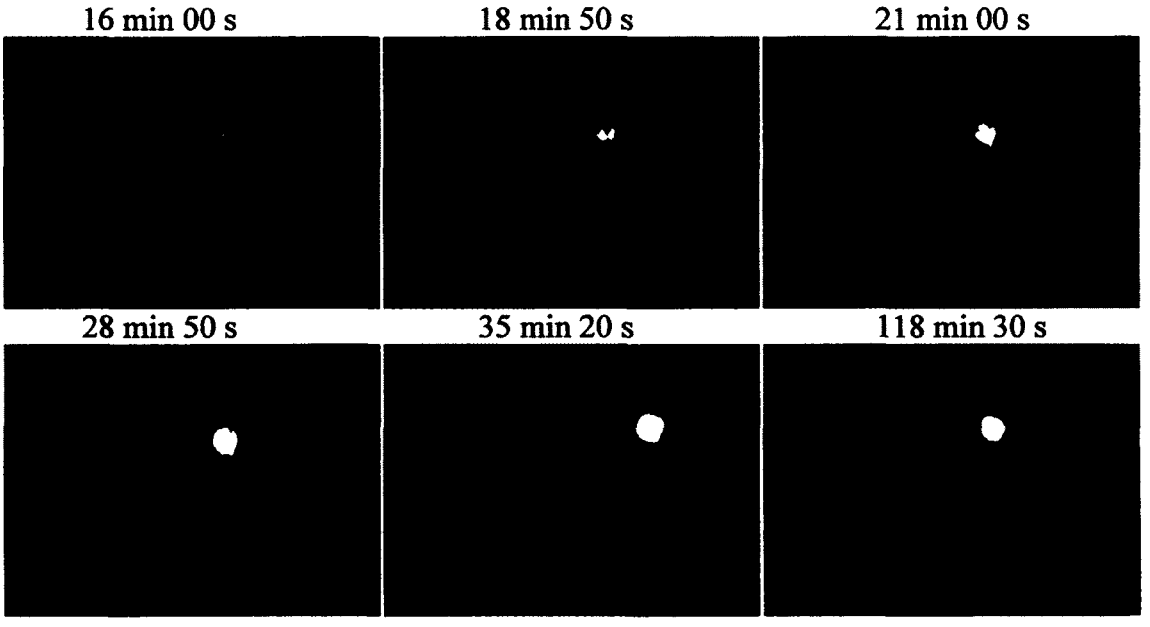

Figure C-7: Select images of hole growth from Table 4-1 (Figure 4-12).

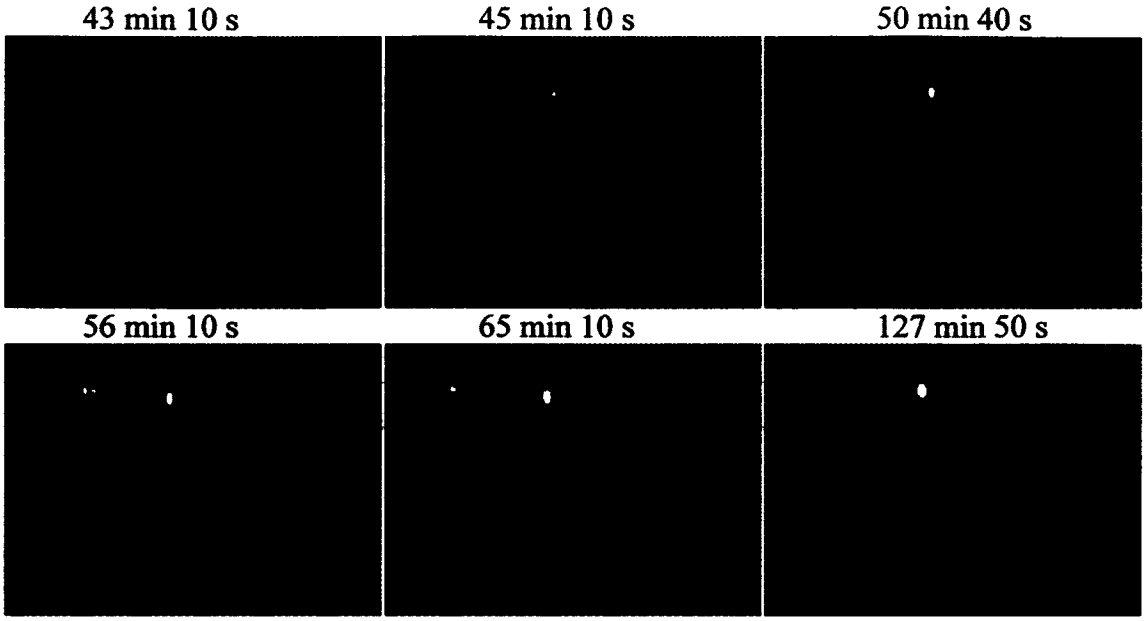

Figure C-8: Select images of hole growth from Table 4-1 (Figure 4-14).

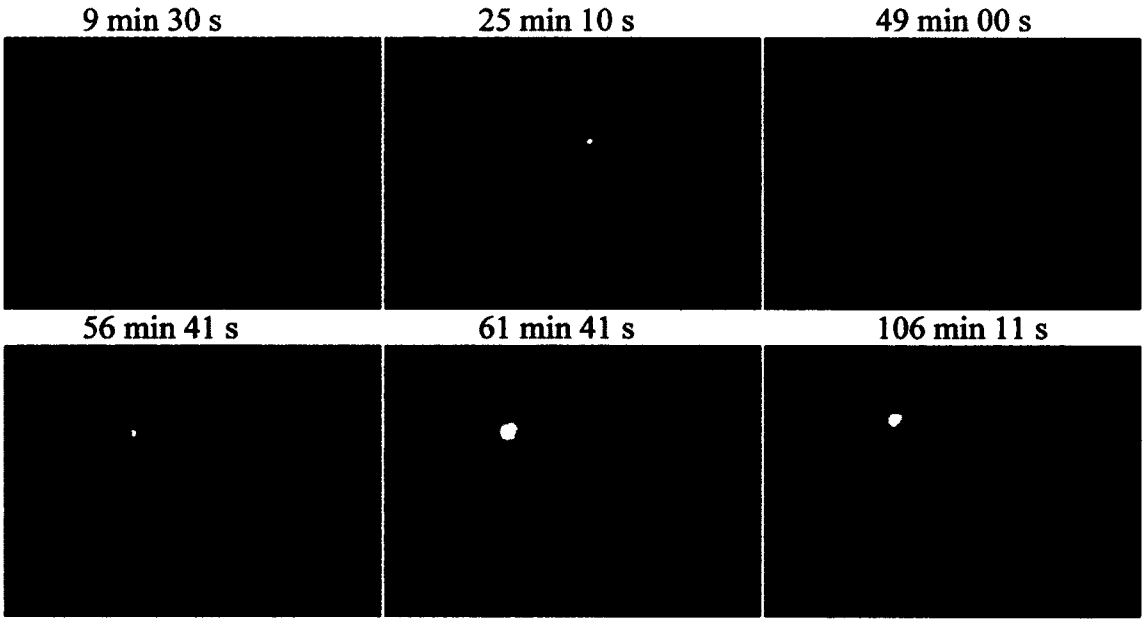

Figure C-9: Select images of hole growth from Table 4-1 (Figure 4-15).

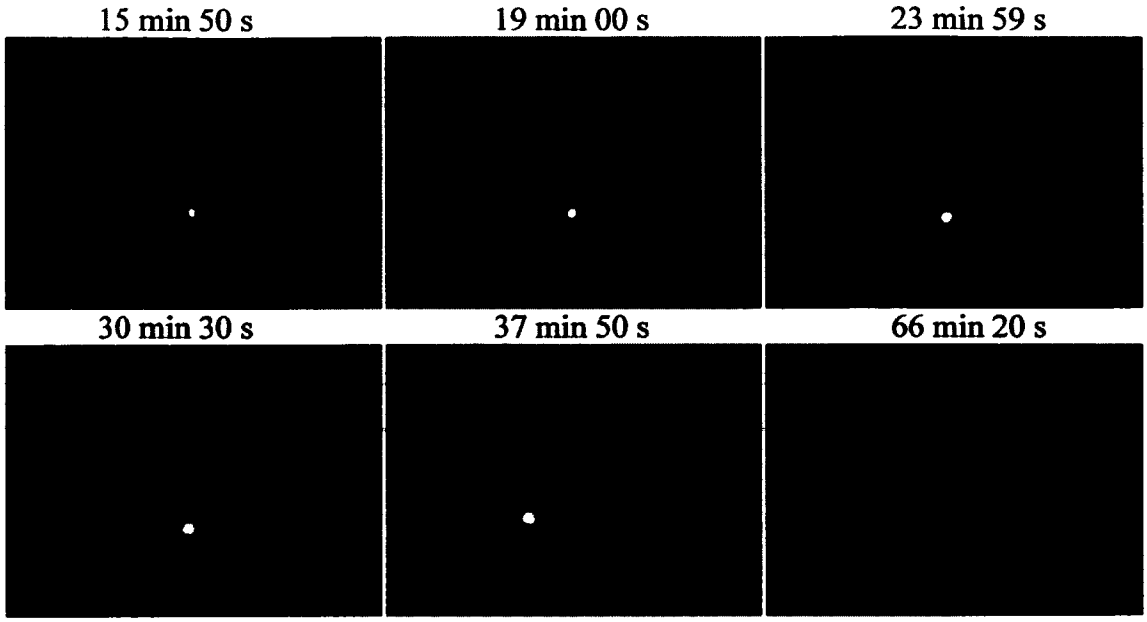

Figure C-10: Select images of hole growth from Table 4-1 (Figure 4-16).

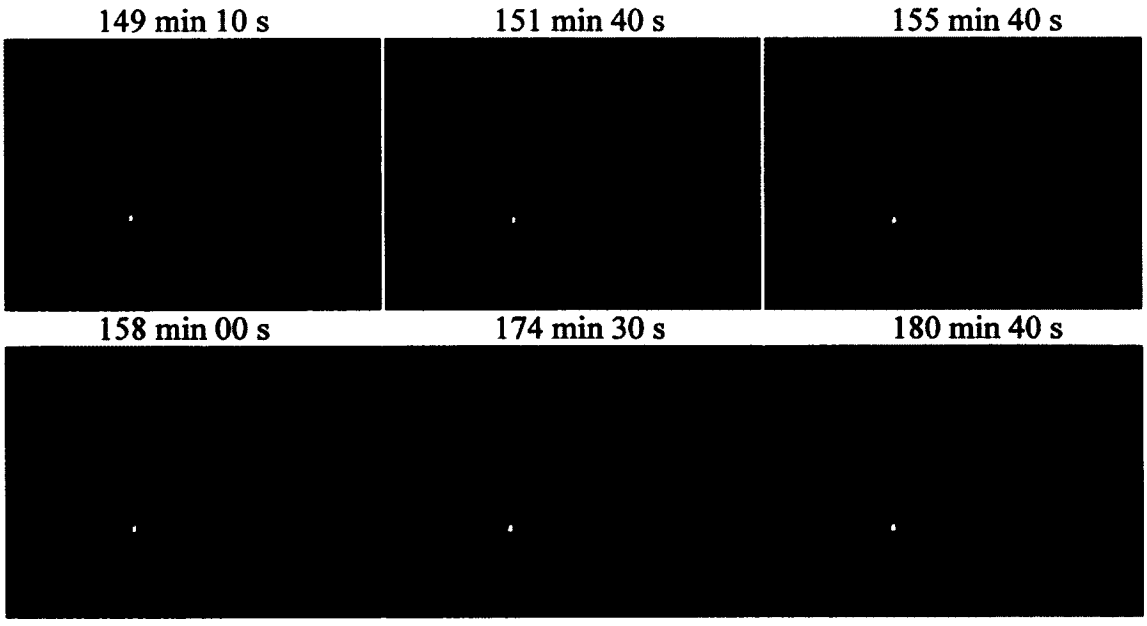

Figure C-11: Select images of hole growth from Table 4-1 (Figure 4-17).

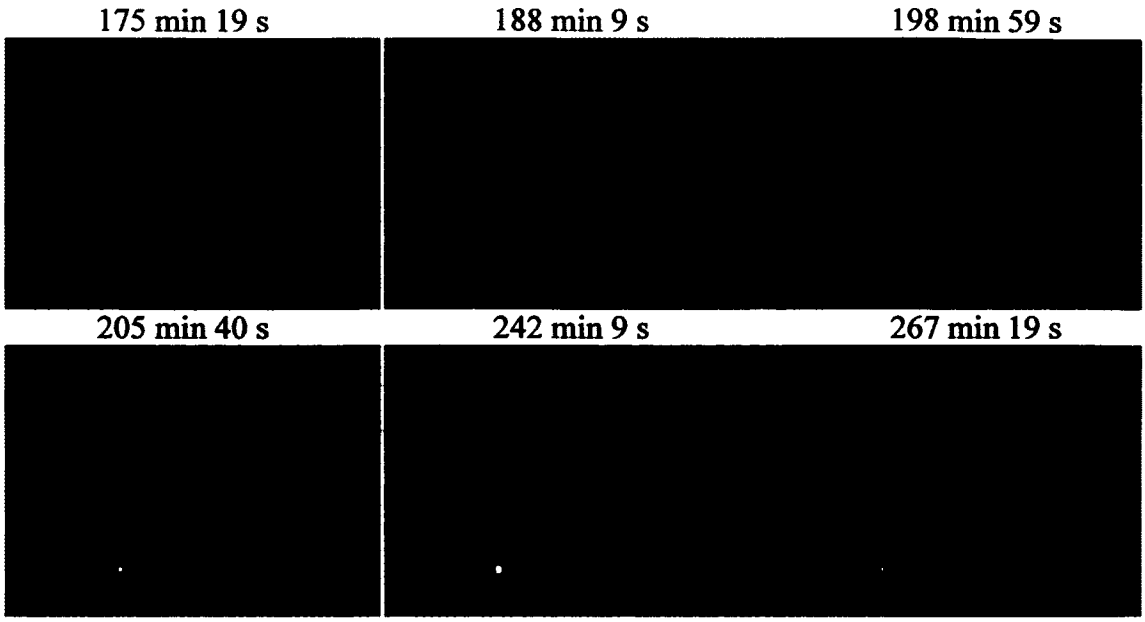

Figure C-12: Select images of hole growth from Table 4-1 (Figure 4-18).

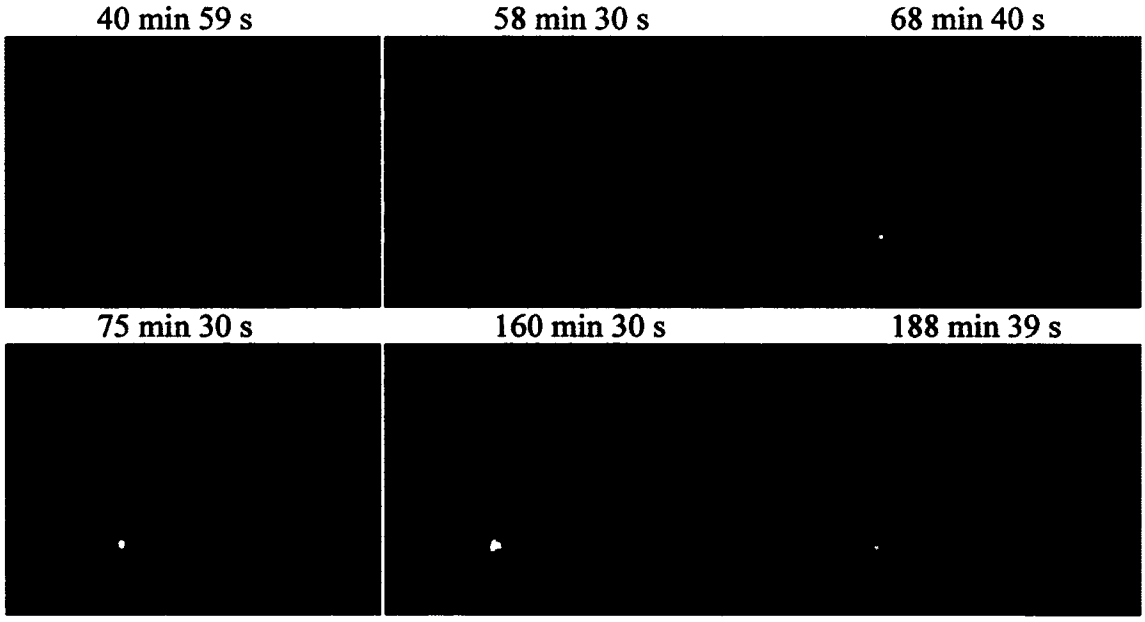

Figure C-13: Select images of hole growth from Table 4-1 (Figure 4-19).

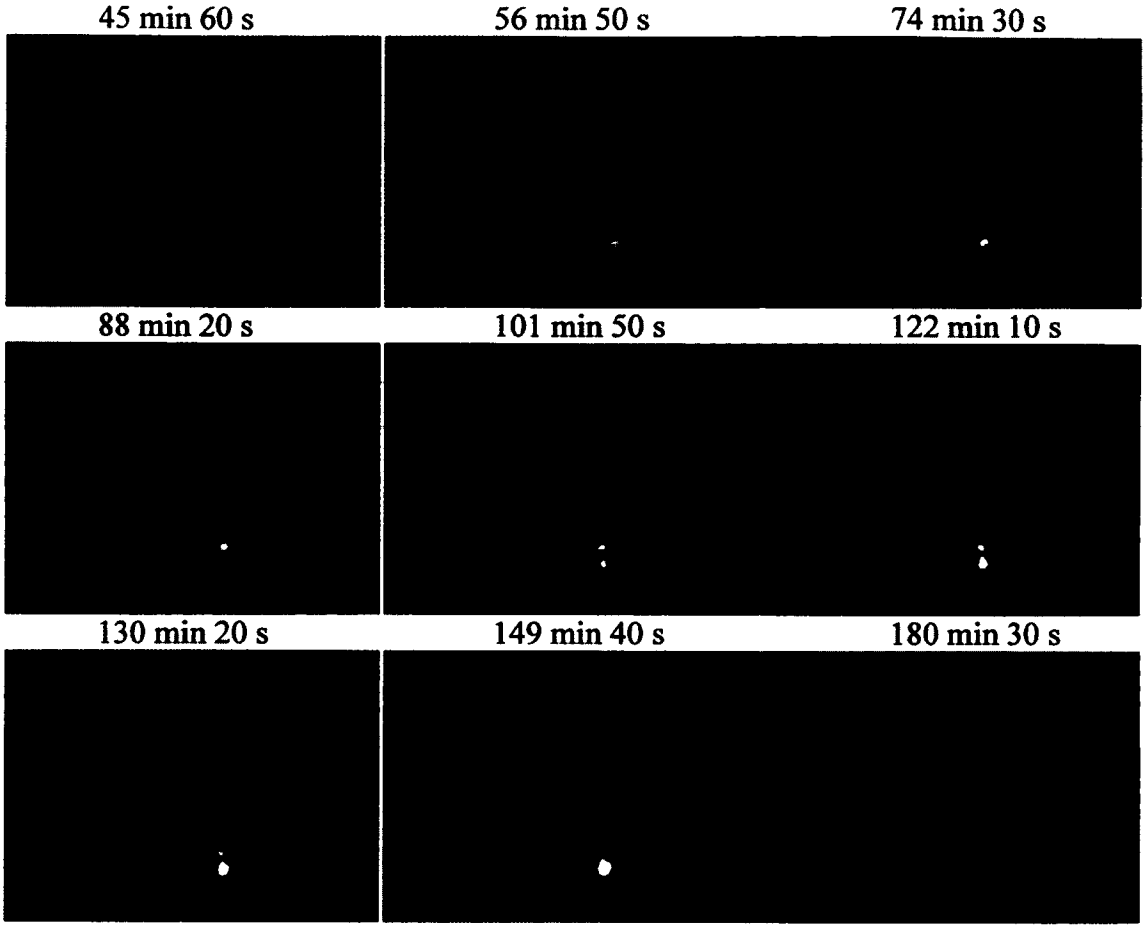

Figure C-14: Select images of hole growth from Table 4-1 (Figure 4-20).

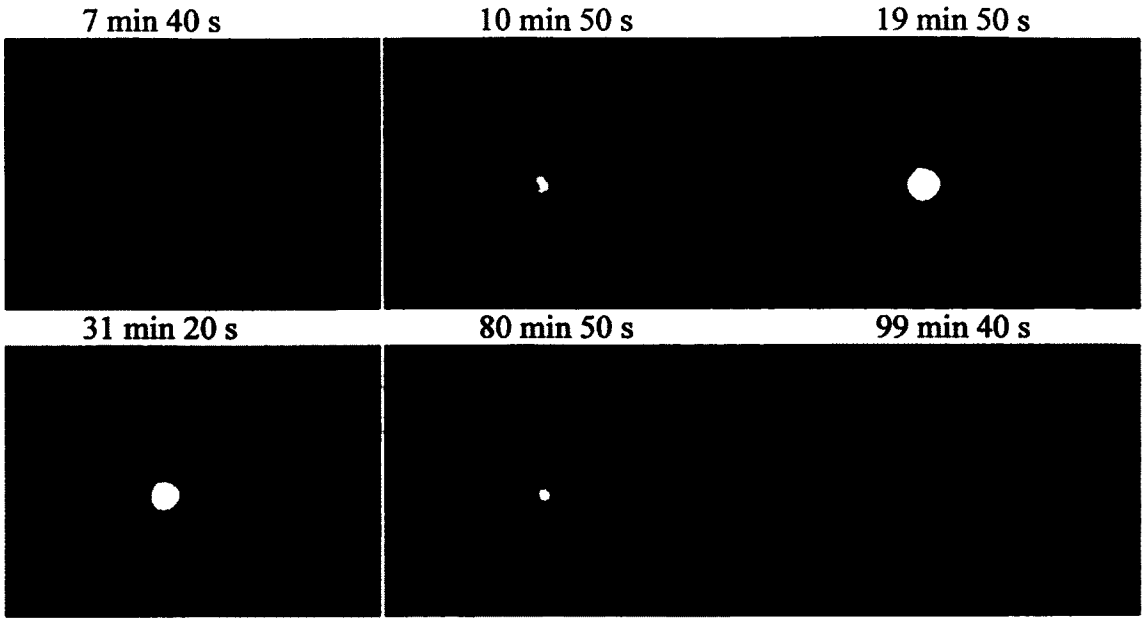

Figure C-15: Select images of hole growth from Table 4-1 (Figure 4-21).

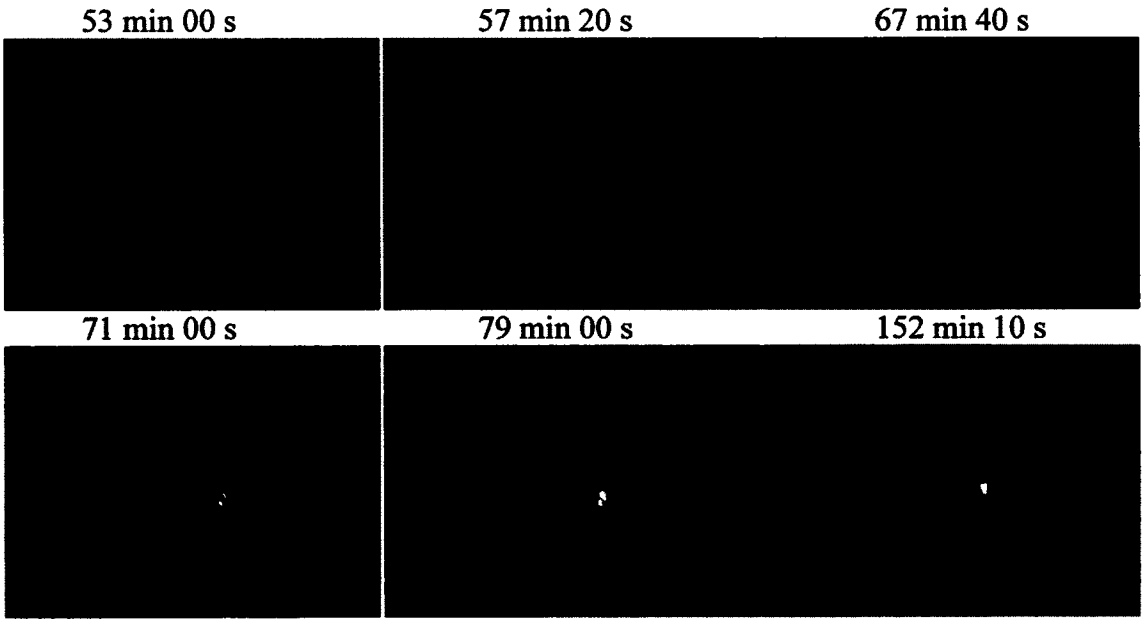

Figure C-16: Select images of hole growth from Table 4-1 (Figure 4-22).

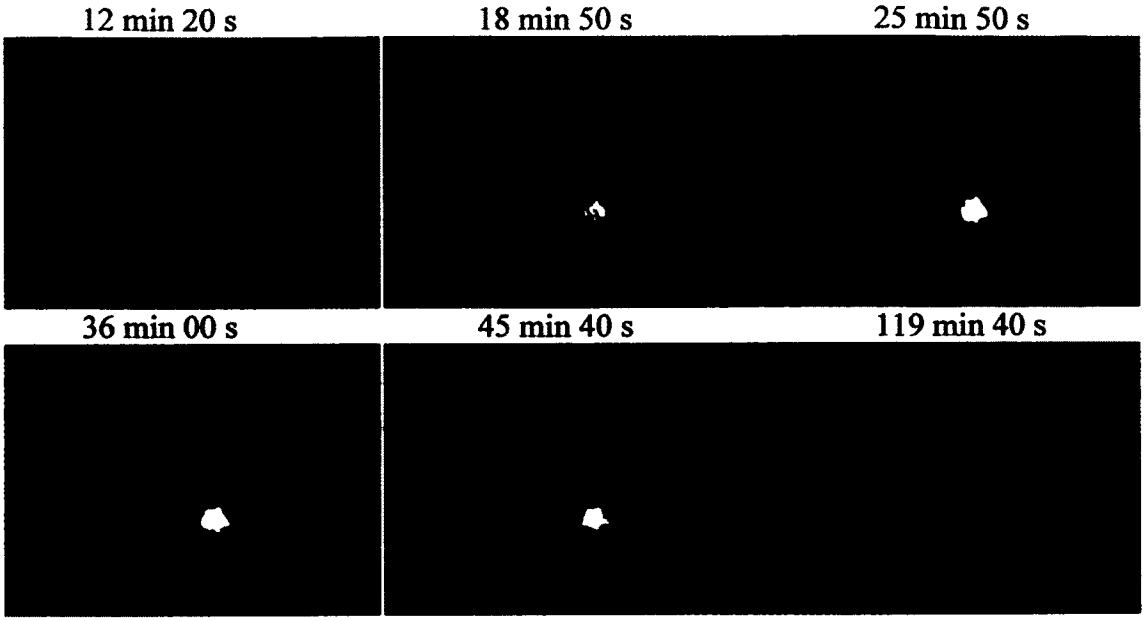

Figure C-17: Select images of hole growth from Table 4-1 (Figure 4-23).

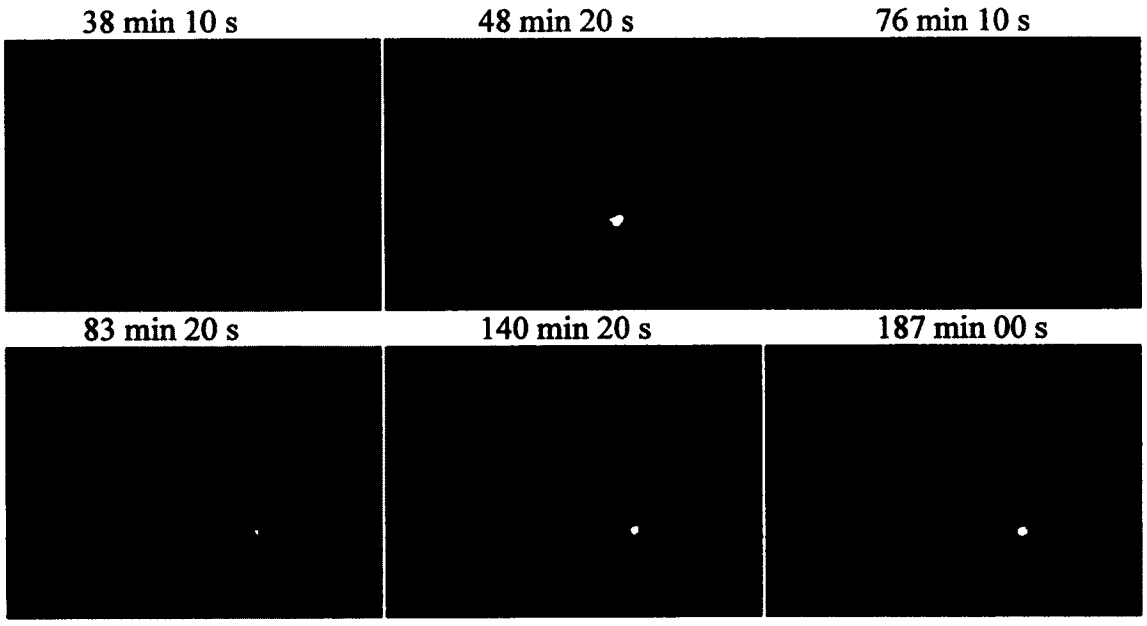

Figure C-18: Select images of hole growth from Table 4-1 (Figure 4-24).

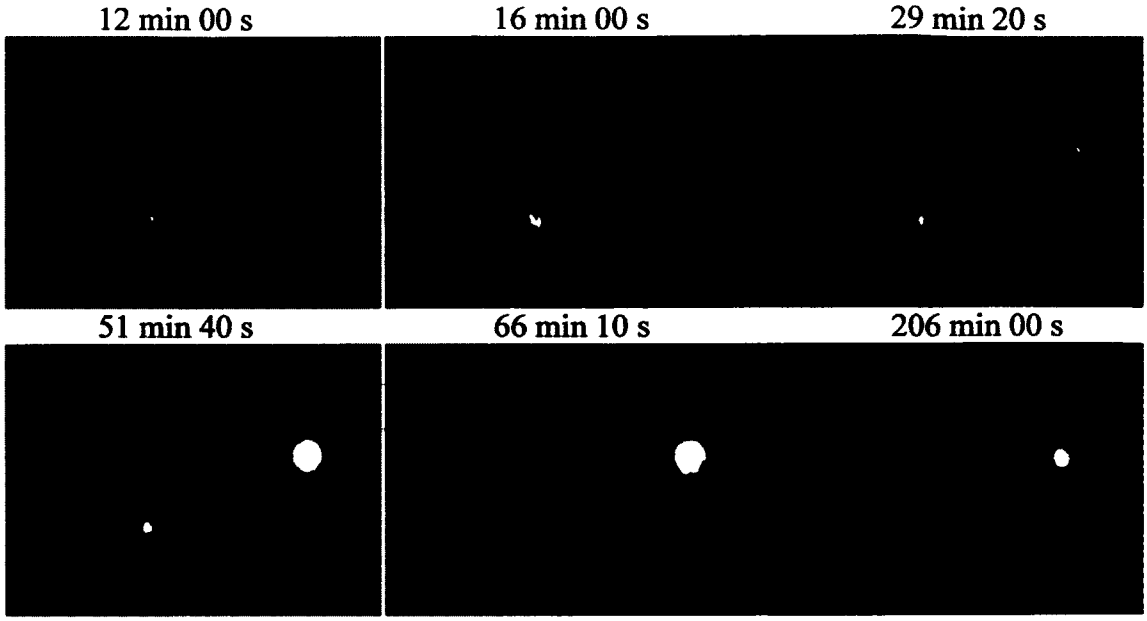

Figure C-19: Select images of hole growth from Table 4-1 (Figure 4-25).

APPENDIX D

TEST MATRIX FOR DEWETTING AND SAMPLE PROPERITES

Table D-1: Test matrix for dewetting of asphalt films.

Asphalt	Neat/Additive	Set/(Sample)	pH	Thickness (μm)	Average (μm)	No. of holes	Average	Dewetted Area (mm^2)	Average Area (mm^2)
PG58-28	*Neat*	*1(1)*	*8*	*181*		*6*		*0.021*	
PG58-28	*Neat*	*2(2)*	*8*	*173*		*9*		*0.172*	
PG58-28	*Neat*	*3(3)*	*8*	*165*		*52*		*1.461*	
PG58-28	*Neat*	*1(4)*	*8.1*	*157*		*23*		*0.120*	
PG58-28	*Neat*	*2(5)*	*7.9*	*213*		*4*		*0.037*	
PG58-28	*Neat*	*3(6)*	*7.9*	*150*	*204.5*	*24*	*12.1*	*0.117*	*0.183*
PG58-28	*Neat*	*1(7)*	*8*	*220*		*0*		*0.000*	
PG58-28	*Neat*	*3(8)*	*8*	*150*		*22*		*0.242*	
PG58-28	*Neat*	*5(9)*	*8*	*181*		*3*		*0.012*	
PG58-28	*Neat*	*1(10)*	*7.8*	*304*		*1*		*0.000*	
PG58-28	*Neat*	*3(11)*	*8*	*308*		*1*		*0.010*	
PG58-28	*Neat*	*5(12)*	*7.8*	*252*		*0*		*0.000*	
PG58-28	1%Adhere HP Plus	1(1)	8	181		443		4.046	
PG58-28	1%Adhere HP Plus	2A(2)	8	118		275		3.475	
PG58-28*	1%Adhere HP Plus	3(3)	8	230	190.5	42	216	0.456	2.586
PG58-28	1%Adhere HP Plus	1(4)	8	283		23		0.258	
PG58-28	1%Adhere HP Plus	3(5)	8	142		369		6.414	
PG58-28	1%Adhere HP Plus	5(6)	8	189		144		0.867	

Table D-1: Test matrix for dewetting of asphalt films (Continued).

Asphalt	Neat/Additive	Set/(Sample)	pH	Thickness (μm)	Average (μm)	No. of holes	Average	Dewetted Area (mm^2)	Average Area (mm^2)
PG58-28	1%Adhere LOF 6500	1(1)	8.1	126	199.3	201	121.7	2.125	1.043
PG58-28*	1%Adhere LOF 6500	2(2)	7.9	172		180		1.082	
PG58-28	1%Adhere LOF 6500	3(3)	7.9	181		142		1.009	
PG58-28	1%Adhere LOF 6500	1(4)	7.8	268		26		0.368	
PG58-28	1%Adhere LOF 6500	3(5)	8	197		110		1.071	
PG58-28	1%Adhere LOF 6500	5(6)	7.9	252		71		0.605	
PG58-28	Neat	2(1)	10	197	184.5	63	189.5	0.436	2.400
PG58-28	Neat	4(2)	10	110		328		6.507	
PG58-28	Neat	6(3)	10	173		291		3.302	
PG58-28	Neat	2(4)	10	257		33		0.178	
PG58-28	Neat	4(5)	10	165		304		3.365	
PG58-28	Neat	6(6)	10	205		118		0.612	
PG58-28	1%Adhere HP Plus	2(1)	10	244	166.6	21	256.7	0.114	4.767
PG58-28	1%Adhere HP Plus	4(2)	10	150		348		5.910	
PG58-28	1%Adhere HP Plus	6(3)	10	244		90		0.878	

Table D-1: Test matrix for dewetting of asphalt films (Continued).

Asphalt	Neat/Additive	Set/(Sample)	pH	Thickness (μm)	Average (μm)	No. of holes	Average	Dewetted Area (mm^2)	Average Area (mm^2)
PG58-28	1%Adhere HP Plus	1A(4)	10	102		345		10.580	
PG58-28	1%Adhere HP Plus	1B(5)	10	142		440		6.355	
PG58-28	1%Adhere HP Plus	2A(6)	10	118		296		4.768	
PG58-28	1%Adhere LOF 6500	2(1)	10	260		27		0.223	
PG58-28	1%Adhere LOF 6500	4(2)	10	244		23		0.137	
PG58-28	1%Adhere LOF 6500	6(3)	10	220		67		0.415	
PG58-28	1%Adhere LOF 6500	1A(4)	10	142	189.7	177	146	1.834	1.997
PG58-28	1%Adhere LOF 6500	2A(5)	10	150		271		3.898	
PG58-28	1%Adhere LOF 6500	2B(6)	10	119		311		5.477	
PG64-22	*Neat*	*1*(1)	*7.7*	*157*		*292*		*5.833*	
*PG64-22**	*Neat*	*2*(2)	*7.7*	*205*		*86*		*0.721*	
*PG64-22**	*Neat*	*3*(3)	*7.9*	*251*		*19*		*0.301*	
PG64-22	*Neat*	*1*(4)	*8*	*228*	*246.8*	*63*	*49.5*	*0.389*	*0.735*
*PG64-22**	*Neat*	*2*(5)	*8*	*287*		*21*		*0.507*	
PG64-22	*Neat*	*3*(6)	*8*	*276*		*30*		*0.310*	

Table D-1: Test matrix for dewetting of asphalt films (Continued).

Asphalt	Neat/Additive	Set/(Sample)	pH	Thickness (μm)	Average (μm)	No. of holes	Average	Dewetted Area (mm^2)	Average Area (mm^2)
PG64-22	*Neat*	*1*(7)	*8*	*244*		*3*		*0.084*	
PG64-22	*Neat*	*3*(8)	*7.8*	*291*		*11*		*0.066*	
PG64-22	*Neat*	*5*(9)	*7.9*	*213*		*69*		*0.604*	
PG64-22	*Neat*	*1*(10)	*7.8*	*254*		*0*		*0.000*	
PG64-22	*Neat*	*3*(11)	*7.8*	*257*		*0*		*0.000*	
PG64-22	*Neat*	*5*(12)	*8.1*	*299*		*0*		*0.000*	
PG64-22	1%Adhere HP Plus	1(1)	7.7	213		312		13.239	
PG64-22*	1%Adhere HP Plus	2(2)	7.7	205		256		6.819	
PG64-22*	1%Adhere HP Plus	3(3)	7.9	230	232.7	275	182.7	2.872	4.793
PG64-22	1%Adhere HP Plus	1(4)	8	252		89		3.464	
PG64-22	1%Adhere HP Plus	3(5)	7.8	213		121		1.860	
PG64-22	1%Adhere HP Plus	5(6)	7.9	283		43		0.504	
PG64-22	1%Adhere LOF 6500	1(1)	8	291		54		0.511	
PG64-22*	1%Adhere LOF 6500	2(2)	8	197	249.3	286	125	4.863	2.051
PG64-22	1%Adhere LOF 6500	3(3)	8	315		83		1.406	

Table D-1: Test matrix for dewetting of asphalt films (Continued).

Asphalt	Neat/Additive	Set/(Sample)	pH	Thickness (μm)	Average (μm)	No. of holes	Average	Dewetted Area (mm^2)	Average Area (mm^2)
PG64-22	1%Adhere LOF 6500	1(4)	7.8	260		86		1.266	
PG64-22	1%Adhere LOF 6500	3(5)	7.8	252		46		1.433	
PG64-22	1%Adhere LOF 6500	5(6)	8.1	181		195		2.829	
PG64-22	Neat	2(1)	10	220		35		0.270	
PG64-22	Neat	4(2)	10	268		86		1.171	
PG64-22	Neat	6(3)	10	260	241.3	12	411	0.054	0.680
PG64-22	Neat	2(4)	10	228		74		0.869	
PG64-22	Neat	4(5)	10	236		124		0.970	
PG64-22	Neat	6(6)	10	236		80		0.745	
PG64-22	1%Adhere HP Plus	*2*(1)	*10*	283		3		0.181	
PG64-22	1%Adhere HP Plus	*4*(2)	*10*	225		138		2.016	
PG64-22	1%Adhere HP Plus	*6*(3)	*10*	236		118		1.344	
PG64-22	1%Adhere HP Plus	1A(4)	10	252	232.8	13	78.7	0.131	1.093
PG64-22	1%Adhere HP Plus	1B(5)	10	220		40		0.438	
PG64-22	1%Adhere HP Plus	2A(6)	10	181		160		2.446	

Table D-1: Test matrix for dewetting of asphalt films (Continued).

Asphalt	Neat/Additive	Set/(Sample)	pH	Thickness (μm)	Average (μm)	No. of holes	Average	Dewetted Area (mm^2)	Average Area (mm^2)
PG64-22	1%Adhere LOF 6500	2(1)	10	220	207.2	98	162.3	1.628	2.716
PG64-22	1%Adhere LOF 6500	4(2)	10	189		199		2.411	
PG64-22	1%Adhere LOF 6500	6(3)	10	228		198		2.722	
PG64-22	1%Adhere LOF 6500	1A(4)	10	228		113		0.829	
PG64-22	1%Adhere LOF 6500	2A(5)	10	244		69		0.520	
PG64-22	1%Adhere LOF 6500	2B(6)	10	134		297		8.188	
PG76-22M	*Neat*	*1*(1)	*8*	*213*	*289.8*	*12*	*4.5*	*1.815*	0.559
PG76-22M	*Neat*	*2*(2)	*7.9*	*228*		*2*		*0.081*	
PG76-22M	*Neat*	*3*(3)	*8*	*339*		*0*		*0.000*	
PG76-22M	*Neat*	*1*(4)	*8*	*228*		*3*		*0.623*	
PG76-22M	*Neat*	*2*(5)	*8.1*	*315*		*0*		*0.000*	
PG76-22M	*Neat*	*3*(6)	*7.9*	*251*		*3*		*0.835*	
PG76-22M	*Neat*	*1*(7)	*8*	*394*		*0*		*0.000*	
PG76-22M	*Neat*	*3*(8)	*7.8*	*375*		*0*		*0.000*	
PG76-22M	*Neat*	*5*(9)	*8*	*315*		*2*		*0.039*	
PG76-22M	*Neat*	*1*(10)	*7.8*	*323*		*2*		*0.078*	
PG76-22M	*Neat*	*3*(11)	*8*	*283*		*3*		*0.329*	
PG76-22M	*Neat*	*5*(12)	*8*	*213*		*27*		*2.906*	

Table D-1: Test matrix for dewetting of asphalt films (Continued).

Asphalt	Neat/Additive	Set/(Sample)	pH	Thickness (μm)	Average (μm)	No. of holes	Average	Dewetted Area (mm^2)	Average Area (mm^2)
PG76-22M	1%Adhere HP Plus	1(1)	8	291	313	64	91.5	0.497	1.163
PG76-22M	1%Adhere HP Plus	2(2)	7.9	328		5		0.021	
PG76-22M	1%Adhere HP Plus	3(3)	8	220		421		5.727	
PG76-22M	1%Adhere HP Plus	1(4)	8	386		9		0.055	
PG76-22M	1%Adhere HP Plus	3(5)	7.8	307		11		0.083	
PG76-22M	1%Adhere HP Plus	5(6)	8	346		39		0.593	
PG76-22M	1%Adhere LOF 6500	1(1)	8	236	253.2	103	74.7	1.103	0.751
PG76-22M	1%Adhere LOF 6500	2(2)	8.1	205		92		0.744	
PG76-22M	1%Adhere LOF 6500	3(3)	7.9	220		104		1.128	
PG76-22M	1%Adhere LOF 6500	*1*(4)	*7.8*	*307*		*33*		*0.386*	
PG76-22M	1%Adhere LOF 6500	*3*(5)	*8*	*260*		*22*		*0.129*	
PG76-22M	1%Adhere LOF 6500	*5*(6)	*8*	*291*		*94*		*1.014*	

Table D-1: Test matrix for dewetting of asphalt films (Continued).

Asphalt	Neat/Additive	Set/(Sample)	pH	Thickness (μm)	Average (μm)	No. of holes	Average	Dewetted Area (mm^2)	Average Area (mm^2)
PG76-22M	Neat	*2*(1)	*9.9*	*378*	*292.7*	*20*	*133.8*	0.232	2.694
PG76-22M	Neat	*4*(2)	*10*	*252*		*135*		2.435	
PG76-22M	Neat	*6*(3)	*10*	*409*		*17*		0.242	
PG76-22M	Neat	*2*(4)	*9.9*	*244*		*198*		4.145	
PG76-22M	Neat	*4*(5)	*10*	*197*		*356*		7.814	
PG76-22M	Neat	*6*(6)	*10*	*276*		*77*		1.296	
PG76-22M	1%Adhere HP Plus	2(1)	9.9	370	275.5	13	301	0.260	0.597
PG76-22M	1%Adhere HP Plus	4(2)	10	299		59		0.700	
PG76-22M	1%Adhere HP Plus	6(3)	10	252		106		1.049	
PG76-22M	1%Adhere HP Plus	1A(4)	10	236		23		0.307	
PG76-22M	1%Adhere HP Plus	1B(5)	10	268		29		0.478	
PG76-22M	1%Adhere HP Plus	2A(6)	10	228		71		0.787	
PG76-22M	1%Adhere LOF 6500	2(1)	9.9	236	230.8	191	184.3	3.585	2.913
PG76-22M	1%Adhere LOF 6500	4(2)	10	228		383		5.098	
PG76-22M	1%Adhere LOF 6500	6(3)	10	283		90		1.214	

Table D-1: Test matrix for dewetting of asphalt films (Continued).

Asphalt	Neat/Additive	Set/(Sample)	pH	Thickness (μm)	Average (μm)	No. of holes	Average	Dewetted Area (mm^2)	Average Area (mm^2)
PG76-22M	1%Adhere LOF 6500	1A(4)	10	181		258		4.992	
PG76-22M	1%Adhere LOF 6500	2A(5)	10	181		143		1.654	
PG76-22M	1%Adhere LOF 6500	2B(6)	10	276		41		0.938	
PG58-28	2%Adhere HP Plus	1A(1)	7.9	110		38		0.544	
PG58-28	2%Adhere HP Plus	1A(2)	8.3	236		25		0.439	
PG58-28	2%Adhere HP Plus	1B(3)	8.3	189	169.2	127	132.5	0.768	1.978
PG58-28	2%Adhere HP Plus	2B(4)	7.8	102		411		8.392	
PG58-28	2%Adhere HP Plus	3A(5)	7.9	181		128		1.447	
PG58-28	2%Adhere HP Plus	2A(6)	7.8	197		66		0.279	
PG76-22M	2%Adhere HP Plus	1A(1)	8.4	354		5		0.028	
PG76-22M	2%Adhere HP Plus	1B(2)	7.9	276	*254.7*	97	*108.8*	1.017	1.557
PG76-22M	2%Adhere HP Plus	2A(3)	8	307		32		0.305	

Table D-1: Test matrix for dewetting of asphalt films (Continued).

Asphalt	Neat/Additive	Set/(Sample)	pH	Thickness (μm)	Average (μm)	No. of holes	Average	Dewetted Area (mm^2)	Average Area (mm^2)
PG76-22M	2%Adhere HP Plus	2B(4)	8	268		136		1.812	
PG76-22M	2%Adhere HP Plus	3A(5)	7.9	150		286		4.657	
PG76-22M	2%Adhere HP Plus	3B(6)	7.9	173		97		1.522	
PG58-28	0.25%Adhere HP Plus	1A(1)	7.8	260		13		0.042	
PG58-28	0.25%Adhere HP Plus	1B(2)	8.2	213		21		0.077	
PG58-28	0.25%Adhere HP Plus	2A(3)	8.2	197	*189*	123	*160.2*	1.621	2.311
PG58-28	0.25%Adhere HP Plus	2B(4)	8.2	118		337		8.188	
PG58-28	0.25%Adhere HP Plus	3A(5)	8.2	189		229		1.947	
PG58-28	0.25%Adhere HP Plus	3B(6)	8.2	157		238		1.989	
PG64-22	0.25%Adhere HP Plus	1A(1)	8.5	165		63		0.542	
PG64-22	0.25%Adhere HP Plus	2A(2)	8	213	191.5	82	134.8	0.808	2.484
PG64-22	0.25%Adhere HP Plus	2A(3)	8.6	142		241		5.416	

Table D-1: Test matrix for dewetting of asphalt films (Continued).

Asphalt	Neat/Additive	Set/(Sample)	pH	Thickness (μm)	Average (μm)	No. of holes	Average	Dewetted Area (mm^2)	Average Area (mm^2)
PG64-22	0.25%Adhere HP Plus	2B(4)	8.3	157		314		5.420	
PG64-22	0.25%Adhere HP Plus	3A(5)	8.2	244		7		0.176	
PG64-22	0.25%Adhere HP Plus	3B(6)	8.2	228		102		2.542	
PG76-22M	0.25%Adhere HP Plus	1A(1)	8.3	260		99		1.620	
PG76-22M	0.25%Adhere HP Plus	1B(2)	8.3	323		1		0.000	
PG76-22M	0.25%Adhere HP Plus	2A(3)	8.3	323	291.3	11	60	0.118	1.180
PG76-22M	0.25%Adhere HP Plus	2B(4)	8.3	276		219		4.966	
PG76-22M	0.25%Adhere HP Plus	3A(5)	8.3	283		2		0.005	
PG76-22M	0.25%Adhere HP Plus	3B(6)	8.3	283		28		0.369	
PG58-28	Neat	1 A(1)	7.9	228		43		0.226	
PG58-28	[Neat]	1 B(2)	7.9	291		13		0.060	
PG58-28	Neat	2 A(3)	8.4	299	*204.7*	10	*151.2*	0.057	2.057
PG58-28	[Neat]	2 B(4)	8.4	220	*[191.5]*	162	*[198]*	1.852	[3.491]
PG58-28	[Neat]	3 A(5)	8	142		303		3.100	
PG58-28	Neat	3 B(6)	8	197		136		1.214	

Table D-1: Test matrix for dewetting of asphalt films (Continued).

Asphalt	Neat/Additive	Set/(Sample)	pH	Thickness (μm)	Average (μm)	No. of holes	Average	Dewetted Area (mm^2)	Average Area (mm^2)
PG58-28	Neat	4 A(7)	8.1	181		239		1.371	
PG58-28	Neat	4 B(8)	8.1	205		132		0.642	
PG58-28	[Neat]	5 A(9)	8.2	118		311		5.735	
PG58-28	[Neat]	5 B(10)	8.2	181		321		9.799	
PG58-28	[Neat]	6 A(11)	8.2	197		78		0.401	
PG58-28	Neat	6 B(12)	8.2	197		66		0.228	
PG 64-22	[Neat]	1 A(1)	8.5	283		41		0.463	
PG 64-22	Neat	1 B(2)	8.5	307		46		0.808	
PG 64-22	Neat	2 A(3)	8.3	307		3		0.015	
PG 64-22	[Neat]	2 B(4)	8.3	315		16		0.429	
PG 64-22	[Neat]	3 A(5)	8.1	134		364		9.169	
PG 64-22	[Neat]	3 B(6)	8.1	189	251.3	305	*150.8*	6.737	2.620
PG 64-22	Neat	4 A(7)	8.2	197	[232.2]	226	*[190.5]*	2.262	[3.751]
PG 64-22	[Neat]	4 B(8)	8.2	228		272		4.230	
PG 64-22	Neat	5 A(9)	8.3	299		12		0.065	
PG 64-22	Neat	5 B(10)	8.3	173		366		5.596	
PG 64-22	Neat	6 A(11)	8.4	339		13		0.193	
PG 64-22	[Neat]	6 B(12)	8.4	244		145		1.478	
PG76-22M	[Neat]	1 A(1)	8.4	268		41		0.976	
PG76-22M	[Neat]	1 B(2)	8.4	331		15		0.399	
PG76-22M	Neat	2 A(3)	8.3	260	294	32	29.8	0.361	0.345
PG76-22M	Neat	2 B(4)	8.3	315	[282.2]	5	[30.3]	0.036	[0.446]
PG76-22M	Neat	3 A(5)	8.4	402		7		0.047	
PG76-22M	[Neat]	3B (6)	8.4	252		43		0.539	

Table D-1: Test matrix for dewetting of asphalt films (Continued).

Asphalt	Neat/Additive	Set/(Sample)	pH	Thickness (μm)	Average (μm)	No. of holes	Average	Dewetted Area (mm^2)	Average Area (mm^2)
PG76-22M	Neat	4 A(7)	7.8	354		16		0.235	
PG76-22M	Neat	4 B(8)	7.8	252		38		0.240	
PG76-22M	[Neat]	5 A(9)	7.9	228		36		0.202	
PG76-22M	Neat	5 B(10)	7.9	252		78		0.553	
PG76-22M	[Neat]	6 A(11)	7.8	291		44		0.547	
PG76-22M	[Neat]	6 B(12)	7.8	323		3		0.011	
PG58-28	*1%Adhere HP Plus*	*2(2)*	*8*	*150*		*418*		*17.086*	
PG58-28	*2%Adhere HP Plus*	*1B*(2)	*7.9*	*102*		*481*		*6.798*	
PG58-28	*2%Adhere HP Plus*	*2A*(3)	*7.8*	*165*		*6*		*0.262*	
PG58-28	*2%Adhere HP Plus*	*3B*(6)	*7.9*	*110*		*78*		*0.736*	
PG76-22M	*2%Adhere HP Plus*	*1A*(1)	*7.9*	*244*		*27*		*0.164*	
PG76-22M	*2%Adhere HP Plus*	*2A*(3)	*8*	*291*		*1*		*0.004*	
PG58-28	*0.25%Adhere HP Plus*	*1A*(1)	*8.2*	*220*		*1*		*0.004*	
PG64-22	*0.25%Adhere HP Plus*	*1B*(2)	*8.5*	*173*		*22*		*1.029*	

Note: *These samples measure approximately 2.4 x 5.08 cm while all other samples measure approximately 2.5 x 5.08 cm
Italized neat samples were not used in analysis as they were affected by light source from microscope
Neat asphalt samples, per six, placed in [] were used in the dewetted area analysis. All 12 samples were used to evaluate the critical film thickness.

APPENDIX E

CHEMISTRY OF TAP WATER USED IN EXPERIMENTS

Table E-1: Approximate chemistry of water used in experiments except where deionized water is used (Courtesy Public Works, City of Ruston, LA).

Pace Analytical
www.pacelabs.com

Pace Analytical Services, Inc.
6 East Tower Circle
Ormond Beach, FL 32174
(386)672-5668

ANALYTICAL RESULTS

Project: CR04180 Annual
Pace Project No.: 35152083

Sample: Well 1 Lab ID: 35152083006 Collected: 08/25/14 09:00 Received: 08/26/14 11:40 Matrix: Water

Parameters	Results	Units	PQL	MDL	DF	Prepared	Analyzed	CAS No.	Qual
200.7 MET ICP, DW No Prep	Analytical Method: EPA 200.7								
Calcium	1.5	mg/L	0.50	0.25	1		09/05/14 03:58	7440-70-2	
Ca Hardness as CaCO3 (SM 2340B	3.8	mg/L	1.2	0.62	1		09/05/14 03:58		
Mg Hardness as CaCO3 (SM 2340B	1.5 I	mg/L	2.0	1.0	1		09/05/14 03:58		
Iron	0.11	mg/L	0.040	0.020	1		09/05/14 03:58	7439-89-6	
Magnesium	0.37 I	mg/L	0.50	0.25	1		09/05/14 03:58	7439-95-4	
Potassium	1.1	mg/L	1.0	0.50	1		09/05/14 03:58	7440-09-7	
Silica	29.8	mg/L	0.21	0.11	1		09/05/14 03:58	7631-86-9	
Sodium	78.9	mg/L	1.0	0.50	1		09/05/14 03:58	7440-23-5	
Tot Hardness asCaCO3 (SM 2340B	5.2	mg/L	3.3	1.6	1		09/05/14 03:58		
200.8 MET ICPMS Drinking Water	Analytical Method: EPA 200.8								
Aluminum	0.019 I	mg/L	0.020	0.012	2		09/08/14 08:52	7429-90-5	D3
Arsenic	0.0016U	mg/L	0.0020	0.0010	2		09/08/14 08:52	7440-38-2	D3
Copper	0.0016U	mg/L	0.0020	0.0010	2		09/08/14 08:52	7440-50-8	D3
Lead	0.50U	ug/L	1.0	0.50	1		09/05/14 13:25	7439-92-1	
Manganese	0.0034	mg/L	0.0020	0.0014	2		09/08/14 08:52	7439-96-5	D3
Zinc	0.0060U	mg/L	0.010	0.0050	2		09/08/14 08:52	7440-66-6	D3
2120B Apparent Color	Analytical Method: SM 2120B								
Apparent Color	10.0	units	5.0	5.0	1		08/27/14 08:25		
2320B Alkalinity	Analytical Method: SM 2320B								
Alkalinity, Total as CaCO3	135	mg/L	5.0	5.0	1		08/27/14 10:39		
4500H+ pH, Electrometric	Analytical Method: SM 4500-H+B								
Temperature, Water (C)	23.0	deg C	0.010	0.010	1		08/27/14 09:15		
pH at 25 Degrees C	7.7	Std. Units	0.10	0.10	1		08/27/14 09:15		Q
300.0 IC Anions	Analytical Method: EPA 300.0								
Nitrogen, NO2 plus NO3	0.043U	mg/L	0.050	0.043	1		08/27/14 01:32		
Orthophosphate as P	0.25	mg/L	0.10	0.066	1		08/27/14 01:32		
300.0 IC Anions 28 Days	Analytical Method: EPA 300.0								
Chloride	16.2	mg/L	5.0	2.5	1		08/28/14 07:37	16887-00-6	
Sulfate	12.4	mg/L	5.0	2.5	1		08/28/14 07:37	14808-79-8	
365.4 Phosphorus, Total	Analytical Method: EPA 365.4 Preparation Method: EPA 365.4								
Phosphorus, Total (as P)	0.23	mg/L	0.10	0.050	1	08/27/14 08:30	08/27/14 18:16	7723-14-0	

REPORT OF LABORATORY ANALYSIS

APPENDIX F

MODIFIED BOIL TEST AND SCORE SHEET

Table F-1: Initial temperature and pH used for modified boil test.

Asphalt	Initial Temperature (°C)	pH
PG 58-28	22	8.3
PG 58-28 + 1% Adhere HP Plus	23.5	8.4
PG 58-28 + 1% Adhere LOF 6500	22.5	8.4
PG 64-22	23	8.4
PG 64-22 + 1% Adhere HP Plus	24	8.4
PG 64-22 + 1% Adhere LOF 6500	23	8.3
PG 76-22M	23	8.2
PG 76-22M + 1% Adhere HP Plus	23	8.3
PG 64-22M + 1% Adhere LOF 6500	22	8.3

Instructions: Insert 1, 2, or 3 in the spaces provided for each binder type based on their performance after being subjected to the modified *ASTM D* 3625 boil test.

Key:

1: Worst

2: Moderate

3: Best

Score in this direction →

PG64-22 Neat	PG64-22 + 1%Adhere HP Plus	PG64-22 + 1% Adhere LOF 6500
2	1	3
PG58-28	PG58-28+1%Adhere HP Plus	PG58-28+1 % Adhere LOF 6500
1	2	3
PG76-22M	PG76-22M + 1 % Adhere HP Plus	PG76-22M + 1 % LOF 6500
3	2	1

Score in this direction ↓

PG64-22 Neat	PG64-22 + 1%Adhere HP Plus	PG64-22 + 1% Adhere LOF 6500
1	1	2
PG58-28	PG58-28+1%Adhere HP Plus	PG58-28+1 % Adhere LOF 6500
2	3	3
PG76-22M	PG76-22M + 1 % Adhere HP Plus	PG76-22M + 1 % LOF 6500
3	2	1

Student 1

MRI

Figure F-1: Student 1 test score distribution.

Instructions: Insert 1, 2, or 3 in the spaces provided for each binder type based on their performance after being subjected to the modified ASTM D 3625 boil test.

Key:

1: Worst

2: Moderate

3: Best

Score in this direction →

PG64-22 Neat	PG64-22 + 1%Adhere HP Plus	PG64-22 + 1% Adhere LOF 6500
1	2	3
PG58-28	PG58-28+1%Adhere HP Plus	PG58-28+1 % Adhere LOF 6500
1	2	3
PG76-22M	PG76-22M + 1 % Adhere HP Plus	PG76-22M + 1 % LOF 6500
3	2	1

Score in this direction ↓

PG64-22 Neat	PG64-22 + 1%Adhere HP Plus	PG64-22 + 1% Adhere LOF 6500
1	3	2
PG58-28	PG58-28+1%Adhere HP Plus	PG58-28+1 % Adhere LOF 6500
1	2	3
PG76-22M	PG76-22M + 1 % Adhere HP Plus	PG76-22M + 1 % LOF 6500
1	2	3

Student 2

H. M

Figure F-2: Student 2 test score distribution.

Instructions: Insert 1, 2, or 3 in the spaces provided for each binder type based on their performance after being subjected to the modified ASTM D 3625 boil test.

Key:

1: Worst

2: Moderate

3: Best

Score in this direction

PG64-22 Neat	PG64-22 + 1%Adhere HP Plus	PG64-22 + 1% Adhere LOF 6500
3	2	1
PG58-28	PG58-28+1%Adhere HP Plus	PG58-28+1 % Adhere LOF 6500
2	1	3
PG76-22M	PG76-22M + 1 % Adhere HP Plus	PG76-22M + 1 % LOF 6500
3	3	2

Score in this direction

PG64-22 Neat	PG64-22 + 1%Adhere HP Plus	PG64-22 + 1% Adhere LOF 6500
3	3	1
PG58-28	PG58-28+1%Adhere HP Plus	PG58-28+1 % Adhere LOF 6500
2	2	3
PG76-22M	PG76-22M + 1 % Adhere HP Plus	PG76-22M + 1 % LOF 6500
1	1	2

Student 3 L.E.

Figure F-3: Student 3 test score distribution.

Instructions: Insert 1, 2, or 3 in the spaces provided for each binder type based on their performance after being subjected to the modified ASTM D 3625 boil test.

Key:

1: Worst

2: Moderate

3: Best

Score in this direction

PG64-22 Neat	PG64-22 + 1%Adhere HP Plus	PG64-22 + 1% Adhere LOF 6500
1	2	3
PG58-28	PG58-28+1%Adhere HP Plus	PG58-28+1 % Adhere LOF 6500
1	2	3
PG76-22M	PG76-22M + 1 % Adhere HP Plus	PG76-22M + 1 % LOF 6500
2	3	1

Score in this direction

PG64-22 Neat	PG64-22 + 1%Adhere HP Plus	PG64-22 + 1% Adhere LOF 6500
1	1	2
PG58-28	PG58-28+1%Adhere HP Plus	PG58-28+1 % Adhere LOF 6500
3	2	3
PG76-22M	PG76-22M + 1 % Adhere HP Plus	PG76-22M + 1 % LOF 6500
2	3	1

Student 4

Figure F-4: Student 4 test score distribution.

Instructions: Insert 1, 2, or 3 in the spaces provided for each binder type based on their performance after being subjected to the modified ASTM D 3625 boil test.

Key:

1: Worst

2: Moderate

3: Best

Score in this direction →

PG64-22 Neat	PG64-22 + 1%Adhere HP Plus	PG64-22 + 1% Adhere LOF 6500
1	1 3	2
PG58-28	PG58-28+1%Adhere HP Plus	PG58-28+1 % Adhere LOF 6500
1	2	3
PG76-22M	PG76-22M + 1 % Adhere HP Plus	PG76-22M + 1 % LOF 6500
3	2	1

Score in this direction ↓

PG64-22 Neat	PG64-22 + 1%Adhere HP Plus	PG64-22 + 1% Adhere LOF 6500
1	1	2
PG58-28	PG58-28+1%Adhere HP Plus	PG58-28+1 % Adhere LOF 6500
3	2	3
PG76-22M	PG76-22M + 1 % Adhere HP Plus	PG76-22M + 1 % LOF 6500
2	3	1

Student 5 KSM

Figure F-5: Student 5 test score distribution.

APPENDIX G

ANALYSIS OF #100 SIEVE SIZE GRAVEL AGGREGATE

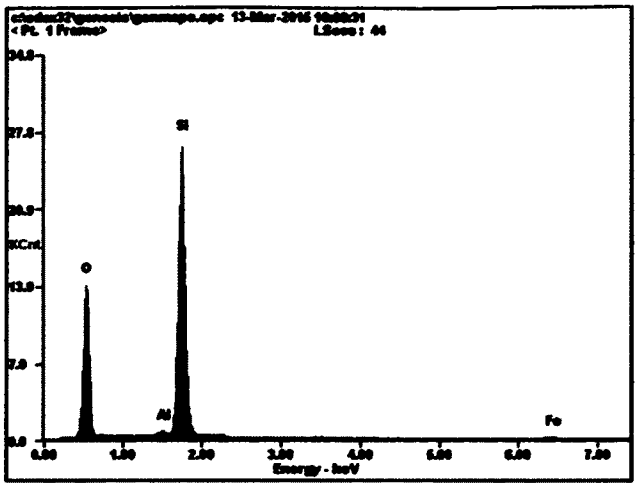

Figure G-1: SEM analysis of gravel particle retained on # 100 sieve.

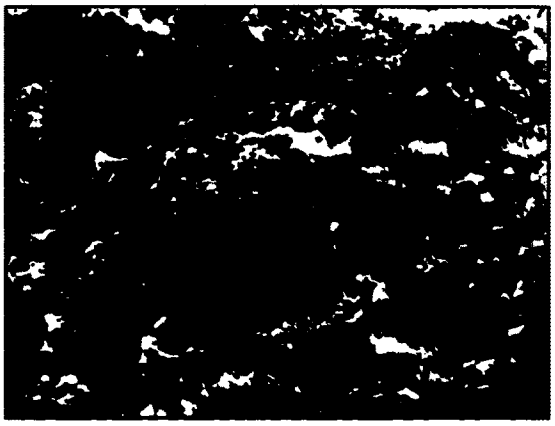

Figure G-2: SEM image of gravel retained on # 100 sieve.

Element	Wt %	At %
OK	53.05	66.77
AlK	00.65	00.49
SiK	45.04	32.29
FeK	01.26	00.45
Matrix	Correction	ZAF

Figure G-3: Weight and atomic weight percent of gravel retained on # 100 sieve.

REFERENCES

(AASHTO T165-86) Standard method of test for effect of water on compressive strength of compacted bituminous mixtures.

(AASHTO T283-03) Standard method of test for resistance of compacted asphalt mixtures to moisture-induced damage.

(AASHTO TP 4) Standard method for preparing and determining the density of hot mix asphalt (hma) specimens by means of the superpave gyratory compactor.

(AASHTO PP2-94) Standard practice for short and long term aging of hot mix asphalt hma edition 1a.

(ASTM D 4541) Standard test method for pull-off strength of coatings using portable adhesion testers.

Alam, M. M, and Picornell, M. (1998). "A test method for identifying moisture susceptible asphalt concrete mixes." Research Report 1455-2F. The Center for Highway Materials Research, The University of Texas at El Paso, El Paso, TX.

Albritton, G. E., Barstis, W. F. and Crawley, A. B. (1999). "Polymer modified hot mix asphalt field trial." Final Report. FHWA/MS-DOT-RD-99-111.

Anderson, D. A., Dukatz, E. L., and Peterson, J. C. (1982). "The effect of antistrip additives on the properties of asphalt cement."*Asphalt Paving Technology*, 400 Selby Ave., St. Paul, MN, 298-316.

Arabani, M., and Hamedi, Gh. H. (2011). "Using the surface free energy method to evaluate the effects of polymeric aggregate treatment." *J. of Mater.in Civ. Eng.*, 23(6), 802-811.

Arambula, E., Caro, S., and Masad, E. (2010). "Experimental measurement and numerical simulation of water vapor diffusion through asphalt pavement materials. *J. of Mater. in Civil Eng.*, 22(6), 588-598.

Aschenbrener, T., Terrel, R. L., and Zamor, R. A. (1994). "Comparison of the hamburg wheel tracking device and the environmental conditioning system to pavements of known stripping performance." *FinalReport. No. COOT -DTD-R-94*-1, Colorado Department of Transportation, Denver, CO.

Asphalt Handbook (2007). *MS-4, 7th Edition*. Asphalt Insititute. Printed in USA.

Bagampadde, U. (2004). "On investigation of stripping propensity of bituminous mixtures." Licentiate thesis, Royal Institute of Technology, Stockholm, Sweden.

Basu, S., Nandakumar, K., and Masliyah, J. H. (1996). "A study of oil displacement on model surfaces." *J. Colloid Interface Sci.,* 182, 82-94.

Beckman, A. O., Badger, R. M., Gullekson, E. E., and Stevenson, D. P. (1941). "Bituminous coatings. *Ind. Eng. Chem.*" 33(8), 984-990.

Bertrand, E., Blake, T.D., De Coninck, J. (2010). "Dynamics of dewetting."*Colloids and surfaces A: physicochem. Eng., Aspects*, 369(2010), 141-147.

Bhasin, A. (2006). "Development of methods to quantify bitumen-aggregate adhesion and loss of adhesion due to water." Ph.D. dissertation, Texas A & M Univ. College Station, TX.

Bhasin, A., and Little, D. (2007). "Characterization of aggregate surface energy using the universal sorption device." *J. of Mater. In Civ. Eng.*, 19 (8), 634-641.

Bonner, D. G. (2001). "Construction materials, their nature and behavior." 3rd Ed., J. M. Illston, and P. L. J. Domone, eds., *Spon Press*. New York, NY.

Brochard-Wyart, F., Debregeas, G., Fondecave, R., and Martin, P. (1997). "Dewetting of supported viscoelastic polymer films: Birth of Rims." *Macromolecules*, 30, 1211-1213.

Brown, E. C., and Kuntze, R. A. (1972). "A Study of Stripping in Asphalt Pavements." Final Report on Project O.R.F.-1, Ontario Research Foundation, Department of Transportation and Communications, ON.

Butz, T., Rahimian, I., Hildebrand, G. (2001). "Modification of road bitumen with the Fischer-Tropsch paraffin Sasobit." *J. Appl. Asphalt Binder Tech.*, 1(2), 70-86.

Cardenas, H. E., Kupwade-Patil, and Eklund, S. E. (2010). "Recovery from sulfate attack in concrete via electrokinetic nanoparticle treatment." *J. Mater. Civ. Eng.*, 23, 7, 2011.

Caro, S., Masad, E., Bhasin, A., and Little, D. N. (2008). "Moisture susceptibility of asphalt mixtures, part 2: characterization and modeling." *Int. J. Pavem. Eng.*, 9(2), 99-114.

Chadbourn, B. A., Skok, E. L., Jr., Newcomb, D. E., Crow, B. L., and Spindle, S. (1999). "The effects of voids in mineral aggregate (VMA) on hot mix asphalt pavements. Report No. MN/RC-2000-13, Univ. of Minnesota, Minneapolis, MN.

Cheng, D. (2002). "Surface free energy of asphalt-aggregate system and performance analysis of asphalt concrete based on surface free energy." Ph.D. dissertation, Texas A & M Univ., College Station, TX.

Cheng, D., Little, D. N., Lytton, R. L., Holste, J. C. (2002). "Surface energy measurement of asphalt and its application to predicting fatigue and healing in asphalt mixtures." *Transp. Research Record: J. Transportation Research Board,* 1810, 44-53.

Composto, R. J., and Chung, H-J. (2005). "Surface-induced structure formation of polymer blends." *Nanolithography and Patterning Techniques in Microelectronics*, Bucknall, D. G., ed.,WoodHead Publishing Ltd., Sawston, Cambridge, UK., 39-75.

Copeland, A. (2005). "Moisture in asphalt pavements in the united states: a financial perspective." *First international workshop on moisture damage,* (in CD-ROM) *Delf, The Netherlands.*

Copeland, A., Kringos, N., Scarpas, A., Youtcheff, J., and Mahadevan, S. (2006b). "Determination of bond strength as a function of moisture content at the aggregate-mastic Interface." *10th International Conference on Asphalt Pavements,* Quebec City, QC, August., 12-17.

Copeland, A. R. and Youtcheff, J. (2006a). "Moisture Sensitivity of Modified Asphalt Binders: Factors Influencing Bond Strength." *10th International Conference on Asphalt Pavements*, Quebec City, QC, August, 12-17.

Copeland, A. R. (2007). "Influence of moisture on bond strength of asphalt-aggregate systems." Ph.D. dissertation, Vanderbilt Univ., Nashville, TN.

Crank, J. (1975). "The Mathematics of Diffusion." Oxford University Press, N.Y.

Curtis, C. W. (1990). "A literature review of liquid anti-stripping and tests for measuring stripping." *Strategic Highway Research Program,* National Research Council, Washington, D.C.

Curtis, C. W., Ensley, K., and Epps, J. (1993). "Fundamental properties of asphalt-aggregate interactions including adhesion and absorption." *Strategic Highway Research Program*, National Research Council,Washington, D.C.

Czarnecki, J., Radoev, B., Scharamm, L. L., and Slavchev, R. (2005). "On the nature of athabasca oil sands." *Adv. in Colloid and Interface Science,*114-115, 53-60.

Davies, J. T., and Rideal, and E. K. (1961). "Interfacial Phenomena." *Academic Press Inc.,*New York, NY.

deGennes, P-G., Brochard-Wyart, F., and Quere, D. (2010). "Capillarity and Wetting Phenomena." *Springer Science + Business Media, Inc.*, New York, NY.

DiBeneddetto, A. T. (1970). "General Concepts of Adhesion." *49th Annual Meeting of the Highway Research Board*, Washington, D.C., (340), 1-12.

Donaldson, E. C., and Alam, W. (2008). "Wettability." *Gulf Publishing Company*, Houston, TX.

Drelich, J. (1993). "The role of wetting phenomena in the hot water process from bitumen recovery from tar sand." Ph.D. dissertation, Univ. of Utah, UT.

Edwards, Y., and Redelius, P.(2003). "Rheological effects of waxes in bitumen." *Energy and Fuels.*, 17(3), 511-520.

Edwards, Y., Tasdemir, Y., and Isacsson, U. (2006). "Rheological effects of commercial waxes and polyphosphoric acid in bitumen 160/220 – low temperature performance." *Fuel.*, 85(7-8), 989-997.

Elseifi, M. A., Al-Qadi, I. L., Yang, S-H, and Carpenter, H. S. (2008). "Validity of asphalt binder film thickness concept in hot-mix asphalt." *Transp. Research Rec. J. Transp. Research Board*, Washington D.C., 2057, 37-45.

Ensley, E. K. (1975). "Multilayer absorption with molecular orientation of asphalt on mineral aggregate and other substrates." *J. of Appl. Chem. Bio.*, 25, 671-82.

Feng, J. (2001). "Interaction and permeability of water with liquid crystalline thermoset." Ph.D. dissertation, Univ. of Florida, Gainesville, FL.

Field, F., and Phang, W. A. (1967). "Stripping in asphaltic concrete mixes: observations and test procedures." *12th Annual conference of the Canadian Technical Asphalt Association*, Halifax, NS.

Francisca, F. M., Rinaldi, V. A., and Santamarina, J. C. (2003). "Instability of hydrocarbon films over mineral surfaces: microscale experimental studies." *J. Env. Eng.*, 129(12), 1120-1128.

Fromm, H. J. (1974). "The mechanisms of asphalt stripping from aggregate surfaces." *Assoc. of Asphalt Paving Techn.*, Minneapolis, MN, 43, 191-223.

Fowkes, F. M. (1983). "Acid-base interactions in polymer adhesion." *Physico-Chemical Aspects of Polymer Surfaces*, K.L. Mittal, ed., Plenum, NY, 2, 583.

George, S. C., and Thomas, S. (2000). "Transport phenomena through polymeric systems." *Prog. in Poly. Sci.*, 26(2001), 985-1017.

Good, R. J. (1992). "Contact angle wetting and adhesion: a critical review." *J. Adh. Sci. Tech.*, 6(12), 1269-1302.

Harnish, C. I. (2010). "Liquid anti-strip technology & best practices." ArrMaz Custom Chemicals, NCAUPG, Overland Park, KS.

Hefer, A. W., Bhasin, A., and Little, D. N. (2006). "Bitumen surface energy characterization using a contact angle approach." *J. of Mater. Civ. Eng.*, 18 (6), 759-767.

Herminghaus, S., Pompe, T., and Fery, A. (2000). "Scanning force microscopy investigation of liquid structures and its application to fundamental wetting research." *J. Adhesion Sci. Techn.*, 14(14), 1767-1782.

Hicks, R. G. (1991). "Moisture damage of asphalt concrete." *National Cooperative Highway Research Program Synthesis,* Transportation Research Board, Washigton D.C., *No.* 175.

Hicks, G., Santucci, L., and Aschenbrener, T. (2003). "Introduction and seminar objectives."*Moisture Sensitivity of Asphalt Pavements: A National Seminar.* San Diego, CA: Transportation Research Board, Washington, D.C.

Hurley, G. C., and Prowell, B. D. (2005). "Evaluation of Sasobit® for use in warm mix asphalt." *NCAT Report 05-06,* National Center for Asphalt Technology (NCAT), Auburn Univ., Auburn, AL.

Isacsson, W., and T. Jorgensen. (1987). "Laboratory methods for determination of the water susceptibility of bituminous pavements." Report, Swedish Road and Traffic Research Institute, Sweden.

Jacobs, K., Herminghaus, S., and Mecke, K. R. (1998). "Thin liquid polymer films rupture via defects." *Langmuir*, 14(4), 965-969.

Kandhal, P. S., Foo, Y. F., and Mallick, R. B. (1998). "A critical review of vma requirements in superpave." *NCAT Report,* No. 98-1, National Center for Asphalt Techn.,Auburn Univ., AL.

Kandhal, P.S., and Chakraborty, S. (1996). "Effect of asphalt film thickness on short and long term aging of asphalt paving mixtures." *NCAT Report 96-01*, National Center for Asphalt Techn., Auburn Univ., AL.

Kandhal, P. S. and Rickards, I. J. (2001). "Premature failure of asphalt overlays from stripping: case histories." *NCAT Report 01-01*, National Center for Asphalt Techn., Auburn Univ., AL

Kandil, K., Abd El Halim, A. O., Hassan, Y., and Mostafa, A. (2007). "Investigation of the effects of different polymer-modified asphalt cements on asphalt mixes at low temperature." *Can. J. Civ. Eng.*,34(5), 589-597.

Kanitpong, K. (2005). "Evaluation of the roles of adhesion and cohesion properties of asphalt binders in moisture damage of HMA." Ph.D. dissertation, Univ. of Wisconsin, Madison, WI.

Kanitpong, K. and Bahia, H. U. (2003). "Role of adhesion and thin film tackiness of asphalt binders in moisture damage of HMA." *J. of the Assoc. of Asphalt Paving Technologists.*, 72, 502-528.

Kanitpong, K. and Bahia, H. U. (2005). "Relating adhesion and cohesion of asphalts to effect of moisture on asphalt mixtures' laboratory performance." *Presented at the 84th Annual Meeting*, Transportation Research Board,Washington, D.C.

Kassem, E., Masad, E., Lytton, R. L., and Bulut, R. (2009). "Measurements of moisture diffusion coefficient of asphalt mixtures and its relationship to mixture composition." *Int. J. Pave. Eng.,* 10(6), 389-399.

Kim, Y-R., Lutif, J. S., Bhasin, A., Little, D. N. (2008). "Evaluation of moisture damage mechansisms and effects of hydrated lime in asphalt mixtures through measurements of mixture component properties and performance testing." *J. Mater. Civ. Eng.,* 20(10), 659-667.

Kennedy, T. W. and Ping, W. (1991). "Evaluation of effectiveness of antistripping additives in protecting asphalt mixes from moisture damage." J. of the Assoc. of Asphalt Paving Techn., St. Paul, MN.

Kennedy, W. T., Roberts, F. L., and Anagnos, J. N. (1984). "Texas boiling test for evaluating moisture susceptibility of asphalt mixtures." *Report. FHWA/TX-85/63+253-5*,Center for Transportation Research, Univ. of Texas, Austin, TX.

Kennedy, T. W., Roberts, F. L., Lee, K. W., and Anagnos, J. N. (1982). "Texas freeze-thaw pedestal test for evaluating moisture susceptibility for asphalt mixtures." *Report.FHWA/TX-81/47+253-3*. Center for Transportation Research, Univ. of Texas, Austin, TX.

Kiggundu, B. M., and Roberts, F. L.(1988). "The success/failure or methods used to predict the stripping propensity in the performance of bituminous pavement mixtures." *NCAT Report 88-03*, National Center for Asphalt Technology (NCAT), Auburn, AL.

Kim, K. W, Kweon, S.J., Doh, Y. S. and Park, T-S. (2003). "Fracture toughness of polymer-modified asphalt concrete at low temperatures." *Can. J. Civ. Eng.,*30(2), 406-413.

Kim, Y-R., Lutif, J. S., Bhasin, A., Little, D. N. (2008). "Evaluation of moisture damage mechanisms and effects of hydrated lime in asphalt mixtures through measurements of mixture component properties and performance testing." *J. Mater. Civ. Eng.,* 20(10), 659-667.

Kristjánsdóttir, O., Muench, S. T., Michael, L., and Burke, G. (2007). "Assessing potential for warm-mix asphalt technology adoption." *Transportation Research Record. J. Transp. Research Board*, 2040, 91-99.

Kumar, P., and Anand, P. (2012). "Laboratory Study on Moisture Susceptibility of Dense Graded Mixes." *J. of Transp. Eng.*,138(1), 105-113.

Lavin, P. (2002). "The effects of dusty aggregates towards stripping in asphalt pavements." *The Asphalt Institute Spring Meeting,* The Woodlands,TX.<http://www.asphaltinstitute.org/wp-content/uploads/public/engineering/pdfs/ materials /Dusty_Aggregates.pdf>

Lee, S. H., Yoo, P. J., Kwon, S. J., and Lee, H. H. (2004). "Solvent-driven dewetting and rim instability." *J.Chem. Phys.*,121(9), 4346-4351.

Lelinki, D., Drelich, J., Miller, J. D., and Hupka, J. (2004). "Rate of bitumen film transfer from a quartz surface to an air bubble as observed by optical microscopy." *Can. J. Chem. Eng.*, 82(4), 794 – 800.

Li, X., Williams, R. C., Maransteanu, M. O., Clyne, T. R., Johnson, E. (2009). "Investigation of in-place asphalt film thickness and performance of hot-mix asphalt mixtures." *J. Mater. in Civil Eng.*, 21(6), 262-270.

National Lime Association. (2006). "Hydrated lime-a solution for high performance high performance hot mix asphalt." *National Lime Association.* Arlington, VA. <http://www.lime.org/documents/publications/free_downloads/fact-asphalt.pdf>

Little, D. N., and Epps, J. A. (2001). "The benefits of hydrated lime in hot mix asphalt." *National Lime Association.* Arlington, VA, 1-79.

Little, D. N., and Jones IV, D. R. (2003). "Chemical and mechanical processes of moisture damage in hot-mix asphalt pavements." *Moisture Sensitivity of Asphalt Pavements*, A National Seminar, San Diego, CA.

Lorenz-Haas, C., Müller-Buschbaum, P., Kraus, J., Bucknall, D. J., and Stamm, M. (2002). "Nucleated dewetting of thin polymer films." *J. Appl. Phys. A.,* 74(1), 383-385.

Lolly, R. (2013). "Evaluation of short term aging effect of hot mix asphalt due to elevated temperatures and extended aging time." M.S. thesis, Arizona State Univ., Tempe, AZ.

Lottman, R. P. (1978). "Predicting moisture-induced damage to asphaltic concrete-field evaluation phase." *Interim Report NCHRP*.Univ.of Idaho, Moscow, ID.

Lottman, R. P., Johnson, D. L. (1969). "The moisture mechanism that causes asphalt stripping in asphalt pavement mixtures." *Second Annual Report*, Univ. of Idaho, Moscow, ID.

Martin, J. S. T., Cooley, L. A. Jr., and Hainin, H. R. (2003). "Production and construction issues for moisture sensitivity of hot-mix asphalt pavements." *Moisture Sensitivity of Asphalt Pavements: A National Seminar.* San Diego, CA: Transportation Research Board, Washington, D.C.

Maupin, G. W. Jr. (1995). "Effectiveness of anti-stripping additives in the field." *ReportVTRC 96-R5.* Virginia Transportation Research Council, Charlottesville, VA.Virginia Department of Tranportation, Richmond, VA.

Maupin, G. W. Jr. (1997). "Follow-up field investigation of the effectiveness of antistrippingadditives in Virginia." *Report VTRC 97 TAR-6.*Virginia Transportation Research Council, Charlottesville, VA.Virginia Department of Tranportation, Richmond, VA.

Meridith, J. C., Smith, A. P., Karim, A., and Amis, E. J. (2000). "Combinatorial materials science for polymer thin-film dewetting." Macromolecules, 33,(26), 9747-9756.

Miknis, F. P., Pauli, A. T, Beemer, A., Wilde, B. (2005). "Use of NMR imaging to measure interfacial properties of asphalts." *Fuel,*84, 1041-1051.

Mugele, F., Becker, T., Nikopoulos, R., Kohonen, M., and Herminghaus, S. (2005). "Capillarity at the nanoscale: an AFM view." *Atomic Force Microscopy in Adhesion Studies,* J. Drelich and K. L. Mittal, eds.,CRC Press, Taylor and Francis Group, Boca Raton, FL, 541-554.

Nejad, F. M., Hamedi, Gh. H., Azarhoosh, A. R. (2013). "Use of surface free energy method to evaluate effect of hydrated lime on moisture damage in hot-mix asphalt." *J. of Mater.in Civ. Eng.*, 25(8), 1119-1126.

Nguyen, T., Byrd, E., Bentz, D., and Seiler, J. (1996). "Development of a method for measuring water stripping resistance of asphalt/siliceous aggregate mixtures." *Report. Transp. Res. Board*National Research. Council, Washington, D.C.

Plancher, H., Miyake, G., Venable, R. L., and Petersen, J. C. (1980). "A simple laboratory test to indicate moisture susceptibility of asphalt-aggregate mixtures to moisture damage during repeated freeze-thaw cycling. *Canadian Tech. Asphalt Assoc. Proc.,*247-262.

Rahim, A. (2010). "Mitigating moisture susceptibility of asphalt mixes." *Final Report 2010-NBG-1060,* Leonard Transportation Center, San Bernardino, CA.

Read, J., and Whiteoak, D. (2003). "The shell bitumen handbook." R. Hunter, ed.,Thomas Telford Publishing, Thomas Telford Ltd, 1 Heron Quay, London.

Redon. C., Brochard-Wyart, F., and Rondelez, F. (1991). "Dynamics of dewetting". *Phys. Rev. Lett.*, 66 (6), 715-717.

Redon, C., Brzoska, J. B., and Brochard-Wyart, F. (1994). "Dewetting and slippage of microscopic polymer films." *Macromolecules*, Vol. 27(2), 468 - 471.

Reiter, G. (2005). "Evolution of rim instabilities in the dewetting of slipping thin polymer films." *J. Adhes.*, 81, 381-395.

Reiter, G. (2013). "Probing properties of polymers in thin films via dewetting." *Adv. Polym. Sci.*, 252, 29-64.

Reynolds, P. (2005). "Wetting of surfaces." *Colloid Science: Principles, Methods and Applications,* T. Cosgrove, ed., Blackwell Publishing Ltd, Oxford, UK,159-179.

Rice, J. M. (1958). "Relationship of aggregate characteristics to the effect of water on bituminous mixtures." *Symp. on effects of water on bituminous paving mixtures, Sixty-first Annual Meeting Papers,* ASTM STP 240, Boston, MA,17-34.

RoadScience.(2014). Tulsa, OK.www.roadscience.net/sites/default/files/AdHere%20HP%Plus_0.pdf

Sharma, A. (1993). "Disintegration of Macroscopic Fluid Sheets on Substrates: A Singular Perturbation Approach." *J. Coll. Int. Sci.*,156(1), 1993, 96-103.

Shute, J. W., Hicks, R. J., Wilson, J. E., and Scholl, L. G. (1989). "Effectiveness of antistripping additives volume 1." *Report FHWA-OR-RD-89-03A*, Materials and Research Division, Oregon Department of Tranportation, Salem, OR.

Skok, E., Johnson, E., Turk, A. (2002). "Asphalt pavement analyzer (APA) evaluation." *Report MN/RC 2003-02,* Univ. of Minnesota, Minneapolis, MN.

Slavchov, R., Radoev, B., and Stöckelhuber, K. W. (2005). "Equilibrium profile and rupture of wetting film on heterogeneous substrates." *Colloids and Surfaces A: Physicochem. Eng. Aspects*, 261,135-140.

Solaimanian, M., Harvey, J., Tahmoressi, M. and Tandon, V. (2003). "Test methods to predict moisture sensitivity of hot mix asphalt pavements." *Moisture Sensitivity of Asphalt Pavements: A National Seminar,* San Diego, CA, Transportation Research Board Washington D.C.

Tarefder, R. A., and Zaman, A. M. (2010). "Nanoscale evaluation of moisture damage in polymer modified asphalts". *J. Mater.Civ. Eng.* 22(7), 714-725.

Tarrer, A. R. (1996). "Use of hydrated lime to reduce hardening and stripping in asphalt mixtures." *Presented at the 4th Annual International Center for Aggregate Research Symp.*, Atlanta, GA.

Tayebali, A. A., Knappe, D. R. U., and Chen, C. (2005). "Quantifying Antistrip Additives in Asphalt (Binder and Mixes)." *Report FHWA/NC/2005-16,* North Carolina State Univ. Raleigh, NC.

Tex-530-C. (2008). Test Procedure for "Effect of water on bituminous paving mixtures."

Thelen, E. (1958). "Surface energy and adhesion properties in asphalt-aggregate systems." *Bulletin 192, HRB*, National Research Council, Washington, DC, 63-72.

van Oss, C. J. (1994). "Interfacial forces in aqueous media." *Marcel Dekker, Inc.*, New York, NY.

van Oss, C. J., Chaudhury, M. K., and Good, R. J. (1987). "Monopolar surfaces." *Adv. Coll. Int. Sci*, 28, 35-64.

Vasconcelos, K. (2010). "Moisture diffusion in asphalt binders and fine aggregate mixtures." Ph.D. dissertation, Texas A&M Univ., College Station, TX.

Vilmin, T., and Raphaël, E. (2006). "Dewetting of thin polymer films." *Eur. Phy. J. E,* 21, 161-174.

Wan, J., and Wilson, J. L. (1992). "Colloid transport and the gas-water interface in porous media." *In Transport and Remediation of Subsurface*. D. A. Sabatini, and R. C. Knox, eds., American Chemical Society, Washington, DC, 55-70.

Wasiuddin, N. M. (2007). "Effect of additives on surface free energy characteristics of aggregates and binders in hot mix asphalt." Ph.D. dissertation, Univ. of Oklahoma, OK.

Wasiuddin, N. M., Fogle, C. M., Zaman, M. M. and O'Rear, E. A. (2007a). "Characterization of thermal degradation of liquid amine anti-strip additives in asphalt binders due to RTFO and PAV-aging." *J. of Test. and Eval.*, 35(4), 387-394.

Wasiuddin, N. M., Fogle, C. M., Zaman, M. M. and O'Rear, E. A. (2007b). "Effect of amine anti-strip additives on surface free energy characteristics of asphalt binders for moisture-induced damage potential." *J. of Test. and Eval.,* 35(1), 36-44.

Wasiuddin, N. M., Selvamohan, S., Zaman, M. M. and Guegan, M. L. T. (2007c). "A comparative laboratory study of Sasobit® and Aspha-Min® in warm mix asphalt." *Transp. Research Record: J. Transportation Research Board*, 1998, 82-88.

Wasiuddin, N. M., Zaman, M. M. and O'Rear, E. A. (2008). "Effect of Sasobit® and Aspha-Min® on wettability and adhesion between asphalt binders and aggregates." *Transp. Research Record: J. Transportation Research Board.,* 2051, 80-89.

Wasiuddin, N. M., and Saltibus, N. E. (2010). "Theoretical and experimental determination of adhesion between asphalt binders and aggregates in dry and wet conditions." *Report No.00-4 TIRE for* Louisiana Transportation Research Center, Baton Rouge, LA.

Wasiuddin, N. M., Saltibus, N., and Mohammad, L. (2011a). "Effects of a wax-based warm mix additive on cohesive strengths of asphalt binders." *Proceedings. T&DI Congress, Chicago, IL, 528-537.*

Wasiuddin N. M., Saltibus, N. E., Mohammad, L. N. (2011b). "A novel moisture conditioning method for adhesive failure of hot and warm mix asphalt." *Transp. Research Record: J. Transportation Research Board,*2208,108-117.

Wei, J., Huang, X., and Zhang, Y. (2010). "Influence of commercial wax on performance of asphalt." *J. of Mater. In Civ. Eng.*, 22 (8), 760-766.

Wekumbura, C., Stastna, J., and Zanzotto, L. (2007). "Destruction and recovery of internal structure in polymer-modified asphalts." *J. Mater.Civ. Eng.* 19 (3), 227-232.

West, R. C., Zhang, J., Cooley, A. Jr. (2004). "Evaluation of the asphalt pavement analyzer for moisture sensitivity testing." *NCAT Report04-04,* National Center for Asphalt Technology, Auburn Univ., Auburn, AL.

Wheeler, J. A. (1996). "Introduction to engineering experimentation." *Prentice-Hall, Inc.,* Englewood Cliffs, NJ.

Xiao, F., Zhao, W., Gandhi, T., and Amirkhanian, S. N. (2010). "Influence of antistripping additives on moisture susceptibility of warm mix asphalt mixtures." *J. Mater. Civ. Eng.,* 22(10), 1047-1055.

Xu, L., Shi, T., and Lijia, A. (2007). "Nonsolvent-Induced Dewetting of Thin Polymer Films." Langmuir, 23,9282-9286.

Yildirim, Y., Jayawickrama, P. W., Hossain, M. S., Alhabshi, A., Yildirim, C., Smit, A. F., and Little, D. (2007). "Hamburg wheel tracking database analysis." *Report No. FHWA/TX-05/0-1707-7.* Texas Department of Transportation, Austin, TX.

Yoon, H. H. and Tarrer, A. R. (1988). "Effect of aggregate properties on stripping." *Transp. Research Record: J. Transportation Research Board,* 1171, 37-43.

Youtcheff, J., and Aurilio, V. (1997). "Moisture Sensitivity of Asphalt Binders: Evaluation and Modeling of the Pneumatic Adhesion Test Results." *42nd Annual Conference of Can. Tech. Asphalt Assoc.,* Ottawa, ON.